Autophagic degradation of peroxisomes in the alkane-assimilating yeast *Yarrowia lipolytica*

A dissertation submitted to the

Technical University of Dresden

For the degree of

Doctor rerum naturalium

In Biology

Presented by

Iryna Parshyna

Institute of Microbiology, Technical University of Dresden

Reviewers:

Prof. Dr. Gerold Barth

Prof. Dr. Marten Veenhuis

Prof. Dr. Richard Rachubinski

Autophagischer Abbau von Peroxisomen in der alkanverwertenden Hefe *Yarrowia lipolytica*

DISSERTATION

Zur Erlangung des akademischen Grades
Doktor der Naturwissenschaften
(Dr. rer. nat.)

eingereicht an
der Fakultät Mathematik und Naturwissenschaften
der Technischen Universität Dresden

von

Diplom-Biologin Iryna Parshyna

geboren am 02.09.1976 in Kiew, Ukraine

Gutachter:
Prof. Dr. Gerold Barth
Prof. Dr. Marten Veenhuis
Prof. Dr. Richard Rachubinski

Parts of this work were published:

Publication:

Parshyna, I. and Barth, G. (2003) Detection of biosynthesis and degradation of peroxisomes by different carbon sources. In: Non-Conventional Yeasts in Genetics, Biochemistry and Biotechnology. Eds: Wolf, K., Breunig, K., Barth, G. Springer-Verlag, Berlin Heidelberg New York, pp. 385-392.

Posters:

Parshyna, I., Gunkel, K., Sibirny, A. and Barth, G. (2001) Selection of peroxisome degradation defective (*pdd*) mutants by expression of the chimeric gene *lacZ-eGFP(SKL)* in the yeast *Yarrowia lipolytica*. 21th International Specialized Symposium on Yeasts (Lwiw, Ukraine)

Parshyna, I. and Barth, G. (2002) Searching for mutants impaired in selective peroxisome degradation in the yeast *Yarrowia lipolytica*. 3rd *Yarrowia lipolytica* International Meeting (Dresden, Germany)

Parshyna, I. and Barth, G. (2002) *APG1* homologue of *Yarrowia lipolytica* is essential for selective peroxisome degradation. 17th Meeting on Yeasts and Related Organisms (Ober-Ramstadt, Germany)

Parshyna, I., Hoffmann, C. and Barth, G. (2003) Analysis of two autophagy-deficient mutants of the yeast *Yarrowia lipolytica*. Yeast, Vol. 20, Number S1, S150

Hoffmann, C., Jacobi, A., Parshyna, I and Barth, G. (2004) Cloning and characterisation of the *ATG6* gene from the yeast *Yarrowia lipolytica*. International Meeting on the Topogenesis of Organellar Proteins (Bochum, Germany)

Parshyna, I., Gunkel, K., Kasper, M and Barth, G. (2004) A novel approach to study the peroxisomal turnover in the dimorphic yeast *Yarrowia lipolytica*. International Meeting on the Topogenesis of Organellar Proteins (Bochum, Germany)

Bodinus, C., Parshyna, I. and Barth, G. (2004) A *Yarrowia lipolytica ATG18/CVT18* homologue is required for nitrogen starvation-induced pexophagy. International Meeting on the Topogenesis of Organellar Proteins (Bochum, Germany)

Contents

Abbreviations

aa	amino acid
ABC	ATP-binding cassette
ALD	adrenoleukodystrophy
amp^R	β-lactamase encoding gene, which confers resistance to ampicilline
Ams1	α-mannosidase
Ape1	aminopeptidase I
APG	autophagy (genes)
APS	ammonium persulfate
ARS	autonomously replicating sequence
ARP	actin-related protein(s)
Atg	autophagy-related
ATP	adenosine triphosphate
AUTO	autophagy
bp	base pairs
BSA	bovine serum albumin
Cdc	cell cycle
Ce	*Caenorhabditis elegans*
CEN	centromere sequence
C-terminal	carboxy-terminal
Cvt	cytoplasm-to-vacuole targeting
Da	Dalton
Dd	*Dictiostelium discoideum*
Dm	*Drosophila melanogaster*
DMSO	dimethyl sulfoxide
DNA	deoxyribonucleic acid
dNTP	2´-desoxynucleoside-5´-triphosphate
EDTA	ethylenediaminetetraacetatic acid
eGFP	enhanced green fluorescent protein
eIF2	eukaryotic initiation factor 2α
eYFP	enhanced yellow fluorescent protein
END	endosome-to-vacuole transport
ER	endoplasmatic reticulum
FM4-64	N-(3-triethylammoniumpropyl)-4-(p-diethylaminophenylhexatrienyl) pyridinium dibromide
G6PDH	glucose-6-phosphat-dehydrogenase

gsa	glucose-induced selective autophagy of peroxisomes (mutants)
HOPS	homotypic fusion and vacuole protein sorting
Hp	*Hansenula polymorpha*
Hs	*Homo sapiens*
Ig	immunoglobulin
ICL	isocitrate lyase
ICL1	gene encoding isocitrate lyase
kb	kilobase (1000 bp)
kDa	kilodalton
lacZ	gene encoding ß-galactosidase from *E. coli*
LEU2	gene encodig β-isopropylmalate dehydrogenase
MIPA	micropexophagy-specific membrane apparatus
Mm	*Mus musculus*
MNNG	N-methyl-N'-nitro-N-nitrosoguanidine
Mox	methanol oxidase
MPT	mitochondrial permeability transition
MU	Miller units
N-terminal	amino-terminal
OD	optical density
ONPG	o-nitrophenyl-β-D-galactopyranoside
ORF	open reading frame
ORI	origin of replication
PAS	pre-autophagosomal structure
paz	pexophagy zeocin-resistant (mutants)
PBD	peroxisome biogenesis disorder
PCD	programmed cell death
PCR	polymerase chain reaction
pdd	peroxisome degradation-deficient (mutants)
PEG	polyethylene glycol
PE	phosphatidyl ethanolamine
PEX	peroxisome biogenesis (genes)
PEXO	pexophagy
PI3K	phosphatidylinositol 3 phosphat kinase
PMSF	phenylmethylsulfonylfluoride
Pp	*Pichia pastoris*
PTS	peroxisomal targeting signal
PVDF	polyvinylidene fluoride

RE	restriction endonuclease
RNA	ribonucleic acid
RNase	ribonuclease
rpm	revolutions per minute
Sc	*Saccharomyces cerevisiae*
SDS	sodium dodecyl sulfate
SDS-PAGE	sodium dodecyl sulfate polyacrylamide gel electrophoresis
SNX	sorting nexin
SPO	sporulation
TEMED	N,N,N',N'-tetramethylethylenediamine
Tris	tris(hydroxymethyl)aminomethane
U	Unit
UBL	ubiquitin-like
URA3	gene encoding orotidine-5´-phosphate decarboxylase
VAC	vacuolar organization and/inheritance (genes)
VAM	vacuolar membrane (genes)
VPS	vacuolar protein sorting
WD	tryptophan and aspartic acid reach repeats
WIPI	WD-repeat protein interacting with phosphoinosides
X-gal	5-bromo-4-chloro-3-indolyl-β-D-galactopyranoside
Yl	*Yarrowia lipolytica*
YNB	yeast nitrogen base
YPD	yeast extract/peptone/dextrose

1 Introduction

1.1 Autophagy in eukaryotic cells

Living cells are able to detect environmental changes and convert them into a variety of anabolic and catabolic responses facilitating cell adaptation to altering conditions. For instance, adaptation to nutrient deprivation is favored by the recycling of cellular components through distinct degradation pathways which are necessary for cell maintenance. Eukaryotic cells possess two powerful hydrolytic machineries. A first one, the ubiquitin/proteasome pathway, occurs predominantly in the cytosol and maintains a continuous turnover of poly-ubiquitin tagged proteins. On the other hand, a large-scale degradation of bulk cytoplasm takes place in the lysosomes in mammals and plants and in the vacuoles in fungi. The mechanisms responsible for delivery of cytoplasmic cargo to the lysosome/vacuole are known collectively as autophagy and are shown to play an essential role in both uni- and multicellular organisms.

1.1.1 Modes of autophagy and autophagy-related degradation pathways

The word "autophagy" is derived from Greek *"auto"* meaning *self* and "*phagos"* that means *to eat*. In eukaryotic cells, two morphologically distinct modes of autophagy have been identified - microautophagy and macroautophagy (see **Fig. 1.1**). In microautophagy, portions of cytoplasm are sequestered by direct invagination of the lysosomal/vacuolar membrane and subsequently degraded by means of proteolytic enzymes (Marzella *et al.*, 1981; de Waal *et al.*, 1986). In mammalian cells, the morphology of microautophagy has not been well characterized yet. In *Saccharomyces cerevisiae*, a formation of a specialized tubular vacuolar membrane invagination, called an autophagic tube, has been described (Müller *et. al.*, 2000).

Macroautophagy is considered to be the major degradation route for turnover of cellular constituents. In this process, portions of cytoplasm are sequestered within double-membrane vesicles, termed autophagic vacuoles in mammalian cells and autophagosomes in yeasts (Mortimore *et al.*, 1989; Dunn, 1990; Baba *et al.*, 1994). Macroautophagy has been extensively characterized morphologically in both yeast and mammalian systems (for reviews, see Klionsky and Ohsumi, 1999; Stromhaug and Klionsky, 2001; Klionsky, 2005) and will be described in detail below.

Recently, a new lysosomal degradation pathway, called chaperon-mediated autophagy, has been observed in mammalian cells (reviewed in Majeski and Dice, 2004). During this process,

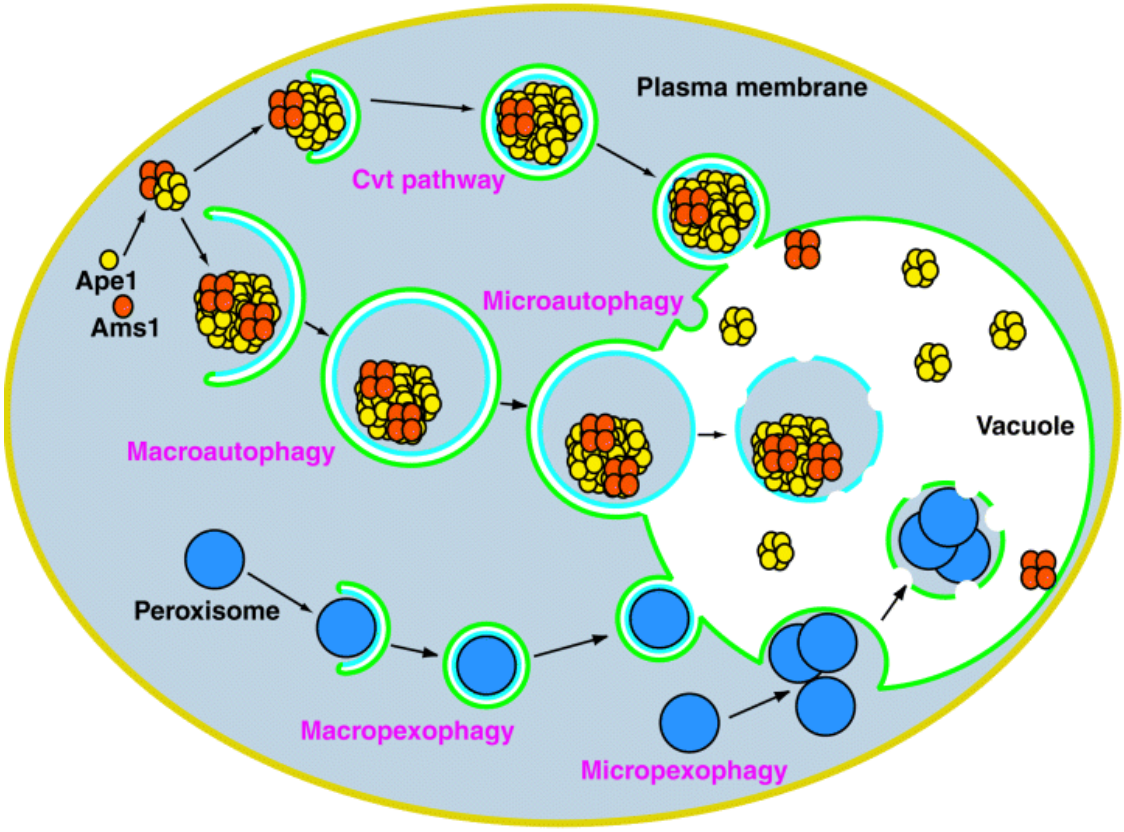

Figure 1.1 Schematic representation of the morphology of autophagy, pexophagy and the Cvt pathway in the yeast *S. cerevisiae* (from Stromhaug and Klionsky, 2001). The basic mechanism of macroautophagy, macropexophagy and the Cvt pathway is the sequestration of cargo material (bulk cytoplasm, peroxisomes or precursors of Ape1 and Ams1, respectively) by cytosolic double-membrane vesicles. Following completion, the sequestering vesicles target and fuse with the vacuole, releasing single-membrane vesicles within the lumen where they are subsequently degraded by vacuolar hydrolases. In microautophagy and micropexophagy, cytoplasm and peroxisomes are taken up directly at the vacuole surface. Abbreviations: Ape1, precursor of aminopeptidase I; Ams1, precursor of α-mannosidase.

cytosolic proteins with particular peptide sequence motifs are recognized by a complex of molecular chaperones and subsequently delivered to lysosomes for degradation. Thus, lysosomes, classically considered to be non-specific protein degradation systems, are able to selectively degrade intracellular proteins.

Although the term "autophagy" reflects cellular "cannibalism", this pathway may also serve a biosynthetic purpose. For example, autophagy in yeast overlaps with the biosynthetic cytoplasm-to-vacuole targeting (Cvt) pathway (**Fig. 1.1**) that transports aminopeptidase I (Ape1) and α-mannosidase (Ams1) to the vacuole (Klionsky *et al.*, 1992; Hutchins and Klionsky, 2001). Ape1 is synthesized as a precursor in the cytosol and rapidly oligomerizes into a dodecamer (Kim *et*

al., 1997). The dodecameric Ape1 precursors assemble into a larger complex termed the Cvt complex, which is then selectively enwrapped by a double-membrane forming a cytosolic vesicle. After fusion with vacuole, the inner vesicle is degraded in the lumen allowing release and maturation of precursor Ape1 (Baba *et al.*, 1997). Therefore, being topologically similar to macroautophagy, Cvt pathway fulfils another physiological function and proceeds constitutively during vegetative growth.

Autophagy was primary believed to be a non-selective bulk degradation process. However, some protein components required for autophagic uptake are also used in specific degradation processes involved in regulation of the organelle homeostasis. The levels of organellar proteins and organelles fluctuate depending on the current needs of the cell. In particular, cells synthesize specific organelles in response to changing environmental conditions. Conversely, organelles are specifically degraded when they become redundant or damaged (reviewed in Kim and Klionsky, 2000). The best examples of regulated organellar degradation are specific turnover of peroxisomes (pexophagy) and mitochondria (mitophagy). Pexophagy can be viewed as a multistage process which may occur in macroautophagic (macropexophagy) or microautophagic (micropexophagy) manner (**Fig. 1.1**). Moreover, it was also shown that selective peroxisome degradation morphologically at least partially overlaps with general autophagy (Scott and Klionsky, 1998; Hutchins et al., 1999). Detailed description of molecular mechanisms of pexophagy in different yeast species will be a subject of later discussion (see *Chapter 1.2.2*).

A morphological overview of autophagy-related processes in a yeast cell is shown schematically in **Fig. 1.1**.

1.1.2 Molecular machinery of autophagy

1.1.2.1 Genes associated with autophagy

While autophagy has been first described in mammalian cells, it has been the application of yeast genetics that allowed us to develop a molecular understanding of this process (reviewed in Ohsumi, 1999; Huang and Klionsky, 2002; Levine and Klionsky, 2004; Mariño and López-Otin, 2004). Most of autophagy-related genes were originally identified in the yeasts *S. cerevisiae* (Tsukada and Ohsumi, 1993; Thumm *et al.*, 1994), *Hansenula polymorpha* (Titorenko *et al.*, 1995) and *Pichia pastoris* (Tuttle and Dunn, 1995; Sakai *et al.*, 1998; Mukaiyama *et al.*, 2002). Subsequent discovery of a number of genes involved in autophagy in higher eukaryotes has been possible because of their homology with the corresponding yeast counterparts. There are also several genes involved in other intracellular transport processes, such as the Cvt route or vacuolar protein sorting (Vps), known to overlap with those functioning in the autophagic

pathway (Scott *et al.*, 1996; Klionsky, 1998). This has led to a confused situation in which a certain autophagy-related gene may have different names due to its involvement in distinct overlapping processes. Therefore, a unified nomenclature for yeast autophagy-related genes and proteins (*ATG* and Atg, respectively) has been established recently (Klionsky *et al.*, 2003). A brief summary of genes and corresponding proteins from yeasts and higher eukaryotes implicated in different stages of autophagy are included in the **Table 1.1**.

Table 1.1 Overview of autophagy-related genes from yeasts and higher eukaryotes (after Reggiori and Klionksy, 2002; Klionsky *et al.*, 2003). Abbreviations used for processes: AUTO, autophagy; CVT, cytoplasm-to-vacuole targeting; PEXO, pexophagy; SPO, sporulation; VAC, vacuolar organization and/or inheritance; VPS, vacuolar protein sorting.

Overview of autophagy-related genes from yeasts and higher eukaryotes

Gene designation		Organisms	Protein characteristics	Processes involved
Current	**Former**			
ATG1	*APG1/AUT3/PDD7/ GSA10/PAZ1/CVT10*	Sc, Pp, Hp, Ce, Dd	Serine/threonine protein kinase	AUTO, PEXO, CVT
ATG2	*APG2/AUT8/GSA11/PAZ7/SPO72*	Sc, Pp	Peripheral membrane protein, interacts with Atg9p	AUTO, PEXO, SPO
ATG3	*APG3/AUT1/GSA20*	Sc, Pp, Dm, Hs	E2-like protein, conjugates Atg8p to PE	AUTO, PEXO, VPS
ATG4	*ATG4/AUT2/PAZ8*	Sc, Pp, Dm	Cystein endopeptidase, cleaves Atg8p, mediates attachment of autophagosomes to microtubules	AUTO, VPS, Micropexophagy in Pp
ATG5	*APG5*	Sc, Dm	Atg12-conjugated protein	AUTO, SPO
ATG6	*ATG6/VPS30*	Sc, Ce, Dd, Mm, Hs	Component of the PIK3-kinase complexes I and II	AUTO, VPS
ATG7	*APG7/GSA7/PAZ12/CVT2*	Sc, Pp, At, Ce, Dd, Mm, Hs	E1-like protein, mediates the conjugation of Atg12p to Atg5p	AUTO, CVT, SPO, Micropexophagy in Pp
ATG8	*APG8/AUT7/PAZ2/CVT5*	Sc, Pp, Hp, Ce, Dd, Mm, Hs	Binds to Atg4p, mediates attachment of auto-phagosomes to microtubules	AUTO, PEXO,CVT, SPO
ATG9	*APG9/AUT9/GSA14/PAZ9/CVT7*	Sc, Pp, At	Integral membrane protein, interacts with Atg2p	AUTO, CVT, SPO, Micropexophagy in Pp

Overview of autophagy-related genes from yeasts and higher eukaryotes

Gene designation		Organisms	Protein characteristics	Processes involved
Current	**Former**			
ATG10	*APG10*	Sc, Ce, Mm	E2-like enzyme, conjugates Atg12p to Atg5p	AUTO, SPO
ATG11	*GSA9/PAZ6/PDD18/CVT9*	Sc, Pp, Hp	Peripheral membrane protein, involved in cargo recognition	PEXO, CVT, VPS
ATG12	*APG12*	Sc, Dd, Ce, At, Mm, Hs	Ubiquitin-like protein, conjugated to Atg5p	AUTO, VPS, SPO
ATG13	*APG13*	Sc	Hyperphosphorylated (in rich media) protein, interacts with Vac8p	AUTO, CVT, SPO
ATG14	*ATG14/CVT12*	Sc	Component of the PI3K complex I, required for organization of the pre-autophagosomal structure	AUTO
ATG15	*AUT5/CVT17*	Sc	Lipase, required for breakdown of intravacuolar vesicles	AUTO, CVT
ATG16	*APG16/PAZ3/CVT11*	Sc, Pp, Dd, Mm	Component of the Atg12-Atg5 protein complex	AUTO, CVT, SPO, Micropexophagy in Pp
ATG17	*APG17*	Sc	Probably involved in the Atg1-Atg13 interaction	AUTO
ATG18	*AUT10/GSA12/ CVT18*	Sc, Pp, Ce	PtdIns-3,5-biphosphate-binding protein, required for recycling of Atg9p	AUTO, PEXO, CVT, VAC
ATG19	*CVT19*	Sc	Cytoplasmatic protein, receptor of Ape1 and Ams1 proteins	CVT
ATG20	*CVT20/SNX42*	Sc	PX-domain-containing protein, binds to PtdIns-3-phosphate and Atg17 and Atg24	AUTO, CVT
ATG21	*CVT21/MAI1/HSV1*	Sc	PtdIns-3,5-biphosphate-binding protein	PEXO, CVT
ATG22	*AUT4*	Sc	Putative integral membrane protein, required for the	AUTO

Overview of autophagy-related genes from yeasts and higher eukaryotes

Gene designation		Organisms	Protein characteristics	Processes involved
Current	**Former**			
			breakdown of autophagic vesicles	
ATG23	*CVT23*	Sc	Peripheral membrane protein, molecular function unknown	AUTO, CVT
ATG24	*PAZ16/CVT13/SNX4*	Sc, Pp	Lipid-binding protein	AUTO, CVT, Micropexophagy in Pp
ATG25	*PDD4*	Hp	Coiled-coil protein, involved in macropexophagy	PEXO in Hp
ATG26	*UGT51/PAZ4*	Sc, Pp	Sterol glycosyltransferase with a GRAM-domain, required for micropexophagy	Micropexophagy in Pp
ATG27	*CVT24/ETF1*	Sc	PtdIns-3-phosphate-binding protein	CVT
ATG28	-	Pp	Coiled-coil protein, selectively involved in pexophagy, molecular function unknown	PEXO in Pp

Furthermore, there are a number of genes which mainly function in other cellular processes but also known to be required for autophagy. The additional genes involved in autophagy-related processes are listed in the **Table 1.2**.

Table 1.2 Overview of autophagy-related genes which also function in other intracellular membrane trafficking pathways (after Klionsky *et al.*, 2003). Abbreviation used for processes: AUTO, autophagy; CC, cell cycle; CHR, chromatin remodelling; CVT, cytoplasm-to-vacuole targeting; GLU, glucose metabolism; EXP, gene expression; HOPS, homotypic membrane fusion and vacuolar protein sorting; PB, peroxisome biogenesis; PEXO, pexophagy; SD, signal transduction; SPO, sporulation; VAC, vacuolar organization and/or inheritance; VPD, vacuolar protein degradation; VPS, vacuolar protein sorting.

Overview of autophagy-related genes which also function in other intracellular membrane trafficking pathways

Gene designations	Organisms	Protein characteristics	Processes involved
ARP5/6	Sc	Actin-related proteins, involved in chromatin remodeling, molecular function unknown	CHR, VPS
CCZ1/CVT16	Sc	Guanyl-nucleotide exchange factor, required for autophagic vacuolar fusion, interacts with Mon1p	AUTO, CVT, VAC
GCN1/PAZ10	Sc, Pp, Hs	Translational activator of GCN2 and GCN4 in response to starvation	EXP, micropexophagy in Pp
GCN2/AAS1/PAZ11	Sc, Pp, Hs	Protein kinase, phosphorylates eIF2α in response to starvation, derepression of GCN4	EXP, micropexophagy in Pp
GCN3/AAS2/PAZ5	Sc, Pp	Alpha subunit of the translation initiation factor eIF2B, positively regulates the GCN4 expression	EXP, micropexophagy in Pp
GCN4/AAS3/PAZ19	Sc, Pp, Hs	Transcriptional activator of amino acids biosynthetic genes in response to amino acids starvation	EXP, micropexophagy in Pp
HSV2 (YGR223c, homologous to *ATG18* and *ATG21*)	Sc, Hp, Hs	Phosphatidylinositol 3,5-bisphosphate-binding protein	unknown
MON1/AUT12	Sc	Protein required for fusion of Cvt-vesicles and autophagosomes with the vacuole, interacts with Ccz1p	AUTO, CVT
PEP1/VPS10	Sc	Transmembrane sorting receptor for multiple vacuolar hydrolases	VPS
PEP4/GSA15/PAZ14	Sc, Pp, Hp	Vacuolar proteinase A, required for posttranslational maturation of vacuolar proteinases	VPD, SPO, micropexophagy in Pp
PEX3	Hp	Peroxisomal membrane protein	PB, PEXO in Hp
PEX14	Hp	Peroxisomal membrane protein, a part of the PTS-receptor docking complex	PB, PEXO in Hp
SNF1/CAT1	Sc	AMP-activated serine/threonine-protein kinase, required for transcription of glucose-repressed genes, regulates *ATG1* and *ATG13* expression	GLU, SD, AUTO
TOR1/2	Sc	Protein kinases, subunits of the TOR-complexes, regulation of growth and cell cycle, regulates *ATG1* expression	CC, SD, AUTO

Overview of autophagy-related genes which also function in other intracellular membrane trafficking pathways

Gene designations	Organisms	Protein characteristics	Processes involved
TUP1/PDD2	Sc, Hp	General repressor of transcription, mediates glucose repression	SD, PEXO in Hp
VAC8/YEB3	Sc, Pp	Vacuolar membrane protein, interacts with Atg13p, required for homotypic vacuole fusion	AUTO, CVT, VAC
VPS15/VAC4/GSA19/ PAZ13/PDD19	Sc, Pp, Hp	Serine/threonine protein kinase, activates Vps34p	VPS, PEXO
VPS16/CVT15/VAM9	Sc	Required for homotypic vacuole fusion, molecular function unknown	VPS, VAC
VPS34/END12/PEP15/ PDD1	Sc, Hp	PI3K, forms a membrane-associated complex with Vps15p	VPS, PEXO, AUTO, VAC
VPS41/CVT8/VAM2	Sc	Component of the HOPS complex	VPS, VAC
VPS51/CVT22	Sc	Forms a tetramer with Vps52p, Vps53p and Vps54p, molecular function unknown	VPS

1.1.2.2 Basic steps of autophagy in yeasts

The autophagic route can be divided into several basic steps, such as signaling, autophagosome formation, vesicle targeting, docking and fusion with the vacuole. At each step, a certain functional subgroup of the *ATG* genes is involved. A brief description of these steps and associated components will be given below.

Induction of autophagy

There are three main signaling pathways known to be crucial for the development of an autophagic response. These include a Tor signaling pathway and Atg1 and Vps34/class III phosphatidylinositol 3-kinase (PI3K) complexes.

Tor (for: target of rapamycin) is a serine/threonine kinase, which coordinates different aspects of cell growth in response to changes in nutrient conditions (Cutler *et al.*, 1999; Schmelzle and Hall, 2000). Starvation, for instance, inhibits Tor activity, provoking various cellular responses, such as cell arrest in the early G1 phase, inhibition of protein synthesis, transcriptional changes and autophagy (Noda and Ohsumi, 1998). The possible mechanisms of the negative controlling of autophagy by Tor are discussed by Raught *et al.* (2001).

The second autophagy signaling pathway involves the Atg1p, a serine/threonine protein kinase which is a part a dynamic protein complex implied in triggering both the Cvt and autophagy routes (Scott *et al.*, 1996; Matsuura *et al.*, 1997; Straub *et al.*, 1997, see also **Fig. 1.2**). The composition of the Atg1 complex varies depending on nutrient conditions. Under nutrient-rich conditions, active Tor directly or indirectly causes the hyperphosphorylation of Atg13p, another component of the Atg1 complex (Funakoshi *et al.*, 1997). The highly phosphorylated form of Atg13p has a lower affinity for the Atg1p. This leads to the interaction of Atg1p with the Atg11/Cvt9 component, which possibly determines the use of the autophagic machinery in the selective Cvt pathway (Kim *et al.*, 2001). On the other hand, inhibition of Tor by starvation or rapamycin treatment results in partial dephosphorylation of Atg13p. This event promotes the Atg1-Atg13 interaction which subsequently triggers autophagy (Kamada *et al.*, 2000). Thus, Atg1p, Atg11p and Atg13p are probably involved in switching from the Cvt pathway to macroautophagy in response to nutrient deprivation, but molecular mechanisms underlying this process are still unknown. Other autophagy- or Cvt-related proteins, such as Atg17 and Vac8, are known to be associated with the Atg1 complex (Wang *et al.*, 1998; Scott *et al.*, 2000). However, physiological functions of these proteins remain to be elucidated.

The third type of molecular components required for the regulation of autophagy is the PI3K complex. The PI3Ks represent a family of enzymes implicated in diverse cellular processes, such as intracellular trafficking, proliferation and assembly of cytoskeletal elements (de Camilli *et al.*, 1996). In *S. cerevisiae*, only one PI3K, Vps34, has been shown to be involved in vacuolar protein sorting and autophagy (Herman and Emr, 1990; Schu *et al.*, 1993; Kihara *et al.*, 2001, see also **Fig. 1.2**). Furthermore, it was demonstrated that ScVps34p in association with a membrane-anchored protein kinase Vps15 (Stack *et al.*, 1993) can form two distinct functional complexes which are involved in a variety of membrane transport events. Complex I including Vps34p, Vps15p, Atg6/Vps30p and Atg14p is shown to be essential for autophagy, whereas complex II, composed of Vps34p, Vps15p, Atg6/Vps30p and Vps38p, controls vesicular transport from the Golgi to the vacuole (Kihara et al., 2001). It was also proposed, that the PI3K complex I may play a role in further autophagic events, such as vesicle nucleation, although its molecular mechanism is still unclear (Levine and Klionsky, 2004). Interestingly, a *H. polymorpha PDD1* gene product homologous to ScVps34p was found to be implied in the selective macroautophagic degradation of peroxisomes in this yeast species (Kiel *et al.*, 1999). These observations suggest that phosphoinositides may have various functions in the regulation of membrane traffic events.

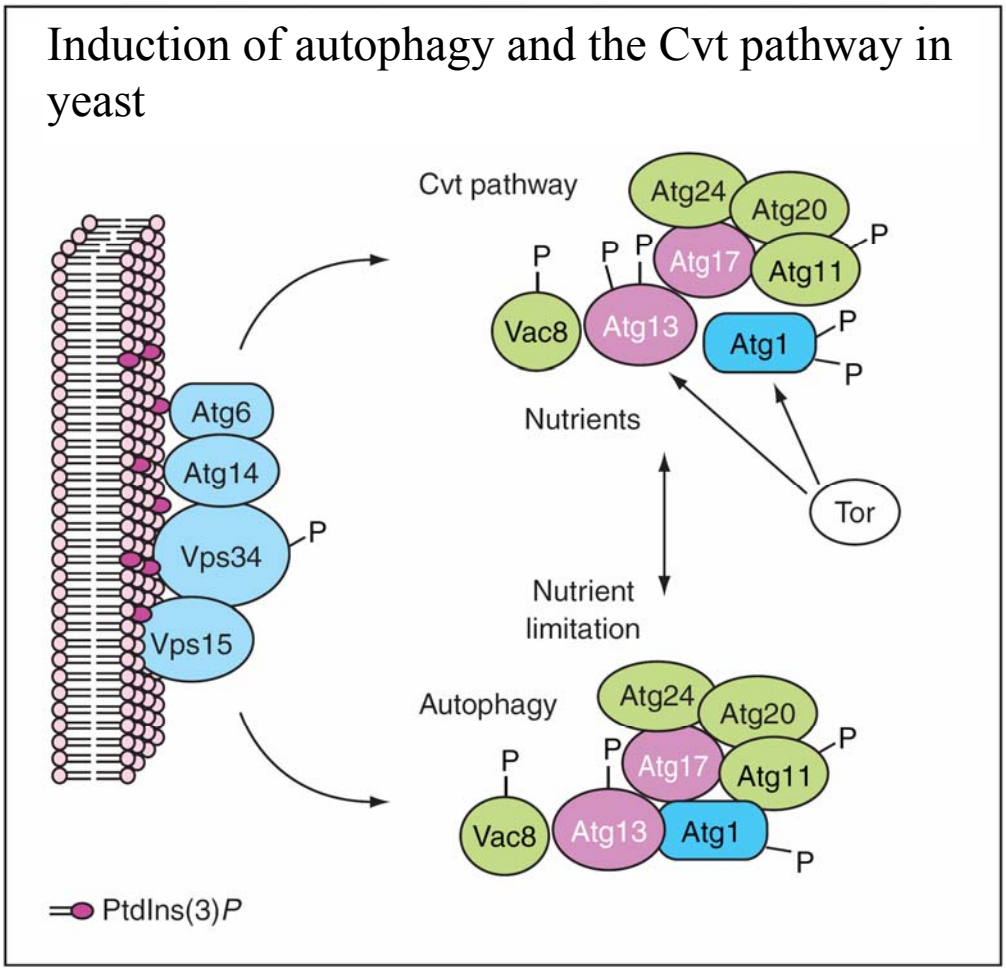

Figure 1.2 Regulation of induction and vesicular nucleation in autophagy and the Cvt pathway in yeast (after Klionsky, 2005).

In yeasts, two protein complexes are required for the induction of autophagy and the Cvt pathway. A first protein complex concerns the PI3K Vps34 and may function at the pre-autophagosomal membrane. A second putative complex consists of the Atg1 kinase and several other proteins and appears to be a downstream effector of Tor kinase. During nutrient-rich conditions, Tor kinase is active, Atg13p is hyperphosphorylated, and Atg1p is a part of a putative protein complex functioning in the Cvt pathway (upper complex). During starvation, activity of the Tor kinase is inhibited that, in turn, causes partial dephosphorylation of Atg13p and subsequent formation of an Atg1-Atg13 protein complex (lower complex) required for the course of autophagy. The Apg17p seems to participate in the stabilization of the Apg1-Apg13 complex. Other components, such as Vac8p, Atg11p, Atg20p and Atg24p, might by able to modulate the activities of Atg1p and Atg13p in order to favor one of the two pathways. The PI3K complex I, consisting of Vps34p, Vps15p, Atg6/Vps30p and Atg14p, is required for both the Cvt pathway and autophagy.

Autophagosome formation

After induction of autophagy, double-membrane vesicles, called autophagosomes, start to form in the cytosol resulting in the sequestration of cytoplasmic components (Baba *et al.*, 1994). This sequestration process involves a protein conjugation mechanism. In yeast, two ubiquitin-like (UBL) systems were shown to be essential for autophagosome formation (Ohsumi, 2001). Both systems are similar to those described for the proteasomal degradation, and include three different enzymes: ubiquitin-activating enzyme (E1), ubiquitin-conjugating enzyme (E2) and ubiquitin-protein ligase (E3) (see **Fig. 1.3**).

A first UBL system found to be essential for macroautophagy implies a participation of the Atg12-Atg5 protein conjugate (Mizushima *et al.*, 1998). In this system, Atg12p is covalently attached to the Atg5p through a COOH-terminal glycine and an internal lysine residue, respectively. This process requires action of the Atg7p, which is homologous to the E1-family of enzymes (Kim *et al.*, 1999), and the Atg10p, which functions as a protein-conjugating enzyme (Shintani *et al.*, 1999). A third protein, Atg16, binds to the conjugated Atg5p and dimerizes to link a pair of Atg12-Atg5 conjugates (**Fig. 1.3**). The Atg12-Atg5 UBL system is shown to be constitutively active and is required for formation of sequestering vesicles in both the Cvt and macroautophagy pathways (George *et al.*, 2000).

Atg8p, a second ubiquitin-like protein involved in autophagy, is conjugated to phosphatidyl-ethanolamine by a serial action of three autophagy proteins, Atg4p, Atg7p and Atg3p (Ichimura *et al.*, 2000; see also **Fig. 1.3** for details). This unusual lipid-protein conjugate was revealed to be essential for the completion of autophagosomes. Atg8p is the first autophagy protein found to be localized to autophagosomes during starvation making it a suitable marker to monitor the autophagosome formation (Kirisako *et al.*, 1999). In addition, recent observations have shown that Atg8p is also essential for macropexophagy in *H. polymorpha* (Monastyrska *et al.*, 2005). These data indicate that Atg8 has an essential role in both selective and non-selective autophagy-related degradation processes.

One of the most intriguing questions concerns the origin of the autophagosomal membrane. Autophagosomes do not appear to bud off from pre-existing organelles, but is thought to be formed *de novo* (for review, see Noda *et al.*, 2002; Wang and Klionsky, 2003). In mammalian cells, a ribosome-free region of the endoplasmatic reticulum has been proposed to be a source of membranes during autophagosome formation (Dunn, 1990; Mizushima *et al.*, 2002). In yeast, a novel perivacuolar structure, called PAS (pre-autophagosomal structure), has been detected (Suzuki *et al.*, 2001). Several autophagy-related proteins, such as Atg1p, Atg2p, Atg9p, Atg11p, Atg18p, and most components of the UBL conjugation systems were found to co-localize, at

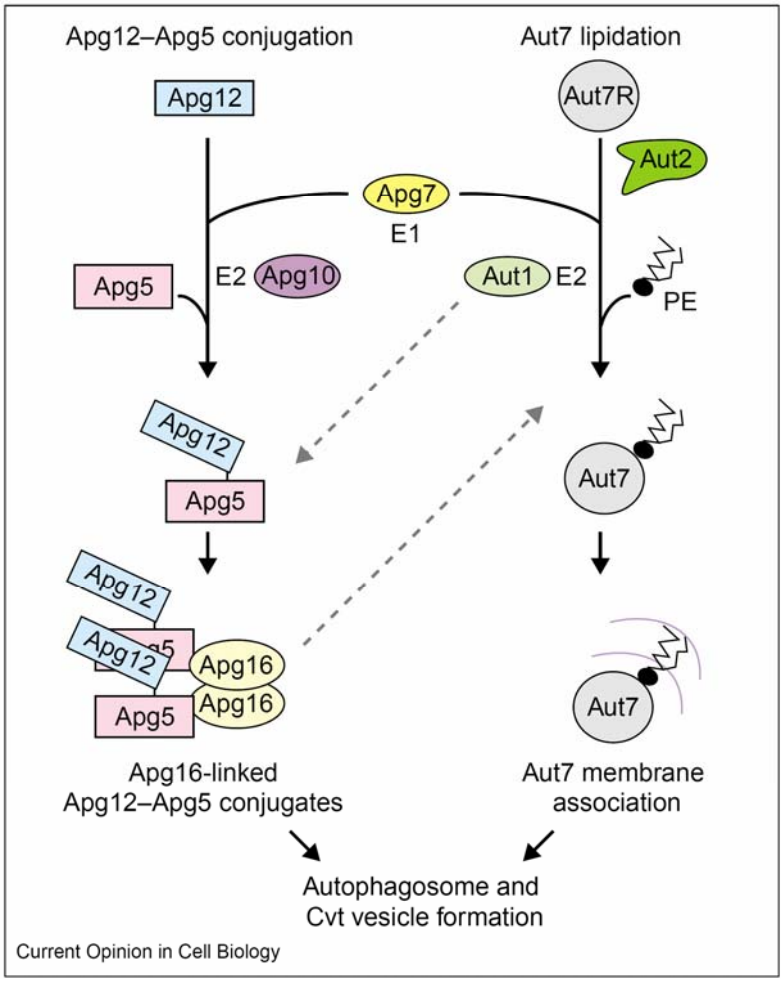

Figure 1.3. Two yeast conjugation systems essential for vesicle formation during autophagy and the Cvt pathway (from Khalfan and Klionsky, 2002).

In the first system, Apg12p is covalently attached to Apg5p to form Apg12-Apg5 protein conjugates. The Apg12-Apg5 interaction is controlled by a serial action of Apg7p (E1-enzyme) and Apg10p (E2-enzyme). Apg7p hydrolyzes ATP and activates Apg12 through formation of a thioester bond. The activated Atg12 is then transferred to Atg10, which in turn transfers Atg12 to Atg5. The Apg12-Apg5 conjugates can interact with Apg16, a small protein with a coiled-coil region which facilitates its oligomerization. The Apg16-linked Apg12-Apg5 multiple conjugates are directly required for vesicle formation in autophagy and the Cvt pathway.

The second conjugation system involves lipidation and subsequent membrane association of the Aut7p. Aut7p is first proteolytically processed by the protease Aut2. Then, the E1-enzyme Apg7 activates processed Aut7p and transfers it to the Aut1p (functions like E2-and E3-enzymes). Aut1 finally conjugates Aut7 to phosphatidylethanolamine (PE) resulting in a tight association of Aut7p to the membrane. Membrane-associated Aut7-PE functions in the formation of autophagosomes and Cvt vesicles. Apg5 = Atg5, Apg7 = Atg7, Apg10 = Atg10, Apg12 = Atg12, Apg16 = Atg16, Aut1 = Atg3, Aut2 = Atg4, Aut7 = Atg8.

least transiently, in this new structure (Kim *et al.*, 2002). These data support the hypothesis that PAS may act as a site of vesicle development during both autophagy and the Cvt pathway. However, a detailed mechanism of the autophagosome formation is waiting to be elucidated.

Vesicle fusion and degradation

Following targeting to the vacuole, the outer membrane of the autophagosome fuses with the vacuole membrane. In yeast, the autophagic membrane fusion implies several components shown to be involved in other types of intracellular vesicular transport events. The molecular machinery, required for this process, includes SNARE proteins (Ishihara *et al.*, 2001), regulatory factors, such as Rab GTP-ases (Wurmser *et al.*, 2000), and the class C of the Vps proteins, also known as the HOPS (for: homotypic fusion and vacuole protein sorting) complex (Sato *et al.*, 2000). Nevertheless, specific proteins playing a crucial role in the autophagosome-vacuole fusion also exist. A detailed overview of these components is given by Kim and Klionsky (2000).

Fusion of the autophagosome with the vacuole allows release of the interior single-membrane vesicles, termed autophagic bodies, into the vacuolar lumen. Autophagic bodies are then broken down by vacuolar hydrolases, and yeast mutants deficient in vacuolar hydrolase activity were shown to accumulate the autophagic bodies within the vacuole (Takeshige *et al.*, 1992). The degradation of lumenal vesicles is pH-dependent and requires the action of at least two proteases (mainly proteinases A and B) and probably lipases (a putative lipase Atg15/Cvt17) (Kim and Klionsky, 2000; Reggiori and Klionsky, 2002). However, it is not clear whether the *ATG15* gene product directly cleaves intravacuolar vesicles. To label membranes destined for degradation, the lipid bilayer composition of autophagic bodies should be different from that of the delimiting vacuolar membrane. Therefore, autophagic bodies may represent a distinct population of subvacuolar vesicles that are degraded within the vacuolar lumen.

1.1.3 Physiological significance of autophagy

From the evolutionary point of view, autophagy originally arose as a mechanism to protect unicellular organisms against starvation or other forms of environmental stress. However, in multicellular organisms, roles of this degradative pathway appear to be more diverse than in lower eukaryotes. A number of comprehensive reviews have covered many aspects of physiological functions of autophagy in worms, insects and especially in mammals, including human (Klionsky and Emr, 2000; Levine and Klionsky, 2004; Mariño and López-Otin, 2004; Shintani and Klionsky, 2004). The most interesting examples of the roles of autophagy are discussed below.

1.1.3.1 Autophagy in programmed cell death

In multicellular organisms, programmed cell death (PCD) is an active process by which a cell or class of cells is eliminated from tissue during both normal development and pathological events (reviewed in Bursch *et al.*, 2000). A "classical" apoptosis, or Type I programmed cell death, is characterized by DNA fragmentation, condensation of cytoplasm and its fragmentation into apoptotic bodies, followed by degradation of the dying cell. In contrast, autophagic, or Type II, cell death involves accumulation of autophagic vacuoles, containing Golgi apparatus, polyribosomes and the endoplasmatic material, in the cytoplasm of dying cells. Remarkably, skeletal elements seem to be largely preserved during the second process, presumably because of their role in autophagocytosis (Ogier-Denis and Codogno, 2003).

The correlation between the autophagic and apoptotic processes is still poorly understood. An excellent example of apoptotic cell death involving autophagic events can be found in insect metamorphosis. Recent investigations of *Drosophila* dying salivary glands have shown that the destruction of useless larval tissues is associated with apoptotic features such as caspase activation and DNA fragmentation. On the other hand, massive accumulation of lysosomal vesicles was also observed in cells fated to die (Baechrecke, 2003). These data illustrate the complexity in elucidation of independent roles of autophagy and apoptosis during the developmental cell death in insects.

The connection between type I and type II PCD is complicated by the sharing of signaling components. For example, it was reported that some apoptosis-related regulatory factors (i.e. death-associated protein kinases and the tumor necrosis factor-related apoptosis-inducing ligand) are implicated in induction of caspase activity and the autophagic PCD (Shintani and Klionsky, 2004). On the other hand, there are also multiple evidences of caspase-independent type II cell

death (Mariño and López-Otin, 2004). These facts underline the hypothesis considering autophagic cell death to be an alternative death program triggered when apoptosis is defective. From this point of view, both types of PCD appear to be distinct processes represented different shades of physiological cell death.

1.1.3.2 Autophagy in human pathology

There are many lines of evidence which connect autophagy to human diseases. It was shown that several human cardiomyopathies and hereditary skeletal myopathies are associated with the accumulation of multiple vacuoles of autophagic and lysosomal origin (Mariño and López-Otin, 2004). The accumulation of autophagic vesicles has been also observed during course of many neurodegenerative disorders, such as Alzheimer's, Huntington's and Parkinson's diseases (reviewed in Larsen and Sulzer, 2002). However, as with myopathies, it is not known whether these molecular events are resulted from the induction of autophagy or are simply a consequent of much more complex pathological processes. Interestingly, increasing evidences indicate that autophagy may also play a neuroprotective role by facilitating the removal of newly formed mutant protein aggregates characteristic for different neurodegenerative disorders. It may be possible, that autophagy is initially activated as a "housekeeping" mechanism to facilitate the proteasome machinery, but it finally contributes to neuropathology. Genetic studies of *ATG* null mutants are required to solve this controversy.

Another issue of interest involves a potential link between autophagy and carcinogenesis (discussed in Ogier-Denis and Codogno, 2003). In theory, the process of autophagy may protect against cancer by sequestering damaged organelles, increasing protein catabolism and promote autophagic cell death. Alternatively, autophagy may contribute to cancer by allowing the survival of transformed cells under nutrient-limiting conditions. Recent advances in understanding of molecular mechanisms of autophagy support mainly the first hypothesis. It is generally believed that autophagic degradation is downregulated in cancer cells. Cell lined derived from hepatic, pancreatic and breast carcinomas were shown to exhibit low autophagic activity when compared to their normal counterparts. Otherwise, autophagy may also act as a tumor suppressor. Probably, the best example illustrating genetic link between these two processes is a tumor suppressor gene *beclin-1*, a mammalian homolog of the yeast autophagy gene *ATG6/VPS30* (Liang *et al.*, 1999). It was demonstrated, that beclin 1 promoted autophagy in autophagy-defective *atg6* yeast mutants and in human MCF7 breast carcinoma cells. The autophagy-promoting activity of beclin 1 was associated with inhibition of MCF7 cellular proliferation and *in vitro* carconigenesis. Furthermore, protein expression experiments revealed

high levels of the endogenous beclin 1expression in normal human cells. In contrast, tumor cell lines showed defective expression of this protein. These observations suggest a possible correlation between the autophagic potential of cancer cells and the expression levels of different autophagy-related genes. Development of drugs which could target the signal transduction elements of the autophagic pathway would be of potential interest for molecular therapy of cancer.

1.1.3.3 Selective autophagy of organelles

Bulk autophagic degradation is generally believed to be important for turnover of cellular components under different physiological and pathological conditions. However, autophagy may also play an essential homeostatic function performing selective degradation of organelles. In general, maintenance of organelles is energetically costly for a cell. Organelles, like peroxisomes or mitochondria, are specifically degraded via an autophagy-like process when they become damaged or are no longer needed. There are two examples of regulated organellar degradation – pexophagy and mitophagy (briefly reviewed in Scott and Klionsky, 1998). Pexophagy, or selective degradation of peroxisomes, involves uptake of the organelles by additional membranes or specific vacuolar membrane invaginations following their degradation by the vacuole/lysosome (for review, see Dunn *et al.*, 2005). This process has been shown to occur in both yeast and mammalian cells. The molecular aspects of pexophagy in yeasts will be discussed below (see *Chapter 1.2.2*).

Autophagy may also contribute to the regulation of mitochondria maintenance. As with peroxisomes, mitochondrial levels fluctuate in response to growth conditions (Scott and Klionsky, 1998). Mitochondria were occasionally seen inside autophagic bodies, indicating that these organelles can be degraded through macroautophagy (Takeshige *et al.*, 1992). It was also revealed, that certain types of stress may induce a loss of integrity of the inner and outer mitochondrial membranes resulting in depolarization, a process termed the mitochondrial permeability transition (MPT). Mitochondrial dysfunction because of MPT is a pathological process, and it usually leads to a cell death via apoptosis and necrosis (reviewed by Kim and Lemasters, 2003). It has been observed, that increasing number of MPT events within a mammalian cell leads to selective mitochondrial degradation in an autophagy-like manner (Elmore *et al.*, 2001). Thus, mitophagy can protect cells against oxidative damage that could result from a loss of mitochondrial integrity without triggering apoptosis.

1.1.4 Conserved character of autophagy

Autophagy has been observed in all eukaryotic cells including plants, yeasts and mammals, indicating a widespread occurrence of this evolutionary conserved pathway. Similarly, molecular machinery required for autophagic degradation appears to be common for both uni- and multicellular organisms. In yeast, 28 *ATG* genes which have exclusive role in autophagy and autophagy-related processes have been identified so far, and at least 40 other genes have been implicated in these events (Klionsky, 2003; see also **Tables 1.1 and 1.2**). Most of the yeast *ATG* genes have candidate homologs in higher eukaryotes, although not for all of them their autophagy-related functions were experimentally proved. On the other hand, studies of already known *ATG* orthologs in higher eukaryotes have revealed essential roles of autophagy in many aspects of development, stress-induced adaptation, aging, cell death and growth control (Levine and Klionsky, 2004). For example, a component of the autophagy induction complex, the serine-threonine kinase Atg1, is important for autophagy and development in *Caenorabditis elegans* and *Dictyostelium*; a putative homolog of Apg1p in mouse, Unc51, is shown to be required for normal neuronal elongation (Tomoda *et al.*, 1999). A component of the PI3K complex, Atg6p, in addition to its tumor suppression function, is also known to be involved in development in *C. elegans* and mice, and target disruption of the mouse *beclin1* results in early embryonic lethality (Yue *et al.*, 2003). Mammalian counterparts of the yeast Atg5-Atg12 conjugation system have been identified suggesting their conserved character among eukaryotes (Mizushima *et al.*, 1998). Furthermore, it has been reported, that *ATG* genes are essential for the life span extension in *C. elegans* (Melendez *et al.*, 2003). Finally, identification of the mammalian protein ASP (apoptosis-specific protein) which displays a high level of similarity to its yeast Atg5 counterpart provides an additional molecular link between apoptosis and autophagy (Hammond *et al.*, 1998).

It is also important to consider possible differences between autophagy and autophagy-related processes in yeasts and higher eukaryotes. Firstly, as already mentioned above, some components of the mammalian autophagic machinery may function in cellular pathways which differ from autophagy. Secondly, it also seems likely that in higher eukaryotes molecular functions of many yeast *ATG* genes are executed by genes with no apparent structural homology to the appropriate yeast counterparts. Lastly, functional redundancy as well as functional divergence has been observed for some autophagy counterparts in higher eukaryotes (Levine and Klionsky, 2004). For an example of functional redundancy, two *Drosophila ATG4* homologues appear to exist, and both of them can complement defects in autophagy in the yeast *atg4* mutant. As an example of functional divergence, there are multiple mammalian homologues to the yeast

Atg8p, although only one of these proteins may function in autophagy in each organism. So, the molecular machinery of autophagy in higher eukaryotes is still poorly understood and physiological functions of these and many other proteins are waiting to be elucidated.

1.2 Peroxisomes as cellular organelles

Compartmentalization of biochemical pathways is a most characteristic feature of eukaryotic cellular metabolism. Apart from various kinds of endocytotic vesicles, which appear to have variable protein compositions, peroxisomes are the last class of "true" cellular organelles discovered by Rhodin (1954). Originally classified as microbodies, these organelles became a biochemical definition as peroxisomes due to the pioneer studies of Christian de Duve and his colleagues (de Duve and Baudhuin, 1966). In the following chapter, morphological features, physiological functions and principles of turnover of peroxisomes will be discussed.

1.2.1 Morphology and functions of peroxisomes

Peroxisomes are almost ubiquitous eukaryotic cellular organelles and, together with the related glyoxysomes of plants and glycosomes of trypanosomes, constitute a so-called microbody family (for reviews, see Lazarow and Kunau, 1997; Michels *et al.*, 2005). These organelles are surrounded by a single membrane that encloses a fine granular matrix and measure up to 1 μm in diameter. Peroxisomes are metabolic organelles and typically contain enzymes that are involved in lipid metabolism, such as hydrogen peroxide (H_2O_2)-producing oxidases, and the enzyme catalase, which converts H_2O_2 to water and O_2 (van den Bosch *et al.*, 1992). Fundamental functions of human peroxisomes are β-oxidation of fatty acids, biosynthesis of cholesterol, bile acids and ether-based lipids (Parsons *et al.*, 2001). In yeasts, peroxisomes are the sites of fatty acids and methanol oxidation and, therefore, are required for cell growth on these compounds as sole carbon sources (van den Bosch *et al.*, 1992; Veenhuis and Harder, 1988). Biosynthesis of some secondary metabolites, such as β-lactam antibiotic penicillin, by filamentous fungi was also shown to take place in these organelles (Müller *et al.*, 1992). Thus, despite their simple morphology, peroxisomes display remarkable functional diversity that widely varies among different species.

The importance of human peroxisomes is well illustrated by the existence of numerous diseases linked with both peroxisomal dysfunction and lack of the organelles (reviewed in Fujiki, 1997; Gould and Valle, 2000; Wanders and Waterham, 2005). The peroxisomal disorders are usually subdivided into two main subgroups: the peroxisome biogenesis disorders (PBDs) and the single

peroxisomal enzyme deficiencies. The PBD group is comprised of four different disorders including Zellweger syndrome, neonatal adrenoleukodystrophy, infantile Refsum's disease and rhizomelic chondrodysplasia punctata. Recent studies have shown that the PBD group is genetically heterogenous with at least 13 distinct linkage groups as concluded from complementation analysis. The genes responsible for all these complementation groups have been already identified which makes molecular diagnostics of PBD patients possible (Shimozawa *et al.*, 2005).

The second group of peroxisomal disorders is characterized by morphologically normal peroxisomes but deficiencies in single peroxisomal enzymes. This group includes the most common X-linked adrenoleukodystrophy (caused by impairment of a peroxisomal membrane protein, termed ALDP), deficiency of β-oxidation enzymes, peroxisomal catalase, etc. Remarkably, the ALD protein was found to possess a significant homology to the ATP-binding cassette (ABC) membrane transporter superfamily (Aubourg, 1994). In general, ABC-transporters constitute a family of large membrane proteins which are able to transport a variety of compounds through biological membranes against steep concentration gradients and at the cost of ATP-hydrolysis. The available outline of human genome contains 48 ABC genes, and the association with human diseases have been shown for 14 of them (Borst and Elferink, 2002). Based on the observations in yeast, peroxisomal ABC-transporters were suggested to mediate the transport of fatty acids or enzymes required for β-oxidation into the peroxisomal matrix. Defects in transporters functioning cause inability of these compounds to cross the peroxisomal membrane, which, in turn, may result in pathological progression. Therefore, studies on peroxisomal integrity and function have also high medical relevance.

1.2.2 Peroxisomal homeostasis

Peroxisomes are dynamic organelles which can be induced or turned over in response to extracellular signals in both yeasts and mammals. The steady-state level (homeostasis) of peroxisomes in any eukaryotic cell is tightly controlled by the balance between the biogenesis and degradation of these organelles. Recent achievements in studies on the molecular aspects of peroxisomal homeostasis are highlighted below.

1.2.2.1 Biogenesis of peroxisomes

Peroxisome biogenesis conceptually consists of (i) formation of the peroxisomal membrane, (ii) import of proteins into the peroxisomal matrix, and (iii) proliferation of the organelles. Combined genetic and biochemical approaches led to the identification of 32 proteins, so-called peroxins, which are remarkably conserved and appear to be required for the biogenesis of peroxisomes in both yeasts and higher eukaryotes (for review, see Heiland and Erdmann, 2005). Some of the peroxins are responsible for the division and inheritance of peroxisomes, however, most of them were shown to be implicated in the topogenesis of peroxisomal components. It is generally known, that peroxisomal membrane and matrix proteins are synthesized on free ribosomes in the cytosol and are post-translationally imported into pre-existing organelles (Lazarow and Fujiki, 1985). The sorting of peroxisomal matrix proteins is now rather well understood, and became a subject of numerous reviews (Subramani, 1998; Subramani *et al.*, 2000; Kunau *et al.*, 2001; Purdue and Lazarow, 2001; Gould and Collins, 2002; Eckert and Erdmann, 2003). To date, two major peroxisomal targeting signals (PTSs), acting in convert with their specific receptors, have been identified. The most common peroxisomal targeting signal is a PTS1. This signal occurs precisely at the carboxyl terminus of a protein and has been defined by the consensus tripeptide sequence (SKL or its derivates). In contrast, the second peroxisomal targeting signal, PTS2, is a conserved N-terminal nonapeptide (R/KL/V/I(X)$_5$H/QL/A) used by a smaller subset of peroxisomal matrix proteins. Nevertheless, existence of other PTSs is also suggested (Karpichev et al., Gunkel *et al.*, 2004; Petriv *et al.*, 2004). Peroxisomal targeting signals 1 and 2 are recognized by cytosolic receptors Pex5p and Pex7p, respectively. Both receptors bind their cargo proteins in the cytosol, deliver them to the docking and translocation sites at the peroxisomal membrane and then shuttle back to the cytosol (Dodt and Gould, 1996; Klei and Veenhuis, 1996). The molecular machinery required for the sorting of peroxisomal membrane proteins is still poorly understood. The peroxisomal membrane targeting signals (mPTS) characterized so far are clearly distinct from PTS1 and PTS2 and has been shown to possess at least part of putative transmembrane segments (Baerends *et al.*, 2000).

The current knowledge concerning organization of the peroxisomal import machinery is summarized by Heiland and Erdmann (2005). The molecular network of peroxin-peroxin interactions includes the receptor-docking complex (Pex13p, Pex14p, Pex17p), the RING-finger complex (Pex2p, Pex10p, Pex12p), the ubiquitin-conjugating complex (Pex4p, Pex22p), the AAA+ proteins (Pex1p, Pex6p) and their membrane anchors (Pex15p, Pex26p). However, the whole picture is not complete, and it is still not clear how folded and even oligomeric proteins are exactly transported across the peroxisomal membrane. Recently, a new model for the

peroxisomal protein import machinery has been developed (Erdmann and Schliebs, 2005). According to this model, the translocation of proteins across the peroxisomal membrane requires a specific protein-conducting channel, called a transient pore, that assembles after the docking of the receptor-cargo complex and is disassembled after translocation is complete. Thus, the transient pore is a short-lived protein assembly which at the same time should be flexible and large enough to allow the translocation of completely folded proteins of varying sizes. Another interesting point of this model is a suggestion that the cargo-loaded import receptor inserts into the peroxisomal membrane and therefore becomes an integral part of the translocation apparatus. Nevertheless, it is so far not known, whether peroxisomal proteins indeed utilize a channel complex or whether they are translocated into peroxisomes via some sort of endocytotic events. Future studies will hopefully tell us more about molecular features distinguishing the peroxisomal translocation machinery from the well-characterized translocons of other organelles. Another exciting question concerns the cellular origin of the peroxisomal membrane. Originally, it was assumed that peroxisomes developed by budding from the endoplasmatic reticulum (ER) (de Duve and Baudhuin, 1966). Since 1985, the "growth and division" model of Lazarow and Fujiki has been broadly accepted (Lazarow and Fujiki, 1985). According to this model, peroxisomes are autonomous organelles formed by division and fission of pre-existing ones after the import of newly synthesized proteins from the cytosol. However, more recent observations support involvement of the ER or other kinds of endomembranes in the peroxisome formation (Titorenko and Rachubinski, 1998; Tabak *et al.*, 2003, Hoepfner *et al.*, 2005). This data implies existence of specific mechanisms which make peroxisomes competent for the import of a defined set of proteins and which ensure their self-propagation. A challenge for the future will be to isolate the pre-peroxisomal membranes and to identify the associated proteins and protein complexes. This, in turn, would provide experimental tools for studying the selective import competency of these organelles.

Another important area of recent studies on peroxisomal biogenesis is a rapidly expanding identification of homologues human genes implicated in this process. Characterization of well-conserved *PEX* (peroxisome assembly) genes of several yeast species has promoted the search for human orthologues in expressed sequence tag libraries (Kunau, 1998). To date, 16 human *PEX* genes are known to be essential for peroxisome biogenesis, multiplication and inheritance; mutations in 13 of them were found to be the cause of PBDs (Gould and Valle, 2000; Shimozawa *et al.*, 2005). This observation strongly supports the view that the basic mechanisms of peroxisomal biogenesis are conserved from yeast to man.

1.2.2.2 Degradation of peroxisomes

Redundant, damaged or non-functional peroxisomes are degraded by a specific autophagy-related process, called pexophagy. Yeasts were proven to be the best model organisms to study this process. In yeasts, peroxisomes can be highly induced during growth of cells in media containing specific carbon and/or nitrogen sources (e.g., oleic acid, methanol, alkanes, or primary amines). Conversely, these organelles are rapidly degraded if preferred carbon sources such as glucose and/or ethanol become available (for review, see Veenhuis *et al.*, 2000; Dunn *et al.*, 2005). Thus, turnover of yeast peroxisomes may be easily manipulated just by changing the carbon source.

Degradation of peroxisomes in methylotropic yeasts

Selective autophagic degradation of peroxisomes was first demonstrated in methylotrophic yeasts, such as *Hansenula polymorpha*, *Pichia pastoris*, *Candida boidinii* and *Pichia methanolica* (Veenhuis *et al.*, 1983; Hill *et al.*, 1985; Tuttle *et al.*, 1993; Kulachkovsky *et al.*, 1997). Methanol-grown cells of these yeast species typically contain several large peroxisomes that harbor key enzymes of methanol metabolism (alcohol oxidase, dihydroxyaceton synthase and catalase). Upon a shift of methanol-grown cells into fresh glucose- or ethanol-containing media, the peroxisomal population becomes redundant for the cell, and, therefore, is selectively degraded by uptake in the vacuole. An additional advantage of the peroxisomes of methylotrophic yeasts is their unusually large size upon proliferation. When grown in a methanol-limited chemostat at low dilution rates, up to 80% of the total cytoplasmic volume of the cell may be occupied with peroxisomes (Veenhuis *et al.*, 2000). This fact facilitates a direct microscopic observation of the organelles that, in turn, allow a high-quality ultrastructural analysis of peroxisomal turnover.

To date, two main modes of pexophagy in methylotrophic yeasts have been described: macropexophagy and micropexophagy (Scott and Klionsky, 1998; Veenhuis *et al.*, 2000; Kiel and Veenhuis, 2003). Both processes are morphologically well understood and were shown to be topologically similar to macro- and microautophagy, respectively (see *Chapter 1.1.1*).

Macropexophagy was first characterized in methanol-grown *H. polymorpha* cells subjected to the carbon catabolite-induced inactivation through glucose or ethanol (Veenhuis *et al.*, 1983). Under these conditions, large mature peroxisomes were specifically sequestered by several (from 2 to up to 12) membranous layers and subsequently degraded in the vacuole (see **Fig. 1.4A**). Remarkably, upon induction of macroautophagy, a single or very few organelles were shown to escape the degradation process (discussed in detail in Kiel *et al.*, 2003). The maintenance of at

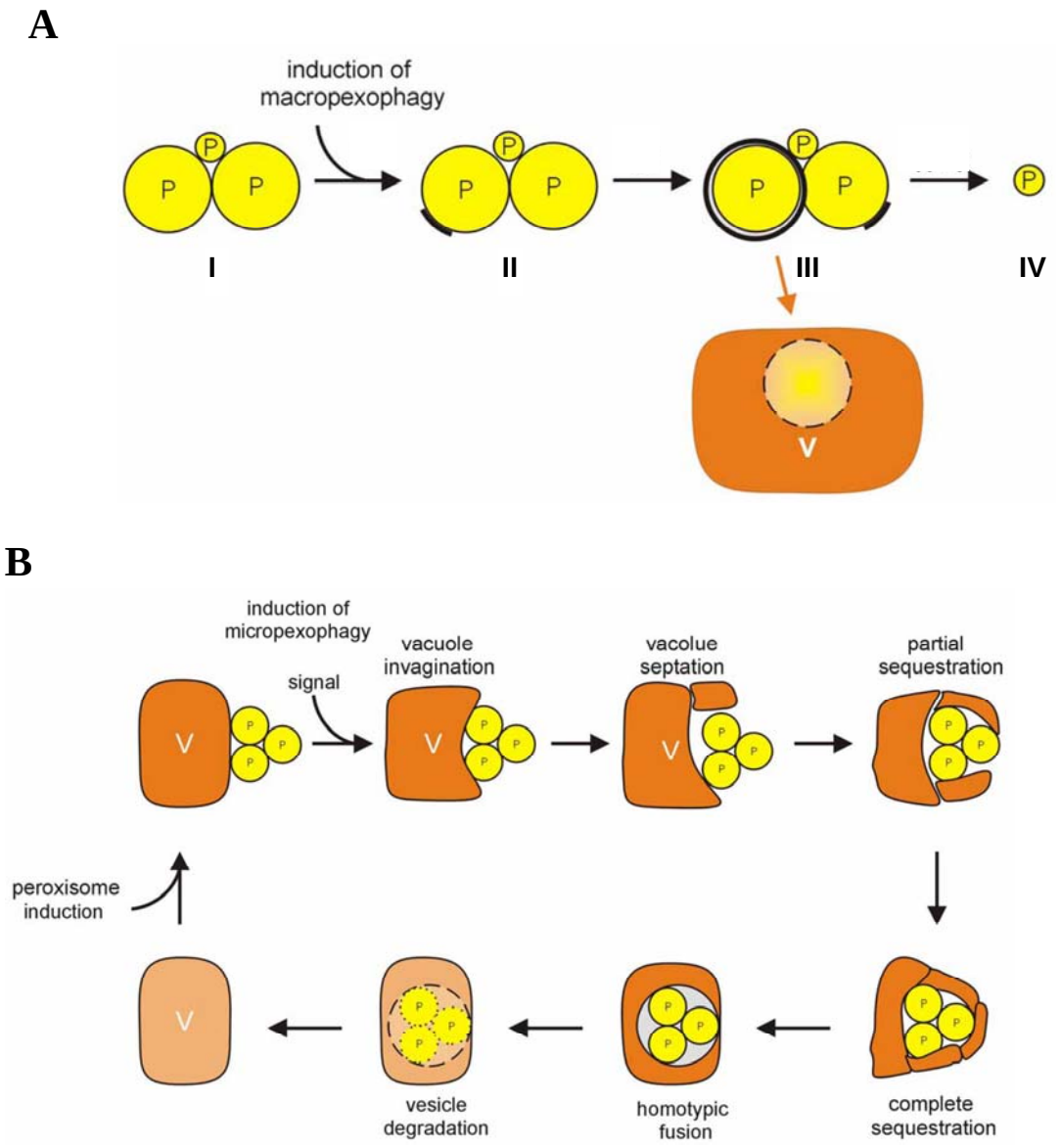

Figure 1.4 Divergent modes of pexophagy in methylotrophic yeasts (from Leão *et al.*, 2003).

A: Macropexophagy in *H. polymorpha*. Methanol-grown *H. polymorpha* cells contain some large peroxisomes (stage I). Upon a shift of these cells into glucose-containing medium (step II), macropexophagy starts with sequestration of a single import-incompetent organelle. After complete sequestration, this organelle fuses with the vacuole and is degraded by vacuolar hydrolases (stage III). Subsequently, other import-incompetent peroxisomes are sequestrated and degraded in the same way, till only the import-competent one remain (stage IV). P, peroxisome; V, vacuole.

B: Micropexophagy in *P. pastoris*. Upon induction of micropexophagy through addition of glucose to methanol-grown *P. pastoris* cells, the vacuole starts to sequester a cluster or peroxisomes. After complete sequestration of the organelles, homotypic fusion of vacuolar membranes occurs. The peroxisomes are then released into the vacuolar lumen where they are degraded by vacuolar hydrolases. P, peroxisome; V, vacuole.

least single peroxisome within the cell may again allow rapid proliferation of the organelles in response to changing nutrient conditions and, thus, has an important role during cell survival.

Sequestration of peroxisomes during macropexophagy was revealed to be a highly selective process. Other cell components (cytosol, ribosomes, mitochondria, etc.) were not taken up by the membrane layers and, thus, were not degraded in the course of macropexophagy in *H. polymorpha* cells (Titorenko *et al.*, 1995). In contrast, during macroautophagy, both cytosol and organelles are randomly sequestered by the autophagosomal membrane (Kim and Klionsky, 2000). Furthermore, macropexophagy in *H. polymorpha* was not dependent on the synthesis of new proteins, since glucose adaptation in the presence of cycloheximide did not block the peroxisomal degradation (Bellu and Kiel, 2003). On the other hand, peroxisomes were not degraded when *H. polymorpha* cells were shifted to 2-deoxyglucose, conditions which still repress synthesis of the alcohol oxidase. Although sequestration of peroxisomes was found to occur under these conditions, fusion events with the vacuole seemed to be blocked (Bellu and Kiel, 2003). These observations suggest the presence of at least two independent signaling pathways which may mediate glucose-induced peroxisome degradation in *H. polymorpha*.

In the related yeast *P. pastoris*, the mode of peroxisome degradation was shown to depend on the carbon source used to induce the degradation process. When methanol-grown *P. pastoris* cells were subjected to ethanol adaptation, peroxisomes were degraded by macropexophagy as described above. Addition of glucose to the methanol-grown cells, however, triggered a micropexophagic engulfment of clusters of peroxisomes directly at the vacuole surface (Tuttle and Dunn, 1995). Micropexophagy in *P. pastoris* was studied in detail *in vivo* using a double-labeling technique. In this experiment, peroxisomes were tagged with a fusion of the green fluorescent protein (GFP) with the C-terminal peroxisomal targeting signal SKL, and the vacuolar membrane was labeled with the vital dye FM4-64 (Sakai *et al.*, 1998). This approach allowed the dissection of micropexophagy into several distinct stages **(Fig. 1.4: B)**. Initially, peroxisomes and the single spherical vacuole are located in close vicinity. Following the induction of micropexophagy, the vacuole invaginates and extends two arms around the peroxisomes. During this stage, the vacuole is usually septated to generate multiple vacuolar compartments, which then coordinately engulf a peroxisomal cluster. Finally, the septated vacuoles or the extended vacuolar arms fuse completely around the peroxisomal cluster, followed by its degradation in the vacuole lumen. The process of micropexophagy appears therefore to be less specific than macropexophagy. In fact, although mitochondrial proteins remain intact, portions of cytoplasm may be sequestered by the vacuolar protrusions and subsequently degraded during glucose adaptation in *P. pastoris* cells (Tuttle and Dunn, 1995).

It must be also noted, that macro- and micropexophagy in *P. pastoris* are not only phenotypically distinct processes. Micropexophagy seems to be carried out slower than macropexophagy, suggesting requirement of a new protein synthesis. Indeed, in contrast to macropexophagy, micropexophagy in *P. pastoris* was shown to be inhibited by cycloheximide (Tuttle and Dunn, 1995). It was also observed, that the protease inhibitor PMSF affected engulfment of peroxisomal clusters during glucose adaptation, but had no effect on the transport of the fluorescent labeled peroxisomes into the vacuole under conditions of the ethanol-induced peroxisome degradation (Sakai *et al.*, 1998). Additionally, the phosphatidylinositol-3-kinase inhibitor wortmannin blocked micropexophagy at an early stage, whereas it did not seem to affect selective peroxisome degradation via macropexophagy (Sakai *et al.*, 1998). So, these processes display both mechanistic and regulatory differences. Recently, a degradation of peroxisomes via a process resembling microautophagy has been observed in methanol-grown *H. polymorpha* cells subjected to nitrogen starvation (Bellu *et al.*, 2001a). Under these conditions, specific vacuolar tubular structures enclosing peroxisomes were formed in the close proximity to the vacuole. In addition, portions of cytosol and mitochondria were also taken up via invaginations of the vacuolar membrane. Moreover, the *H. polymorpha PDD1* (peroxisome degradation deficient) gene product was found to be implicated in both degradation processes, whereas the *PDD2* gene was required only for selective peroxisome degradation via macropexophagy. Thus, glucose-induced and nitrogen starvation-induced peroxisome degradation in *H. polymorpha* are mechanically distinct processes which involve common but also unique genes (Bellu *et al.*, 2001a). Further investigations in this yeast have provided evidences that the processes of macro- and microautophagic peroxisome degradation occur simultaneously in methanol-grown cells subjected to nitrogen depletion and excess of glucose (Monastryska *et al.*, 2004). Therefore, in *H. polymorpha* and *P. pastoris*, both macro- and micro-pexophagy may take place, but they are apparently induced under different conditions.

Selective degradation of peroxisomes was also studied in other methylotrophic yeasts. Similar to *H. polymorpha* and *P. pastoris*, addition of ethanol to methanol-grown *P. methanolica* cells resulted in selective peroxisome degradation via macropexophagy (Kulachkovsky *et al.*, 1997). Also in *C. boidinii*, turnover of peroxisomes has been observed during ethanol adaptation (Hill *et al.*, 1985). However, so far little information is evident regarding the detailed mechanisms of pexophagy in these yeast species.

Degradation of peroxisomes in S. cerevisiae and Y. lipolytica

Selective degradation of peroxisomes was also observed in *S. cerevisiae* and *Y. lipolytica*. In these yeasts, peroxisomes can be induced by growing the cells on fatty acids (e.g., oleic acid) as a carbon and energy source or primary amines as a source of nitrogen. Under these conditions, β-oxidation enzymes or amine oxidase, required for metabolism of fatty acids and primary amines, are present in the peroxisomes and may be used as markers to monitor the degradation of the organelles.

In *S. cerevisiae*, turnover of peroxisomes was studied when oleate-grown cells were gradually shifted to glucose-containing media with or without nitrogen source (Chiang *et al.*, 1996; Hutchins *et al.*, 1999). Under these conditions, peroxisomes were internalized via an engulfment of the vacuolar membrane, a process thought to resemble micropexophagy in *P. pastoris* (Bellu and Kiel, 2003). Also, the peroxisomal marker protein thiolase was shown to degrade much faster than cytosolic or mitochondrial proteins. This observation suggests a specific character of the peroxisome degradation process in baker's yeast. Furthermore, pexophagy was found out to be impaired in some mutants of *S. cerevisiae* also affected in macroautophagy or in the biosynthetic Cvt pathway (Hutchins *et al.*, 1999). Thus, the selective and non-selective intracellular vacuolar transport pathways in *S. cerevisiae* overlap at least partially.

Selective peroxisome degradation was also revealed in the alkane-utilizing yeast *Y. lipolytica*. To induce peroxisomal turnover, cells of this yeast were first grown in acetate/oleic acid/ethylamine medium and subsequently transferred into fresh medium containing glucose and ammonium sulfate. Under these conditions, peroxisomes were shown to be specifically degraded by uptake in the vacuole via the macropexophagic process (Gunkel *et al.*, 1999; Nazarko *et al.*, 2005). However, detailed mechanisms of the pexophagy in *Y. lipolytica* and *S. cerevisiae* are still waiting to be elucidated.

1.2.2.3 Molecular links between peroxisome biogenesis and degradation

Another challenging question that arises from the studies on peroxisomal turnover concerns the specificity of the degradation process. Destruction of cellular components is a hazardous process which must be precisely regulated. Surprisingly, studies on the peroxisomal turnover in *H. polymorpha* have provided first evidences that selective peroxisome degradation is organized at the level of peroxins (Kiel *et al.*, 2003a).

Previously, van der Klei *et al.* (1991a) demonstrated that the peroxisomal membrane is the prime target of a macropexophagic machinery using *H. polymorpha* mutants defective in biogenesis of these organelles. These mutants (called *pex* mutants) lack intact peroxisomes, but still possess

peroxisomal membrane structures (known as "remnants") under conditions which induce peroxisome biogenesis (Veenhuis *et al.*, 1996). In most methanol-grown *pex* mutants, peroxisomal remnants are subjected to the normal glucose-induced peroxisome degradation, except for the Δ*pex14* cells (Veenhuis *et al.*, 1996). Earlier observations showed that Pex14p is involved in the import of peroxisomal matrix proteins at the stage of docking of PTS1 receptor to the peroxisomal membrane (Subramani *et al.*, 2000). Recently, Bellu *et al.* (2001) have also demonstrated that the N-terminus of HpPex14p is essential for macropexophagy in *H. polymorpha*. Electron microscopical analysis revealed that in the yeast strain producing the full-length Pex14p peroxisomes were normally degraded, whereas in cells producing the N-terminally truncated form of Pex14p sequestration of the organelles was prevented. Thus, Pex14p is required early in the degradation process acting probably as a molecular switch between peroxisomal biogenesis and pexophagy.

Further molecular links between inactivation of the peroxisomal matrix import machinery and the onset of pexophagy came from studies on the involvement of another peroxin, Pex3, in macropexophagy in *H. polymorpha* (Bellu *et al.*, 2002). Pex3 is an integral peroxisomal membrane protein which appears to play an essential role in assembly of the membrane-associated peroxisomal matrix protein import complexes (Hazra *et al.*, 2002). It was demonstrated that during glucose adaptation of methanol-grown *H. polymorpha* cells, the level of Pex3p decreased rapidly in a proteasome-dependent way prior to sequestration of the peroxisomes (Bellu *et al.*, 2002). Furthermore, overexpression of *PEX3* was shown to prevent glucose-induced peroxisomal degradation in *H. polymorpha*, suggesting that Pex3p might protect the organelles from degradation. From this point of view, removal of Pex3p from the peroxisomal membrane might disassemble the import complexes and, therefore, in unknown manner provoke the degradation of peroxisomes. Notably, both Pex3 and Pex14 peroxins were found to be parts of the same complex (Hazra *et al.*, 2002). Taken together, these data demonstrate that at least two peroxisomal membrane proteins are involved in the selective degradation of peroxisomes, and that opposite processes of peroxisome biogenesis and degradation converge at the molecular level.

1.2.3 Overlap between pexophagy and other autophagy-related pathways

As has been already indicated above, pexophagy shares a lot of genes with other autophagy-related processes (reviewed in Veenhuis *et al.*, 2000; Bellu and Kiel, 2003; Farré and Subramani, 2004). The first isolated genes involved in macro- and micropexophagy appeared to be homologues of those in *S. cerevisiae* required for the vacuolar protein sorting *(VPS)*, general autophagy *(APG/AUT)*, cytoplasm-to-vacuolar targeting *(CVT)*, and endocytosis *(END)*. For example, the *H. polymorpha PDD1* (for: peroxisome degradation deficient) gene was found to encode the functional homologue of ScVps34p, a PI3K essential for vacuolar protein sorting and endocytosis (Kiel *et al.*, 1999; see also **Table 1.2**). The Vps pathway is generally required to transfer soluble vacuolar proteins (mainly zymogens of proteases, lipases, etc.) via vesicle transport through the ER, Golgi, and the endosome system to the vacuole, where the inactive proteins are activated by removal of their pro-sequences (for review, see Bryant and Stevens, 1998). Since the *H. polymorpha pdd1* mutant was affected in an early stage of macropexophagy, the sequestration of peroxisomes, the degradation defect in this mutant cannot be attributed to a lack of vacuolar proteases due to the *vps* phenotype. However, the involvement of the HpPdd1p in the VPS process was also obvious, since the vacuolar protease carboxypeptidase Y was mislocalized in *pdd1* mutants (Kiel et al., 1999). This data confirms the earlier observations that phosphoinositides have diverse roles in intracellular traffic pathways, most likely through different effectors involved in these processes.

Recently, two other genes form *H. polymorpha*, namely *PDD7* and *ATG8*, were shown to display high levels of similarity with *APG1* and *APG8* from *S. cerevisiae*, respectively. Both *H. polymorpha* genes appeared to be essential for selective peroxisome degradation via macropexophagy as well as for nitrogen starvation-induced microautophagy (Komduur *et al.*, 2003; Monastyrska *et al.*, 2005; see also **Table 1.1**). Conversely, Hutchins *et al.* (1999) studied the effect of mutations in some *APG* genes on pexophagy in *S. cerevisiae*. It was observed that in *apg1*, *apg5*, *apg7*, *apg8*, *apg10* and *apg14* mutants, the peroxisomal marker 3-ketoacyl-CoA thiolase was not degraded when oleate-grown cells were shifted to glucose medium lacking nitrogen (Hutchins *et al.*, 1999). This data indicates that al least these *APG* genes are required for autophagic peroxisome degradation which occurs in baker's yeast under conditions of nitrogen starvation.

Similar to *H. polymorpha*, the genes shown to be necessary for macro- and micropexophagy in *P. pastoris* comprise those involved in the induction of autophagy and the Cvt pathway (homologues of *S. cerevisiae APG1* and *VPS15*), as well as those required for the cargo sequestration (homologous of *S. cerevisiae APG2*, *APG7*, *APG8*, *APG9*, *AUT10* and *APG16*)

(Kim *et al.*, 1999; Stasyk *et al.*, 1999; Yuan *et al.*, 1999; Guan *et al.*, 2001; Stromhaug *et al.*, 2001; Mukaiyama *et al.*, 2002). Remarkably, most of the proteins encoded by these genes were found to be located to the PAS (pre-autophagosomal structure) which was proposed to be a central compartment for vesicular formation during both autophagy and the Cvt pathway in *S. cerevisiae* (Suzuki *et al.*, 2001). Based on these observations, Kiel *et al.* (2003a) suggested an important function of the PAS in macropexophagy in yeasts, at the stages of signaling and organelle sequestration. Furthermore, it was also speculated that a PAS-like structure might be required for the complete vacuolar engulfment of a peroxisomal cluster during micropexophagy in *P. pastoris* (Subramani, 2001). Experimental evidence for the involvement of such a structure, called micropexophagy apparatus (MIPA), has been published recently (Oku *et al.*, 2003; Mukaiyama *et al.*, 2004). The next question to be elucidated is whether the MIPA and PAS are indeed related structures, or they present completely different intracellular formations displaying variations in modes of peroxisome degradation. Additional investigations are definitely necessary to provide molecular and structural basis to study relations between micropexophagy, macropexopahagy and autophagy.

Although, as denoted above, pexophagy and other related transport and degradation pathways utilize many common genes, there are also components found out to be specific for these processes. For instance, in *P. pastoris*, *GSA9* (for: glucose-induced selective autophagy of peroxisomes), *GCN1*, *GCN2*, *GCN3*, and *ATG26* were shown to be selectively involved in pexophagy, but not in starvation-induced autophagy (Yuan *et al.*, 1997; Kim *et al.*, 2001; Farré and Subramani, 2004). In addition, in *H. polymorpha*, some *PDD* genes required for macro-autophagy have no orthologs in baker's yeast, or appear to have putative homologs known to be unaffected in general autophagy (Bellu and Kiel, 2003; Leão-Helder *et al.*, 2003). An opposite may also occur: ScAtg23p was demonstrated to be essential for the Cvt pathway and efficient autophagy but not for pexophagy (Tucker *et al.*, 2003). Altogether, this data suggests that even if macro- and micropexophagy employ key components of the Apg/Cvt machinery, there must be also a set of unique proteins required for these processes. Further analysis will give insights in common and specific mechanisms of pexophagy, autophagy and their related processes.

1.3 The alkane-assimilating yeast *Yarrowia lipolytica*

Yeasts have a long history as domesticated and cultivated unicellular organisms. The brewing of beer and wine and the leavening of bread are well-known traditional applications of yeasts. However, with development of biological sciences, the exploitation of these eukaryotic microorganisms became much wider. To date, the field of yeast research range from investigation of molecular mechanisms of cellular metabolism to heterologous protein expression, from development of novel diagnostic tools to engineering of metabolic pathways, from classical genetics to modern genomic analysis. In recent years, so-called non-conventional yeasts have been proven to be favorite model organisms to solve some molecular biological and biotechnological problems. The dimorphic alkane-assimilating yeast *Yarrowia lipolytica* is one of the most intensively investigated non-conventional yeast species with strong research and biotechnological potential.

1.3.1 General characteristics of *Y. lipolytica*

The hemiascomycetous yeast *Y. lipolytica* is an obligate aerobic microorganism, which can be normally isolated from different food products, such as cheese, yoghurts, kefir, meat or shrimps. First classified as *Endomycopsis lipolytica*, then as *Saccharomycopsis lipolytica*, this yeast species has been finally assigned to the new genus *Yarrowia* (van der Walt and von Arx, 1980). *Y. lipolytica* is considered as nonpathogenic, as the maximum growth temperature of most isolate does not exceed 32-34 ºC, and intravenous mice injections of *Y. lipolytica* cells are not associated with any mortality (Holzschu *et al.*, 1979).

Nearly all natural isolates of *Y. lipolytica* are haploid, heterothallic, and belong either to the A or to B mating types. Crossing of A and B strains results in the formation of stable diploids, which can be induced to sporulate, forming one to four spores per ascus. Extensive studies on the *Y. lipolytica* life cycle, including mating processes and sporulation, were performed by Barth and Weber (1985), Weber and Kurischko (1989), and Barth and Gaillardin (1996).

Y. lipolytica is a natural dimorphic fungus, which differentiates into yeast, pseudomycelium and true septate mycelial forms (van der Walt and von Arx, 1980). The proportion of the different cellular forms depends on the strain used. However, certain nutrient signals were found to induce so-called yeast-hypha transition, which makes this microorganism a suitable morphogenetic model (Perez-Campo and Dominguez, 2001).

Y. lipolytica can assimilate normally a lot of diverse carbon-containing substrates. In general, this yeast grows well on sugars (mainly glucose, but not sucrose), alcohols, acetate and

hydrophobic substrates (alkanes, fatty acids and oils), as reviewed by Barth and Gaillardin (1997). Ethanol can be used as sole carbon source at concentrations up to 3 %; higher ethanol content inhibits cell growth. A comprehensive review on carbohydrate metabolism in non-conventional yeasts including *Y. lipolytica* has been published recently (Flores *et al.*, 2000).

A characteristic feature of *Y. lipoyltica* is its ability to utilize *n*-alkanes, 1-alkenes, fatty acids and various fats and oils as sole carbon sources (reviewed in Barth *et al.*, 2003; Fickers *et al.*, 2005). Mechanisms of the hydrocarbons utilization have been intensively studied since mid-1980s. It was shown, that a 27 kDa extracellular emulsifier, called liposan, was induced in *Y. lipolytica* cells growing on *n*-alkanes (Cirigliano and Carman, 1984). Next, a presence of several length-specific alkane-uptake systems was proposed based on the characterization of a collection of alkane non-utilizing mutants (Mausberger *et al.*, 2001). After entry into the cell, *n*-alkanes are hydrolyzed by a cytochrom P450 monooxygenase system (Il'chenko *et al.*, 1980). Eight different *Y. lipolytica* genes (*YlALK1* to *YlALK8*) encoding cytochtomes P450 of the CYP52 family have been cloned and analyzed so far (Iida *et al.*, 2000). Interestingly, peroxisome deficiency was shown to repress the *n*-alkane-inducible *YlALK1* expression (Sumita *et al.*, 2002). The n-alkanes are subsequently oxidized to corresponding fatty acids, which are further metabolized through the β-oxidation system located to peroxisomes. The role of peroxisomal β-oxidation enzymes, especially of the acyl-CoA oxidase in γ-decalactone accumulation, has become an objective of extensive studies (Wache *et al.*, 2001; Mlickova *et al.*, 2004).

The ability of *Y. lipolytica* to use hydrophobic substrates as carbon sources has formed the basis of various industrial applications of this yeast. Initial interest was focused on the production of single cell proteins from normal paraffins, during which a basic knowledge on high scale fermentation was achieved. Second, the ability of several isolates of *Y. lipolytica* to excrete organic acids (i.e., citric acid, α-ketoglutaric acid) in growth medium can be used for a large-scale production of these compounds from cheap carbon sources, such as rape seed oil (reviewed in Barth and Gaillardin, 1996). *Y. lipolytica* also possesses a powerful system for protein secretion, which have been applied for production of both homologous (lipases, proteases and phosphatases) and heterologous (i.e., rice α-amilase or human epidermal growth factor) secreted proteins (Park *et al.*, 1997; Hamsa *et al.*, 1998; Dominguez *et al.*, 2003; Fickers *et al.*, 2005a). Remarkably, the secretion pathway in *Y. lipolytica* appeared to be closer to those of mammalian cells than to those of the baker's yeast, a feature, which for sure provides an additional advantage for studies on protein secretion in this yeast species (Beckerich *et al.*, 1998). Recent applications of *Y. lipolytica* concern bioconversion of fatty acids (Wache *et al.*, 2003) and manufacturing of heterologous proteins (Nicaud *et al.*, 2002; Madzak *et al.*, 2004).

The extreme academic and biotechnological interest in *Y. lipolytica* stimulated a rapid development of genetic tools for this non-conventional yeast. Efficient transformation methods as well as a set of appropriate integrative and replicative plasmids became available owing to combined efforts of different research groups (reviewed in Barth and Gaillardin, 1996; Barth *et al.*, 2003). *Y. lipolytica* has no own DNA plasmids, although linear dsRNA molecules encapsulated within virus-like particles were observed in several yeast strains (Tréton *et al.*, 1985). Early searches for *ARS*-containing vectors for *Y. lipolytica* were unsuccessful till it has turned out that only *ARS*s associated with a *CEN* sequence are able to support the extrachromosomal replication (Fournier *et al.*, 1993). Plasmids with *ARS/CEN* regions are mitotically quite stable and exhibit mendelain segregation during meiosis (Vernis *at el.*, 2001). Furthermore, *Y. lipolytica* multicopy integrative systems based on a defective *URA3* marker as well as on rDNA or Zeta regions of the *Y. lipolytica* retrotransposon Ylt1 have been developed (Le Dall *et al.*, 1994; Juretzek *et al.*, 2001); new disruption cassettes for rapid gene disruption and insertion mutagenesis have been described recently (Mauersberger *et al.*, 2001; Fickers *et al.*, 2003). In addition, a highly representative two-hybrid genomic library for *Y. lipolytica* is now available (Kabani *et al.*, 2000), allowing *in vivo* studies of protein-protein interactions in this organism.

Taking together, the alkane-assimilating yeast *Y. lipolytica* has been proven to be an original and exiting model to study protein secretion, morphogenesis, carbon metabolism, as well as signal transduction pathways (for an extensive review, see Barth *et al.*, 2003). More recent developments concerning genome structure and peroxisomal biogenesis in this yeast will be discussed in detail below.

1.3.2 Organization of the genome of *Y. lipolytica*

In the last few years, a particular attention has been paid to the deciphering of the structure and functioning of the genome of *Y. lipolytica*. One of the most important current achievements in this field is the sequencing of the complete *Y. lipolytica* genome conducted by an international consortium in collaboration with *Génolevures* (Dujon *et al.*, 2004).

The genome of *Y. lipolytica* (a reference strain E150) consists in six chromosomes comprising ca. 20.5 Mb of DNA, which were shown to be highly polymorphic among different isolates (Naumova *et al.*, 1993; Casaregola *et al.*, 1997). The total number of protein-coding genes is predicted to be about 6700, among which 510 genes correspond to tRNA; the average GC content of the coding DNA regions is estimated as 52.9 % (for comparison, in *S. cerevisiae* it is

39.6 %) (Dujon *et al.*, 2004). About 13 % of *Y. lipolytica* genes contain one or two introns, often a relatively large size (about 400 bp). Repeated sequences are presented by one to six subtelomeric clusters of rDNA (Casaregola *et al.*, 1997), at least two retrotransposons of the Ty3 family (Schmid-Berger *et al.*, 1994; Kovalchuk *et al.*, 2005) as well as non-LTR and DNA mobile elements (Casaregola *et al.*, 2002; Neuveglise *et al.*, 2005). Further analysis of the *Y. lipolytica* genomic sequence, e.g. classification and comparison of protein families, study of gene expansion and conservation, etc., has verified a high level of genome redundancy, confirming the rapid sequence evolution assumed for this yeast species. Furthermore, several features of its genome organization, such as high GC content, dispersion of the rDNA clusters and of the 5S RNA genes, higher eukaryotic-like size of snRNA, and, in particular, the signal recognition particle 7S RNA, bring this yeast species evolutionary closer to higher eukaryotes (Casaregola *et al.*, 2000). Phylogenetic tree based on the comparison of 25S rDNA sequences located *Y. lipolytica* on an isolated branch clearly separated from *S. cerevisiae* on the one hand, and from a bulk of other hemiascomycetes on the other hand (Dujon *et al.*, 2004). This data confirms the unique taxonomical position which *Y. lipolytica* occupies among other hemiascomycetous yeasts.

1.3.3 *Y. lipolytica* as a model to study the biogenesis of peroxisomes

The alkane-assimilating yeast *Y. lipolytica* was proved to be an excellent model to study the molecular mechanisms involved in peroxisomal assembly, division and turnover. In *Y. lipolytica*, extensive peroxisome proliferation was shown to take place during growth of yeast cells in medium containing oleic acid as a sole carbon source, and mutants defective in peroxisome biogenesis were simply isolated because they fail to grow on oleate (Nuttley *et al.*, 1993). This feature combined with the availability of well-developed genetic tools resulted in identification of *Y. lipolytica* genes involved in peroxisomal biogenesis (reviewed in Barth and Gaillardin, 1996). In the main, molecular studies on peroxisome biogenesis in *Y. lipolytica* have provided new insights on this process. In the classical model of peroxisome biogenesis, structurally and functionally homogenous organelles were proposed to divide from pre-existing one and subsequently grow via constant import of membrane and matrix proteins (Lazarow and Fujiki, 1985). Recent findings in *Y. lipolytica* have challenged this conception. It was shown, that the population of peroxisomes in one *Y. lipolytica* cell consists of many structurally and functionally distinct compartments (subforms) which differ in their import competency for peroxisomal proteins and undergo a specific time-dependent conversion to mature organelles (Titorenko and

Rachubinski, 2001). Several earlier reports provided evidences that, in *H. polymorpha*, newly formed import-competent peroxisomes have a lower density compared to the mature organelles (Veenhuis *et al.*, 2000). On the basis of investigations in the yeast *Y. lipolytica*, Titorenko *et al.* (2000) proposed a new model for peroxisome biogenesis via so-called multistep peroxisome assembly pathway. According to this model, six different peroxisomal subforms, termed P1 to P6, undergo a morphological and biochemical conversion through several consecutive steps. The initial step in the peroxisome assembly pathway involves the fusion of early intermediates, small peroxisomal vesicles P1 and P2, to form a P3 organelle. Remarkably, peroxisomal membrane fusion events were revealed to require the action of two peroxins from the AAA family, Pex1p and Pex6p (Titorenko and Rachubinski, 2000a). Further steps of the peroxisome assembly pathway involve uptake of phospholipids and selective import of matrix proteins resulting in the formation of P4 and P5 intermediates. Finally, a mature peroxisome, P6, carrying the complete set of matrix proteins is formed. Further molecular analysis of the peroxisome assembly pathway operating in *Y. lipolytica* will facilitate elucidation of precise structure and functioning of the peroxisome import machinery as well as its selectivity for distinct sets of peroxisomal matrix proteins.

Studies on *Y. lipolytica* have also contributed to our knowledge about the role of endoplasmatic reticulum (ER) in the peroxisome biogenesis. As recently shown, the ER may serve as a source for the formation of early peroxisomal precursors (Titorenko et al., 1998). In this model, a limited set of peroxisomal membrane proteins is first post-translationally targeted to the ER-subdomain, called the pre-peroxisomal template (Titorenko *et al.*, 2000b). The peroxisomal precursors P1 and P2 are subsequently formed via budding of the pre-peroxisomal template accomplished by uptake of distinct subsets of the peroxisomal membrane proteins (Titorenko and Rachubinsky, 2001a; 2001b). Thus, peroxisomes in *Y. lipolytica* are heterogenous organelles dynamically integrated into intracellular membrane turnover.

1.4 Aim of the work

The work presented in this thesis is aimed at understanding molecular mechanisms of the autophagic degradation of peroxisomes in the yeast *Y. lipolytica*. In this microorganism, peroxisomes were revealed to be subjected to selective degradation via macropexophagy after a shift of peroxisomes-containing cells into a minimal medium with glucose and a source of nitrogen (Gunkel *et al.*, 1999; Nazarko *et al.*, 2005). Recently, a homolog of *S. cerevisiae TRS85* gene, encoding the 85 kDa subunit of the transport protein particle (TRAPP) complex, has been shown to be required for both pexophagy and general autophagy in *Y. lipolytica* (Nazarko *et al.*, 2005a). This mutant was obtained by means of insertional mutagenesis and a peroxisomal amine oxidase activity plate screening assay (Nazarko *et al.*, 2002). However, this screen has not so far revealed any *Y. lipolytica ATG* genes homologous to those previously described in other organisms.

At the beginning of this thesis project, very little was known about the molecular mechanisms of peroxisome degradation in *Y. lipolytica* and no genes involved in this process were identified in this microorganism. Therefore, the main interest of this study was focused firstly on the development and optimization of *Y. lipolytica* as a model system to study peroxisome degradation. Furthermore, *Y. lipolytica* genes and proteins implicated at different stages of pexophagy should be found and their feasible role in the autophagic degradation of peroxisomes should be investigated. Finally, a proper easy-to-handle selection procedure for isolation of novel *pdd* mutants of *Y. lipolytica* should be devised. In particular, the following tasks were proposed:

1. The construction of a recombinant strain of *Y. lipolytica* expressing a peroxisome-targeted βGal-eGFP(SKL) fusion protein.
2. The fluorescence microscopic analysis of pexophagy in *Y. lipolytica* cells expressing βGal-eGFP(SKL) fusion under nitrogen-rich and nitrogen-starved conditions.
3. The investigation of the influence of PMSF on the course of pexophagy in *Y. lipolytica*.
4. A bioinformatic screen of the genome of *Y. lipolytica* for autophagy-related proteins.
5. Biochemical and fluorescence microscopic studies of pexophagy in *atg1, atg6, atg11, atg18, gcn2* and *pep4* mutants of *Y. lipolytica*.
6. The development of a visual screening assay for isolation of *Y. lipolytica pdd* mutants based on the expression of heterologous β-galactosidase.

2 Materials and methods

2.1 Laboratory equipment

Incubators and shakers

Incubator Memmert BE500 (set at 37 °C for the cultivation of *E. coli*)

Incubator Heraeus BK 600 (set at 28 °C for the cultivation of *Y. lipolytica*)

Shaker Infors HT Novotron® AK82 (set at 37 °C for the cultivation of *E. coli*)

Shaker Infors HT Multitron® (set at 28 °C for the cultivation of *Y. lipolytica*)

Centrifuges

Heraeus Biofuge fresco (microcentrifuge)

Heraeus Sepatech Biofuge 15R with rotor HFA 5.50

Sorvall RC 5C with rotors SS-34, SLA-1500 and SLA-3000

Sterilizers

Benchtop steam sterilizer KSG 112

Steam sterilizer H+P Varioklav 500E

Hot air sterilizer Memmert Modell 500

Electroporators

BioRad GenePulser® II

BioRad MicroPulser™

Thermocyclers

Biometra T1 Thermocycler

MWG-Biotech Primus 25

MWG-Biotech Primus 96 plus

DNA sequencers

Beckman Coulter CEQ™ 2000XL DNA analysis system with CEQ sequence analysis 4.3.9 software

Electrophoresis systems

BioRad Sub-Cell® GT electrophoresis system (for horizontal DNA electrophoresis)

Hoefer HE 99X Max submarine unit (for horizontal DNA electrophoresis)

Phase PROT-RESOLV MINI-LC vertical gel electrophoresis system (for protein electrophoresis)

Electroblotters

PeqLab ThePanther™ semi-dry electroblotter model HEP-1

Power supplies

BioRad PowerPac 300 (for DNA-electrophoresis)

Biometra Standart Power Pack P25 (for protein electrophoresis)

Pharmacia Biotech electrophoresis power supply EPS 3500 (for semi-dry protein transfer)

Spectrometers

Pharmacia Biotech Ultospec 2000 (UV/visible spectrophotometer)

Kontron Instruments Uvikon 943

Balances

Sartorius MC1

Sartorius BP310P

Kern 770 (microbalance)

pH Meters

WTW pH526 (for pH 4–7)

WTW pH537 (for pH 7–10)

Microscopes

Olympus light microscope BX40

Olympus fluorescent microscope BX60

Further equipment

Bandelin Sonopuls HD 2070 ultrasound homogenizer

Biometra Vacu-Blot system

Biometra OV5 hybridization oven

Heidolph Promax 1020 reciprocal shaker

Heidolph Reax 2000 vibrating mixer

Heraeus HERAsafe safety cabinet

Kleinfeld Labortechnik block-thermostat BT100

MWG-Biotech UV transilluminator TEX-35M (312 nm) (with Biophotonics GelPrint 2000 software)
Retsch MM200 vibrating shaker (used for cell disruption)
Savant DNA Speed Vac® concentrator 110
Techne Tempcold refrigerated thermostat
Ultrasonic homogenizer USD30

2.2 Chemicals and reagents

All chemicals and reagents used in this work are commercially available.

2.2.1 Fine chemicals

Agarose	Sigma-Aldrich
Ampicillin	Roth
Ammonium persulfate	Merck
Bacto® Yeast Nitrogen Base w/o amino acids	Difco
Bacto™ Yeast Nitrogen Base w/o amino acids and ammonium sulphate	Difco
BechMark™ prestained protein ladder	Invitrogen/Gibco BRL
BSA	Roth
Coomassie® Brillantblau G250	Ferak
Glycogen	Roche
Cyanosine	Sigma-Aldrich
DMSO	Sigma-Aldrich
Ethidium bromide	Serva
DNA from salmon sperm, MB grade	Roche
FM4-64	Molecular Probes Inc.
GeneRuler™ 1 kb DNA ladder	Fermentas
IPTG	AGS
MNNG	Sigma-Aldrich
PMSF	Fluka
Poly L-lysine	Sigma-Aldrich
Protease inhibitors cocktail (complete™)	Roche
TEMED	Serva
X-gal	AGS

2.2.2 Enzymes und PCR reagents

Restriction endonucleases and appropriate buffers	Fermentas
BioTherm™ DNA polymerase	GeneCraft
Combi*Zyme* DNA polymerase mix	Invitek
dNTPs	Fermentas
Glusulase	NEN Life Science Products
Klenow fragment	Fermentas
Pfu DNA polymerase	Fermentas
Pwo DNA polymerase	Roche
Ribonuclease A	USB
T4 DNA ligase	Promega
Taq DNA polymerase	Fermentas
Thermosensitive alkaline phosphatase	Gibco BRL
OptiPerform buffer III	Invitek
Zymolyase 20T	ICN Biomedicals

2.2.3 Kits and related products

JETQUICK PCR Product Purification Spin Kit	Genomed
JETQUICK Gel Extraction Spin Kit	Genomed
JETSORB Gel Extraction Kit	Genomed
JETQUICL Plasmid Miniprep Spin Kit	Genomed
JETSTAR Plasmid Midiprep Kit	Genomed
CEQ™ DTCS Quick Start Kit	Beckman Coulter
ECL^{Plus} Western blotting detection system	Amersham Biosciences
Gene Images random prime labelling module	Amersham Biosciences
Gene Images CDP-*Star* detection module	Amersham Biosciences
Immobilon™-P PVDF transfer membrane	Millipore
White VSWP Membrane	Millipore
Hybond-N nylon membrane	Amersham Biosciences
Hyperfilm ECL X-ray film	Amersham Biosciences
GB-003 blotting paper	Schleicher & Schüll

2.2.4 Antibodies

Antibodies used in this work were diluted and stored according to supplier's information. Stock solutions were further diluted in a block solution (*see 2.7.5*) in proportions as described below and then used for Western blots detection.

Primary antibodies

Mouse anti-β-galactosidase (Sigma-Aldrich)	1:1000
Rabbit anti-thiolase (kindly provided by Prof. R. Rachubinski)	1:10000
Rabbit anti-ICL (kindly provided by Prof. R. Rachubinski)	1:5000
Rabbit anti-G6PDH (Sigma-Aldrich)	1:5000
Rabbit anti-GroEL (kindly provided by Prof. van der Klei)	1:2000
Rabbit anti-aconitase (kindly provided by Prof. G. Rödel)	1:5000

Secondary antibodies

Sheep anti-mouse Ig-HRP (Amersham Biosciences)	1:5000
Donkey anti-rabbit Ig-HRP (Amersham Biosciences)	1:5000
Rabbit anti-mouse Ig coupled to Texas red (Dianova)	1:80

2.2.5 Nucleic acids

2.2.5.1 Acquired plasmids

Table 2.1 An overview of the acquired plasmids used in this work. Restriction map of the plasmid pLG3 can be found in Appendix (Chapter 7.1).

Plasmid	Genetic markers	Description	Reference
pUCBM21	*amp^R*	Standard *E. coli* cloning vector	Roche Molecular Biochemicals Mannheim
pINA443	*amp^R YlURA3 ARS68*	Low copy *ARS/CEN Y. lipolytica/ E. coli* shuttle vector	Barth and Gaillardin, 1996
pINA354-lacZ-GFP (pLG3)	*amp^R YlLEU2 lacZ eGFP(SKL)*	*Y. lipolytica* integrative vector containing a chimerical l*acZ-eGFP (SKL)* gene fusion under control of the *Y. lipolytica ICL1* promoter	Gunkel, 2000

2.2.5.2 Constructed plasmids

All plasmids constructed in the course of the work are listed in the **Table 2.2**.

Table 2.2 An overview of plasmids constructed during the work. Plasmids indicated with symbol "*" were made by C. Hoffmann (2004), and those with symbol "#" - by C. Bodinus (2004). For restriction maps of the plasmids pATG1URA3, pAPG6URA3, pCVT18URA3, pVAC8URA3, pGCN2URA3, and pPEP4URA3, see Appendix (Chapter 7.1).

Plasmid	Genetic markers	Description
pUCATG1	*amp*^{R}	pUCMB21-based plasmid containing *Pst*I/*Bam*HI-fragment of the *YlATG1* gene
pAPG6*	*amp*^{R}	pUCMB21-based plasmid containing *Sal*I-fragment of the *YlATG6* gene
pUCATG11	*amp*^{R}	pUCMB21-based plasmid containing *Xba*I/*Bam*HI -fragment of the *YlATG11* gene
pUCCVT18#	*amp*^{R}	pUCMB21-based plasmid containing *Nco*I/*Bgl*II -fragment of the *YlATG18* gene
pUCVAC8	*amp*^{R}	pUCMB21-based plasmid containing *Sal*I/*Nco*I -fragment of the *YlVAC8* gene
pUCGCN2	*amp*^{R}	pUCMB21-based plasmid containing *Pae*I -fragment of the *YlGCN2* gene
pUCPEP4	*amp*^{R}	pUCMB21-based plasmid containing *Pae*I -fragment of the *YlPEP4* gene
pATG1URA3	*amp*^{R} *YlURA3*	integrative plasmid for disruption of the *YlATG1* gene, which contains the *YlATG1::YlURA3* cassette in the vector pUCBM21
pAPG6URA3*	*amp*^{R} *YlURA3*	integrative plasmid for disruption of the *YlATG6* gene, which contains the *YlATG6::YlURA3* cassette in the vector pUCBM21
pAPG11URA3	*amp*^{R} *YlURA3*	integrative plasmid for disruption of the *YlATG11* gene, which contains the *YlATG11::YlURA3* cassette in the vector pUCBM21
pCVT18URA3#	*amp*^{R} *YlURA3*	integrative plasmid for disruption of the *YlATG18* gene, which contains the *YlATG18::YlURA3* cassette in the vector pUCBM21
pGCN2URA3	*amp*^{R} *YlURA3*	integrative plasmid for disruption of the *YlGCN2* gene, which contains the *YlGCN2::YlURA3* cassette in the vector pUCBM21
pPEP4URA3	*amp*^{R}, *YlURA3*	integrative plasmid for disruption of the *YlPEP4* gene, which contains the *YlPEP4::YlURA3* cassette in the vector pUCBM21

2.2.6 Synthetic oligonucleotides

Table 2.3 A list of synthetic oligonucleotides used in this work. Oligonucleotides NN^{o} 1-23 were used for cloning purposes, NN^{o} 24-32 were applied for sequencing of the obtained fragments and NN^{o} 33-38 were used for screening of *Y. lipolytica* mutants with disrupted genes of interest. Recognition sites for restriction endonucleases are shown underlined and in bold. All oligonucleotides were purchased from MWG-Biotech.

N^{o}	Name	Sequence (5′ → 3′)	RE	Application
1	p181neu	AGCCACGGAGCTGTTGTT	-	Amplification of the *Pst*I/*Bam*HI-fragment of the *YlATG1* gene
2	p182neu	AAGCTGTCCATCTCCCTG	-	Amplification of the *Pst*I/*Bam*HI-fragment of the *YlATG1* gene
3	p121w	ATATAT**GTCGAC**TCCCTCATCAC ACAG	*Sal*I	Amplification of the *Sal*I-fragment of the *YlATG6* gene
4	p122w	ATATAT**GTCGAC**TGTGACCACCA CGTA	*Sal*I	Amplification of the *Sal*I-fragment of the *YlATG6* gene
5	ATGXba	CTAGTTAGGAGCTGTCTGC	-	Amplification of the *Xba*I/*Bam*HI-fragment of the *YlATG11* gene
6	ATGBam	TCGTCCAACCAACCAATCC	-	Amplification of the *Xba*I/*Bam*HI-fragment of the *YlATG11* gene
7	AUTvor	GCTGCACTGGTCTCATGT	-	Amplification of the *Nco*I/*Bgl*II-fragment of the *YlATG18* gene
8	AUTrev	GAGATTGGAGGCCAGATT	-	Amplification of the *Nco*I/*Bgl*II-fragment of the *YlATG18* gene
9	Vac1	TATACGAGACGCGGTAGG	-	Amplification of the *Sal*I/*Nco*I-fragment of the *YlVAC8* gene
10	Vac3	CTGGACGTCGAGATAGTG	-	Amplification of the *Sal*I/*Nco*I-fragment of the *YlVAC8* gene
11	Y283-1	ATATAT**GCATGC**ATGTACTCTTTG GGTATCATCTTT	*Pae*I	Amplification of the *Pae*I-fragment of the *YlGCN2* gene
12	Y283-2	ATATAT**GCATGC**GAAGACGTTGT CGGCCTT	*Pae*I	Amplification of the *Pae*I-fragment of the *YlGCN2* gene
13	pPEP4vor	CAATGGCTGGATCGCTCT	-	Amplification of the *Pae*I-fragment of the *YlPEP4* gene
14	pPEP4rev	GAGGTGGAATCTCGTGTC	-	Amplification of the *Pae*I-fragment of the *YlPEP4* gene
15	pURA22	ATA**CCGCGG**/**GTCGAC**GAGTATC TGTCT	*Cfr*42I, *Sal*I	Amplification of the *YlURA3* gene with *Cfr*42I extensions

N°	Name	Sequence (5′ → 3′)	RE	Application
16	pURA2	ATA**CCGCGG/GTCGAC**AAAGGC CTGTTT	*Cfr*42I, *Sal*I	Amplification of the *YlURA3* gene with *Cfr*42I extensions
17	pURA3	ATATAT**TCGCGA/GTCGAC**GAGT ATCTGTCT	*Bsp*68I, *Sal*I	Amplification of the *YlURA3* gene with *Bsp*68I extensions
18	pURA4	ATATAT**TCGCGA/GTCGAC**AAAG GCCTGTTT	*Bsp*68I, *Sal*I	Amplification of the *YlURA3* gene with *Bsp*68I extensions
19	pURANru1	ATA**TCGCGA**CTTGGATCACTTTG ACGATAC	*Bsp*68I	Amplification of the *YlURA3* gene with *Bsp*68I extensions (w/o *Sal*I-restriction site)
20	pURANru2	ATA**TCGCGA**GTGTACAGAGCTTG GTCCT	*Bsp*68I	Amplification of the *YlURA3* gene with *Bsp*68I extensions (w/o *Sal*I-restriction site)
22	pURAcla1	ATA**ATCGAT/GTCGAC**GAGTATC TGTCT	*Bsu*15I, *Sal*I	Amplification of the *YlURA3* gene with *Bsu*15I extension
23	URA-ClaI	ATA**ATCGAT**TTCTGCCTCCAGGA AGTC	*Bsu*15I	Amplification of the *YlURA3* gene with *Bsu*15I extensions (w/o *Sal*I-restriction site)

Sequencing primers

24	pECHseq 3vor	TAGCTCACTCATTAGGCAC	-	Sequencing of the DNA-fragments inserted in the MCS of the plasmid pUCBM21
25	pIGAseq5 rev	TGCAAGGCGATTAAGTTGG	-	Sequencing of the DNA-fragments inserted in the MCS of the plasmid pUCBM21
26	pSEQ1	TCCTGCTCTCGTGGCAAGTCA	-	Sequencing of the *YlATG1*-fragment
27	pSEQ2	GATGGCCACCGGAGAGCC	-	Sequencing of the *YlATG1*-fragment
28	pSEQ3	AAGGAGCTCATTGAGCTTGCCG	-	Sequencing of the *YlURA3-ORF*
29	pSEQ7	ACATATACTTCACTGCCCCA	-	Sequencing of the *YlURA3-ORF*
30	pSEQ8	ATACAAGCTGAACAAGCGCT	-	Sequencing of the *YlURA3-ORF*
31	CVTseqvor	ATCCGACGACTGGATCAG	-	Sequencing of the *YlATG18*-fragment
32	CVTseqrev	CTGCAAACGGAGTGTCTC	-	Sequencing of the *YlATG18*-fragment

Screening primers

Nº	Name	Sequence (5′ → 3′)	RE	Application
33	p180w-1	CAGTTATTTGTAGTCACCTGT	-	Searching for *Y. lipolytica atg1* disrupted strains
34	p180w-2	GAGGCCGATCTTCCTAAG	-	Searching for *Y. lipolytica atg1* disrupted strains
35	CVTscreenvor	GCGTCTTGTTCGATCTTGAG	-	Searching for *Y. lipolytica atg18* disrupted strains
36	CVTscreenrev	CCACATTCCAGTGAAGGTCT	-	Searching for *Y. lipolytica atg18* disrupted strains
35	pScreen5	AACACTGCGATGGAGCGT	-	Searching for *Y. lipolytica gcn2* disrupted strains
36	pScreen6	GGCACCGACAGAGTACTT	-	Searching for *Y. lipolytica gcn2* disrupted strains
37	pPEP4screenvor	ATGGCTGGATCGCTCTAC	-	Searching for *Y. lipolytica pep4* disrupted strains
38	pPEP4screenrev	GAGGTGGAATCTCGTGTC	-	Searching for *Y. lipolytica pep4* disrupted strains

2.3 Microorganisms

2.3.1 *Escherichia coli*

E. coli strain DH5αC (*gyrA96 recA1 endA1 endA1 thi-1 hsdR*17 ($r_k^- m_k^+$) *supE44 deoR Δ(lacZYA-argF) U169 [ϕ80 Δ(lacZ) M15)* from Gibco-BRL was used for molecular cloning.

2.3.2 *Yarrowia lipolytica*

Table 2.4 *Y. lipolytica* strains used in this work.

Strain	Genotype	References
PO1d	*MATA leu2*-270 *ura3*-302 *xpr2*-322	Le Dall *et al.*, 1994
PO1d(pLG3)	*MATA leu2*-270 *ura3*-302 *xpr2-322 LEU2 lacZ-eGFP(SKL)*	this work
PO1d(pLG3)atg1	*MATA leu2*-270 *ura3*-302 *xpr2-322 LEU2 lacZ-eGFP(SKL) atg1::URA3*	this work
PO1d(pLG3)atg6	*MATA leu2*-270 *ura3*-302 *xpr2-322 LEU2 lacZ-eGFP(SKL)* atg6::*URA3*	Hoffmann, 2004

Strain	Genotype	References
PO1d(pLG3)atg11	*MATA leu2*-270 *ura3*-302 *xpr2-322 LEU2 lacZ-eGFP(SKL)* a*tg11::URA3*	this work
PO1d(pLG3)atg18	*MATA leu2*-270 *ura3*-302 *xpr2-322 LEU2 lacZ-eGFP(SKL) atg18::URA3*	Bodinus, 2004
PO1d(pLG3)gcn2	*MATA leu2*-270 *ura3*-302 *xpr2-322 LEU2 lacZ-eGFP(SKL) gcn2::URA3*	this work
PO1d(pLG3)pep4	*MATA leu2*-270 *ura3*-302 *xpr2-322 LEU2 lacZ-eGFP(SKL) pep4::URA3*	this work
PO1d(pINA443)	*MATA leu2*-270 *ura3*-302 *xpr2*-322 *plasmid URA3*	this work

2.4 Growth media

All media for cultivation of microorganisms were prepared as described below. For solid media, agar was added to the final concentration of 20 g/l.

2.4.1 LB medium (Luria-Bertani medium) (Sambrook *et al*, 1989)

	Final concentration
Pepton	1 % (w/v)
Yeast extract	0.5 % (w/v)
NaCl	1 % (w/v)

2.4.2 SOC medium (Sambrook *et al*, 1989)

	Final concentration
Pancreatic pepton from casein	2 % (w/v)
Yeast extract	0.5 % (w/v)
NaCl	10 mM
$MgCl_2$	10 mM
KCl	2.5 mM
Glucose	20 mM

2.4.3 Complete media for *Y. lipolytica*

2.4.3.1 Yeast extract - Pepton - Glucose medium (YPD)

	Final concentration
Yeast extract	1 % (w/v)
Bacto peptone	2 % (w/v)
Glucose	2 % (w/v)

2.4.3.2 Yeast extract – Pepton – Glucose – Citrate medium (YPD-citrate)

	Final concentration
Yeast extract	1 % (w/v
Bacto peptone	2 % (w/v)
Glucose	2 % (w/v)
Citric acid-Na citrate (pH 4.0)	50 mM

2.4.4 Minimal media for *Y. lipolytica*

2.4.4.1 Minimal medium with thiamine (Reader medium)

Mineral salts	*Final concentration (g/l)*
$(NH_4)_2SO_4$	3.0
KH_2PO_4	1.0
$K_2HPO_4 \cdot 3H_2O$	0.16
$MgSO_4 \cdot 7H_2O$	0.7
NaCl	0.5
$Ca(NO_3)_2 \cdot 4H_2O$	0.40

Trace elements	*Final concentration (mg/l)*
H_3BO_3	0.6
$CuSO_4 \cdot 5H_2O$	0.048
$MnSO_4 \cdot 4H_2O$	0.48
$Na_2MoO_4 \cdot 2H_2O$	0.24
$ZnSO_4 \cdot 7H_2O$	0.048
$FeCl_3 \cdot 6H_2O$	2.0
$Ca(NO_3)_2 \cdot 4H_2O$	2.0
KI	0.12
$CoCl_2$	0.1

Vitamins	*Final concentration (mg/l)*
Thiamine hydrochloride	0.3

Supplements	*Final concentration (mg/l)*
Uracil (Ura)	20
Leucin (Leu)	60

Carbon sources	*Final concentration*
Glucose (G)	1 % (w/v)

2.4.4.2 Minimal media for induction of biogenesis and degradation of peroxisomes

Yeast Nitrogen Base (YNB)	*Final concentration (g/l)*
YNB w/o amino aids	6.7
YNB w/o amino acids and Ammonium sulphate	1.7

Carbon and nitrogen sources	*Final concentration*
Glucose (G)	2 % (w/v)
Ethanol (E)	1 % (w/v)
Oleic acid (O)	1 % (w/v)
Ethylamine (M)	2 % (w/v)

Supplements	*Final concentration*
K_2HPO_4	0.5 % (w/v)
KH_2PO_4	0.5 % (w/v)
Yeast extract	0.1 % (w/v)
Uracil (if need)	20 mg/l

Minimal media were signed according to the contained carbon and nitrogen sources and supplements, for instance:

YEM – YNB medium with ethanol and ethylamine

YOM - YNB medium with oleic acid and ethylamine

YGA – YNB medium with glucose and ammonium sulphate

YGW – YNB medium with glucose w/o nitrogen source

YEM and **YOM** media were used for induction of peroxisomal biogenesis.

YGA and **YGW** media were used for induction of degradation of peroxisomes or for both the organelle degradation and nitrogen starvation events.

2.5 Cultivation of microorganisms

2.5.1 Cultivation of *E. coli*

E. coli cells were grown either in liquid or on solid LB medium (*see 2.4.1*) at 37 °C. Liquid cultures were agitated continuously at 220 rpm. For selection of bacterial transformants, ampicillin was added to media to the final concentration 100 µg/ml. For blue-white selection, IPTG und X-gal were added to the solid medium to the final concentrations 30 µg/ml and 150 µg/ml, respectively.

2.5.2 Cultivation of *Y. lipolytica*

Y. lipolytica strains were generally grown at 28 °C in complete (*2.4.3*) or minimal (*2.4.4*) media. Liquid cultures were incubated with continuous agitation at 220 rpm. Transformed yeast cells were selected on appropriate minimal media with glucose. For induction of peroxisome biogenesis, cells were first pre-grown either in YPD or YGA (*see 2.4.4.2*) for 24 h (pre-culture I), diluted in fresh YPD or YGA and cultivated for 8-9 h till the mid-log phase (pre-culture II). Cells were then harvested by centrifugation, washed once with minimal medium w/o carbon source and transferred into fresh YEM or YOM (*see 2.4.4.2*) to the initial OD_{600} 0.6 or 0.2 respectively (main culture I). For degradation experiments, cells incubated in the main culture I overnight were washed once with minimal medium w/o carbon source and shifted to the YGA or YGW (see *2.4.4.2*) to the initial OD_{600} 0.8-1.0 (main culture II). For subsequent biochemical and

microscopical analyses, samples were taken every two hours and processed as described below (*see chapter 2.7*).

2.5.3 Cultivation for determination of cell viability

To determine cell viability under conditions of nitrogen starvation, a phloxin B (cyanosine) staining was applied (Tsukada and Ohsumi, 1993). Briefly, yeast cells were pre-grown in liquid minimal medium overnight and then placed onto YGW (*see 2.4.4.2*) plates containing 10 µg/ml of phloxine B by the drop-plate technique. After incubation for 3-4 days, cells with defects in viability became pink whereas wild type cells remained uncolored.

2.6 DNA techniques

Standard genetic manipulations were performed as described by Sambrook *et al.* (1989) and Ausubel *et al.* (1997).

2.6.1 Agarose gel electrophoresis

Solutions:

50 x TAE buffer:	242 g Tris base 57.1 ml glacial acetic acid 100 ml 0.5 M EDTA (pH 8.0)
EB-stock solution:	10 mg/ml
6 x gel-loading buffer:	10 mM Tris-HCl (pH 7.6) 60 % (v/v) glycerol 60 mM EDTA (pH 8.0) 0.03 % bromphenol blue

For visualization and separation of DNA fragments, a standard horizontal agarose gel electrophoresis was used. The electrophoresis was performed in 1 x TAE buffer at 8-10 V/cm at room temperature. Gels percentage was determined according to the size range of the DNA fragments and was typically 0.6-1.5 % (w/v) of agarose. Ethidium bromide was added to gels, except ones used for Southern blotting, to the final concentration of 0.4 mg/ml. The DNA samples were mixed with 1/5 volume of 6 x gel-loading buffer and loaded into the sample wells. GeneRuler 1 kb ladder (*see 2.2.1*) was used as a molecular weight standard. After electrophoresis, the EB-DNA complexes were visualized directly under UV light (312 nm).

2.6.2 DNA extraction from agarose gel

DNA extraction from agarose gel was performed using JETQUICK Gel Extraction Spin Kit (for fragments up to 2 kb) or JETSORB Gel Extraction Kit (for larger fragments) according to the manufacture's manual (*see 2.2.3*).

2.6.3 Digestion of DNA with restriction endonucleases

Restriction enzyme digestions were generally performed by incubating of DNA molecules with an appropriate amount of a restriction enzyme under proper conditions. For analytical digestion, 500 ng of DNA were mixed with 2 U of enzyme and a corresponding buffer in a volume of 20 µl and incubated at 37 ºC for 2 h. Digestion of preparative amounts of DNA (2-5 µg) was carried out in a volume of 40-60 µl overnight with 10-20 U of enzyme. In the case of double digestion with two different endonucleases, a buffer providing a maximal activity for both enzymes was selected.

2.6.4 DNA precipitation

For concentration of DNA samples, a standard procedure of alcohol precipitation was used. Typically, 0.7 volumes of ice-cold isopropanol were added to the DNA sample and incubated on an ice-water bath for 10 min. After centrifugation, the DNA pellet was washed with cold 70 % ethanol solution, dried in a speed-vac and dissolved in HPLC-grade water.

2.6.5 Treatment of DNA with alkaline phosphatase

To reduce a self-ligation rate by ligation of lineralized vector DNA molecules, their 5′-phosphate groups were removed by treatment with the thermosensitive bacterial alkaline phosphatase (*see 2.2.2*). The reaction was performed according to the manufacture's instructions. The fragments of interest were then purified through agarose gel as described before (*see 2.6.2*).

2.6.6 Treatment of DNA with Klenow

Klenow fragment (DNA polymerase I large fragment) (*see 2.2.2*) was used to fill-in recessed 3′-termini of double-stranded DNA fragments. The reaction was carried out in accordance with the manufacture's manual.

2.6.7 Ligation of DNA with T4 ligase

For a ligation reaction, vector and insert DNA were usually taken in the molar ratio 1:3 to 1:6. Basic amount of the vector DNA varied from 30 to 50 ng. Ligations were carried out in 15 µl of 1 x ligation buffer at 16 ºC overnight or at 20 ºC for 4 h. In the case of ligation of blunt-ended DNA fragments, PEG 4000 was added to the final concentration of 5 %. The T4 ligase was then inactivated at 70 ºC for 10 min. The ligation mixture was finally dialyzed for 10 min through the Millipore White VSWP membrane (*see 2.2.3*) and subsequently used for bacterial transformation (*see 2.6.13*).

2.6.8 Amplification of DNA by PCR

Polymerase Chain Reaction (PCR) is a general method to amplify in vitro a specific nucleotide sequence from a matrix molecule, called template. In this work, PCR amplification was used to obtain specific DNA fragments from yeast genome and for the screening of yeast transformants with disrupted genes of interest. For cloning purposes, the Combi*Zyme* DNA polymerase mix and the *Pfu* DNA polymerase (*see 2.2.2*) were used, whereas the *Taq* and *Pwo* DNA polymerases (*see 2.2.2*) were taken to conduct the analytical tests.

Components of a typical PCR reaction were as follows:

- DNA template (20 -200 ng)

- downstream and upstream primers (both 50 pmol)

- dNTPs mix (dATP, dCTP, dGTP and dTTP in the final concentration of 100 µm) *- 10 x reaction buffer (10 µl)*

- $MgCl_2$ (in the final concentration of 250 µM)

- 2 U of the DNA polymerase

The following cycling conditions were generally used:

Initial denaturation		*94 °C, 5 min*
5 cycles	*Denaturation*	*94 °C, 1 min*
	Annealing	*T_m - 6 °C, 30 sec – 2 min*
	Elongation	*72 °C, 1 min/1000 bp*
25 cycles	*Denaturation*	*94 °C, 1 min*
	Annealing	*T_m - 3°C, 30 sec – 2 min*
	Elongation	*72 °C, 1 min/1000 bp*
Final elongation		*72 °C, 7 min*

Melting temperature of the primers was determined from the following equation:

$$T_m = 63.9 + 0.42\ (G + C) - 650/n,$$

where T_m is a melting temperature, in ºC, $(G + C)$ – a GC content of the primer, and n – a primer length. The composition of reaction mix and cycling conditions were slightly modified depending on the expected product length as well as enzyme and template used. PCR products were then purified by means of JETQUICK PCR Product Purification Spin Kit (*see 2.2.3*) in accordance with manufacture's instructions and sequenced as described below (*see 2.6.10*).

2.6.9 DNA sequencing

DNA sequencing was performed by the modified dideoxy-mediated chain termination method (Sanger *et al.*, 1977). For sequencing reactions, a CEQ™ DTCS Quick Start Kit (*see 2.2.3*) was used as described by manufacture. Sequencing itself was done with CEQ™ 2000XL DNA analysis system made by Beckman Coulter (*see 2.1*).

2.6.10 Isolation of plasmid DNA from *E. coli*

Plasmid DNA was usually isolated from *E. coli* cells grown overnight in 3 ml selective medium (*see 2.5.1*). For analytical digestions, plasmid isolation was carried out by the alkaline lysis method as described by Sambrook *et al.*, (1989). For sequencing and cloning procedures, DNA was separated with JETQUICK Plasmid Midiprep Spin Kit (*see 2.2.3*). For large-scale DNA preparations, JETSTAR Plasmid Midiprep Kit was generally used (*see 2.2.3*).

2.6.11 Isolation of DNA from *Y. lipolytica*

2.6.11.1 Rapid small-scale DNA isolation with glass beads

Solutions:

TEST buffer:	10 mM Tris-HCl (pH 8.0) 1 mM EDTA 100 mM NaCl 2 % Triton X-100 1 % SDS
TE buffer:	10 mM Tris-HCl (pH 8.0) 1 mM EDTA

Isolation of yeast DNA was performed according to the procedure described by Hoffman and Winston (1987) with minor modification. This method was used for the preparation of yeast chromosomal DNA from *Y. lipolytica* transformants for analytical needs.

In brief, yeast cells were grown in 10 ml of YPD medium (*see 2.4.3*) until stationary phase, harvested by centrifugation (for 5 min at 5000 rpm), washed once with water and resuspended in 200 µl of TEST buffer. Then 200 µl of phenol and 0.3 g of glass beads were added to cells, and they were disrupted by vortex mixing for 3 min. The obtained suspension was mixed with 200 µl of TE buffer and centrifugated for 5 min at 13000 rpm. The aqueous phase was then transferred to a new tube and treated with 400 µl of phenol-chloroform-isoamyl alcohol (25:24:1) mix. Phenol traces were subsequently extracted with 400 µl of chloroform-isoamyl alcohol (24:1). At last, DNA was precipitated by 1 ml of absolute ethanol, washed once with 70 % ice-cold ethanol, dried in a speed-vac and resuspended in 40 µl of TE buffer containing 100 µg/ml of RNase A.

2.6.11.2 Isolation of yeast DNA by spheroplast lysis

Solutions:

SP buffer:	1.2 M sorbitol 0.1 M potassium phosphate buffer (pH 6.5)
SPβ buffer:	20 mM β-mercaptoethanol in SP buffer
Zymolyase 20T:	10 mg/ml in SP buffer
Tris-EDTA buffer:	50 mM Tris-HCl (pH 7.4) 20 mM EDTA

This method was preferably used for the preparation of larger amounts of a high molecular weight yeast DNA for the following analysis by Southern blotting.

For this purpose, yeast cells were first pre-grown in 10 ml of YPD (*see 2.4.3*) medium for 24 h. Then 100 ml of fresh YPD medium were inoculated with 1 ml of the pre-culture and incubated for 8-12 h. Cells were harvested, washed once with water and resuspended in 10 ml of SPβ buffer. Next, 250 µl of zymolyase 20T and 200 µl of glusulase (*see 2.2.2*) were added to the cell suspension, and it was incubated at 37 ºC for 60-90 min (at least 90 % of cells should lost their cell wall). Spheroplasts were spun down by gently centrifugation, washed once with 10 ml of SP buffer and resuspended in 10 ml of Tris-EDTA buffer. For spheroplasts lysis, 1 ml of 10 % SDS was added to the suspension, and the lysate was incubated at 70 ºC for 30 min. Afterwards, proteins were precipitated by the addition of 3 ml of 5 M potassium acetate and following incubation on ice for 1 h. The probes were centrifuged for 10 min at maximal speed, and the supernatant was transferred to a new tube. Nucleic acids were precipitated with 0.7 volume of isopropanol for 10 min at room temperature, centrifuged at maximal speed for 10 min, washed once with 70 % ice-cold ethanol and dissolved in 5 ml of TE buffer (pH 8.0) containing 100 µg/ml of RNase A. Subsequently, probes were incubated at 37 ºC for 30 min to degrade RNA molecules. Remaining proteins were then extracted twice with phenol, once with phenol-

chloroform-isoamyl alcohol (25:24:1) mix and, finally, once with chloroform-isoamyl alcohol (24:1). DNA was then precipitated by adding 0.5 ml of 3 M sodium acetate and 5 ml isopropanol. The probes were incubated at room temperature for 10 min, centrifuged, washed once with ice-cold 70 % ethanol and air-dried. Finally, DNA pellet was dissolved in 500 µl of HPLC-grade water or TE buffer (pH 8.0).

2.6.12 Transformation of microorganisms

2.6.12.1 Transformation of *E. coli* by electroporation

Competent *E. coli* cells were prepared as described by Dower *et al.* (1998). The cells were then portioned in 40 µl aliquots and stored by -80 ºC.

For transformation, aliquots were firstly thawed on ice, mixed with 5 ng of plasmid DNA or 2 µl of ligation mix and transferred to the chilled electroporation cuvette (0.1 cm, PeqLab). Then electric pulse of 1.8 kV was applied to cell suspension, and 960 µl of SOC medium (*see 2.4.2*) were added to cell immediately. Cells were incubated at 37 ºC for 1 h and, finally, plated out on selective plates (*see 2.5.1*) and incubated at 37 ºC overnight.

2.6.12.2 Transformation of *Y. lipolytica* by lithium acetate method

Solutions:

Lithium acetate buffer:	0.1 M lithium acetate (pH 6.0)
Carrier DNA:	5 mg/ml salmon sperm DNA in 50 mM TE buffer (pH 8.0), sonicated in the 500 bp range
PEG solution:	40 % PEG 4000 in lithium acetate buffer

Transformation of *Y. lipolytica* was performed according to the lithium acetate method described by Barth and Gaillardin (1996) with minor modification. This technique was mainly used for generation of mutant *Y. lipolytica* strains with genes of interest disrupted through homologous recombination.

For preparation of competent cells, yeast strain was first pre-grown in 5 ml of YPD-citrate medium (*see 2.4.3.2*) at 28 ºC for 24 h. Then three cultures (50 µl, 100 µl and 200 µl of pre-culture) were inoculated in 10 ml of YPD-citrate and incubated overnight. One of the cultures with cell density between 9 x 10^7 and 1,5 x 10^8 cells/ml was then harvested by centrifugation, washed twice with 10 ml TE buffer, resuspended in 10 ml of 0.1 M lithium acetate and incubated at 28 ºC for 1 h with gentle shaking. Afterwards, the cell suspension was spun down and resuspended in 1 ml of lithium acetate buffer. Competent cells were used immediately for transformation procedure.

For the transformation, 200 -500 ng of a linearized plasmid DNA were mixed with 5 µl of carrier DNA and incubated at 60 ºC for 5 min. Next, 100 µl of competent cells were added to the DNA, gently mixed and incubated at 28 ºC for 15 min. The cell suspension was then treated with 0.7 ml of 40 % PEG 4000 for 1 h with shaking. After the following heat shock at 39 ºC for 10 min, 1.2 ml of lithium acetate buffer was added to the cells, mixed gently once again, plated out on selective medium (*see 2.4.4*) and incubated at 28 ºC for several days.

2.6.13 Southern blotting

Solutions:

Depurination solution:	0.25 M HCl
Denaturation solution:	1.5 M NaCl, 0.5 M NaOH
Neutralization solution:	1.5 M NaCl, 0.5 M Tris-HCl (pH 7.5)
SSC solution:	0.3 M sodium acetate, 3 M NaCl

Southern blotting is a well-known technique commonly used for detection of specific DNA fragments by gel-transfer hybridization. In the course of this work, southern blotting and hybridization were performed in order to examine specific DNA fragments in genomes of transformed *Y. lipolytica* strains carrying gene disruption cassettes. Genomic DNA required for this method was prepared as described above (*see 2.6.12.2*).

In the beginning, approximately 600 ng of genomic DNA were overnight digested with appropriate restriction endonucleases (*see 2.6.3*) and resulting digest was separated in agarose gel without ethidium bromide as explained above (*see 2.6.1*). The separated DNA was consecutively treated with depurination, denaturation and neutralization solutions in order to get smaller single-stranded fragments, and then transferred from gel to a Hybond-N nylon membrane (*see 2.2.3*). Transfer of DNA was carried out in SSC solution using a Biometra Vacu-Blot system (*see 2.1*) and following recommendations of manufacture. After transfer, the DNA was permanently attached to the membrane by cross-linking using UV light.

For hybridization, probes were prepared with *Gene Images* random prime labeling module (*see 2.2.3*) as described in the manufacture's manual. Pre-hybridization, hybridization, re-hybridization (if needed) and washing steps were done according to the recommendations of the same manual. For membrane detection*, Gene Images* CDP-*Star* detection module (*see 2.2.3*) was used.

2.6.14 Plasmid construction

In the course of this work, several predicted *Y. lipolytica* genes, which may be involved in the autophagic peroxisome degradation in this yeast, should have been disrupted in order to confirm their functions. Towards this aim, two sets of plasmids were constructed. First set included plasmids carrying fragments of genes of interest amplified from *Y. lipolytica* genomic DNA. Second set was created by cloning of *Y. lipolytica URA3* gene into these fragments in order to destroy respective ORFs. Plasmids from the second set were then used for the disruption of selected *Y. lipolytica* genes by integrative transformation (*see 2.6.13.2*).

2.6.14.1 Construction of plasmids carrying fragments of selected *Y. lipolytica* genes

Fragments of seven *Y. lipolytica* genes probably implicated in peroxisome degradation were amplified from the genomic DNA of *Y. lipolytica* strain PO1d by PCR using specific oligonucleotides as primers (*see 2.2.6*). Obtained PCR products were treated with corresponding restriction endonucleases as described above *(see 2.6.3*) and cloned into the multiple cloning site of the vector pUCBM21. Primers used for fragment amplifications as well as restriction enzymes for their cloning are listed in the **Table 2.5**. Created plasmids were further used for construction of corresponding gene disruption cassettes.

Table 2.5 Overview of gene fragments, primers and restriction enzymes (RE) used for construction of plasmids carrying fragments of *ATG1*, *ATG6*, *ATG11*, *ATG18*, *VAC8*, *GCN2* and *PEP4* genes of *Y. lipolytica*. Plasmids indicated with symbols were made either by C. Hoffmann (*) or by C. Bodinus ($^{\#}$).

***Y. lipolytica* gene**	**Size of a cloned DNA-fragment**	**Primers for a fragment amplification**	**RE for molecular cloning**	**Obtained plasmid**
ATG1	1.82 kb	p181neu, p182neu	*Pst*I, *Bam*HI	pUCATG1
ATG6	0.82 kb	p121w, p122w	*Sal*I	pAPG6*
ATG11	3.4 kb	ATGXba, ATGBam	*Xba*I, *Bam*HI	pUCATG11
ATG18	2.08 kb	AUTvor, AUTrev	*Nco*I, *Bgl*II	pUCCVT18$^{\#}$
GCN2	1.06 kb	Y283-1, Y283-2	*Pae*I	pUCGCN2
PEP4	2.61 kb	pPEP4vor, pPEP4rev	*Pae*I	pUCPEP4

2.6.14.2 Construction of plasmids carrying cassettes for gene disruption

Plasmids described in the chapter 2.6.15.1 were then used for construction of disruption cassettes for corresponding *Y. lipolytica* genes. For this purpose, *URA3* gene from *Y. lipolytica* was inserted into the cloned fragments of the first plasmid set. General strategies for the *YlURA3* cloning as well as sizes of obtained *URA3*-flanked regions are presented in the **Table 2.6**. In most cases, the *YlURA3* fragment was amplified from the plasmid pINA443 by PCR using specific primers with additional recognition sites for restriction endonucleases (RE) in their 5′-regions (*see 2.2.6*). Functionality of the amplified *YlURA3* gene was tested either by sequencing (*see 2.6.10*) or directly by transformation of *Y. lipolytica ura3*$^{-}$ cells. For the construction of plasmids pCVT18URA3 and pPEP4URA3, a fragment carrying *YlURA3* gene was cut out directly from the plasmid pINA443 with the endonuclease *Sal*I. Obtained *URA3* fragments were then cloned into corresponding recognition sites of plasmids described in the **Table 2.5** (*see 2.6.15.1*), so that protein-coding sequences of *Y. lipolytica* genes of interest were disrupted by the *URA3* insertion. Constructed plasmids were further used as a source of fragments for integrative transformation of *Y. lipolytica* strain PO1d[pLG3] (*see 2.3.2*) in order to generate mutants with disrupted genes of interest.

Table 2.6 General strategies for cloning of the *Y. lipolytica URA3* gene and plasmids obtained after *YlURA3* insertion. Abbreviation "RE" means restriction endonuclease. Plasmids indicated with symbols were made either by C. Hoffmann (*) or by C. Bodinus ($^{\#}$).

***ORF* to be disrupted**	**Origin of the *YlURA3*-gene**	**RE for *YlURA3* cloning**	**Obtained plasmid**	**Sizes of the *YlURA3*-flanked regions**
ATG1	pINA443; PCR with primers pURA2 and pURA22	*Cfr*42I	pATG1URA3	2.8 kb; 0.9 kb
ATG6	pINA443; PCR with primers pURANru1 and pURANru2	*Bsp*68I	pAPG6URA3*	0.27 kb; 0.55 kb
ATG11	pINA443; PCR with primers pURAcla1 and pURA-ClaI	*Bsu*15I	pATG11URA3	1.54 kb; 1.33 kb
ATG18	pINA443; RE-digestion	*Sal*I	pCVT18URA3$^{\#}$	1,6 kb; 0.49 kb
GCN2	pINA443; PCR with primers pURA3 and pURA4	*Bsp*68I	pGCN2URA3	0.4 kb; 0.66 kb
PEP4	pINA443; RE-digestion	*Sal*I	pPEP4URA3	1.31 kb; 1,3 kb

2.7 Protein techniques

2.7.1 Preparation of cell-free extracts

Cell-free extracts were prepared by mechanical disruption of cells using glass beads. Cell were harvested by centrifugation at 3000 rpm for 5 min, washed once with 1 volume of ice-cold 0.05 M potassium phosphate buffer (pH 7.4) and resuspended in 1 ml of ice-cold phosphate buffer containing protease inhibitor cocktail (*see 2.2.1*). Probes were then stored at -20 ºC overnight. For protein extraction, probes were thawed on ice, washed once with fresh chilled phosphate buffer and resuspended in 300-500 µl of phosphate buffer with protease inhibitor cocktail. All following steps were performed at 4 ºC! About 0.3 g of chilled glass beads (0.25-0.5 mm) was added to the cells, and they were disrupted by mixing on the Retsch vibrating shaker (*see 2.1*) for 10 min. The probes were then centrifuged for 10 min at 3000 rpm, the supernatants were collected and centrifuged once again for 5 min. The obtained supernatants (crude extracts) were then transferred into new tubes and used for further experiments.

2.7.2 Determination of protein concentration by the Lowry method

Solutions:

Solution A:	2 % (w/v) Na_2CO_3 in 0.1 M NaOH
Solution B:	1 % (w/v) $CuSO_4 \cdot 5H_2O$
Solution C:	2 % (w/v) sodium potassium tartrate
Solution D:	49 ml of solution A mixed with 0.5 ml of solution B and 0.5 ml of solution C
Solution E:	1N Folin reagent (commercially available, diluted with distilled water)

To determine the protein concentration, the Lowry protein assay (Lowry *et al.*, 1951) was used. Briefly, samples were diluted 50- or 100-fold with 0.1 M NaOH, and 1 ml of the solution D was added to each probe, mixed well with vortex and incubated for 10 min at room temperature. Then 0.1 ml of solution E was added, the probes were immediately mixed and allowed to develop for the next 30 min. The extinctions were finally measured at λ = 720 nm against a blank probe (0.1 M NaOH instead of protein extract), and protein concentrations were determined by the comparison of absorbance values with a standard curve prepared using different BSA concentrations (0.01-0.4 mg/ml) dissolved in 0.1 M NaOH.

2.7.3 SDS polyacrylamide gel electrophoresis (SDS-PAGE)

Solutions:

Electrophoresis buffer:	0.25 M Tris 1.92 M glycine 1 % SDS

6 x sample buffer: 0.35 M Tris-HCl (pH 6.8)
30 % (v/v) glycerol
10 % (w/v) SDS
0.6 M DTT
0.012 % bromphenol blue

For electrophoretic separation of proteins, a discontinuous polyacrylamide gel (PAGE) under denaturating (i.e., SDS-presence) conditions was used (Laemmli, 1970). Electrophoresis was carried out in a PROT-RESOLV MINI-LC vertical gel electrophoresis system (*see 2.1*). Gel concentration was selected so that the proteins of interest were best resolved. The recipe for a commonly used gel composition is given in the **Table 2.7.**

Table 2.7 A typical composition of separating and stacking gels.

Components	Separating gel (10 %)	Stacking gel (5 %)	Stock solutions
Acrylamide solution	3.3 ml	0.83 ml	30 % acrylamide, 0.8 % bisacrylamide
Separating gel buffer	2.5 ml	-	1.5 M Tris-HCl (pH 8,8)
Stacking gel buffer	-	0.63 ml	0.5 M Tris-HCl (pH 6.8)
SDS solution	100 µl	50 µl	10 % (w/v) SDS
TEMED	5 µl	5 µl	undiluted
APS solution	100 µl	50 µl	10 % (w/v) APS
H_2O	4.0 ml	3.4 ml	
Total volume	10 ml	5 ml	

The separation gel solution was first poured, layered with isopropanol and allowed to polymerize for 30 min at room temperature. After its polymerization, the isopropanol was removed, the stacking gel was poured and a comb was inserted into the layer of stacking gel solution, and incubated another 30 min. Afterwards, the gel was placed into the electrophoresis apparatus filled with 1 x electrophoretic buffer, and the comb was carefully removed. Crude extracts prepared as described above (*see 2.7.1*) were mixed with 1/5 volume of 6 x sample buffer and heated at 95 ºC for 5 min. Probes containing 25-30 µg of denaturated protein were loaded per sample well. As a protein standard, the BechMark™ prestained protein ladder (*see 2.1*) was used. The proteins were then electrophoretically separated at the current of 25-30 mA (for stacking gel) and 50-60 mA (for separating gel) for 2-3 h.

2.7.4 Western blotting

Solutions:

Transfer buffer:	25 mM Tris 192 mM glycine 5 % methanol 0.001 % SDS
10 x Ponceau S solution:	2 % (w/v) Ponceau S 30 % (w/v) trichloracetic acid 30 % (w/v) 5-sulfosalicylic acid

Proteins sufficiently separated in SDS-PAGE were then transferred to the Immobilon-P PDVF transfer membrane (*see 2.2.3*) to enable their following immunodetection (*see2.7.5*). The protein transfer was done by means of semi dry electroblotting. For this procedure, stacking gel was first removed from separating gel, and the last one was equilibrated in transfer buffer for 15 min. At the same time, membrane was wetted in methanol for 30 sec, rinsed with distilled water and also equilibrated in transfer buffer. Afterwards, the gel and the membrane were placed between filter paper soaked in transfer buffer. This assembly was put into the PeqLab semidry electroblotter (*see 2.1*), and a current of 0.8 mA/cm_2 was passed. After 2 h of transfer, the membrane was removed from the blotter and stained with 1 x Ponceau S to visualize protein bands. At last, the membrane was left in blocking buffer (*see 2.7.5*) at 4 ºC overnight.

2.7.5 Immunodetection of blotted proteins

Solutions:

Washing buffer:	20 mM Tris-HCl (pH 7.6) 137 mM NaCl 0.1 % Tween 20
Blocking buffer:	5 % non-fat dry milk in washing buffer
Stripping buffer:	62.5 mM Tris-HCl (pH 6.7) 100 mM β-mercaptoethanol 2 % (w/v) SDS

Proteins transferred to a PDVF membrane were subsequently detected with specific antibodies directed against the proteins of interest. For this purpose, the overnight blocked membrane was briefly washed with washing buffer and incubated for 1 h with primary antibodies diluted in blocking solution as described above (*see 2.2.4*). The membrane was then washed three times with fresh washing buffer, incubated for the next 1 h with appropriate secondary antibodies (*see 2.2.4)* and finally washed three times with washing buffer. The detection of membrane was performed using ECL^{Plus} Western blotting detection system (*see 2.2.3*) according to the manufacture's instructions. For re-probing with another antibody, membrane was first incubated

with a stripping buffer at 50 ºC for 30 min, well washed with fresh washing buffer and then detected as described above.

2.7.6 Immunofluorescent detection of β-galactosidase

Solutions:

Zymolyase 20T solution:	15 mg/ml in water
Poly L-lysine solution:	0.5 % in water
Mounting solution:	1 % n-propyl gallate in SP buffer

Immunofluorescent labelling of the heterologous β-galactosidase in *Y. lipolytica* was performed according to the method described by Barth and Gaillardin (1996) with minor modifications. Cells were grown in 25 ml of minimal YEM medium (*see 2.4.4.2*) until a density of 1-$2 \cdot 10^7$ cells/ml. Then 2.5 ml of 37 % formaldehyde was added directly to the culture and incubated for 30 min at 28 ºC with occasional mixing. For spheroplasting, the cells were spun down, washed twice with SP solution (*see 2.6.12.2*), resuspended in 4 ml of SPβ (*see 2.6.12.2*) containing 40 µl of fresh zymolyase 20T mix and incubated at 30 ºC for 1 to 1.5 h with gently shaking. The spheroplasts were subsequently harvested by centrifugation (2000 rpm, 10 min), and the pellet was resuspended in 0.5 ml SP. About 30 µl of spheroplasts were spotted onto glass slides (9 mm reaction wells, Marienfield, Germany) covered before with poly L-lysine. The slides were then washed with SP solution until cells were not overlapping and let air dry. For cell permeabilization, slides were immersed in chilled methanol for 3 min, then in chilled acetone for 10 sec and again air dried. All next steps were performed in a humid box! Spots were covered with 50 µl of blocking solution (*see 2.7.5*) and incubated for 30 min at room temperature. Blocking solution was then removed, and about 50 µl of anti-β-galactosidase antibody (*see 2.2.4*) diluted 1:100 in blocking buffer were added to each spot. After 1 h of incubation, primary antibody was removed, spots were washed with blocking solution, and the cells were finally covered with 50 µl of 1:80 diluted Texas red-conjugated secondary antibody (*see 2.2.4*) and incubated another 1 h. For control, secondary antibody was replaced by blocking solution. At last, slides were covered with mounting solution to protect against photo-bleaching and with a coverslip (edges of coverslip can be sealed with a nail polish). Slides were stored at -20 ºC in the dark and then viewed with fluorescent microscope as described below (*see 2.9*).

2.7.7 Enzyme assays

2.7.7.1 Determination of the activity of isocitrate lyase

The activity of isocitrate lyase (ICL) was assayed spectrophotometrically as described by Dixon and Kornberg (1959). In the course of this assay, glyoxylate produced as a result of the

enzymatic conversion of isocitrate reacts with phenylhydrazine. The absorbance of resulting phenylhydrozone can be measured at 324 nm. Since the reaction requires a certain time to reach a steady-state, measurements were recorded starting 3 min after the onset of activity. Changes in absorbance were then followed continuously on a Pharmacia Biotech spectrometer (*see 2.1*). Components essential for the assay performance are listed in the **Table 2.8**.

Table 2.8 Components required for the measurement of the ICL activity.

Component	**Stock solution**	**Final concentration**	**Volume (ml)**
Tris-HCl (pH 7.4)	100 mM	67 mM	0.8 (± x)
$MgCl_2$	50 mM	5 mM	0.15
Cystein HCl	20 mM	2 mM	0.15
D,L-isocitrate	16,7 mM	1.67 mM	0.15
Phenylhydrazine HCl	33 mM	3.3 mM	0.15
Sample			0.1 (± x)

The specific activity of isocitrate lyase was then calculated using the following equation:

$$A_{ICL} = \frac{\Delta E_{324}}{17 \times \Delta t \times C_{prot}} \times k,$$

where A_{ICL} is a specific ICL-activity, in U/mg of the whole protein: ΔE_{324} corresponds to the changes in the extinction at 324 nm determined during time Δt, in min; C_{prot} means a protein concentration in the sample; 17 is the absorbance coefficient for phenylhydrozone, in $mM^{-1}cm^{-1}$, and k is a dilution coefficient.

Cell-free extracts used for the measurement of the specific ICL activity were prepared as described above (*see 2.7.1*).

2.7.7.2 Determination of the activity of β-galactosidase

Solutions:

Z-buffer (pH 7.0): 60 mM Na_2HPO_4
40 mM $NaH_2PO_4 \cdot H_2O$
10 mM KCl
1 mM $MgSO_4 \cdot 7H_2O$
50 mM β-mercaptoethanol (fresh added)

ONPG solution: 13.3 mM in Z-buffer w/o mercaptoethanol

The activity of β-galactosidase (β-Gal) was determined in cell-free extracts (*see 2.7.1*) by the continuous method. The basis of this method is a β-galactosidase-catalyzed hydrolysis of *o*-nitrophenyl-β-D-galactopyranoside (ONPG) in the course of which a yellow-coloured *o*-nitrophenol is released. The formation of *o*-nitrophenol was monitored spectrophotometrically at 420 nm for 3 min. The activity of β-galactosidase was then determined according to the following equation:

$$A_{GAL} = \frac{\Delta E_{420}}{1.91 \times \Delta t \times C_{prot}} \times k ,$$

where A_{GAL} means specific β-galactosidase activity, in U/mg of the protein; ΔE_{420} is the change in the extinction at 420 nm determined during time Δt, in min; C_{prot} means a protein concentration in the sample; 1.91 is the absorbance coefficient for *o*-nitrophenol, in $mM^{-1}cm^{-1}$, and k is a sample dilution coefficient.

2.8 Construction of *Y. lipolytica* mutants via gene disruption technique

The fulfilment of this work required elucidation of functions of some predicted autophagy-related proteins from *Y. lipolytica*. For this purpose, wild type alleles of the corresponding *Y. lipolytica* genes were disturbed by use of the gene disruption technique. This method is based on the *in vivo* homologous recombination between chromosomal and plasmid copies of the targeted DNA fragment. As a marker for selection of transformed yeast cells, homologous *YlURA3* gene was used. *Y. lipolytica* strain PO1d(pLG3) was generally transformed by the lithium acetate method (*see 2.6.12.2*) using a linearized plasmid carrying a recombinant cassette for gene disruption (*see 2.6.14.2*). Yeast transformants were selected on minimal medium without uracil. Correct integration of the gene disruption cassettes was first checked by PCR (*2.6.8*) using synthetic oligonucleotides as screening primers (*listed in 2.2.6*) and then confirmed by the Southern hybridization (*2.6.13*) with specific probes against both analyzed and homologous *YlURA3* genes (a 1.7 kb *Sal*I-fragment of the plasmid pINA443). Obtained mutant strains were then used for further biochemical and microscopical analyses in order to characterize the course of pexophagy in *Y. lipolytica*.

2.8.1 Construction of the *Y. lipolytica atg1* mutant

To construct the *Y. lipolytica atg1* mutant, the plasmid pATG1URA3 was used. This plasmid was digested with restriction endonucleases *Pst*I and *Bam*HI and then transformed into *Y. lipolytica* strain PO1d(pLG3). Yeast transformants were selected for correct integration of the

gene disruption cassette by PCR analysis with synthetic oligonucleotides p180w-1 and p180w-2 as primers (*see 2.2.6*), and two clones (№№ 14 and 15) were chosen for the subsequent Southern blot hybridization. Genomic DNA samples from the initial strain as well as from the selected clones were digested with enzymes *Pst*I and *Bam*HI. The plasmid pUCATG1 was treated with *Bam*HI and *Kpn*2I, and the resulted fragment of 0.32 kb was labelled and used as a probe for the followed hybridisation. After the detection, the membrane was washed and probed with the labelled *Sal*I-fragment that carries *YlURA3* gene. A schematic view of the *YlATG1* wild-type and disrupted loci as well as the obtained Southern blots are presented in **Fig. 2.1**. Hybridization of the *YlATG1* probe with genomic DNA from the wild-type strain produced a single fragment with estimated length about 1.82 kb. At the same time, strains with disrupted *atg1* locus (*YlATG1**) gave a smaller 1.25 kb fragment **(Fig. 2.1: B)**. These results agree well with the predicted ones **(Fig. 2.1: A)**. Disruption of the *YlATG1* locus was also confirmed by hybridization with the *YlURA3* probe. The appearance of additional bands due to the introduction of plasmid-borne *YlURA3* gene into the host nuclear genome was observed in this case **(Fig. 2.1: C)**. Another *URA3*-specific signals, which were also observed in the untransformed strain, resulted from hybridization of the probe with the remains of *YlURA3* locus previously disrupted by insertion of the heterologous *ScSUC2* gene into the genome of *Y. lipolytica* strain PO1d (Nicaud *et al.*, 1989).

2.8.2 Construction of the *Y. lipolytica atg6* mutant

Construction of the *Y. lipolytica atg6* mutant strain was done by C. Hoffmann and is described in details in her diploma thesis (Hoffmann, 2004). Briefly, cells of the strain PO1d(pLG3) were transformed with the *Sal*I-flanked gene disruption cassette from the plasmid pAPG6URA3, and transformants with restored uracil prototrophy were examined as described above. Genomic DNA was then isolated from three clones of interest (№№ 37, 42 and 64), digested with the *Eco*RI enzyme, separated through electrophoresis and hybridized with *YlATG6*-specific and *YlURA3*-specific probes. As shown on **Fig. 2.2**, *YlATG6* locus of the wild-type strains PO1d and PO1d(pLG3) remained intact, whereas it was disrupted by homologous integration of the cassette into genomic DNA of all three transformants.

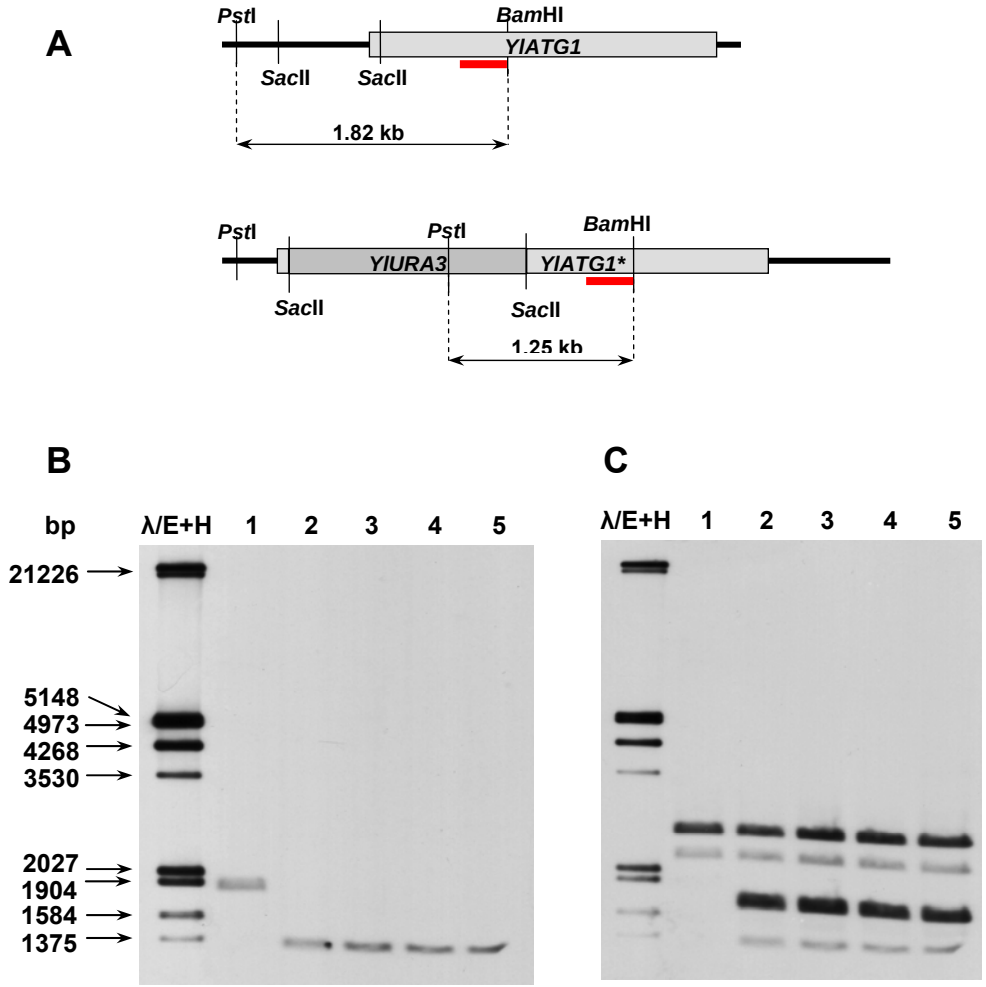

Figure 2.1 Disruption of the *YlATG1* gene.

(A) Schematic view of the intact (*YlATG1*) and disrupted (*YlATG1**) *ATG1* allele from the *Y. lipolytica* strain PO1d(pLG3). The disrupted allele contains the *YlURA3* gene between the *Sac*II recognition sites of the *ATG1* gene. Positions of the *YlATG1*-specific probe (red lines) and sizes of the predicted fragments are indicated.

(B) Hybridization of the *YlATG1*-specific probe with genomic DNA of the initial strain PO1d(pLG3) (lane 1) and selected transformants (lanes 2-5). Genomic DNA samples were digested with restriction enzymes *Pst*I and *Bam*HI. DNA of phage λ digested with *Eco*RI and *Hind*III enzymes was used as a molecular weight marker. The wild-type specific fragment (1.82 kb) is substituted by the smaller one (1.25 kb) in all analyzed transformants, confirming the disruption of the *YlATG1* locus.

(C) Hybridization of the *YlURA3*-specific probe with genomic DNA of the initial strain PO1d(pLG3) (lane 1) and selected transformants (lanes 2-5). Additional bands observed in all analyzed mutants in comparison to the initial strain indicate that *URA3* gene was indeed introduced in these strains upon transformation. The size of the lower fragment (1.25 kb) confirms specific nature of integration of the disruption cassette.

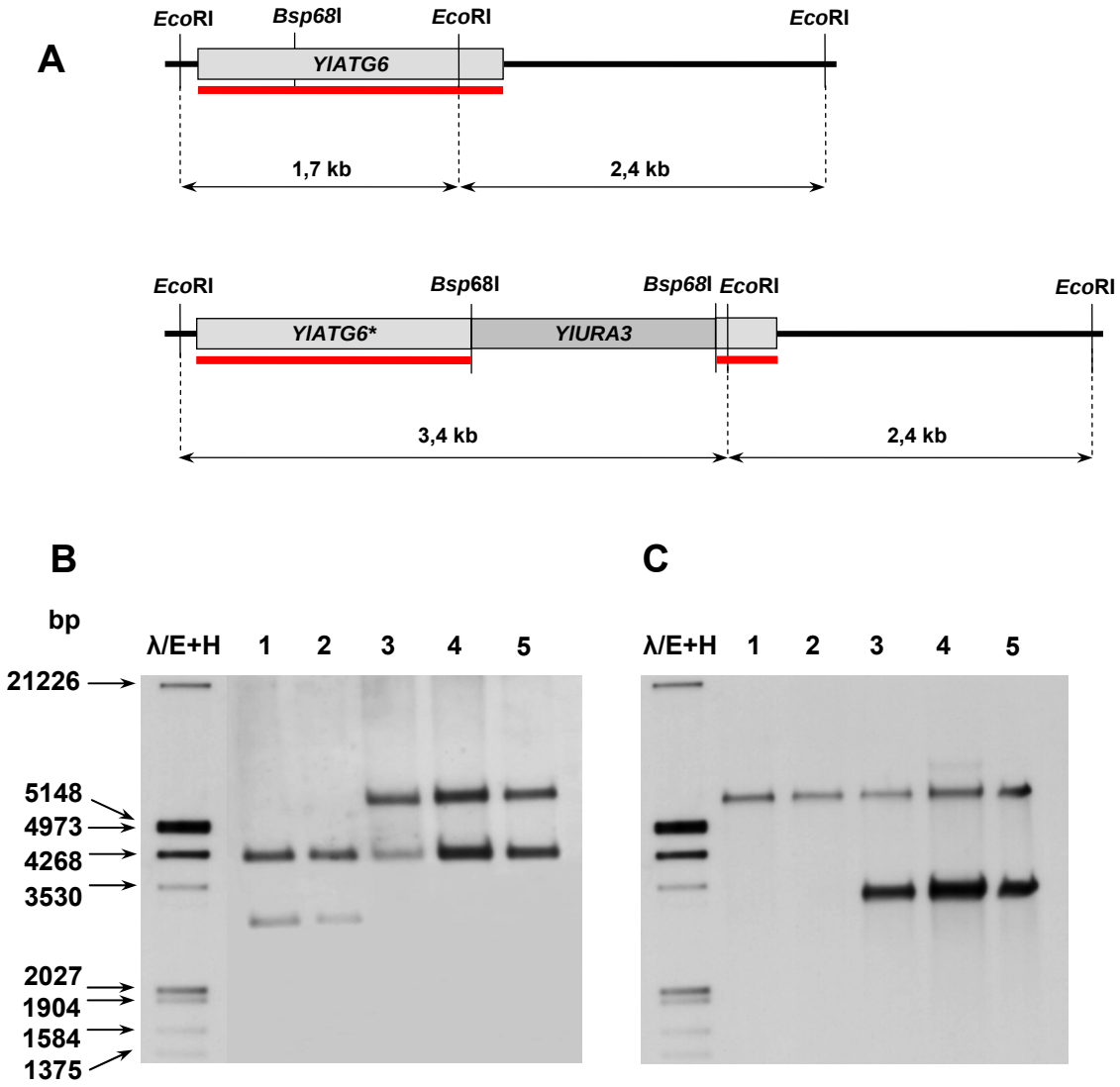

Figure 2.2 Disruption of the *YlATG6* gene (from Hoffmann, 2004).

(A) Schematic view of the intact (*YlATG6*) and disrupted (*YlATG6**) *ATG6* allele from the *Y lipolytica* strain PO1d(pLG3). The disrupted allele contains the *YlURA3* gene between the *Bsp*68I recognition sites of the *ATG6* gene. Positions of the *YlATG6*-specific probe (red lines) and sizes of the predicted fragments are indicated.

(B) Hybridization of the *YlATG6*-specific probe with genomic DNA of initial strains PO1d (lane 1) and PO1d(pLG3) (lane 2) as well as selected transformants (lanes 3-5). Genomic DNA was digested with the restriction enzyme *Eco*RI. DNA of phage λ digested with *Eco*RI and *Hind*III enzymes was used as a marker for indication of molecular weights. In all analyzed transformants, wild-type specific fragments (1.7 and 2.4 kb) are substituted by those specific for the mutant *atg6* allele (2.4 and 3.4 kb) that indicates disruption of the chromosomal *YlATG6* locus.

(C) Hybridization of the *YlURA3*-specific probe with genomic DNA of initial strains PO1d (lame 1) and PO1d(pLG3) (lane 2) as well as selected transformants (lanes 3-5). Additional *URA3* specific bands observed in all analyzed mutants in comparison to the untransformed strains indicate that *URA3* gene was indeed introduced in yeast genome upon transformation.

2.8.3 Construction of the *Y. lipolytica atg11* mutant

To construct the *atg11* mutant of *Y. lipolytica*, the strain PO1d(pLG3) with the wild-type *YlATG11* locus was transformed with plasmid pATG11URA3 previously treated with restriction enzymes *Xba*I and *Bam*HI to release a *URA3*-containing *ATG11*-directed disruption cassette. Transformed yeast cells were selected based on the restored ability to grow without uracil. Then genomic DNA was isolated from randomly selected clones and digested with the *Nco*I enzyme. Obtained samples were used for the following Southern blot analysis. The 1.83 kb *Pst*I-fragment from plasmid pUCATG11 and the 1.7 kb *Sal*I-flanked *YlUAR3* fragment were used as probes. The expected size of a wild-type band corresponding to the intact *YlATG11* gene was about 9.9 kb. In the case of successful gene disruption, this initial band should be broken into two smaller bands of 6.8 kb and 4.3 kb, respectively **(Fig. 2.3: A)**. The expected band pattern was observed in the transformants №№ 14, 15, 43 and 45 **(Fig. 2.3: B)**. Hybridization with the *YlURA3*-specific probe produced bands of the same size as well as some additional bands specific for disrupted *URA3* allele of the initial *Y. lipolytica* strain **(Fig. 2.3: C)**. Obtained results confirmed disruption of the *YlATG11* gene in the analyzed transformants. Appearance of the additional band of approximately 5.5 kb, which was present in both wild type and mutant strains, could be explained through non-specific interactions.

2.8.4 Construction of the *Y. lipolytica atg18* mutant

The *Y. lipolytica* strain with disrupted *ATG18* gene was constructed by C. Bodinus in the course of his diploma thesis (Bodinus, 2004). Briefly, the initial strain PO1d(pLG3) was transformed with the *YlATG18* disruption cassette from the plasmid pCVT18URA3. Yeast transformants were then analysed by PCR with synthetic primers CVTscreenvor and CVTscreenrev (*see 2.2.6*), and two positive clones (numbers 54 and 61) were selected for the followed Southern hybridization. For this purpose, genomic DNA from the initial strain and two transformants was digested with restriction endonucleases *Bam*HI and *Bgl*II. Then hybridizations with specific *YlATG18* (the *Bam*HI/*Bgl*II-fragment from plasmid pUCCVT18) and *YlURA3* probes were performed. The obtained Southern blots are presented in **Fig. 2.4**. These results confirmed disruption of the *ATG18* gene in both *Y. lipolytica* transformants. The wild type band (1.7 kb) is substituted by the novel one (3.7 kb), indicating specific insertion of the disruption cassette into genomic *ATG18* locus.

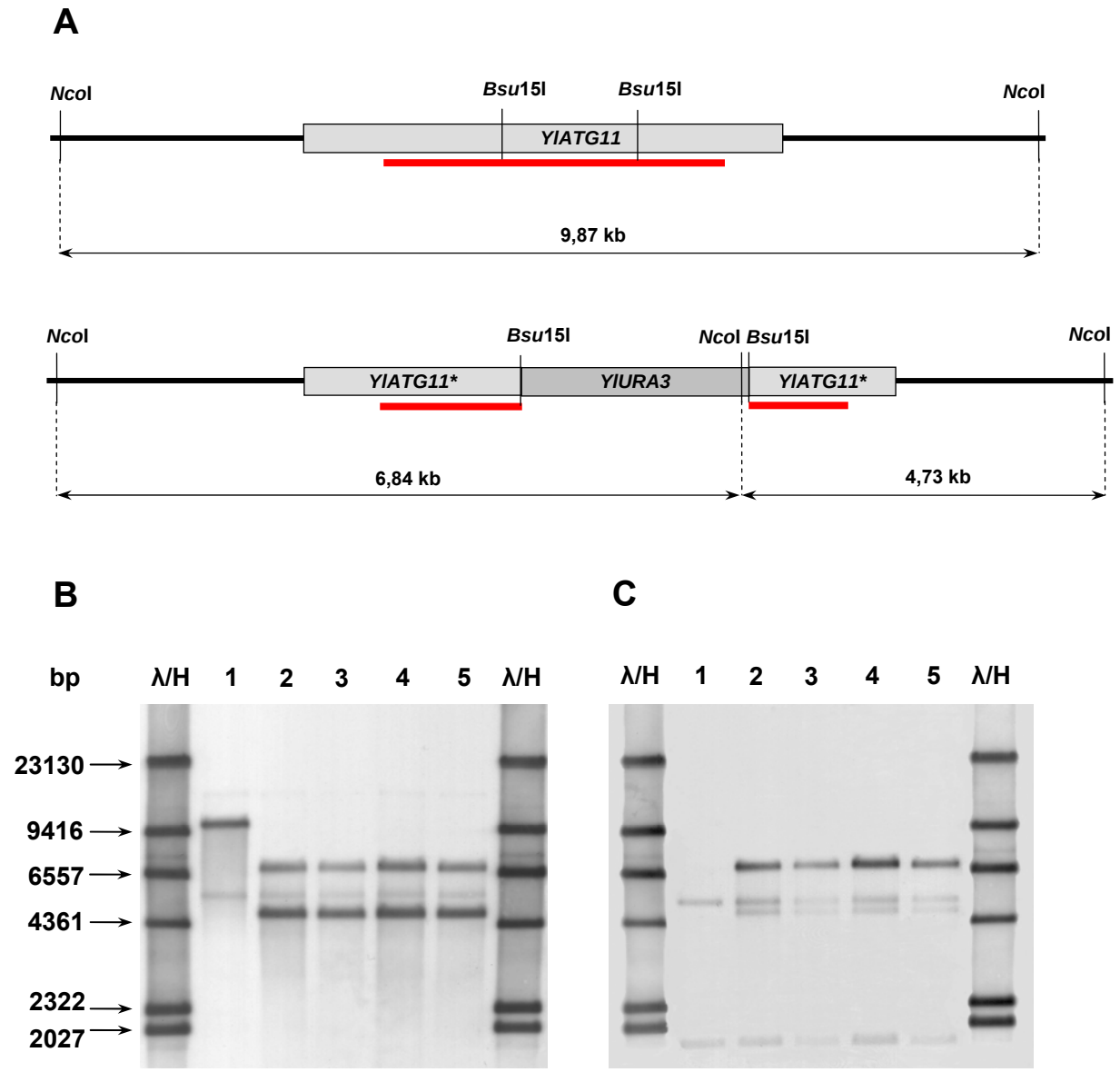

Figure 2.3 Disruption of the *YlATG11* gene.

(A) Schematic view of the intact (*YlATG11*) and disrupted (*YlATG11**) *ATG11* allele from the *Y. lipolytica* strain PO1d(pLG3). The disrupted allele contains the *YlURA3* gene between the *Bsu*15I recognition sites of the target gene. Positions of the *YlATG11*-specific probe (red lines) and sizes of the predicted fragments are indicated.

(B) Hybridization of the *YlATG11*-specific probe with genomic DNA of the initial strain PO1d(pLG3) (lane 1) and selected transformants (lanes 2-5). Genomic DNA samples were treated with the *Nco*I endonuclease. DNA of phage λ digested with the restriction enzyme *Hind*III was used as a molecular weight marker. In the wild-type strain, the fragment of about 9.9 kb corresponding to the intact *YlATG11* gene is observed. In transformants, this band is broken into two smaller bands of 6.8 and 4.7 kb that confirm correct insertion of the *ATG11* gene disruption cassette.

(C) Hybridization of the *YlURA3*-specific probe with genomic DNA of the initial strain PO1d(pLG3) (lane 1) and selected transformants (lanes 2-5). The *URA3*-specific hybridization pattern overlaps with that from the *ATG11*-specific hybridization and produces bands of the same size and two additional bands characteristic for disrupted *URA3* allele of the initial *Y. lipolytica* strain.

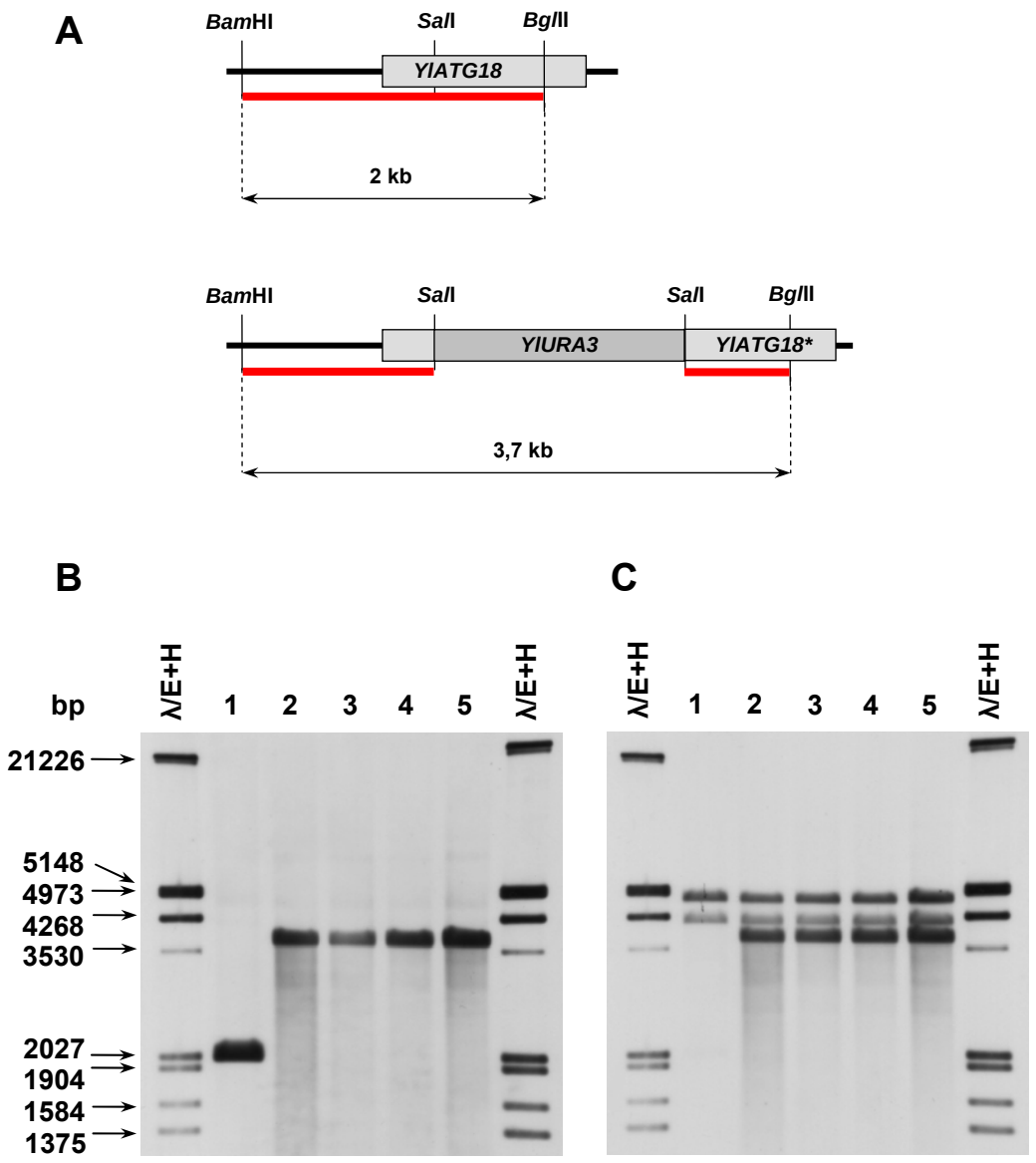

Figure 2.4 Disruption of the *YlATG18* gene (from Bodinus, 2004).

(A) Schematic view of the intact (*YlATG18*) and disrupted (*YlATG18**) *ATG18* allele from the strain PO1d(pLG3) of *Y. lipolytica*. The disrupted allele contains the *YlURA3* gene between the *Sal*I recognition sites of the *ATG18* gene. Positions of the *YlATG18*-specific probe (red lines) and sizes of the predicted fragments are indicated.

(B) Hybridization of the *YlATG18*-specific probe with genomic DNA of the initial strain PO1d(pLG3) (lane 1) and selected transformants (lanes 2-5). Genomic DNA was digested with restriction enzymes *Bam*HI and *Bgl*II. DNA of phage λ digested with *Eco*RI and *Hind*III enzymes was used as a molecular weight marker. The wild-type specific fragment (2 kb) is substituted by the larger one (3.7 kb) in all analyzed transformants, confirming specific disruption of the chromosomal *YlATG18* locus.

(C) Hybridization of the *YlURA3*-specific probe with genomic DNA of the initial strain PO1d(pLG3) (lane 1) and selected transformants (lanes 2-5). A specific 3.7 kb band which corresponds to the size of the disruption cassette is detected in all analyzed transformants. This data confirms the specific insertion of the *ATG18* disruption cassette into the genome of *Y. lipolytica*.

2.8.5 Construction of the *Y. lipolytica gcn2* mutant

Construction of the *Y. lipolytica gcn2* mutant strain was carried out essentially in the same way as described for previous mutant strains. For yeast transformation, the *GCN2* gene disruption cassette from the plasmid pGCN2URA3 was used. Correct integration of the cassette and disruption of the *YlGCN2* gene were first proved by PCR analysis using synthetic oligonucleotides pScreen5 and pScreen6 as primers (*see 2.2.6*) and then confirmed by the Southern blotting. For this purpose, genomic DNA from initial strain and some selected transformants (clones 18, 104, 124 and 169) were treated with enzymes *Eco*RI and *Xho*I. The specific *YlGCN2* probe was prepared by enzymatic digestion of the plasmid pUCGCN2 with the restriction endonuclease *Pae*I. A predicted hybridization pattern with the *GCN2*-directed probe is shown in **Fig. 2.5 (A)**. Insertion of the disruption cassette into the chromosomal *GCN2* locus should lead to substitution of the wild type fragment of 2.1 kb with two fragments of 1.5 kb and 2.3 kb, respectively. As is evident from Southern blots, the *GCN2* probe indeed recognized both predicted fragments in the genomic DNA of the analyzed transformants **(Fig. 2.5: B**). Following hybridization with the *YlURA3*-specific probe also produced two bands of the same length together with an additional one corresponding to the remained chromosomal *URA3* locus **(Fig. 2.5: C)**. Taken together, these data confirmed disruption of the chromosomal *GCN2* gene in all analyzed *Y. lypolytica* transformants.

2.8.6 Construction of the *Y. lipolytica pep4* mutant

For construction of the *pep4* mutant of *Y. lipolytica*, the plasmid pPEP4URA3 was first digested with restriction endonucleases *Pae*I and *Bam*HI and then transformed into *Y. lipolytica* strain PO1d(pLG3). Yeast transformants with disrupted *YlPEP4* gene were selected by PCR with synthetic primers pPEP4screenvor and pPEP4screenvrev (*see 2.2.6*), and two clones (№№ 25 and 54) were chosen for the following blotting. The restriction endonuclease *Sma*I was used for digestion of the genomic DNA. *PEP4*-specific probes were obtained after digestion of the plasmid pUCPEP4 with enzymes *Pae*I and *Hind*III. The Southern hybridization showed that the wild type-specific band of 11.6 kb disappeared in both transformants. The single novel band of 7.5 kb appeared in the transformant 25, whereas two novel fragments, 7.5 kb and 5.7 kb respectively, were observed in the transformant 54 **(Fig. 2.6: B)**. Thus, only band pattern of the transformant 54 corresponds to the predicted one **(Fig. 2.6: A)**. Hybridization with the *YlURA3*-specific probe provided additional support for the insertion of *PEP4* gene disruption cassette into chromosomal *PEP4* locus in this clone **(Fig. 2.6: C)**.

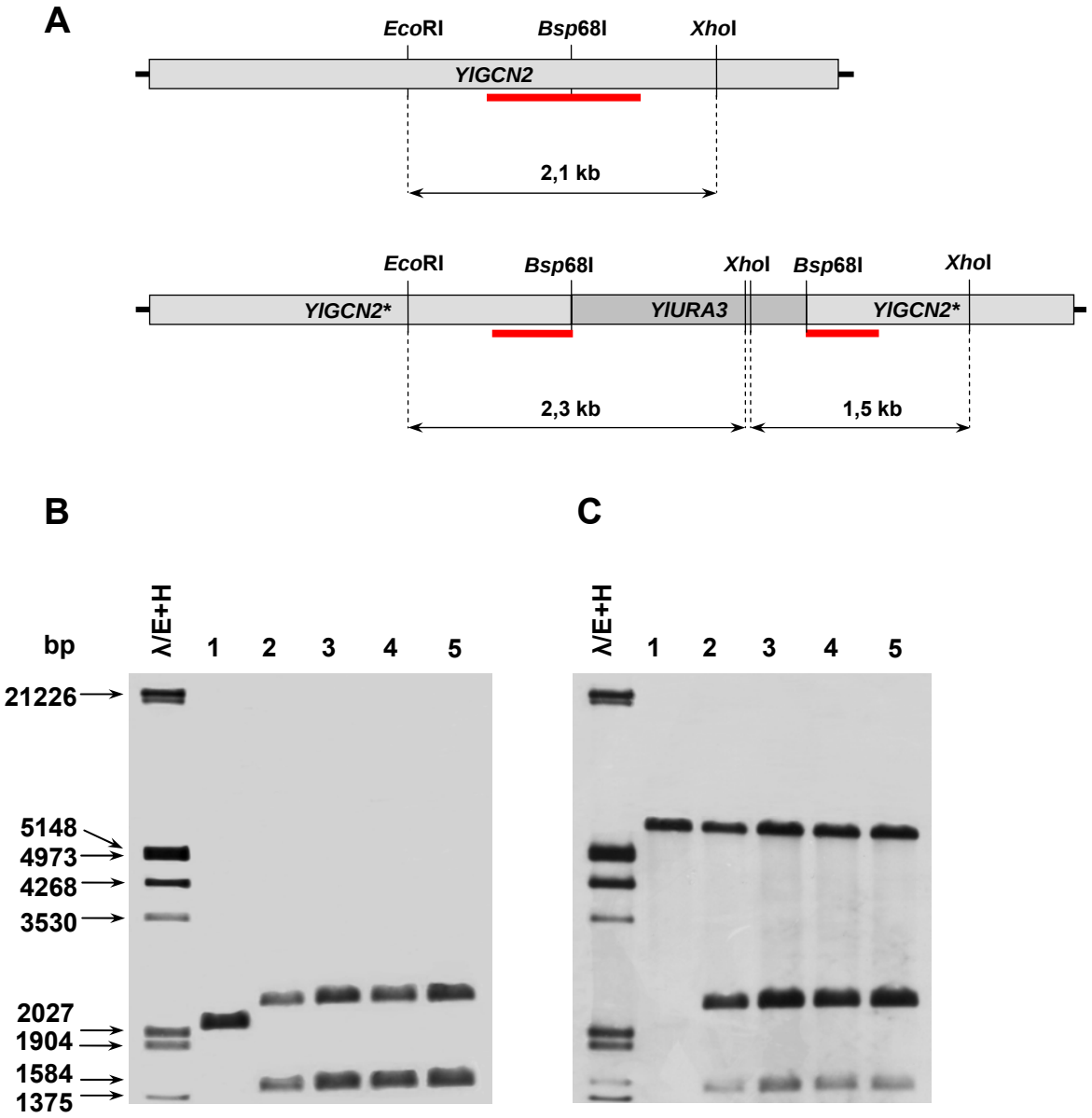

Figure 2.5 Disruption of the *YlGCN2* gene.

(A) Schematic view of the intact (*YlGCN2*) and disrupted (*YlGCN2**) *GCN2* allele from *Y lipolytica* strain PO1d(pLG3). The disrupted allele contains the *YlURA3* gene between the *Bsp*68I recognition sites of the *GCN2* gene. Positions of the *YlGCN2*-specific probe (red lines) and sizes of the predicted fragments are indicated.

(B) Hybridization of the *YlGCN2*-specific probe with genomic DNA of the initial strain PO1d(pLG3) (lane 1) and selected transformants (lanes 2-5). Genomic DNA was digested with restriction enzymes *Eco*RI and *Xho*I. DNA of phage λ digested with *Eco*RI and *Hind*III enzymes was used as a molecular weight marker. The wild-type specific fragment (2.1 kb) is substituted with two novel fragments (1.5 and 2.3 kb) in all analyzed transformants, confirming the disruption of the *YlGCN2* gene.

(C) Hybridization of the *YlURA3*-specific probe with genomic DNA of the initial strain PO1d(pLG3) (lane 1) and selected transformants (lanes 2-5). In all transformed strains, two bands of the same length (1.5 and 2.3 kb) are produced upon treatment with the *URA3*-specific probe. These results indicate that the *URA3* gene was specifically introduced in these strains upon transformation.

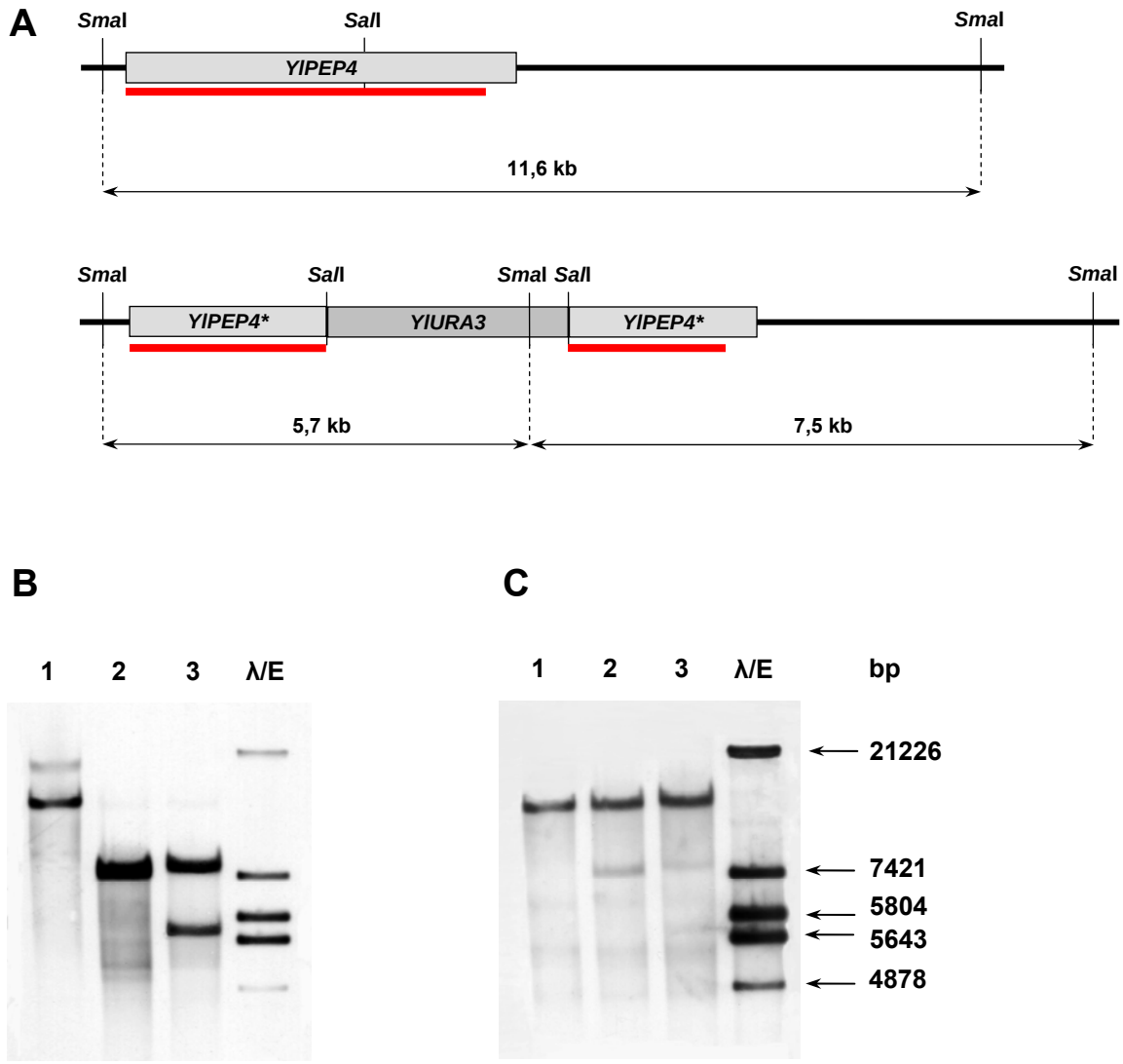

Figure 2.6 Disruption of the *YlPEP4* gene.

(A) Schematic view of the intact (*YlPEP4*) and disrupted (*YlPEP4**) *PEP4* allele from the strain PO1d(pLG3) of *Y. lipolytica*. The disrupted allele contains the *YlURA3* gene between the *Sal*I recognition sites of the *PEP4* gene. Positions of the *YlPEP4*-specific probe (red lines) and sizes of the predicted fragments are indicated.

(B) Hybridization of the *YlPEP4*-specific probe with genomic DNA of the initial strain PO1d(pLG3) (lane 1) and selected transformants (lanes 2,3). Genomic DNA was treated with the restriction enzyme *Sma*I. DNA of phage λ digested with the endonuclease *Eco*RI was used as a molecular weight marker. The single 7.5 kb band is observed in the first mutant strain (lane 2), whereas two bands of predicted sizes of 5.7 and 7.5 kb were detected in the genome of the second mutant (lane 3). Both analyzed transformants lost the11.6 kb fragment specific for the intact *YlPEP4* gene.

(C) Hybridization of the *YlURA3*-specific probe with genomic DNA of the initial strain PO1d(pLG3) (lane 1) and selected transformants (lanes 2,3). Weak signals corresponding to the introduced *YlURA3* gene from the *PEP4* disruption cassette are observed in both transformants confirming its specific insertion into the host genome.

2.9 Mutagenesis and mutant selection

Solutions:

Washing buffer:	0.1 M potassium citrate buffer (pH 5.5)
MNNG-solution:	25µg/ml MNNG in washing buffer
Assay-mixture:	100 ml Z-buffer (see 2.7.7.2) 0.27 ml β- mercaptoethanol 1.67 ml X-gal (of 20 mg/ml stock solution)

Mutants of *Y. lipolytica* were obtained by treatment of cells with N-methyl-N'-nitro-N-nitrosoguanidine (MNNG) as described by Barth and Gaillardin (1996). Briefly, yeast cells were pre-grown in 10 ml of YPD medium (*see 2.4.3*) at 28 ºC overnight. Next day, a main culture of 130 ml was inoculated with 0.5 ml of the pre-culture and incubated at 28 ºC with agitation till the early log phase. The cells were centrifuged, washed twice with one volume of washing buffer, and the cell pellet was then resuspended in MNNG-solution. The obtained cell suspension was incubated with gentle agitation for 20 min at room temperature. Afterwards, cells were well washed with minimal medium w/o carbon source and resuspended in 25 ml of YPD medium containing 15 % of glycerol. The cell aliquots were then plated out on YPD plates and incubated at 28 ºC for several days. The viability of MNNG-treated cells should be under 2 % comparing to the non-treated cells in order to achieve a high percentage of mutant phenotypes.

For selection of *Y. lipolytica* mutants with defects in the process of autophagical degradation of peroxisomes, a β-galactosidase filter assay developed by Gunkel (2000) with some modifications was used. The system is based on the coloured reaction mediated by the P_{ICL1}-regulated expression of heterologous β-galactosidase. The detailed description of this procedure is given in Appendix (Fig. 7.17). Basically, mutagenezied cells expressing chimerical protein βGal-eGFP(SKL) were first pre-grown on YPD-plates and then replica plated onto YEM-plates (*see 2.4.4.2*) containing ethanol as a sole carbon source to stimulate peroxisome proliferation. Plates were incubated at 28 ºC for about 19 h. Cells were subsequently transferred with a filter onto fresh YGA- and YGW-plates (*see 2.4.4.2*) and incubated another 8 h in order to induce degradation of the organelles. Cells were next permeabilized by incubation of the filter for 10 sec in liquid nitrogen and air-dried at room temperature. For the following filter assay, the filter with cells was put onto a new one soaked with the assay mixture and incubated for 1-2 h at 28 ºC. Mutant cells with remained activity of the β-galactosidase were coloured blue, whereas cells of the wild type became pale due to the inactivation and following degradation of the reporter protein.

2.10 Fluorescence microscopy

Solutions:

FM4-64 solution: 2 mg/ml in DMSO

To study morphology of autophagical processes in *Y. liypolytica*, dual fluorescent staining of peroxisomes with eGFP and vacuoles with FM4-64 was performed. For visualization of peroxisomes, cells of *Y. lipolytica* strain PO1d(pLG3) (*see 2.3.2*) expressing chimerical peroxisomal protein βGal-eGFP(SKL) were used. Yeast vacuole membrane staining was carried out using a red fluorescent dye FM4-64 as first proposed by Vida and Emr (1995). Yeast cells were cultivated as described above (*see 2.5.2*). Then, 3 µl of the FM4-64 solution was added to 3 ml of cell suspension from the main culture I and incubated with agitation at 28 ºC for 2 h. Afterwards cells were washed once with 0.05 M potassium phosphate buffer (pH 7.4) and inoculated in 30 ml of the main culture II. For microscopical analysis, aliquots of the main culture II were taken every two hours, washed once with ice-cold potassium phosphate buffer and viewed under Olympus fluorescent microscope BX60 (*see 2.1*). eGFP fluorescent signal was visualized with a F41-017 filter set (excitation wavelength about 480-520 nm) and FM4-64 was visualized with a rhodamine filter (510-550 nm). Images were processed with a "Soft Imaging System analySIS" and Adobe Photoshop 7.0 software.

2.11 Bioinformatics

Sequences of putative *Y. lipolytica* proteins showing homology to known autophagy and autophagy-related proteins from other organisms were found using Internet databases of the Génolevures (http://cbi.labri.fr/Genolevures/) and the National Centre for Biotechnology Information (http://www.ncbi.nlm.nih.gov/). For this purpose, nucleotide-nucleotide (blastn), protein-protein (blastp) as well as translated (tblastn and tblastx) BLAST searches of NCBI and *Y. lipolytica* genome sequencing consortium were performed (Altschul *et al.*, 1990). Multiple sequence alignments were obtained by means of the ClustalX 1.81 programme (Thompson *et al.*, 1997) and further adjusted with the GeneDoc programme (Nicholas *et al.*, 1997). Phylogenetic trees were generated using again the ClustalX 1.81 and then visualized with TreeView, Version 1.5.2 (Page, 1996). Accession numbers of proteins included in the phylogenetic analysis are listed in the **Table 2.6**. For prediction of functional protein domains of *Y. lipolytica* counterparts, NCBI Reverse Position Specific BLAST (Marchler-Bauer and Bryant, 2004), ScanProsite (Gattiker *et al.*, 2002) and TopPred (von Heijne, 1992) tools from the ExPASy proteomics server (http://au.expasy.ch/tools/) were used. *Saccharomyces* Genome Database

(http://www.yeastgenome.org/) was searched for additional information on *S. cerevisiae* proteins of interest.

Table 2.6 List of proteins used in alignments and for generation of phylogenetic trees. Protein designations are as annotated in the NCBI database.

Protein	Organism	NCBI accession number	References
Atg1	*S. cerevisiae*	P53104	Matsuura *et al.*, 1997
Pdd7	*H. polymorpha*	AAL23618	Komduur *et al.*, 2003
Gsa10	*P. pastoris*	AAL77195	Stromhaug *et al.*, 2001
Ulk1	*H. sapiens*	AAC32326	Kuroyanagi *et al.*, 1998
Ulk2	*H. sapiens*	NP_055498	Yan *et al.*, 1999
Atg6	*S. cerevisiae*	Q02948	Kametaka *et al.*, 1998
Beclin1	*H. sapiens*	NP_003757	Liang *et al.*, 1999
Atg11	*S. cerevisiae*	Q12527	Kim *et al.*, 2001
Gsa9	*P. pastoris*	AAG30291	Kim *et al.*, 2001
Pdd18	*H. polymorpha*	AAR12210	Komduur *et al.*, unpubl.
Atg21	*S. cerevisiae*	Q02887	Stromhaug *et al.*, 2004
Atg21	*H. polymorpha*	AAR87854	Leao-Helder *et al.*, 2004
Atg18	*S. cerevisiae*	P43601	Guan *et al.*, 2001
Atg18	*H. polymorpha*	AAV74416	Leao-Helder *et al.*, 2004
Gsa12	*P. pastoris*	AAL67674	Guan *et al.*, 2001
WIPI-1alpha	*H. sapiens*	AAV80760	Proikas-Cezanne *et al.*, 2004
WIPI49-like	*H. sapiens*	AAH07596	Strausberg *et al.*, 2002
Hsv2	*S. cerevisiae*	NP_011739	Tettelin *et al.*, 1997
Hsv2	*H. polymorpha*	AAV74417	Leao-Helder *et al.*, 2004
Gcn2	*S. cerevisiae*	P15442	Roussou *et al.*, 1988
eIF2 alpha kinase	*H. sapiens*	NP_001013725	Berlanga *et al.*, 1999
Pep4	*S. cerevisiae*	P07267	Woolford *et al.*, 1986; Ammerer et al., 1986
Pep4	*H. polymorpha*	AAB68519	Bae *et al.*, unpubl.

Protein	Organism	NCBI accession number	References
Yps1	*H. polymorpha*	AAQ06628	Sohn *et al.*, unpubl.
Yps1	*P. pastoris*	AAR11771	Werten and de Wolf, 2005
Cathepsin D	*H. sapiens*	P07339	Faust *et al.*, 1985

3 Results

3.1 Construction and characterization of *Y. lipolytica* strain PO1d(pLG3) expressing chimerical protein βGal-eGFP(SKL)

In the first part of this thesis project, the non-conventional alkane-assimilating yeast *Y. lipolytica* should be established as an experimental model to explore the process of autophagic degradation of peroxisomes. Towards this end, a genetically modified strain of *Y. lipolytica* possessing properties required for this study should be constructed and characterized.

3.1.1 Construction of *Y. lipolytica* strain expressing a chimerical protein βGal-eGFP(SKL)

The suitability of *Y. lipolytica* as a model system to identify genes involved in the biogenesis of peroxisomes has been already demonstrated by numerous genetic studies (Nuttley *et al.*, 1993; Titorenko *et. al.*, 2000). However, a lack of a proper easy-to-handle genetic marker to visualize peroxisomal compartment appears to be a critical disadvantage for studies on peroxisomal turnover in this yeast. To overcome this problem, an artificial construct bearing the bacterial β-galactosidase (βGal) fused with the enhanced green fluorescent protein (eGFP) and targeted to peroxisomes by the C-terminal PTS1-signal (SKL) was developed (Gunkel, 2000). The sequence encoding this construct was placed under the control of a strong, regulated promoter of the homologous isocitrate lyase (*YlICL1*), the enzyme, previously shown to be localized to peroxisomes in ethanol/ethylamine-grown *Y. lipolytica* cells (Gunkel, 2000). The plasmid pLG3 carrying the *LacZ-eGFP(SKL)* gene fusion was linearized with the restriction endonuclease *Not*I and introduced into the *Y. lipolytica* strain PO1d. Randomly selected transformants were then analyzed by Southern hybridization to confirm a presence of the construct in their genomes. Towards this end, genomic DNA was isolated from six transformants, digested with the endonuclease *Eco*32I, separated in an agarose gel, transferred to a nylon membrane and hybridized with the *LacZ-eGFP(SKL)*-specific probe (1.93 kb *Sac*I-fragment from the plasmid pLG3). The results of the hybridization are shown in **Fig. 3.1**. Obtained data demonstrated a presence of the fragment of interest (2.95 kb) in all tested clones (lines 2-7). Conversely, the initial *Y. lipolytica* strain PO1d (lane 1) was found to lack this fragment. The clone 3 (lane 4) in following named as PO1d(pLG3) was selected for further studies.

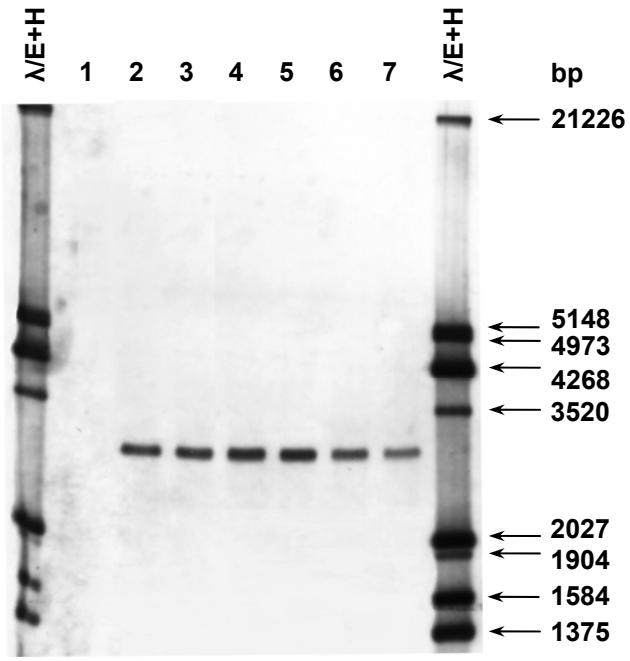

Figure 3.1 Detection of the βGal-eGFP(SKL)-coding fragment in genomes of some *Y. lipolytica* transformants. Hybridization of the *LacZ-eGFP(SKL)*-specific probe with genomic DNA of the initial strain PO1d (lane 1) and selected transformants (lanes 2-7) is shown. Genomic DNA was treated with the restriction endonuclease *Eco*32I. As a molecular weight marker, DNA of phage λ digested with *Eco*RI and *Hind*III enzymes was used. All tested transformants contain the 2.95 kb fragment indicating integration of the *LacZ-eGFP(SKL)* fusion construct in their genomes. In contrast, no *LacZ-eGFP(SKL)*-specific signal could be detected in untransformed *Y. lipolytica* strain PO1d.

3.1.2 Intracellular localization of chimerical protein βGal-eGFP(SKL)

The addition of SKL-motif at the C-terminus of the chimerical protein βGal-eGFP(SKL) ensure its targeting into peroxisomes. To confirm this prediction, the intracellular localization of βGal-eGFP(SKL) was determined by indirect immunofluorescence microscopy as described in *Materials and Methods (2.7.6*). In ethanol/ethylamine-grown cells of the strain PO1d(pLG3), the β-galactosidase-specific staining was almost wholly confined to spot-like structures in the peripheral cytoplasm (see right panel from the **Fig. 3.2**). Such localization pattern is known to be characteristic for vesicle-like compartments. On the other hand, the eGFP-specific signal showed a dual distribution: a homogenous staining associated with the centre of the cell, and a dispersed spot distribution within the cytoplasm (middle panel from the **Fig. 3.2**). The unusual bulk staining pattern may be explained through self-fluorescence of the cellular cytoplasm pulled together due to osmotic pressure on the spheroplast's membrane. The eGFP-specific spot-like structures, in turn, most probably correspond to peroxisomes which are pushed out to the surface of spheroplasts. The overlay of both β-galactosidase- and eGFP-specific localization

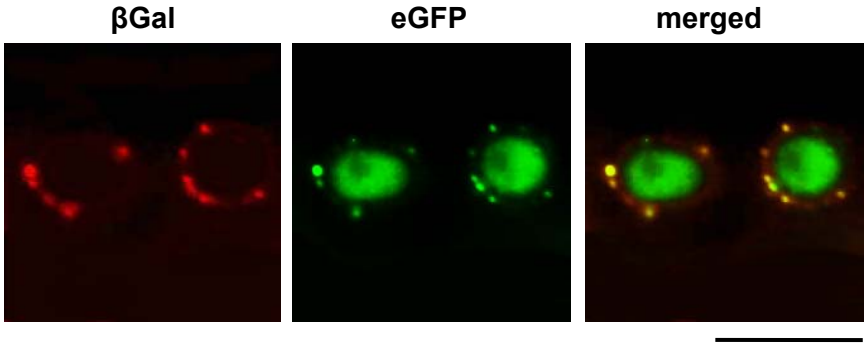

Figure 3.2 Immunocytochemical localization of the recombinant protein βGal-eGFP(SKL) in the ethanol/ethylamine-grown cells of *Y. lipolytica* strain PO1d(pLG3). Cells expressing chromosomal *lacZ-eGFP(SKL)* gene fusion were grown in medium inducing peroxisome proliferation, harvested by centrifugation, dehydrated with formalin, converted to spheroplasts, fixed on slides and subjected to the immunoreaction with specific antibodies. Slides were then mounted with the mounting medium and viewed with a fluorescence microscope. The heterologous β-galactosidase was visualized using Texas Red conjugated Ig (left panel). The eGFP fluorescence is showed in green (middle panel). The merged image of both fluorescent signals was produced computationally using the Adobe Photoshop 7.0 program (right panel). The bar is equal to 20 μm.

patterns revealed a high rate of overlap of these fluorescent signals (right panel from **Fig. 3.2**), indicating that the heterologous eGFP and β-galactosidase were most probably co-localized to peroxisomes in living ethanol/ethylamine-grown cells of *Y. lipolytica*. In contrast, no β-galactosidase-specific fluorescence could be detected in the negative control sample incubated without secondary antibodies (data not shown).

These results demonstrated that, under tested conditions, the chimerical SKL-tagged protein βGal-eGFP(SKL) could be sufficiently expressed and is incorporated in its target organelle, the peroxisome. Next question to be explored was whether the fate of this protein reflected physiological status of peroxisomes under different cultivation conditions affecting peroxisomal homeostasis in yeast cells.

3.1.3 Expression of chimerical protein βGal-eGFP(SKL) under conditions of peroxisome biogenesis

Two media containing either oleic acid (1 %) or ethanol (1 %) as a sole carbon source (YOM and YEM, respectively) were chosen to induce peroxisome biogenesis in *Y. lipolytica*. Additionally, up to 2 % of ethylamine was added to both media in order to intensify the proliferation rates, as recommended by Gunkel (2000). Yeast cells of the strain PO1d(pLG3) were incubated as described in *Materials and Methods* (*2.5.2*), samples were taken at indicated times, and then cell-free extracts were prepared and subjected to the biochemical and Western blot analyses (see *2.7*).

As illustrated in **Fig. 3.3**, the specific activity of peroxisomal ICL increased dramatically upon cell growth in both oleate/ethylamine- **(A)** and ethanol/ethylamine- **(B)** containing media, reaching its maximum after 8-10 h (oleic acid) and 10-13 h (ethanol) of incubation. After these time points, however, a rapid decrease in the ICL activity was observed most obviously due to the glucose-dependent phosphorylation of this protein as shown in *S. cerevisiae* and *Y. lipolytica* (Lopez-Boado *et al.*, 1988, Barth *et al.*, unpublished data). Altogether, these data correlate well with previously reported kinetics of the carbon source-dependent induction of the *YlICL1* promoter (Juretzek, 1999; Gunkel, 2000). Surprisingly, the specific ICL-activity appeared to be slightly higher on the medium containing ethanol as a sole carbon source, although cell growth rates on ethanol were found to be about two times lower comparing to those characteristic for a medium with oleic acid. Similarly, the increase in specific β-galactosidase activity was also observed in both oleate- and ethanol-grown cells. Moreover, the *YlICL1*-driven expression of heterologous β-galactosidase showed essentially the same tendency compared to the homologous ICL expression **(Fig. 3.3)** that is also in line with our previous data on regulation of the *YlICL1* promoter (Juretzek, 1999). As expected, no specific β-galactosidase activity could be determined in cells of the strain PO1d(pINA443) expressing a control "empty" vector (data not shown).

The results described above were confirmed by the following Western blotting using antibodies directed against *Y. lipolytica* ICL and bacterial β-galactosidase **(Fig. 3.4)**. The last antibody was used to detect the protein βGal-eGFP(SKL) in transformed yeast cells. As evident from **Fig. 3.4 (A, B)**, bands corresponding to both native ICL (62 kDa) and heterologous βGal-eGFP(SKL) (106 kDa) proteins could be observed in all analyzed samples. Notably, the 106 kDa band characteristic for the recombinant protein showed much lower intensity if compared with the ICL-specific band, although the same membranes were used for immunodetection. This observation could be explained by (i) a generally low level of the heterologous βGal-eGFP(SKL) protein expression, (ii) an improper protein conformation that may affect specific antigen-antibody interactions, and (iii) intracellular degradation of this artificial protein by the yeast vacuole. The last reason appears to be most probable since a few minor signals with lower molecular weights were observed in some cases with antibodies against β-galactosidase. At the same time, expression of the recombinant protein βGal-eGFP(SKL) itself had no influence on the cell growth (data not shown). However, obvious peaks could be detected on membranes detected with anti-β-galactosidase antibodies after 8-10 h (oleate-grown cells) and

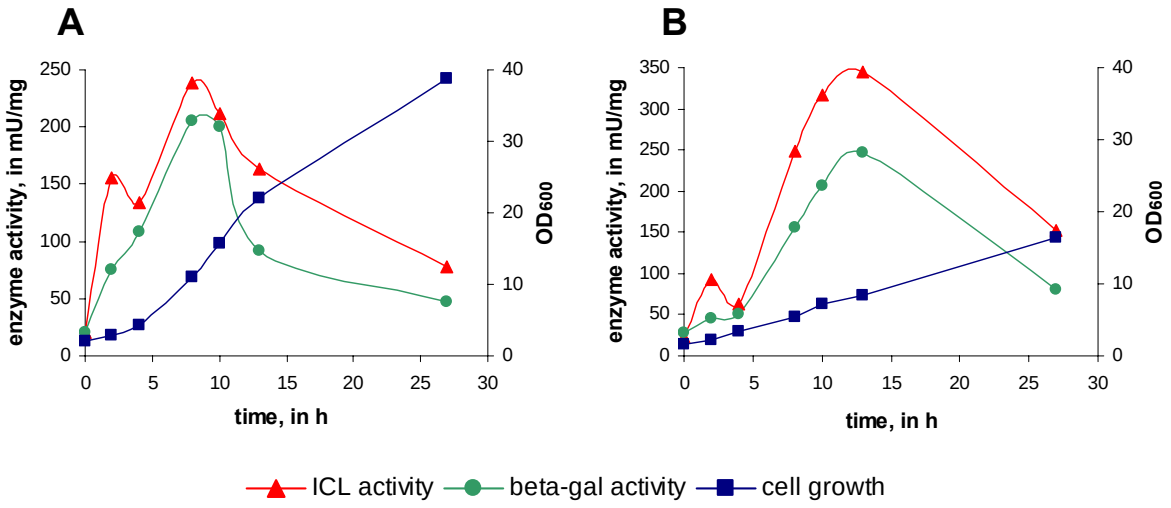

Figure 3.3 Changes in the activities of isocitrate lyase (ICL) and β-galactosidase (beta-gal) under the peroxisome biogenesis inducing conditions. Cells of the *Y. lipolytica* strain PO1d(pLG3) were grown in oleic acid/ethylamine- **(A)** and ethanol/ethylamine- **(B)** containing media in order to induce peroxisome biogenesis. Samples were taken immediately (0 h) and after 2, 4, 8, 10, 13 and 27 h of incubation. Cell-free extracts were prepared and specific enzyme activities were determined, as described *(see 2.7.7)*. Results of one representative experiment are shown.

10-13 h (ethanol-grown cells) of cultivation that generally reproduced the results of enzyme kinetics. The apparent 24 h-decrease in the specific activity of β-galactosidase in the ethanol/ethylamine-grown cells could be most likely because of the inactivation of the whole protein, i.e. by posttranslational modifications. More detailed biochemical experiments should be performed in order to answer this question. Taken together, this data confirmed that the chimerical *YlICL1*-controlled protein βGal-eGFP(SKL) is expressed like a peroxisomal one under conditions leading to proliferation of these organelles.

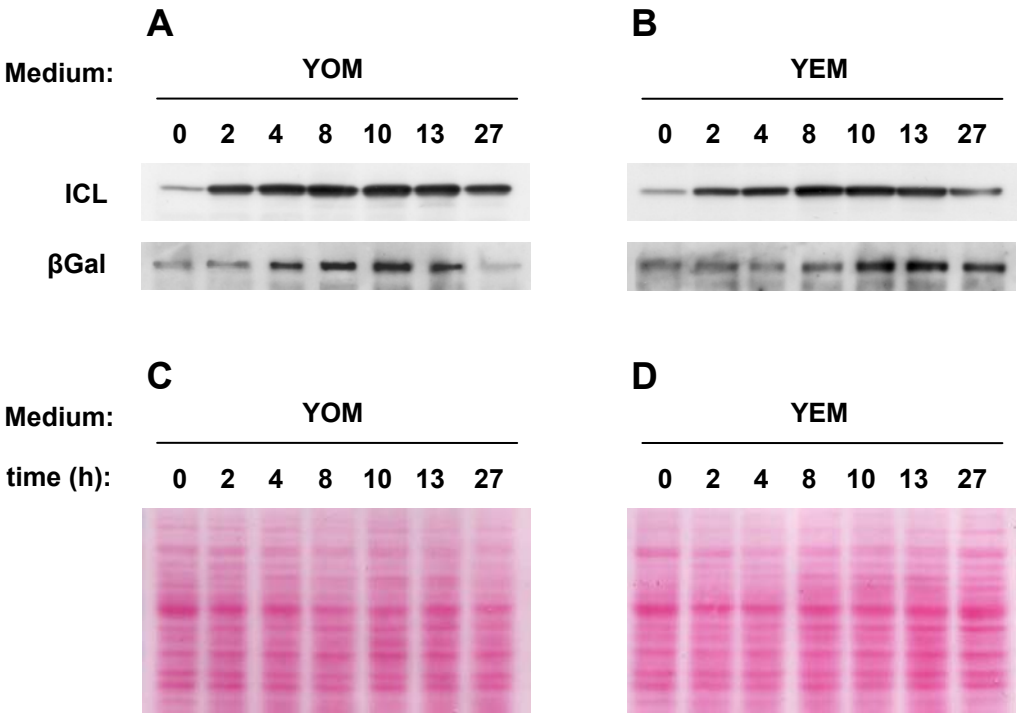

Figure 3.4 Changes in the levels of homologous (ICL) and heterologous (β-galactosidase) peroxisomal proteins under the peroxisome biogenesis inducing conditions. (A, B): Western blots performed with crude extracts of cells of the strain PO1d(pLG3) grown in oleic acid/ethylamine- **(A)** and ethanol/ethylamine- **(B)** containing media. Samples were collected immediately (0 h) and after 2, 4, 8, 10, 13 and 27 h of incubation. Blots were decorated with anti-ICL and anti-β-galactosidase antibodies. **(C, D):** The respective Ponceau S-stained membranes to show that equal amounts of the whole protein were loaded per lane. Abbreviations used for media: YOM, yeast extract/oleate/ethylamine; YEM, yeast extract/ethanol/ethylamine.

3.1.4 Expression of chimerical protein βGal-eGFP(SKL) under conditions of peroxisome degradation

To induce peroxisome degradation, cells of the *Y. lipolytica* strain PO1d(pLG3) were first cultivated as above (*3.1.3*), and then shifted into glucose-containing media with and without nitrogen source (YGA and YGW, respectively) as described in *Materials and Methods (2.5.2)*. Samples were taken at indicated time points and subsequently processed for the biochemical and Western blot analyses *(2.7)*.

The shift of ethanol/ethylamine-grown cells into glucose-containing media led to a rapid inactivation of both ICL and β-galactosidase **(Fig. 3.5)**. A half-reduction of these peroxisomal enzyme activities were found already after 2.5-3 h (for YGA medium) and 4 h (for YGW medium) of incubation. After 8-10 h of glucose adaptation, only 10-15 % of the initial activities could be measured. Although expression of the endogenous *YlICL1* promoter was shown to be

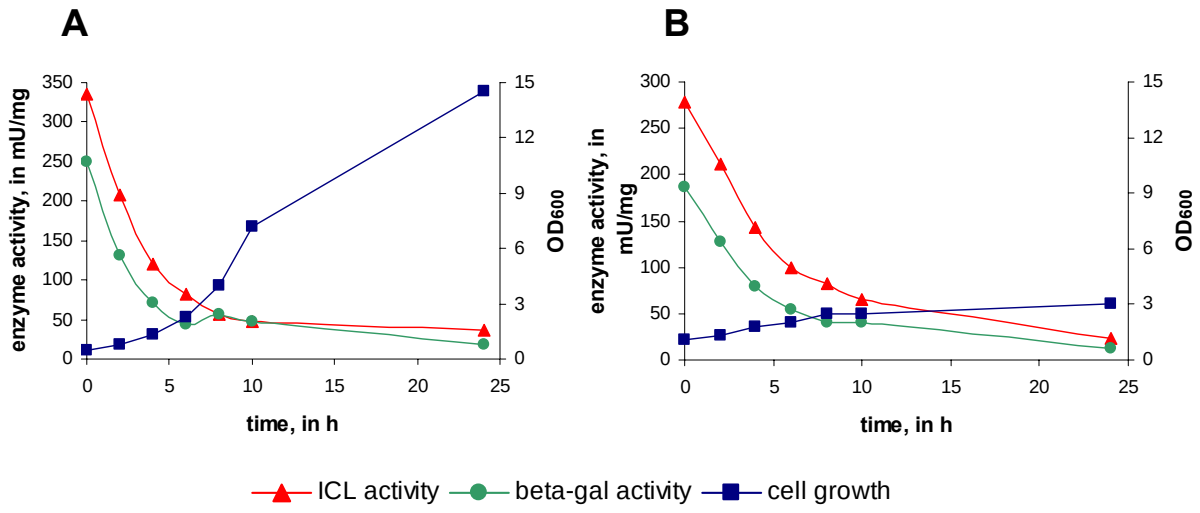

Figure 3.5 Changes in the activities of isocitrate lyase (ICL) and β-galactosidase (beta-gal) under the peroxisome degradation inducing conditions. Yeast cells expressing the chimerical protein βGal-eGFP(SKL) were grown in a ethanol/ethalymine-containing medium in order to induce peroxisome proliferation (*see 2.5.2*), and subsequently shifted into ammonium sulfate **(A)** and nitrogen depleted **(B)** glucose-containing media. Samples were taken immediately (0 h) and after 2, 4, 6, 8 and 24 h of incubation. Cell-free extracts were prepared and specific enzyme activities were determined as described *(see 2.7.7)*. Results of one representative experiment are shown.

rapidly repressed by glucose addition, about 10 % of the basal promoter activity could be still determined in glucose-grown cells (Juretzek, 1999). So, the enzyme activity profiles gained in this experiment correspond well with those observed previously. Essentially similar results were also achieved in the case of oleic acid/ethylamine-grown cells subjected to ammonium sulfate and nitrogen depleted glucose-containing media (data not shown).

To test whether the decreases in activities of peroxisomal enzymes were due to the reduced protein expression or because of specific protein degradation, Western blot analysis was then performed with the same cell-free extracts. As is evident from **Fig. 3.6**, the levels of peroxisomal marker proteins ICL (62 kDa) and THI (43 kDa)* basically decreased after transfer of ethanol/ethylamine-grown cells into both glucose-containing media. Similarly, amounts of the recombinant protein βGal-eGFP(SKL) (106 kDa) detected using specific antibody against bacterial β-galactosidase also reduced in accordance with incubation time. Remarkably, in glucose/ammonium sulfate-grown cells, the decrease in levels of analyzed proteins seemed to occur gradually in the course of cultivation **(Fig. 3.6: A)**. On the other hand, this process took

* In the case of THI detection, two signals showing essentially the same degradation tendencies were obtained in almost all experiments. The second, weak signal most likely corresponds to the acetoacetyl-CoA thiolase described for *Y. lipolytica* some time ago (Yamagami *et al.*, 2001).

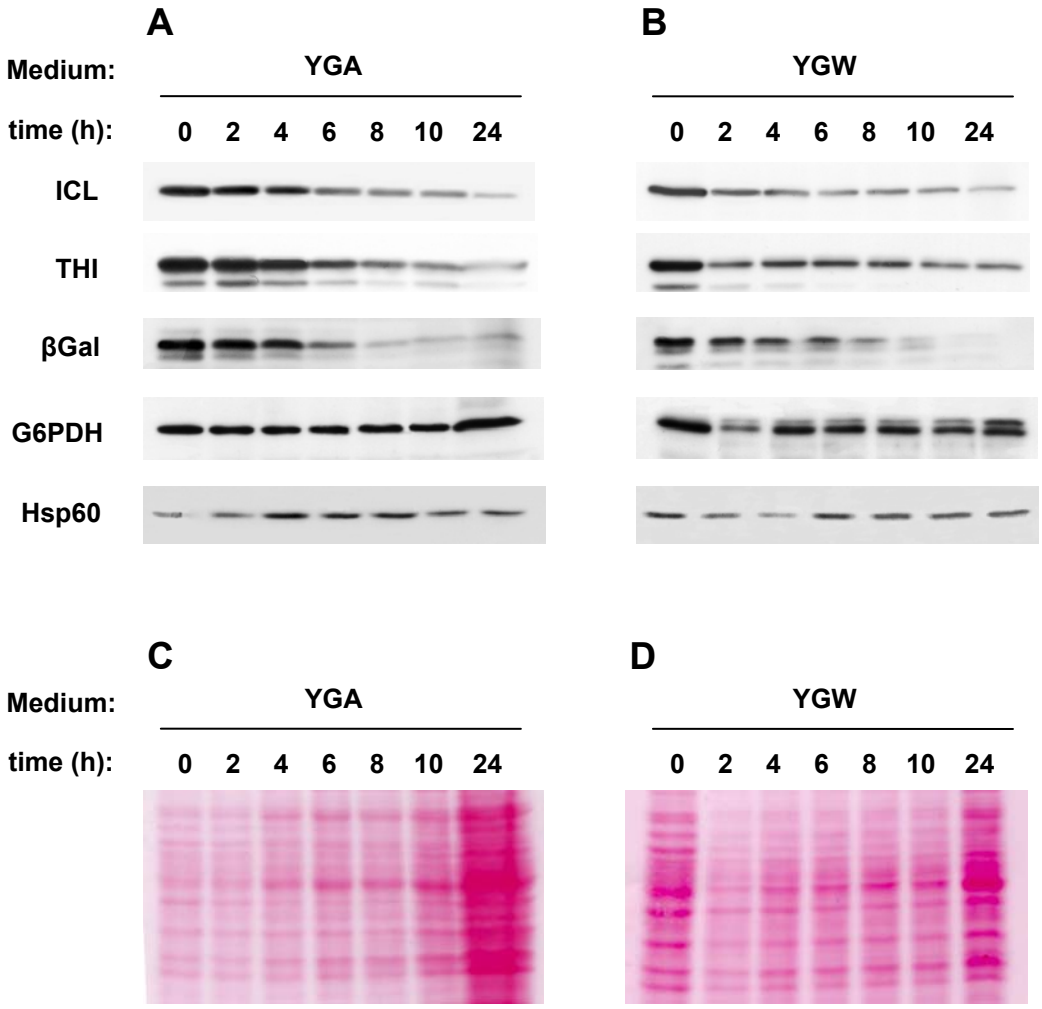

Figure 3.6 Changes in levels of some marker proteins under the peroxisome degradation inducing conditions. (A, B) Western blots performed with crude extracts of ethanol/ethylamine-grown cells of the strain PO1d(pLG3) subjected to glucose-containing media with **(A)** and without **(B)** nitrogen source. Samples were taken immediately (0 h) and after 2, 4, 6, 8, 10 and 24 h of incubation and proceeded as described under *2.7*. Blots were decorated with anti-isocitrate lyase (ICL), anti-thiolase (THI), anti-β-galactosidase (βGal), anti-glucoso-6-phosphate dehydrogenase (G6PDH) and anti-GroEL (Hsp60) antibodies. **(C, D)** The Ponceau S-stained membranes showing that equal volumes of cell-free extracts were loaded per lane. Abbreviations used for media: YGA, yeast extract/glucose/ammonium sulfate; YGW, yeast extract/glucose without nitrogen source.

place more rapidly under glucose/nitrogen starvation conditions: a fast reduction of levels of these proteins could be detected already after 2 h of incubation remaining then almost constant, regardless of the prolonged incubation time **(Fig. 3.6: B)**. So, in *Y. lipolytica*, the glucose-induced degradation of peroxisomal enzymes may occur at different rates depending on the presence or absence of a nitrogen source in growth media.

The cytosolic marker protein G6PDH, in contrast, did not degrade during cell growth in a medium containing glucose and ammonium sulfate **(Fig. 3.6: A)**. Moreover, intensity of the

G6PDH-specific signal was found to considerably increase under these conditions. Such expression pattern is typical for a continuously expressed cytosolic enzyme and corresponds to the increase in quantities of the whole protein due to the cell growth, as illustrated by the Ponceau S-stained membrane **(Fig. 3.6: C)**. On the other hand, under glucose/nitrogen starvation conditions, a 2 h-decrease in G6PDH levels was observed, consistent with that shown for peroxisomal proteins. Such rapid degradation of this cytosolic enzyme may be well explained through its up-taking by the vacuole due to a bulk autophagy triggered in response to nitrogen depletion. After 4 h of cell growth in YGW medium, the G6PDH-specific signal became again more intense and remained unaffected with prolonged incubation time **(Fig. 3.6: B)**. Importantly, the same tendency was noticed for total cellular protein amounts, as is evident from the membrane visualized with Ponceau S **(Fig. 3.6: D)**. A comparable degradation pattern was also observed for the mitochondrial protein Hsp60 detected with the antibody against bacterial chaperonin GroEL, which exhibits cross-reactivity with a respective *Y. lipolytica* counterpart **(Fig. 3.6: A, B).** This data indicated that also mitochondria were degraded during non-specific autophagic processes. At the same time, these organelles remained intact if both C- and N-sources were present in growth media.

Thus, the inactivation of peroxisomal enzymes ICL and β-galactosidase was not only due to the glucose-induced repression of the *YlICL1* promoter but also because of the specific degradation of these proteins. Furthermore, no essential differences could be revealed between the degradation patterns of homologous ICL and thiolase and heterologous β-galactosidase under both tested conditions. Altogether, the above experiments provide strong evidence that the chimerical *YlICL1*-controlled protein βGal-eGFP(SKL) possesses the expression and degradation profiles characteristic for a peroxisomal enzyme under peroxisome degradation-inducing conditions.

3.2 Fluorescence microscopic detection of peroxisomal turnover in *Y. lipolytica* by the use of chimerical protein βGal-eGFP(SKL)

Expression of the recombinant protein βGal-eGFP(SKL) was next used to monitor the course of pexophagy in *Y. lipolytica* by fluorescent microscopy. For this purpose, cells of the strain PO1d(pLG3) were cultivated as in previous experiments *(see chapter 3.1.4)* to induce turnover of peroxisomes. The probes were taken for indicated time points from both glucose-grown cultures and examined by fluorescence microscopy as described in *Materials and Methods (2.9)*. Peroxisomes were specifically visualized by the eGFP fluorescence due to the heterologous

βGal-eGFP(SKL) expression. Vacuolar membranes, in turn, were stained with the hydrophobic vital dye FM4-64 as described in *Materials and Methods (2.9)*.

As shown in **Fig. 3.7**, yeast cells freshly transferred from ethanol/ethylamine- into ammonium sulfate (YGA) and nitrogen depleted (YGW) glucose-containing media possessed a number of green fluorescent dots representing intact peroxisomes (0 h - point). The organelles strongly displayed a dispersed cytoplasmic distribution, and no eGFP-specific fluorescence could be observed inside the vacuoles immediately upon begin of glucose adaptation. After 2 h of cultivation, however, peroxisomes appeared to be localized in the close proximity to the vacuolar membrane **(Fig. 3.7; 2 h - point)**. Furthermore, a spreading green fluorescent signal could be already found in the vacuolar lumen indicating beginning of the degradation process. This tendency became much stronger with the prolonged incubation time. 4 h after shift into glucose-containing media, almost all intracellular green fluorescence were found to be accumulated inside the vacuoles **(Fig. 3.7; 4 h - point)**. After 6 h of cultivation, peroxisome degradation was already completed in the glucose/ammonium sulfate-grown cells, whereas this process remained at least partly active in the glucose/nitrogen starved-cells since a bulk green fluorescence could be still detected in their vacuoles **(Fig. 3.7; 6 h - point)**. Similar nitrogen starvation-modulated differences in the kinetics of peroxisome degradation were also observed in further comparable experiments (for example, see *chapter 3.3*) confirming biochemical data described above *(3.1.4)*. These kinetic variations could be explained through probable differences in the mechanisms contributed to pexophagy in the presence and absence of nitrogen, although no apparent morphological differences could be revealed between peroxisome degradation in YGA- and YGW-grown wild type cells by this method. Remarkably, the formation of numerous invaginations of the vacuolar membranes was observed in the yeast cells subjected to nitrogen starvation **(Fig. 3.7: B, arrows).** At the same time, such vacuolar membrane invaginations were never completed in the glucose/ammonium sulfate-grown cells, since only a few bends in the vacuolar membranes could be found in cells under these growth conditions **(Fig. 3.7: A, arrows)**. Taken together, the results of fluorescence microscopy analysis suggest the chimerical protein βGal-eGFP(SKL) to be a suitable fluorescent marker to visualize peroxisomes in *Y. lipolytica* and, therefore, can be used to study the dynamics of peroxisomal turnover in this yeast under different physiological conditions.

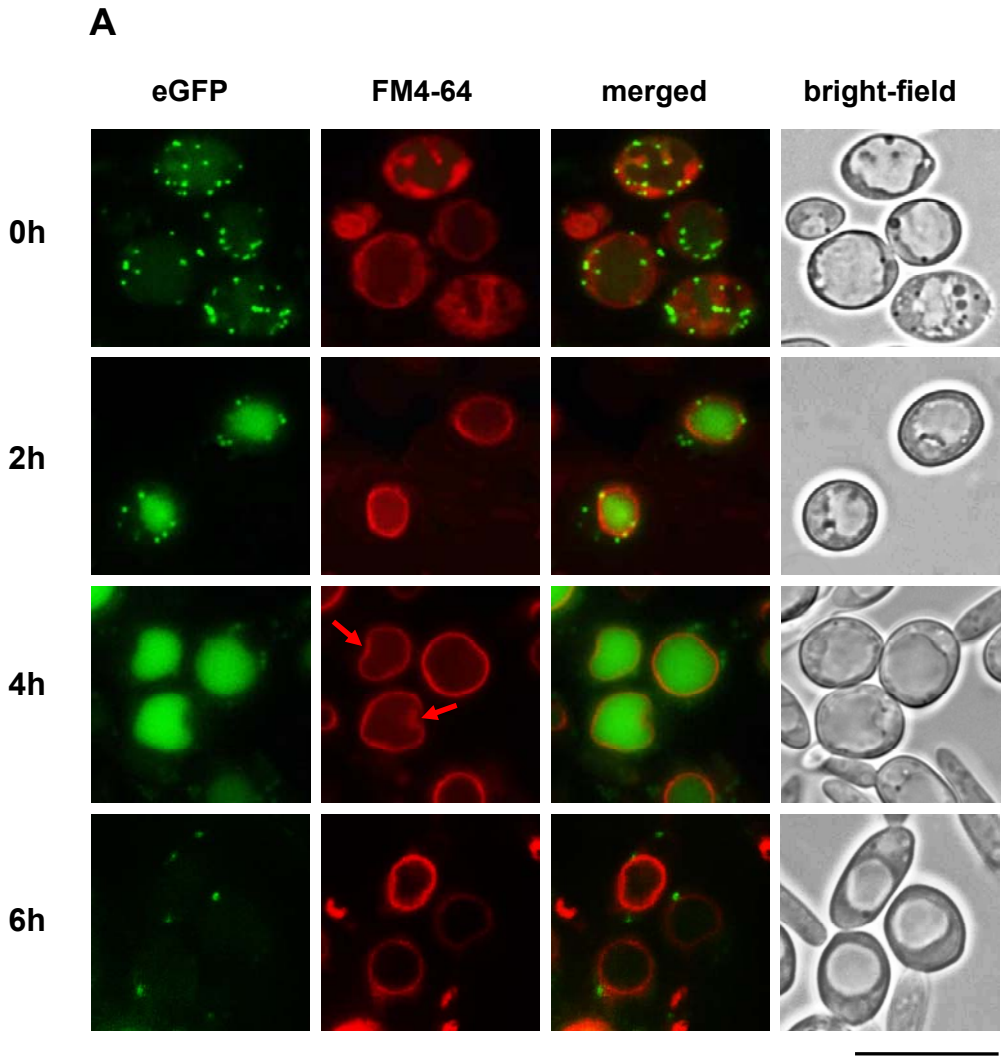

Figure 3.7 Detection of peroxisome degradation in *Y. lipolytica* by fluorescence microscopy. Cells expressing the chimerical protein βGal-eGFP(SKL) were first grown in a ethanol/ethylamine-containing medium to induce peroxisome biogenesis as described in *Materials and Methods (2.5.2)* and subsequently transferred into glucose-containing media with **(A)** and without **(B)** a source of nitrogen. Probes were taken at the indicated time points, processed as described *(2.9)* and viewed under fluorescent microscope. Peroxisomes were labeled with eGFP (green). Vacuolar membranes were stained with FM4-64 (red).
(A) Peroxisomes are selectively degraded in the vacuoles 6 h after transfer into a glucose/ammonium sulfate-containing medium.
Arrows point to bends in the vacuolar membranes.
The scale bar is equal to 20 μm.

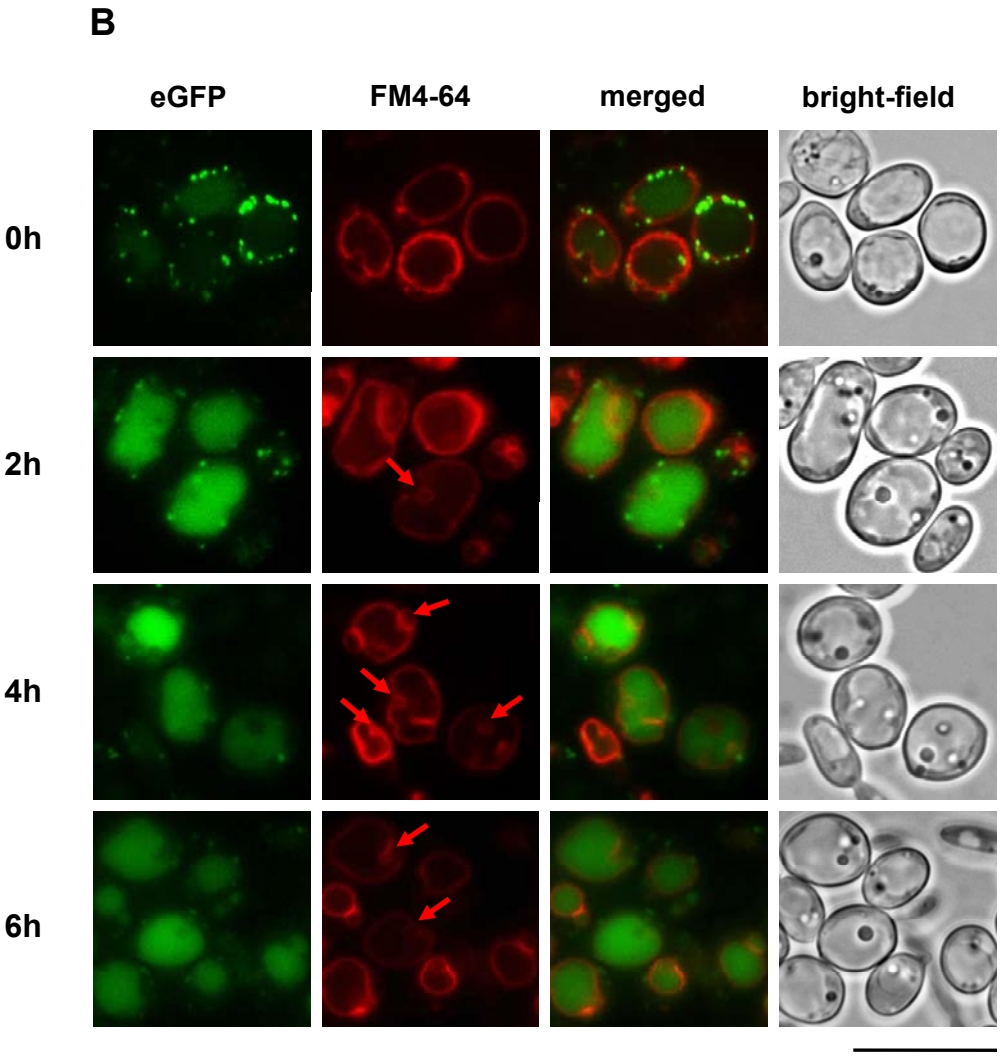

Figure 3.7 (continuation) Detection of peroxisome degradation in *Y. lipolytica* by fluorescence microscopy.
(B) Peroxisomes are seen to be mostly degraded in the vacuoles 6 h after shift into a glucose medium lacking nitrogen.
Arrows point invaginations in the vacuolar membranes.
The scale bar is equal to 20 µm.

3.3 Effect of PMSF on peroxisome degradation in *Y. lipolytica*

PMSF (phenylmethylsulfonyl fluoride) is known to be a specific inhibitor of serine proteases and, therefore, prevents the vacuolar proteolytic degradation of the bulk cellular protein (Lee and Goldberg, 1996). Furthermore, PMSF has been reported to block the nutrient starvation-induced breakdown of autophagic bodies in yeast (Takeshige *et al.*, 1992). To test whether addition of PMSF also affects the degradation of peroxisomes in *Y. lipolytica*, the following experiment was performed. Yeast cells of the strain PO1d(pLG3) were cultivated in a ethanol/ethylamine-containing medium as described in *Materials and Methods* (*2.5.2*), washed once with a minimal medium without carbon source and transferred into fresh YGA and YGW media supplemented with PMSF (dissolved in DMSO) at a final concentration of 1 mM. As a control, glucose-containing media with DMSO were used. Samples were taken immediately after transfer and at indicated time points and subsequently processed for the biochemical, Western blot and fluorescence microscopical analyses as described above *(Materials and Methods, 2.7, 2.9)*. In accord with previous data (*3.1.4*), the decrease in specific ICL and β-galactosidase activities as well as in levels of the ICL protein was observed in cells incubated in both YGA and YGW media containing DMSO **(Fig. 3.8: A, B; Fig. 3.9)**. In contrast, the decrease in enzyme activities was dramatically reduced by more than 50 % in the presence of PMSF **(Fig. 3.8: C, D)**. Furthermore, the degradation of peroxisomal ICL was found to be prevented after PMSF addition, as well **(Fig. 3.9)**. This indicates that observed reduction in the decrease of ICL activity was indeed due to the retarded degradation of this protein caused by PMSF treatment. On the contrary, low concentrations of DMSO alone appeared to have no obvious effect on degradation of this peroxisomal protein **(Fig. 3.9)**. The effect of PMSF addition on pexophagy in *Y. lipolytica* was also confirmed by the following fluorescent microscopy, using the FM4-64 staining to label the vacuolar membranes. As evident from **Fig. 3.10 (A, C)**, the degradation of peroxisomes was clearly delayed in cells subjected to PMSF treatment since intensive eGFP-specific fluorescence could be still observed inside vacuolar lumen 6 h after transfer into glucose. In control cells, consistent with previous results (*Chapter 3.2*), the degradation event was not affected: the majority of peroxisomes were targeted to the vacuoles during the first 4 h followed by their almost complete degradation after 6 h of cultivation **(Fig. 3.10: B, D)**. Another interesting observation concerns the uptake of peroxisomes by the vacuoles for degradation. Whereas this process took place during the first 2 h in control cells, it seemed to be slightly retarded in cells treated with PMSF **(Fig. 3.10; 4 h - point)**. Remarkably, also the number of the vacuolar membrane invaginations appeared to be diminished in the nitrogen-starved cells subjected to PMSF treatment **(Fig. 3.10: C, arrows)**.

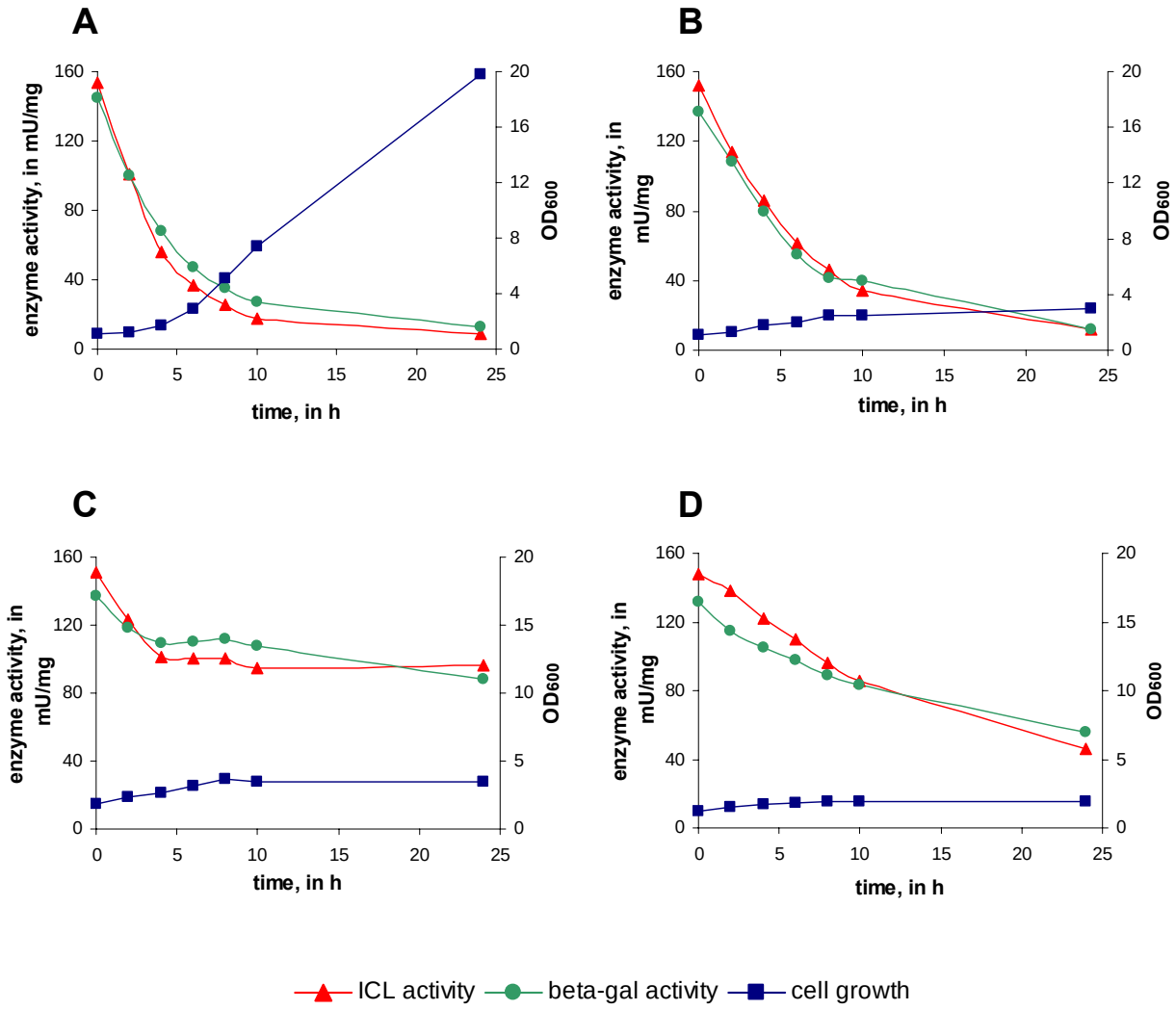

Figure 3.8 Changes in the activities of isocitrate lyase (ICL) and β-galactosidase (beta-gal) under the conditions of peroxisome degradation and PMSF treatment. Cell of the *Y. lipolytica* strain PO1d(pLG3) were first grown in a ethanol/ethylamine-containing medium in order to induce peroxisome proliferation, and then shifted into glucose-containing media with **(A, C)** and without **(B, D)** a source of nitrogen followed by addition of 1 mM PMSF **(C, D)**. Samples were taken immediately (0 h) and after 2, 4, 6, 8 and 24 h of incubation. Addition of PMSF results in reduction of decrease of enzyme activities normally caused by glucose-induced degradation of peroxisomes.

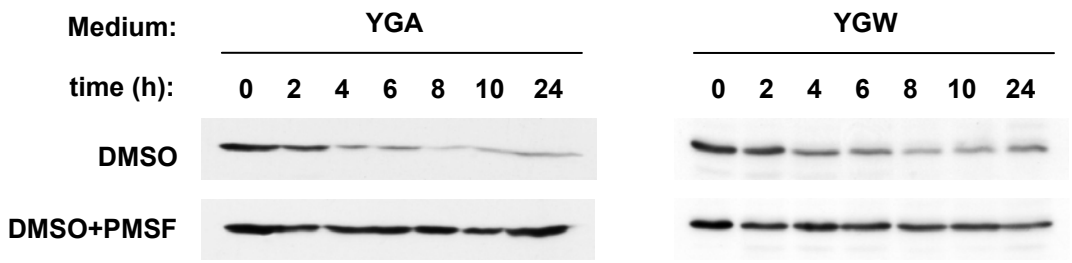

Figure 3.9 Changes in the levels of isocitrate lyase under the conditions of peroxisome degradation and PMSF treatment. Western blots performed with crude extracts of the ethanol/ethylamine-grown cells of strain PO1d(pLG3) subjected to ammonium sulfate **(YGA)** and nitrogen depleted **(YGW)** glucose-containing media in the absence **(DMSO)** or presence **(DMSO+PMSF)** of 1 mM PMSF. Samples were taken immediately after transfer into glucose (0 h) and at the indicated time points and prepared as described (*Materials and Methods, 2.7*). The blots were then decorated with antibodies against isocitrate lyase. Glucose-grown cells exposed to PMSF treatment show significantly less degradation of ICL if compared with control non-treated cells in the presence or absence of a nitrogen source.

Altogether, the results presented above demonstrate that addition of PMSF affects pexophagy in *Y. lipolytica* cells subjected to glucose in the presence or absence of nitrogen. This data provides further evidence that normal functioning of vacuolar serine proteases is essential for the course of peroxisome degradation.

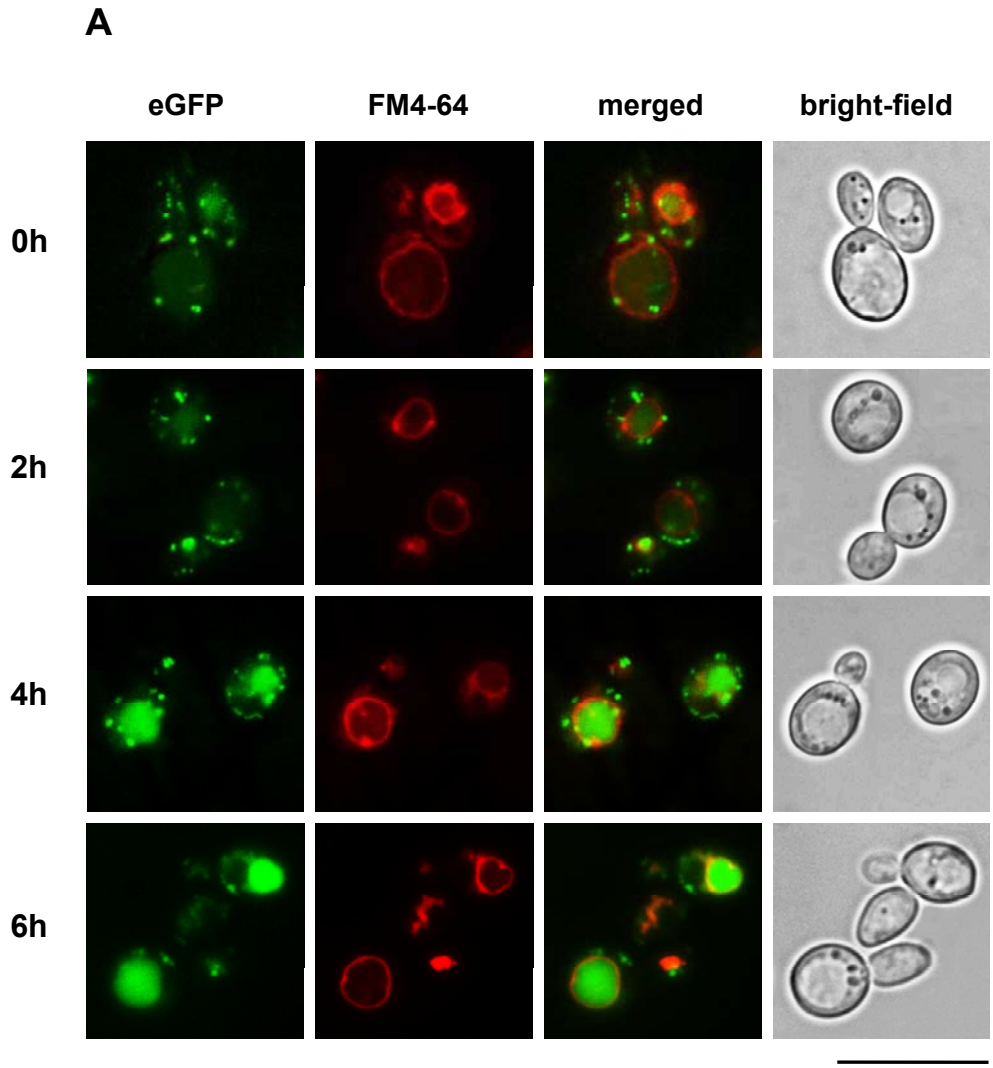

Figure 3.10 Fluorescence microscopy images of peroxisome degradation in the *Y. lipolytica* cells subjected to PMSF treatment. **C**ells of the strain PO1d(pLG3) were grown in an ethanol/ethylamine-containing medium as described *(Materials and Methods, 2.5.2)* and shifted into glucose/ammonium sulfate-containing media with **(A)** and without **(B)** 1 mM PMSF dissolved in DMSO. Cells were then viewed by a fluorescence microscope immediately (0 h) and at the indicated time points. Peroxisomes were labeled with eGFP (green fluorescence). Vacuolar membranes were visualized with FM4-64 (red fluorescence).
(A) Addition of 1 mM PMSF to the glucose/ammonium sulfate-grown cells affects peroxisome degradation in the vacuoles.
The scale bar is equal to 20 µm.

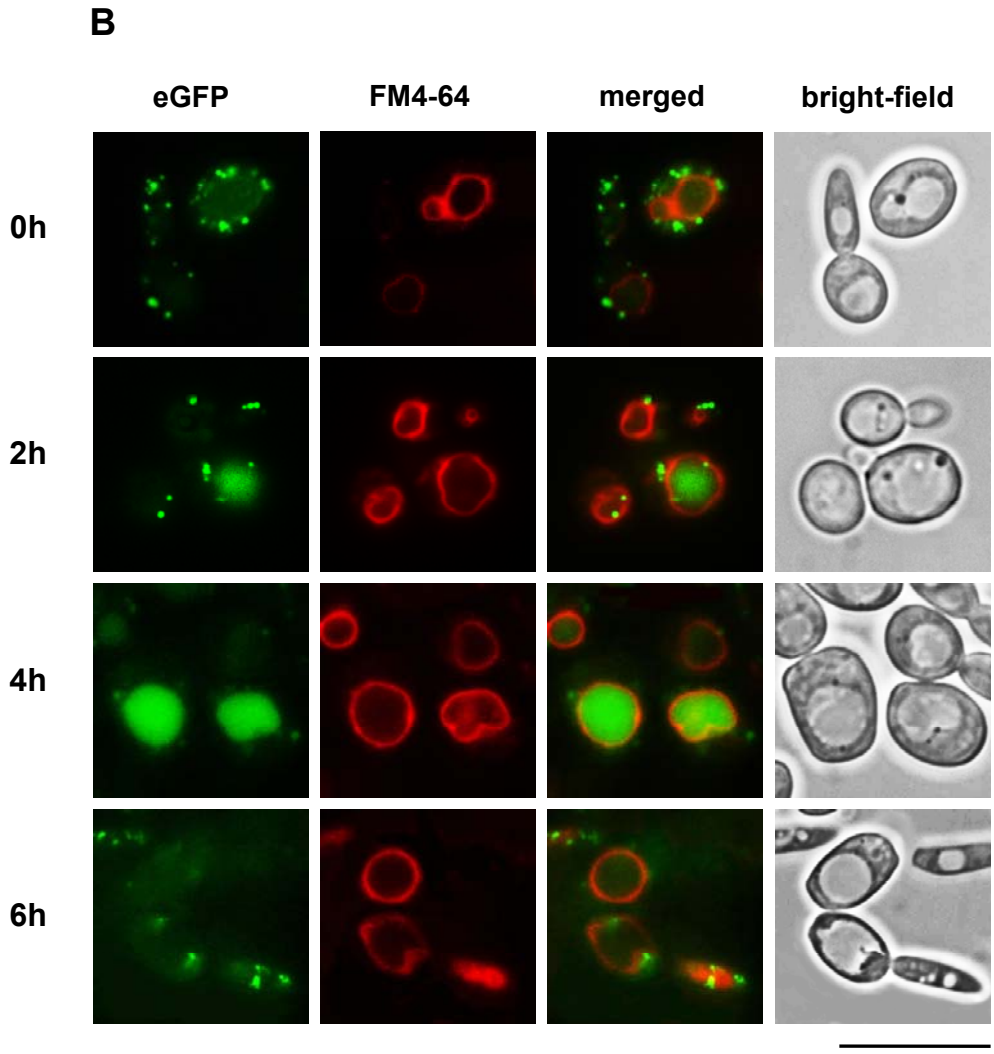

Figure 3.10 (continuation) Fluorescence microscopy images of peroxisome degradation in the *Y. lipolytica* cells subjected to PMSF treatment.
(B) Peroxisomes are normally degraded in the glucose/ammonium sulfate-grown cells subjected to DMSO treatment only.
The scale bar is equal to 20 μm.

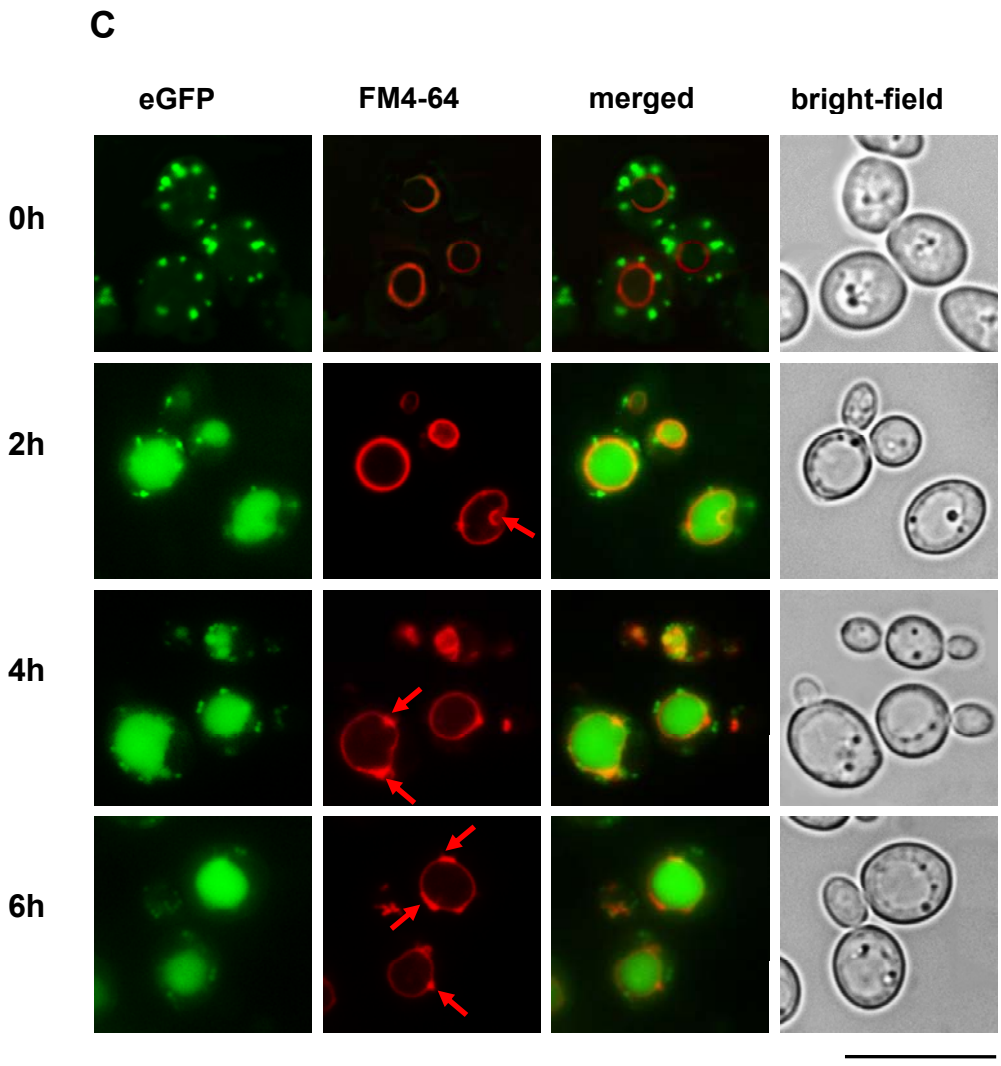

Figure 3.10 (continuation) Fluorescence microscopy images of peroxisome degradation in the *Y. lipolytica* cells subjected to PMSF treatment.
(C) Degradation of peroxisomes in the vacuoles is retarded in cells subjected to nitrogen starvation and 1 mM PMSF simultaneously.
Arrows point to uncompleted invaginations of the vacuolar membranes.
The scale bar is equal to 20 μm.

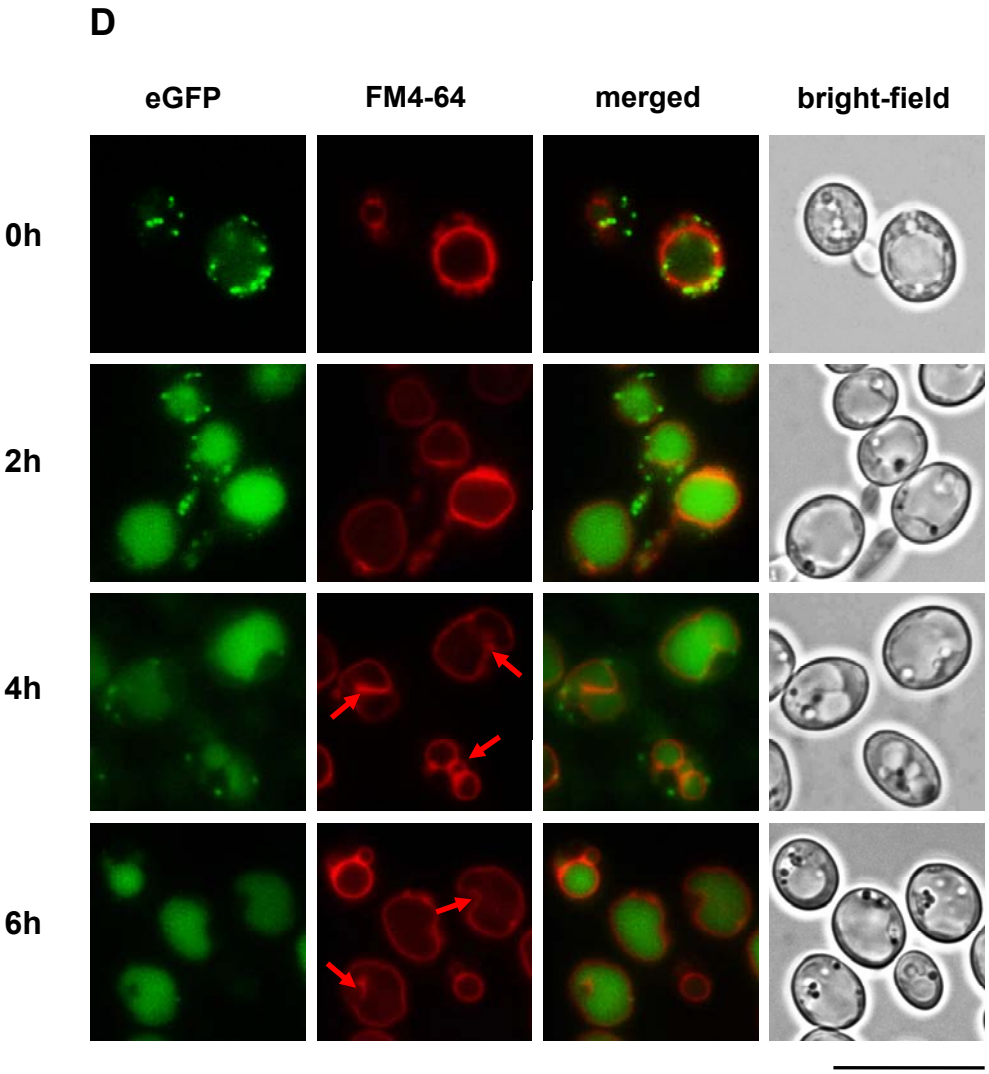

Figure 3.10 (continuation) Fluorescence microscopy images of peroxisome degradation in the *Y. lipolytica* cells subjected to PMSF treatment.
(D) Peroxisome degradation remains unaffected in the control DMSO-treated cells under conditions of nitrogen starvation.
Arrows point to invaginations of the vacuolar membranes.
The scale bar is equal to 20 μm.

3.4 Bioinformatic analysis of autophagy-related proteins from the genome of alkane-utilizing yeast *Y. lipolytica*

The major task of this work was to gain insights into the molecular mechanisms of the autophagic degradation of peroxisomes in the alkane-utilizing yeast *Y. lipolytica*. So, the next part of this thesis was aimed to identify genes and proteins implicated at different stages of pexophagy in this yeast. At first, a bioinformatic genome-wide screening was carried out to search for probable autophagy-related proteins from the *Y. lipolytica* genome.

3.4.1 Genome-wide screening for autophagy-related proteins from *Y. lipolytica*

The course of autophagy has been extensively studied in three yeast model systems, namely baker's yeast *S. cerevisiae* as well as two methylotrophic yeasts, *P. pastoris* and *H. polymorpha* (Bellu and Kiel, 2003; Dunn *et al.*, 2005). A large number of autophagy-related proteins (Atg-proteins) from these microorganisms have been described up to now, and most of them are highly conserved between different yeast species (Scott *et al.*, 1996; Ohsumi, 1999). Moreover, most of the known Atg-proteins appear to be essential not only for general (i.e., autophagy) but also for selective anabolic (i.e., the Cvt-pathway) and catabolic (pexophagy) membrane trafficking processes (Hutchins *et al.*, 1999; Kim and Klionsky, 2000; Klionsky *et al.*, 2003). The last observation suggests that also in *Y. lipolytica* homologous Atg-proteins may be associated with pexophagy. In order to identify such Atg-counterparts from *Y. lipolytica*, a bioinformatic screening of the whole yeast genome was performed. Amino acid sequences of known yeast Atg-proteins were used as queries in different BLAST searches against the complete genome sequence of *Y. lipolytica* (for details, see *Materials and Methods, 2.10*). The obtained results are collected in **Table 3.1**.

Table 3.1 Overview of predicted autophagy-related proteins from the genome of *Y. lipolytica*. Amino acid sequences of known Atg-like proteins from yeasts were queried individually against translated *Y. lipolytica* database as described in *Materials and Methods (2.10)*. All potential hits were then examined additionally for their chromosomal localization as well as for percentage of identities and similarities to corresponding *S. cerevisiae* (Sc), *P. pastoris* (Pp) and *H. polymorpha* (Hp) counterparts. Abbreviations used for mutant phenotypes: *apg*, autophagy; *cvt*, cytoplasm-to-vacuole targeting; *macr*o, peroxisome degradation via macropexophagy; *micro*, peroxisome degradation via micropexophagy; *pdd*, peroxisome degradation by unknown mechanism.

Overview of predicted autophagy-related proteins from the genome of *Y. lipolytica*

Proteins	*Y. lipolytica* homologues (NCBI accession number)	Size in aa	Chromosome	Identity and similarity to, %			Mutant phenotype*
				Sc	Pp	Hp	
Atg1	XP_503272	710	D	35/49	42/58	42/58	*apg* and *pdd* in Sc *macro* and *micro* in Hp
Atg2	XP_503692	1520	E	25/42	26/44	-	*apg* and *micro* in Sc, *micro* in Pp
Atg3	XP_504353	366	E	44/61	-	-	*apg* in Sc
Atg4	XP_500034	345	A	37/51	35/48	-	*apg* in Sc, *micro* in Pp
Atg5	XP_504356	255	E	20/40	-	-	*apg* in Sc
Atg6	XP_502723	434	D	31/50	-	-	*apg* in Sc
Atg7	XP_502039	598	C	40/59	42/58	-	*apg* in Sc, *micro* in Pp
Atg8	XP_503468	137	E	77/89	82/93	78/93	*apg* in Sc, *macro* in Hp, *micro* in Pp
Atg9	XP_505157	788	F	44/65	36/55	-	*apg* in Sc, *micro* in Pp
Atg10	not found	-	-	-	-	-	*apg* in Sc
Atg11	XP_500502	924	B	22/38	25/44	28/42	*macro* in Hp, *micro* in Pp, NOT *apg*
Atg12	XP_506021	205	F	41/65	-	-	*apg* in Sc
Atg13	XP_504947	715	F	24/39	-	-	*apg* in Sc
Atg14	XP_504611	425	E	19/42	-	-	*apg* in Sc
Atg15	XP_505075	559	F	50/64	-	-	*apg* in Sc
Atg16	not found	-	-	-	-	-	*apg* in Sc, *micro* in Pp

Overview of predicted autophagy-related proteins from the genome of *Y. lipolytica*

Proteins	*Y. lipolytica* homologues (NCBI accession number)	Size in aa	Chromosome	Identity and similarity to, %			Mutant phenotype*
				Sc	Pp	Hp	
Atg17	XP_505796	408	F	23/43	-	-	*apg* in Sc
Atg18	XP_505968	400	F	37/56	39/54	43/57	*apg* in Sc, *micro* in Pp
Atg19	not found	-	-	-	-	-	NOT *apg*, NOT *pdd*
Atg20	XP_502542	570	D	28/49	20/40	-	*apg* in Sc
Atg21	not found	-	-	-	-	-	*cvt* in Sc, *apg* and *macro* in Hp
Atg22	XP_501406	589	C	37/55	-	-	*apg* in Sc
Atg23	not found	-	-	-	-	-	*apg* in Sc
Atg24	XP_503920	483	E	36/59	34/54	-	*apg* in Sc, *micro* in Pp
Atg25	XP_505441	318	F	-	-	24/44	*macro* in Hp NOT *apg*
Atg26	XP_502984	1307	D	48/65	50/66	-	*micro* in Pp
Atg27	XP_501883	276	C	23/44	-	-	NOT *apg* NOT *pdd*
Atg28	not found	-	-	-	-	-	*macro* and *micro* in Pp
Gcn1	XP_502953	252	D	37/54	-	-	*micro* in Pp
Gcn2	XP_500907	1609	B	37/56	-	-	*micro* in Pp
Gcn3	XP_501964	307	C	59/75	-	-	*micro* in Pp
Gcn4	XP_504480	281	E	39/65	-	-	*micro* in Pp
Hsv2	XP_500923	359	B	32/54	51/58**	28/47	unknown
Pep4	XP_505932	396	F	65/79	-	64/76	*apg* in Sc
Tor1/2	XP_505106	2316	F	52/68	-	27/39	*apg* in Sc

Overview of predicted autophagy-related proteins from the genome of *Y. lipolytica*

Proteins	*Y. lipolytica* homologues (NCBI accession number)	Size in aa	Chromosome	Identity and similarity to, %			Mutant phenotype*
				Sc	Pp	Hp	
Tup1	XP_500061	647	A	44/57	-	46/58	*macro* in Hp, NOT *apg*
Vac8	XP_503924	573	E	67/81	65/80	-	*apg* in Sc
Vps15	XP_504745	1322	E	30/47	34/54	-	*macro* in Hp, *macro* and *micro* in Pp
Vps34	XP_505213	801	F	41/56	-	34/50	*apg* in Sc, *apg* and *macro* in Hp

* All deletions in *S. cerevisiae* (except for ScAtg4p) are viable.

** Compared with PpGsa12p

The search through genome sequence databases revealed 33 putative proteins from *Y. lipolytica* showing different rates of homology to the Atg-counterparts from other yeast species **(Table 3.1)**. Among them, proteins proven to perform key functions at different stages of the autophagic process could be identified (see also *Introduction, Tables 1.1, 1.2*). For example, *Y. lipolytica* homologs of members of the Atg1 and Vps34 protein signaling complexes were found. Moreover, almost all counterparts of the proteins from both Atg12-Atg5 and Atg8 yeast conjugation systems were present in the genome of *Y. lipolytica*. Remarkably, the *Y. lipolytica* Atg8-homolog exhibited a high level of sequence identity (about 80 %) to its *S. cerevisiae*, *H. polymorpha* and *P. pastoris* counterparts suggesting that this E1-like enzyme is highly conserved between different yeast species. Also homologs of other essential Atg-proteins, such as Tor1/2, Tup1, Pep4 and Gcn1-4 proteins, could be identified in the *Y. lipolytica* genome. On the other hand, no *Y. lipolytica* homologs of *ATG10, ATG16, ATG19, ATG21, ATG23* or *ATG28* genes could be revealed in this search. As the complete genome of *Y. lipolytica* has been already sequenced (Dujon *et al.*, 2004), we can rule out the possibility that the sequences of these genes are still not annotated. It can be proposed that *Y. lipolytica* orthologs of these proteins have very low similarity compared to those from other yeast species and, therefore, could not be found in this experiment. Another alternative, however, is that no such homologous genes are present in

the *Y. lipolytica* genome at all. In this case, other still unknown molecular players should perform their functions.

3.4.2 Bioinformatic analysis of some predicted autophagy-related proteins from *Y. lipolytica*

As already mentioned above, some of predicted *Y. lipolytica* autophagy-related proteins appear to play key functions during autophagic degradation of peroxisomes in other yeasts. Six of these candidates, namely Atg1, Atg6, Atg11, Atg18, Gcn2 and Pep4 proteins, were characterized in detail. Towards this aim, sequence and phylogenetic analysis of these proteins was performed (see Chapter 7.2 in Appendix). The main features of these proteins deduced from computational analyses are discussed below.

The *Y. lipolytica ATG1* gene encodes a putative 710 aa long protein with a predicted molecular weight of 78.7 kDa. It is supposed to be a protein kinase, since a highly conserved protein kinase domain covering residues 7-299 was identified at its N-terminus **(Fig. 7.8)**. Also, a putative ATP-binding region (residues 13-36) and a serine/threonine kinase active site (residues 147-158) could be found within this domain. YlAtg1p shows high levels of similarity to the homologous proteins from *S. cerevisiae* (Atg1), *H. polymorpha* (Pdd7) and *P. pastoris* (Gsa10) **(Table 3.1)** as well as to so-called ULK protein kinases from human. Multiple alignments of the amino acid sequences of YlAtg1p and its homologs revealed two conserved regions located at the N- and C-termini of these proteins **(Fig. 7.8)**. Well-conserved N-terminal regions of the Atg1 proteins are occupied by the described above protein kinase domain. However, no protein domains could be identified at the C-termini of these homologs, although high similarities of the C-terminal residues suggest their important role in the Atg1 functioning. The phylogenetic tree illustrating relationships between Atg1 homologous proteins from *Y. lipolytica*, *S. cerevisiae*, *P. pastoris*, *H. polymorpha* and *H. sapiens* is shown in Appendix **(Fig. 7.14)**.

YlAtg6p protein contains 434 aa residues and has a predicted molecular weight of 49.2 kDa. Searches against the protein domain database allowed me to identify the specific Apg6 domain occupying three quarters of the whole YlAtg6p length (residues 102-433). No conserved amino acid motifs could be found at the N-terminal part of YlAtg6p using the NCBI database. The *Y. lipolytica* Atg6 homolog displays high levels of similarity to its *S. cerevisiae* counterpart **(Table 3.1)** as well as to beclin 1 from human. Multiple alignments of these proteins revealed extended regions of similarity, with the exception for the less conserved N-terminus **(Fig. 7.9)**. No Atg6 homologous proteins from other yeast species have been reported so far.

YlAtg11p is a large protein of 924 aa residues with a deduced molecular weight of 104 kDa. As evident from **Table 3.1**, YlAtg11p displays rather moderate similarity to the homologous proteins from other yeast species. Moreover, no conserved motifs could be predicted within its sequence. Multiple sequence alignments of Atg11-related proteins from *S. cerevisiae* (Atg11), *H. polymorpha* (Pdd18) and *P. pastoris* (Gsa9) did not reveal any extended regions of similarity within these proteins, and most conserved amino acid residues were found at their C-termini **(Fig. 7.10)**. ExPASy topology prediction programs, however, determined two putative membrane-spanning segments (residues 444-464 and 519-539) suggesting that this protein may display a membranous localization.

The *Y. lipolytica ATG18* gene encodes a putative 400 aa long protein with a predicted molecular weight of 43.6 kDa. Analysis of the YlAtg18 protein sequence revealed several WD-repeats (residues 70-273). Furthermore, this protein exhibits a strong similarity to its homologous counterparts from *S. cerevisiae* (Cvt18), *P. pastoris* (Gsa12) and *H. polymorpha* (Atg18) **(Table 3.1)**. These proteins, in turn, share a significant degree of similarity with components of a novel family of phosphoinositide binding proteins, including ScAtg21p and ScHsv2p (Stromhaug *et al.*, 2004) as well as with human WIPI proteins (Proikas-Cezanne *et al.*, 2004). Multiple sequence alignments linked the most conserved regions of these proteins to the WD40 repeats **(Fig. 7.11)**. Reconstruction of phylogenetic relationships between the Atg18 homologs from yeasts and human is shown in **Fig. 7.15** in Appendix. Interestingly, no orthologs of ScAtg21 could be found in the genome of *Y. lipolytica* in this search, although the corresponding *H. polymorpha* protein has been already identified (Leão-Helder *et al.*, 2004).

Presumed *GCN2* gene from *Y. lipolytica* encodes a large protein of 1609 aa with a deduced molecular weight of 173.2 kDa. Two putative protein kinase domains were found in the amino acid sequence of YlGcn2p at the positions of 242-464 and 721-922 residues, respectively. YlGcn2p displays a high similarity to its *S. cerevisiae* counterpart, ScGcn2 **(Table 3.1)**, as well as to the translation initiation factor 2-alpha kinase 4 from human. Multiple sequence alignments of these proteins revealed the second kinase domain to be a most conserved part within their sequences **(Fig. 7.12)**.

Predicted Pep4 protein from *Y lipolytica* is 396 aa long with an estimated molecular weight of 42.6 kDa. It is supposed to belong to the eukaryotic aspartyl proteases family, as the corresponding structurally conserved catalytic domain covering about 90 % of the whole protein length was found within its sequence. YlPep4p possesses a significant degree of similarity with the corresponding *S. cerevisiae* and *H. polymorpha* homologs **(Table 3.1)** and with selected aspartyl proteases of yeast and human origin (see **Fig. 7.13, 7.16** in Appendix).

3.5 Characterization of *atg1*, *atg6*, *atg11*, *atg18*, *gcn2* and *pep4* mutants of *Y. lipolytica*

Having determined putative autophagy-related proteins of *Y. lipolytica*, it was next interesting to test whether these proteins perform the same or other molecular functions if compared to their homologs from other yeasts. To this end, six selected *Y. lipolytica* genes – *ATG1, ATG6, ATG11, ATG18, GCN2* and *PEP4* - were disturbed by the gene disruption technique (see *Materials and Methods, 2.8*). The obtained mutant strains were then examined for the cell viability and the ability to degrade peroxisomes under different physiological conditions.

3.5.1 Cell growth and viability of selected *Y. lipolytica atg* mutants under nitrogen starvation conditions

Previous studies on yeasts showed that deletion of *ATG* genes often results in decreased growth rates and reduced cell viability under conditions of nitrogen starvation (Tsukada and Ohsumi, 1993). Therefore, it was first analyzed whether disruption of selected *Y. lipolytica ATG* genes produced similar phenotypic effects in corresponding yeast mutants. To analyze the cell growth, freshly cloned cells of the wild type and *atg* mutants were grown overnight in a liquid minimal medium with glucose and then transferred into liquid YGA and YGW media at the initial OD_{600} about 0.5-1.0. Cell growth rates (OD_{600}) were then examined in aliquots collected after 2, 4, 6, 8, 10 and 24 h of cultivation. For the viability test, the glucose-grown *Y. lipolytica* wild and mutant cells were dropped onto YGA and YGW agar plates supplemented with 10 µg/ml of phloxin B as described previously (Tsukada and Ohsumi, 1993) and incubated at 28 °C for some days. Dead yeast cells became pink because of accumulation of the non-metabolized phloxin B, while living cells remained uncolored by this method.

As is evident from **Fig. 3.11 (A, B)**, all tested *Y. lipolytica* mutants showed a significant reduction of the growth rates during cultivation of cells in the glucose-containing nitrogen-depleted medium. Comparison of growth curves of the parental and mutant *Y. lipolytica* strains revealed about 2-2.5-fold decrease in the final OD_{600} during 24 h of cultivation for the *atg6, atg11, atg18, gcn2* and *pep4* mutants and a 1.5-fold decrease in the case of the *Y. lipolytica atg1* mutant strain. This observation clearly reflects the fact that a cell undergoes global metabolical alterations in order to survive conditions of nutrient limitation. In contrast, growth of both wild type and mutant cells remained unaffected if a source of nitrogen was present in a growth medium **(Fig. 3.11: C, D)**. It should be, however, taken into account that, according to a general strategy of mutant construction using the *YlURA3* gene as a selective marker for yeast

transformation (see *Material and Methods, 2.8*), all derived *Y. lipolytica* mutant strains were turned to be complete prototrophic. The parental strain PO1d(pLG3), on the contrary, exhibits the uracil auxotrophy which slows down its growth rates in minimal medium. So, an independent yeast transformant carrying additional genomic copies of the *YlURA3* gene should be preferably used as a control to compare growth rates of these yeast strains.

The results obtained in cell growth experiments were verified by the following cell viability test. As shown in **Fig. 3.12**, three of the inspected *Y. lipolytica atg*-mutants, namely *atg1, atg6* and *atg18*, displayed clear defects in their cell viability, as an intensive coloring of the nitrogen starved-cells could be observed after 3 days of incubation on the phloxin B agar plates. However, no apparent differences could be revealed between cell viabilities of the wild type and *atg11, gcn2* and *pep4* mutant strains as probably better seen if 10^6 cells per spot were dropped **(Fig. 3.12)**. This finding correlates well with theoretical predictions, since the corresponding homologous proteins from *S. cerevisiae* and methylotrophic yeasts are known to play no significant role in general autophagy but in other intracellular membrane-mediated pathways (see *Introduction, 1.1.2* for more details). As expected, no obvious phenotypic differences could be found out between the parental and mutant strains on control phloxin B plates in the presence of ammonium sulfate **(Fig. 3.12, right panel)**.

In summary, all examined mutants of *Y. lipolytica* revealed defects in cell growth under the conditions of nitrogen starvation. Furthermore, three out of the selected strains showed defects in cell survival under the same conditions that could be attributed to a diminished autophagic degradation in these mutants.

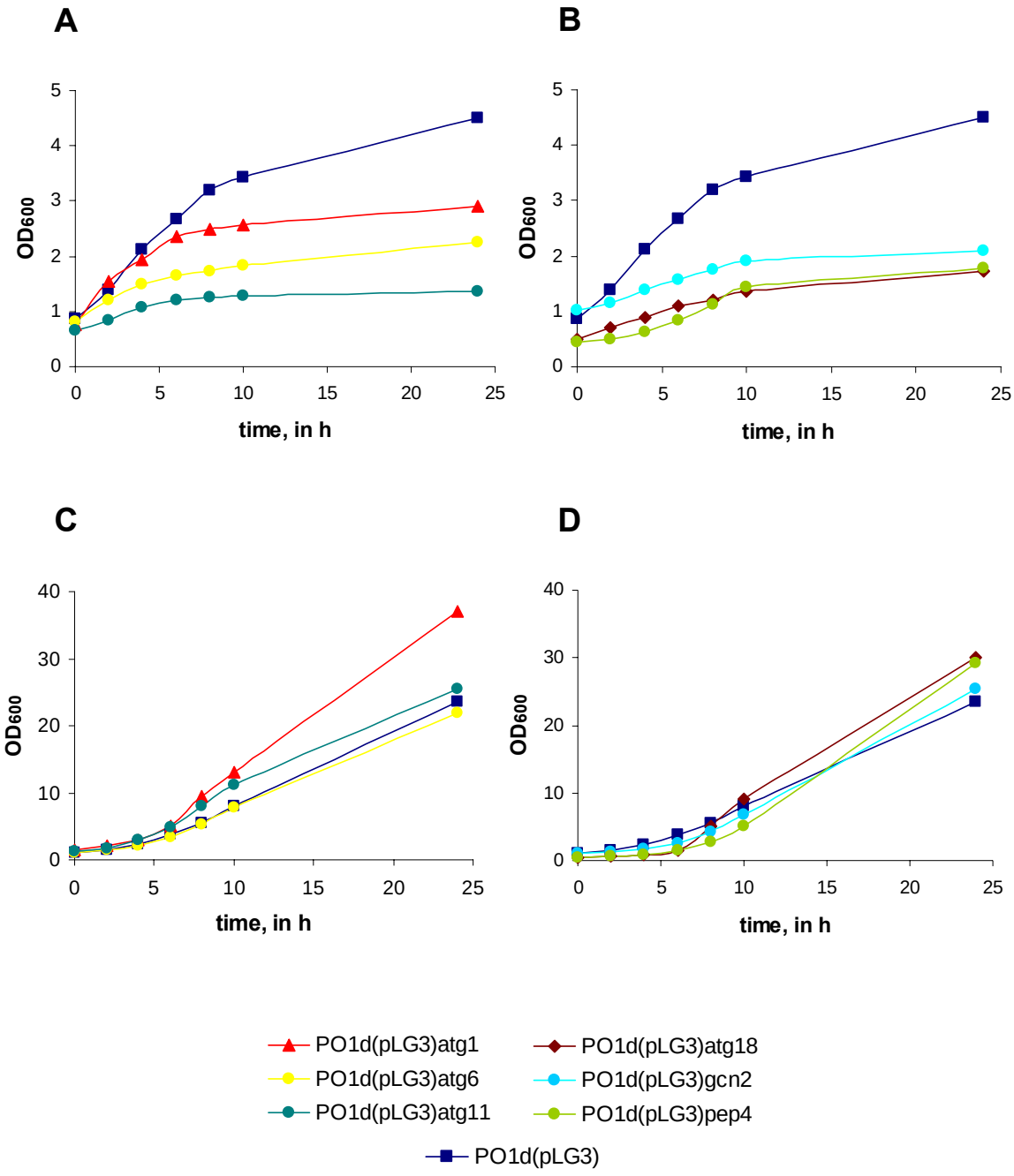

Figure 3.11 Cell growth of selected *Y. lipolytica atg* mutants in the absence (A, B) and presence (C, D) of nitrogen. Overnight cultures of *Y. lipolytica* strain PO1d(pLG3) and derivative *atg1, atg6, atg11, atg18, gcn2* and *pep4* mutants were diluted in liquid YGW **(A, B)** and YGA **(C, D)** media to initial OD_{600} of about 0.5-1 and cultivated for the next 24 h. Aliquots were collected and the OD_{600} were measured at the indicated time points. Results of one representative experiment are shown. The parental strain PO1d(pLG3) displays the *ura3*-auxotrophy. All mutant stains are prototrophic. Abbreviations used of media: YGA, yeast extract/glucose/ammonium sulfate; YGW, yeast extract/glucose without nitrogen.

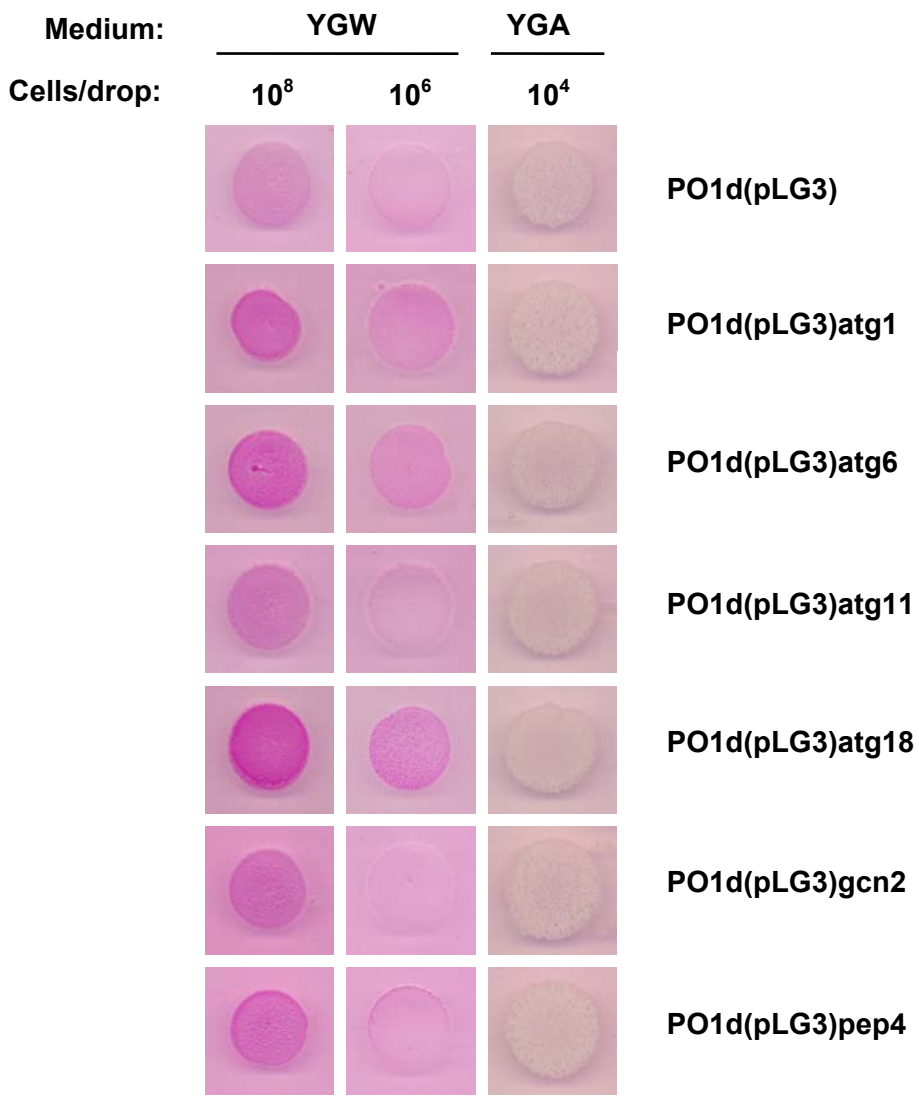

Figure 3.12 Cell viability of selected *atg* mutants of *Y. lipolytica* determined by the staining with phloxin B. Exponentially growing cells of the *Y. lipolytica* initial strain PO1d(pLG3) and derived *atg1, atg6, atg11, atg18, gcn2* and *pep4* mutants were spotted onto YGA and YGW plates supplemented with phloxin B at a final concentration of 10 µg/ml. Plates were incubated for some days, and spots were then examined for dye accumulation by development of the pink colour. Abbreviations used for media: YGA, yeast extract/glucose/ammonium sulfate; YGW, yeast extract/glucose without nitrogen.

3.5.2 Peroxisome degradation in *Y. lipolytica atg* mutants

Results presented in previous chapter clearly demonstrated several phenotypic differences between the *Y. lipolytica* wild type and *atg* mutant strains which are most probably due to defects in the course of autophagy or other related intracellular trafficking pathways in these mutants. Hence, the autophagic peroxisome degradation was next explored in more detail in the *Y. lipolytica atg1, atg6, atg11, atg18, gcn2* and *pep4* strains. To this end, yeast cells of the parental and mutant strains were cultivated in ethanol/ethylamine-containing media as described above *(3.1.3)* and subsequently shifted into glucose-containing media with and without nitrogen source (YGA and YGW, respectively) as described in *Materials and Methods (2.5.2)*. Samples were collected at indicated time points and subjected to further biochemical, immunological and fluorescence microscopic analyses *(Materials and Methods: 2.7, 2.9)*. The results acquired for each mutant strain are shown in the following six chapters.

3.5.2.1 The atg1 mutant of Y. lipolytica

Transfer of the ethanol/ethylamine-grown *atg1* cells into a glucose/ammonium sulfate-containing medium resulted in the inactivation of peroxisomal marker enzymes ICL and β-galactosidase. As is evident from **Fig. 3.13 (A, B)**, only about 20 % of both enzyme activities could be measured in cell-free extracts of the *atg1* cells after 10 h of cultivation. However, no noticeable reduction in activities of these enzymes could be revealed in the *Y. lipolytica atg1* mutant under conditions of nitrogen starvation if compared to the parental strain PO1d(pLG3) **(Fig. 3.13: C, D)**. Degradation kinetics of enzymes determined biochemically were confirmed by the following Western blot analysis. The amounts of peroxisomal enzymes ICL and THI were found to generally decrease in the wild type and *atg1* mutant strains, if both glucose and ammonium sulfate were present in the medium. On the other hand, the levels of cytoplasmic (G6PDH) and mitochondrial (aconitase) proteins remained more or less unchanged under these conditions **(Fig. 3.14: A, B)**. Next, if cells were subjected to glucose without nitrogen source, no apparent alterations in the levels of examined proteins could be detected in the *atg1* mutant, whereas in the wild type cells, consistent with the previous observations *(3.1.4)*, degradation of all tested proteins was obvious **(Fig. 3.14: C, D)**.

To further examine the role of YlAtg1p in peroxisome degradation, fluorescence microscopic analysis of the glucose-grown *Y. lipolytica atg1* cells was performed as described above *(3.2)*. As shown in **Fig. 3.15 (A)**, no apparent defects in peroxisome degradation could be observed in the *atg1* mutant after transfer of cells into the glucose/ammonium sulfate-containing medium:

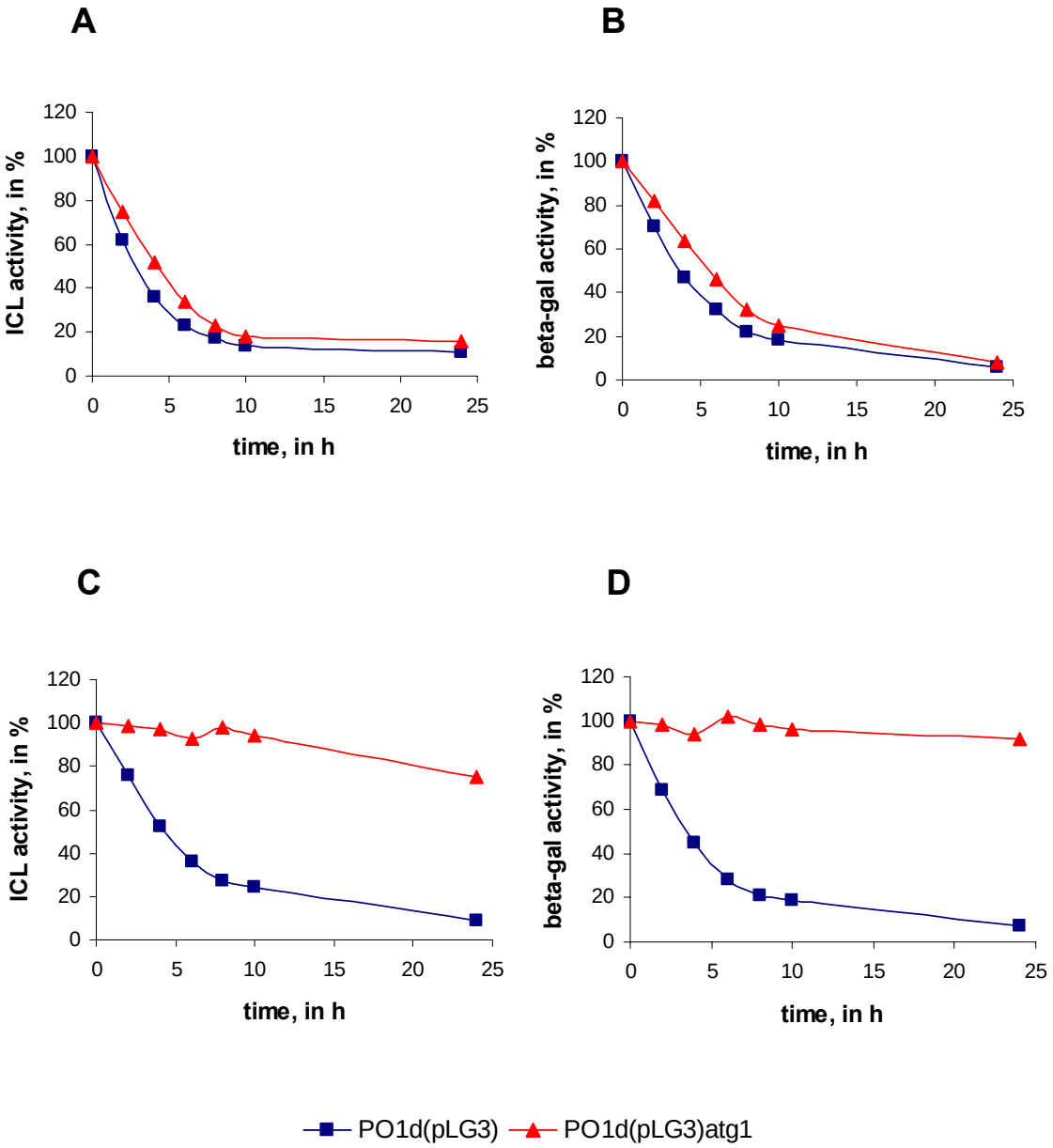

Figure 3.13 Changes in the relative activities of isocitrate lyase and β-galactosidase in the *Y. lipolytica* WT and *atg1* mutant cells under the peroxisome degradation inducing conditions. Ethanol/ethylamine-grown cells of the parental strain PO1d(pLG3) as well as *atg1* mutant were transferred into glucose media with **(A, B)** and without **(C, D)** source of nitrogen as described above *(Materials and Methods, 2.5.2)*. Samples were taken immediately (0 h) and after 2, 4, 6, 8 and 24 h of incubation. Cell-free extracts were then prepared and activities of the peroxisomal ICL **(A, C)** and β-galactosidase **(B, D)** were determined as described *(2.7.7)*. Results of a representative experiment are shown. Specific enzyme activities are expressed as a percentage of the initial value (0 h) which is set to 100 %.

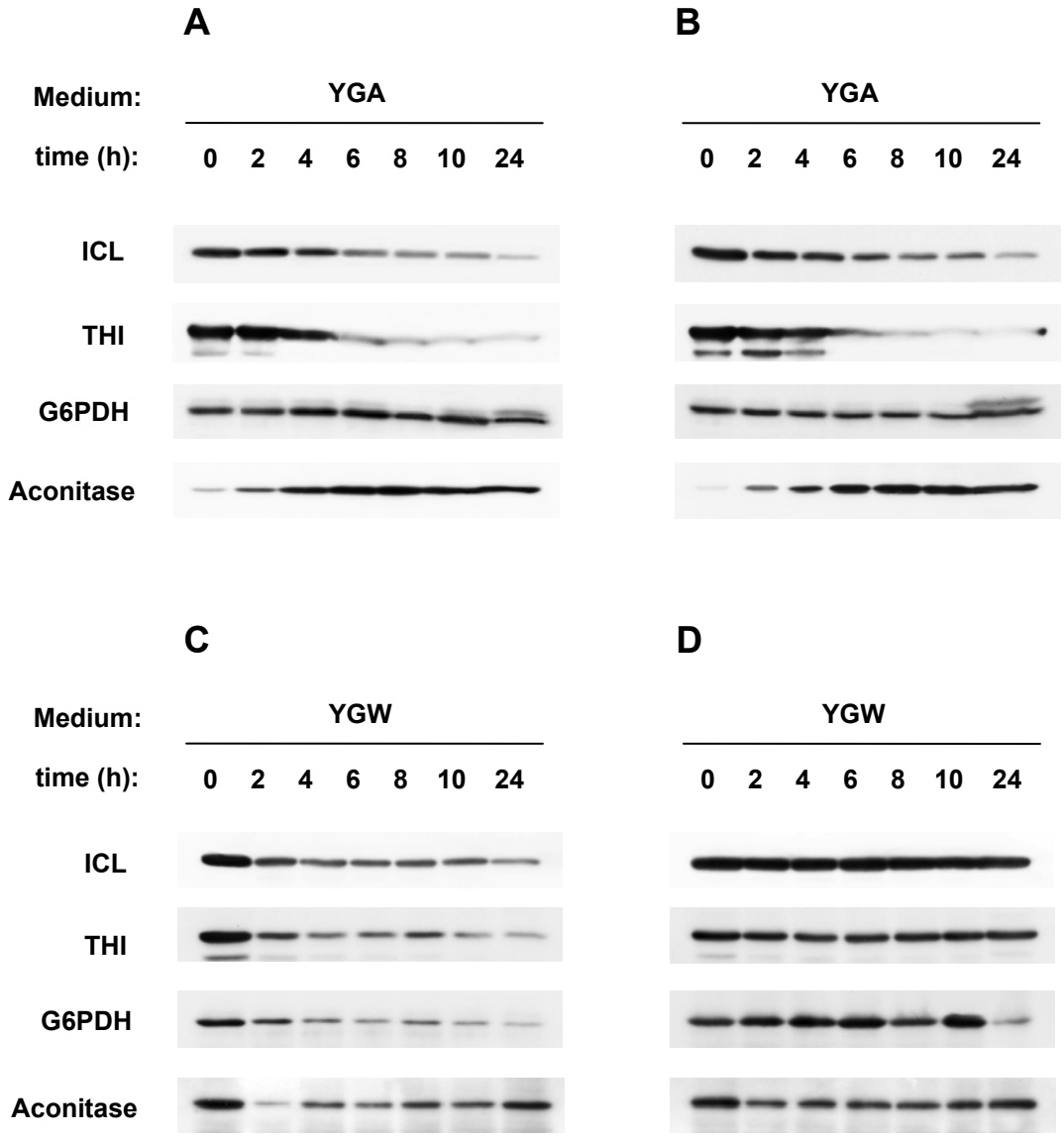

Figure 3.14 Changes in the levels of specific marker proteins in the *Y. lipolytica* WT and *atg1* mutant cells subjected to conditions leading to peroxisome degradation.
(A, B) Western blots performed with cell-free extracts of the ethanol/ethylamine-grown PO1d(pLG3) **(A)** and *atg1* mutant **(B)** cells shifted into glucose/ammonium sulfate-containing medium. Equal volumes of cell-free extracts were loaded per line.
(C, D) Western blots performed with cell-free extracts of the ethanol/ethylamine-grown PO1d(pLG3) **(C)** and *atg1* mutant **(D)** cells shifted into glucose medium lacking nitrogen. Equal volumes of cell-free extracts were loaded per line.
Abbreviations used for marker proteins: ICL, isocitrate lyase; THI, thiolase; G6PDH, glucoso-6-phosphate dehydrogenase.
Abbreviations used for media: YGA, yeast extract/glucose/ammonium sulfate; YGW, yeast extract/glucose without nitrogen source.

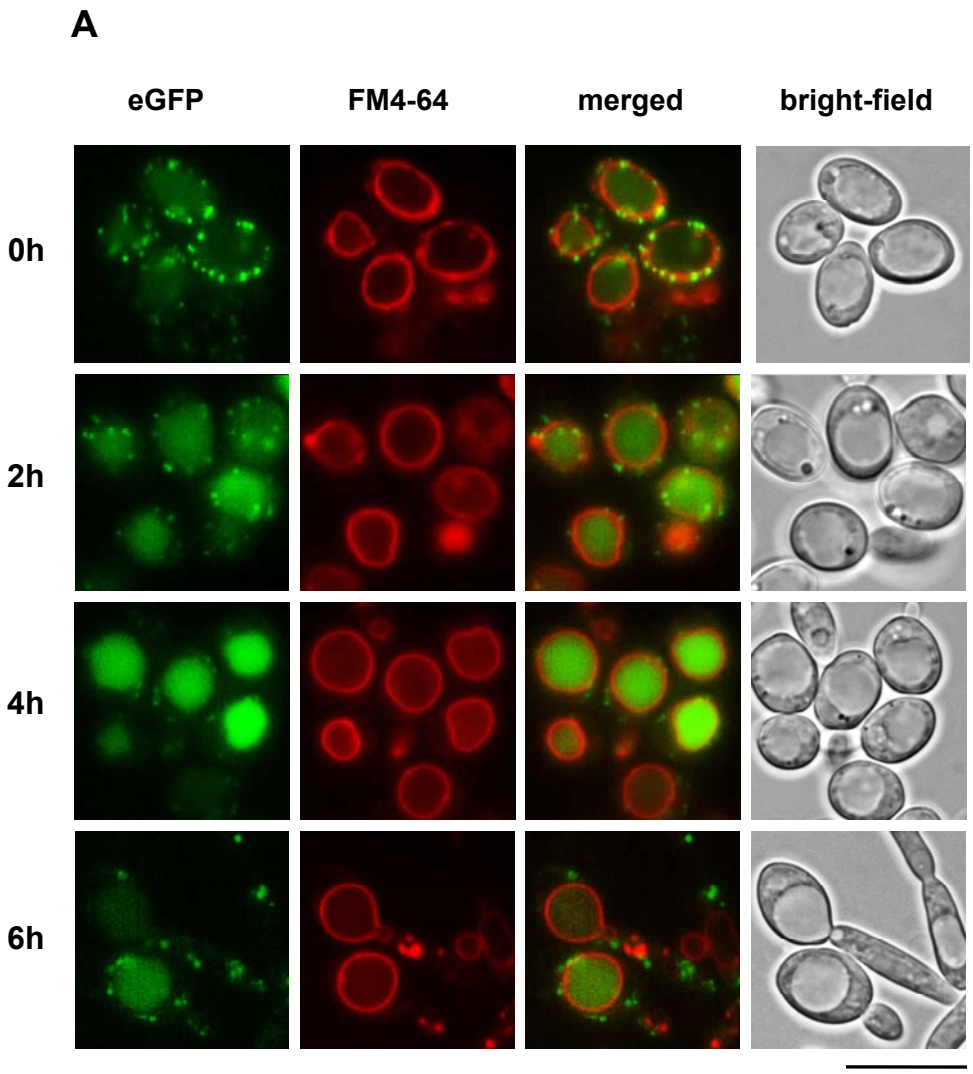

Figure 3.15 Fluorescence microscopic detection of peroxisome degradation in the *atg1* mutant of *Y. lipolytica*. Yeast cells were cultivated in an ethanol/ethylamine-containing medium to induce peroxisome biogenesis as described in *Materials and Methods (2.5.2)* and then transferred into glucose-containing media with **(A)** or without **(B)** a source of nitrogen. Probes were taken at the indicated time points, processed as described *(2.9)* and analyzed by fluorescent microscope. Peroxisomes were viewed with eGFP (green fluorescence). Vacuolar membranes were stained with FM4-64 (red fluorescence).
(A) Peroxisomes are selectively degraded in the vacuoles of the *atg1* mutant cells 6 h after transfer into a glucose/ammonium sulfate-containing medium.
The scale bar is equal to 20 μm.

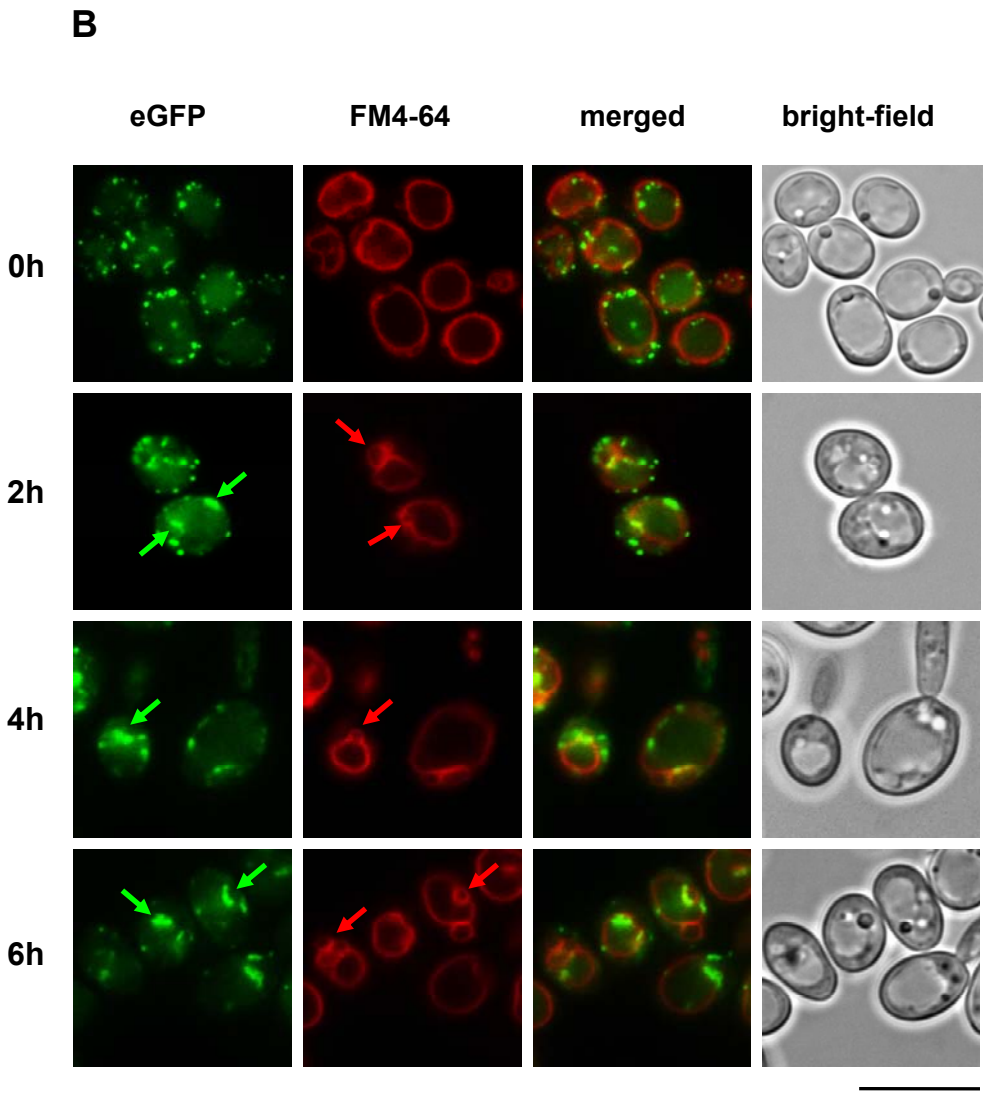

Figure 3.15 (continuation) Fluorescence microscopic detection of peroxisome degradation in the *atg1* mutant of *Y. lipolytica*.
(B) *The d*egradation of peroxisomes is damaged in the *atg1* mutant cells grown on glucose in the absence of a nitrogen source.
Red arrows point to invaginations of the vacuolar membranes. Green arrows indicate peroxisomal clusters.
The scale bar is equal to 20 µm.

the organelles were seen to be targeted to and degraded in the vacuoles during the first 4 h of cultivation. After 6 h, the majority of peroxisomes were already eliminated from the cytoplasm. Conversely, the shift of the *atg1* mutant cells into the glucose-containing medium lacking nitrogen led to clear defects in the course of pexophagy **(Fig. 3.15: B)**. The organelles were found to be directed to the vacuoles during the first 2 h of cultivation. After the next 4 h, however, no peroxisomes were taken up by the vacuoles since clusters of these organelles **(green arrows)** could be still observed at the close proximity to the vacuolar membranes. At the same time, invaginations of the vacuolar membranes didn't seem to be significantly affected in the *Y. lipolytica atg1* mutant under conditions of glucose and nitrogen starvation **(red arrows)**. Taken together, these results suggest that the *Y. lipolytica* Atg1 counterpart plays an important role in the autophagic peroxisome degradation under conditions of nitrogen starvation but is most likely not involved in this process if a source of nitrogen is present in the growth medium.

3.5.2.2 The atg6 mutant of Y. lipolytica

Comparison of the kinetics of inactivation of peroxisomal enzymes ICL and β-galactosidase did not reveal any considerable differences between the parental and *atg6* mutant strains of *Y. lipolytica* under the conditions of glucose and ammonium sulfate **(Fig. 3.16: A, B)**. Conversely, no apparent inactivation of these enzymes were observed in the *atg6* mutant cells grown in a glucose medium lacking nitrogen source **(Fig. 3.16: C, D),** indicating that peroxisomes in this mutant stay intact under these conditions. To further analyze these results, fates of peroxisomal (ICL and THI) as well as cytosolic (G6PDH) and mitochondrial (aconitase) marker proteins were examined by Western blotting. As illustrated in **Fig. 3.17 (C, D)**, no reduction in levels of these proteins was found in the *atg6* mutant under the nitrogen starvation conditions if compared to the parental *Y. lipolytica* strain PO1d(pLG3). This data points at a possible defect in a general autophagic degradation in the *Y. lipolytica atg6* cells that is also in line with the biochemical data described above. On the other hand, analysis of levels of the peroxisomal marker proteins form the glucose/ammonium sulfate-grown *atg6* mutant cells revealed unexpected results. As shown in **Fig. 3.17 (A, B)**, the degradation of both ICL and THI was visibly delayed in the *atg6* mutant in comparison with the initial *Y. lipolytica* strain. This finding indicates that peroxisome degradation may be disturbed in this mutant also during cell growth in the gluocose/ammonium sulfate-containing medium. Characteristically, the levels of cytosolic and mitochondrial proteins remained unaffected in both wild type and mutant strains under these conditions **(Fig. 3.17: A, B)**.

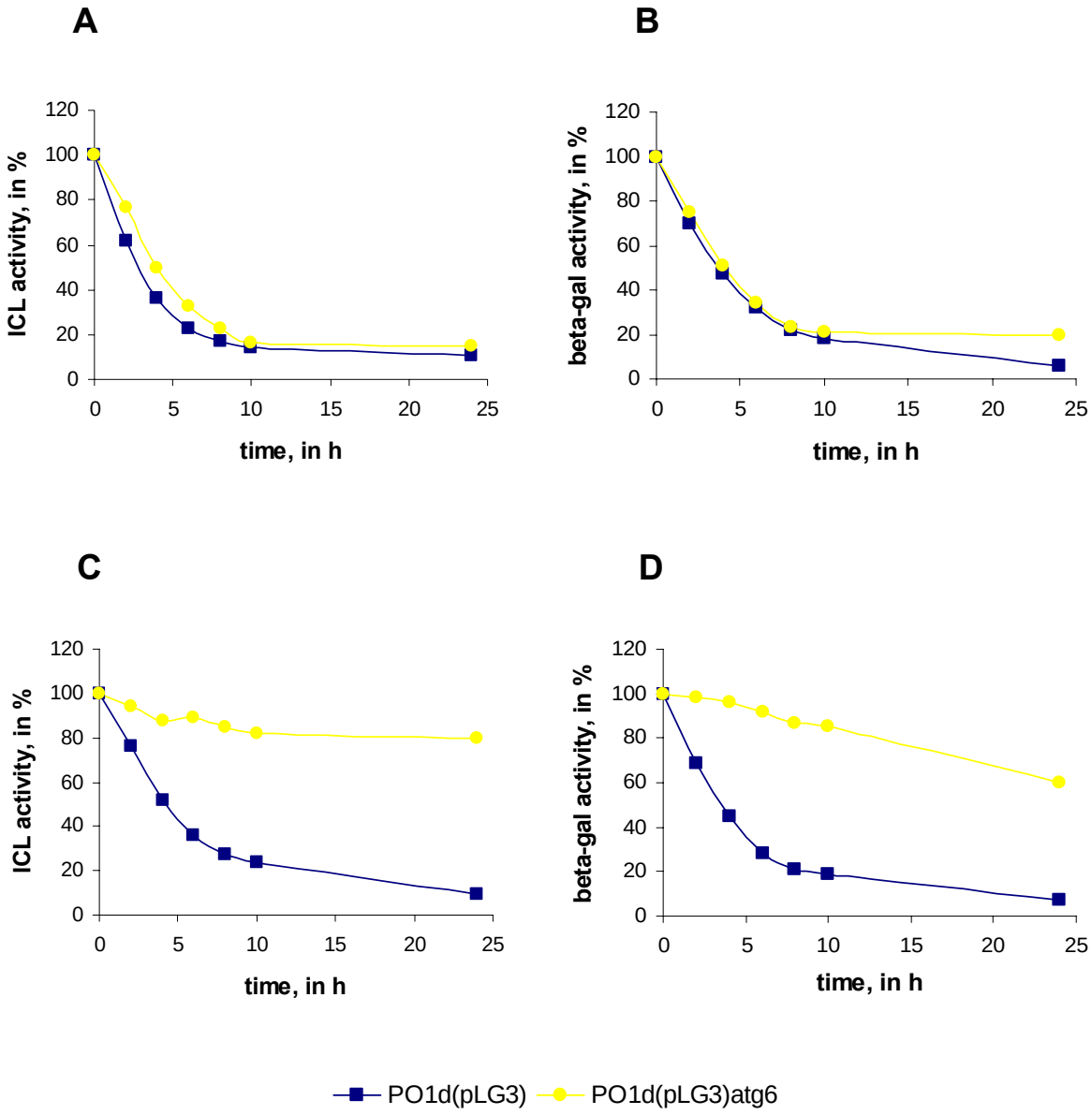

Figure 3.16 Changes in the relative activities of isocitrate lyase and β-galactosidase in the *Y. lipolytica* WT and *atg6* mutant cells under the peroxisome degradation inducing conditions. Ethanol/ethylamine-grown cells of the parental strain PO1d(pLG3) and the *atg6* mutant of *Y. lipolytica* were transferred into glucose media with **(A, B)** and without **(C, D)** nitrogen source as described above *(Materials and Methods, 2.5.2)*. Samples were taken immediately (0 h) and after 2, 4, 6, 8 and 24 h of incubation. Cell-free extracts were prepared and activities of the peroxisomal ICL **(A, C)** and β-galactosidase **(B, D)** were determined as described *(2.7.7)*. Results of a representative experiment are shown. Specific enzyme activities are expressed as a percentage of the initial value (0 h) which is set to 100 %.

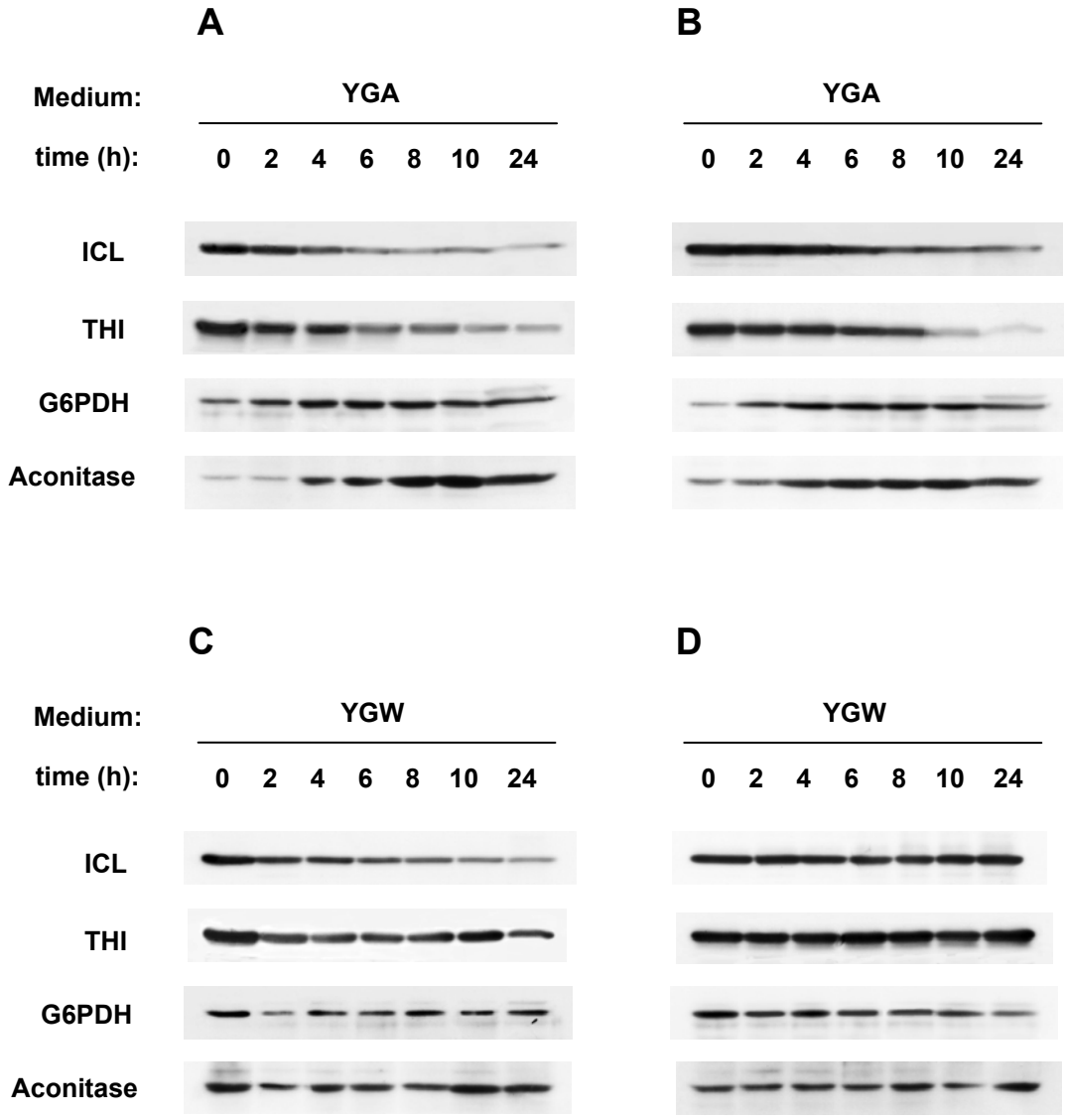

Figure 3.17 Changes in the levels of some marker proteins in the *Y. lipolytica* WT and *atg6* mutant cells subjected to the peroxisome degradation inducing conditions.
(A, B) Western blots performed with cell-free extracts of the ethanol/ethylamine-grown PO1d(pLG3) **(A)** and *atg6* mutant **(B)** cells shifted into a glucose/ammonium sulfate-containing medium. Equal volumes of cell-free extracts were loaded per line.
(C, D) Western blots performed with cell-free extracts of the ethanol/ethylamine-grown PO1d(pLG3) **(C)** and *atg6* mutant **(D)** cells shifted into a glucose medium lacking nitrogen. Equal volumes of cell-free extracts were loaded per line.
Abbreviations used for marker proteins: ICL, isocitrate lyase; THI, thiolase; G6PDH, glucoso-6-phosphate dehydrogenase.
Abbreviations used for media: YGA, yeast extract/glucose/ammonium sulfate; YGW, yeast extract/glucose without nitrogen source.

To confirm the data introduced above, the degradation of peroxisomes in the *Y. lipolytica atg6* mutant was next tested by fluorescence micrcoscopy using specific eGFP and rhodamine filters (see *Materials and Methods, 3.2*). It turned out that pexophagy was impaired in the *atg6* glucose-grown cells both in the presence and absence of a source of nitrogen. As shown in **Fig. 3.18**, peroxisomes were targeted to the vacuoles in the *atg6* mutant cells in the beginning of glucose adaptation. However, the following fusion of the auto(pexo)phagosomal and vacuolar membranes seemed not to occur because individual peroxisomes as well as clusters of these organelles **(arrows)** were observed at the vacuolar membranes of the glucose-grown *atg6* cells after 4 h of cultivation. In support of this, no organelles could be still found inside the vacuoles after 6 h of cultivation. Remarkably, also the formation of invaginations of the vacuolar membranes appeared to be damaged in the *atg6* cells grown under the nitrogen starvation conditions. Another notable observation concerns morphology of the intracellular membranes in the *Y. lipolytica atg6* mutant. Staining with FM4-64 revealed unusual membranous structures in the cytoplasm of cells cultivated in ethanol/ethylamine and glucose/nitrogen-depleted media **(Fig. 3.18: B)**, confirming the assumption that YlAtg6p is in some way involved in organizing (and) functioning of the intracellular membrane trafficking.

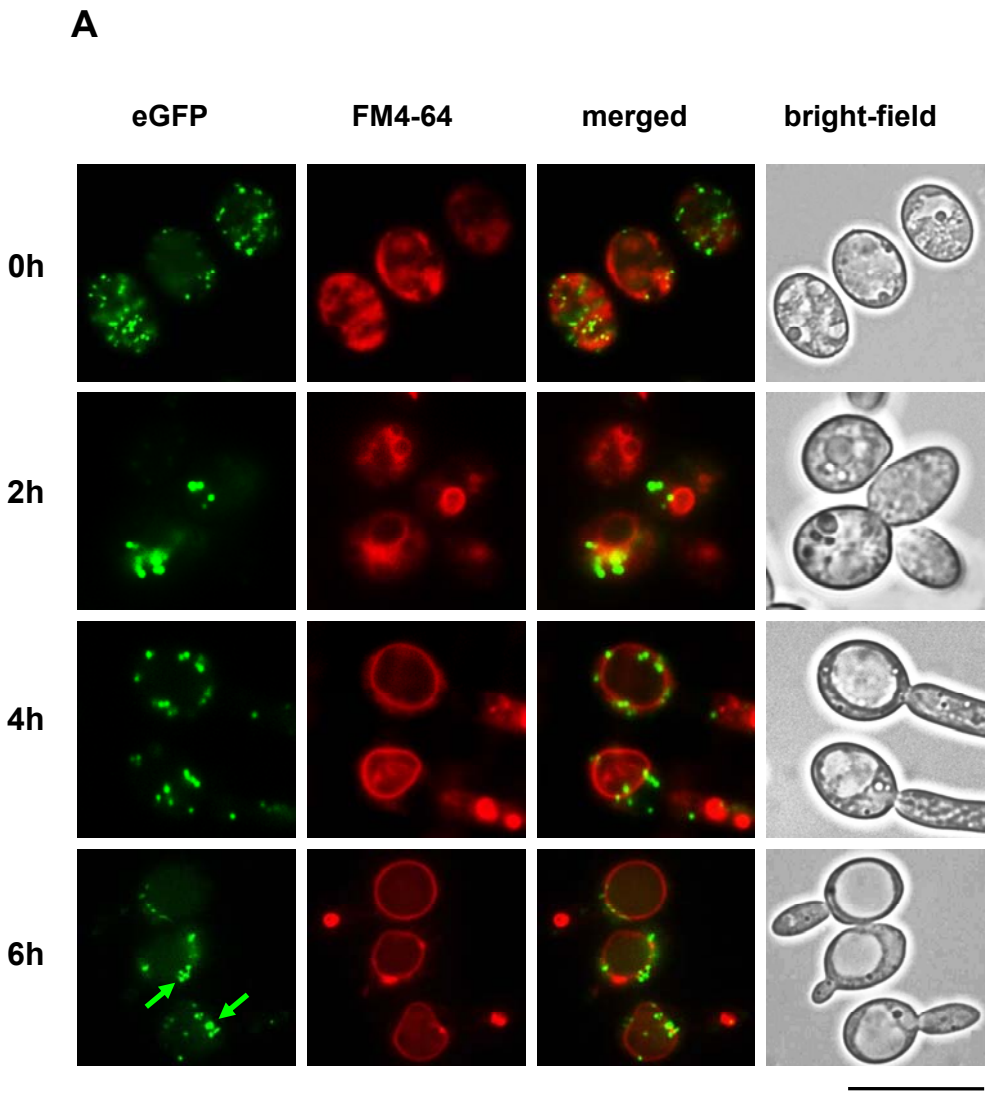

Figure 3.18 Fluorescence microscopic detection of peroxisome degradation in the *atg6* mutant of *Y. lipolytica*. Yeast cells were cultivated in an ethanol/ethylamine-containing medium to induce peroxisome biogenesis as described in *Materials and Methods (2.5.2)* and then transferred into glucose-containing media with **(A)** and without **(B)** a source of nitrogen. Probes were taken at the indicated time points, processed as described *(2.9)* and analyzed by fluorescent microscope. Peroxisomes were viewed with eGFP (green fluorescence). Vacuolar membranes were stained with FM4-64 (red fluorescence).
(A) The degradation of peroxisomes is impaired in the *atg6* mutant cells upon transfer into a glucose/ammonium sulfate-containing medium.
Arrows point to groups of non-degraded peroxisomes.
The scale bar is equal to 20 μm.

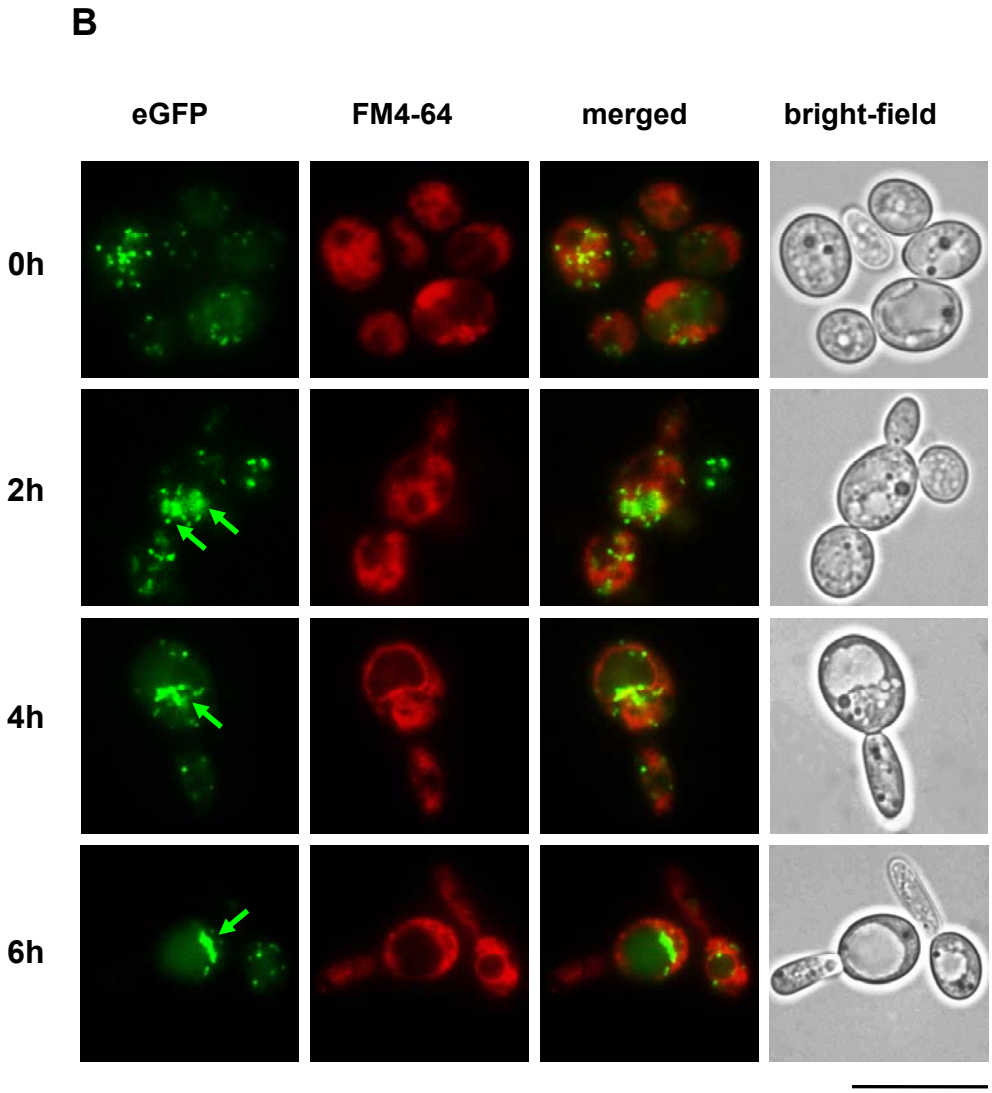

Figure 3.18 (continuation) Fluorescence microscopic detection of peroxisome degradation in the *atg6* mutant of *Y. lipolytica*.
(B) Peroxisomes are not degraded in the *atg6* mutant cells subjected to both glucose and nitrogen starvation simultaneously.
Arrows point to clusters of non-degraded peroxisomes.
The scale bar is equal to 20 μm.

3.5.2.3 The atg11 mutant of Y. lipolytica

No significant differences in the kinetics of inactivation of peroxisomal ICL and β-galactosidase could be observed between the wild type and the *atg11* mutant strains of *Y. lipolytica* upon transfer of cells from ethanol/ethylamine into glucose-containing medium supplemented with ammonium sulfate **(Fig. 3.19: A, B)**. Conversely, shift of the *Y. lipolytica atg11* cells into a glucose medium lacking nitrogen did not lead to a rapid inactivation of these enzymes as in the case of initial *Y. lipolytica* strain PO1d(pLG3) **(Fig. 3.19: C, D)**. The same cell-free extracts were then analyzed by Western blotting using antibodies against peroxisomal enzymes ICL and THI as well as cytoplasmic G6PDH. All examined peroxisomal proteins were found to degrade during cell growth in a glucose/ammonium sulfate-containing medium, whereas amount of the cytoplasmic marker protein considerably increased under the same conditions **Fig. 3.20 (A, B)**. Under the conditions of nitrogen starvation, however, no pronounced 2 h-decrease in the levels of ICL and THI could be detected in the *atg11* mutant if compared to the parental *Y. lipolytica* strain **(Fig. 3.20: C, D)**. Nevertheless, degradation event seemed to occur in the *atg11* cells since a general reduction of levels of the examined peroxisomal proteins were observed. In addition, the degradation of cytosolic G6PDH was unaffected in the *Y. lipolytica atg11* mutant cells starved by nitrogen **(Fig. 3.20: D)**. To verify these results, fluorescence microscopic analysis of the glucose-grown *atg11* strain was conducted as described above *(Materials and Methods, 3.2)*. As is obvious from **Fig. 3.21**, pexophagy was clearly delayed in the *atg11* mutant under both cultivation conditions. Peroxisomes were delivered to the vacuoles 2 h after transfer into glucose media. However, the degradation of peroxisomes did not take place yet since no green fluorescent signal could be observed in the vacuolar lumina of the glucose-grown *atg11* cells. After 4 h of cultivation, the degradation process began in the vacuoles but individual non-degraded peroxisomes could be still found at the close proximity to the vacuolar membranes. Similarly, not all of these organelles were taken up by the vacuoles after 6 h of cultivation. Taken together, this data demonstrates that the course of pexophagy is partially damaged in the *atg11* mutant, most probably at the stage of uptake of peroxisomes by the vacuoles. Conversely, formation of the vacuolar membrane invaginations seemed to be not disturbed in the *atg11* cells subjected to glucose and nitrogen starvation simultaneously. This fact, together with the normal degradation of G6PDH in the *atg11* mutant, suggests that YlAtg11p is not involved in the starvation-induced autophagy but is most likely implicated in the glucose-induced degradation of peroxisomes. In conclusion, it can be proposed that, in *Y. lipolytica*, presence of two different inducers in the growth medium may trigger at least two different degradation mechanisms. This assumption should be undoubtedly confirmed by further investigations.

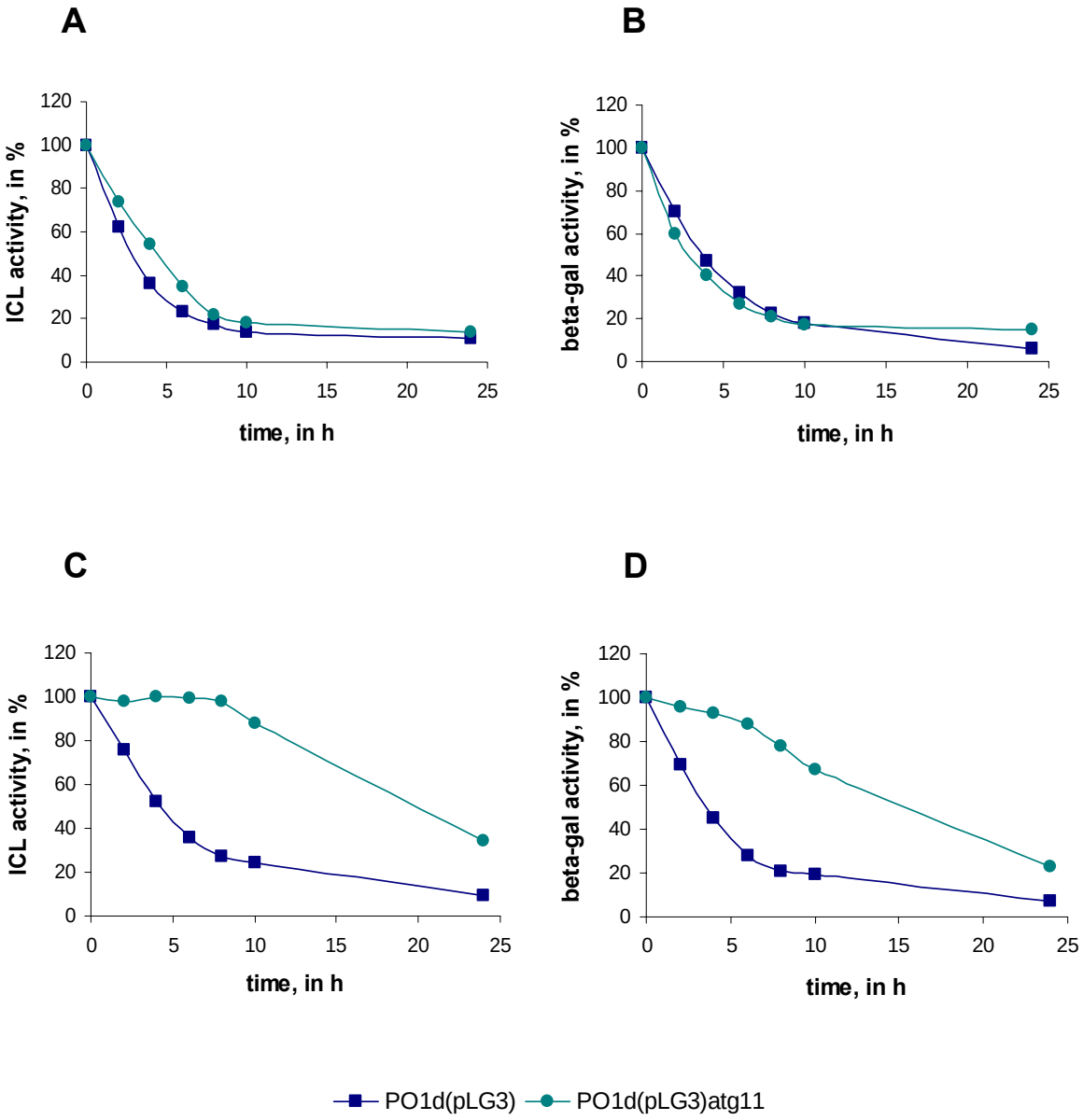

Figure 3.19 Changes in the relative activities of isocitrate lyase and β-galactosidase in the *Y. lipolytica* WT and *atg11* mutant cells under the peroxisome degradation inducing conditions. Ethanol/ethylamine-grown cells of the parental strain PO1d(pLG3) and the *atg11* mutant of *Y. lipolytica* were transferred into glucose media with **(A, B)** and without **(C, D)** nitrogen source as described above *(Materials and Methods, 2.5.2)*. Samples were taken immediately and after 2, 4, 6, 8 and 24 h of incubation. Cell-free extracts were prepared and activities of the peroxisomal ICL **(A,** C) and β-galactosidase **(B, D)** were determined as described *(2.7.7)*. Results of a representative experiment are shown. Specific enzyme activities are expressed as a percentage of the initial value (0 h) which is set to 100 %.

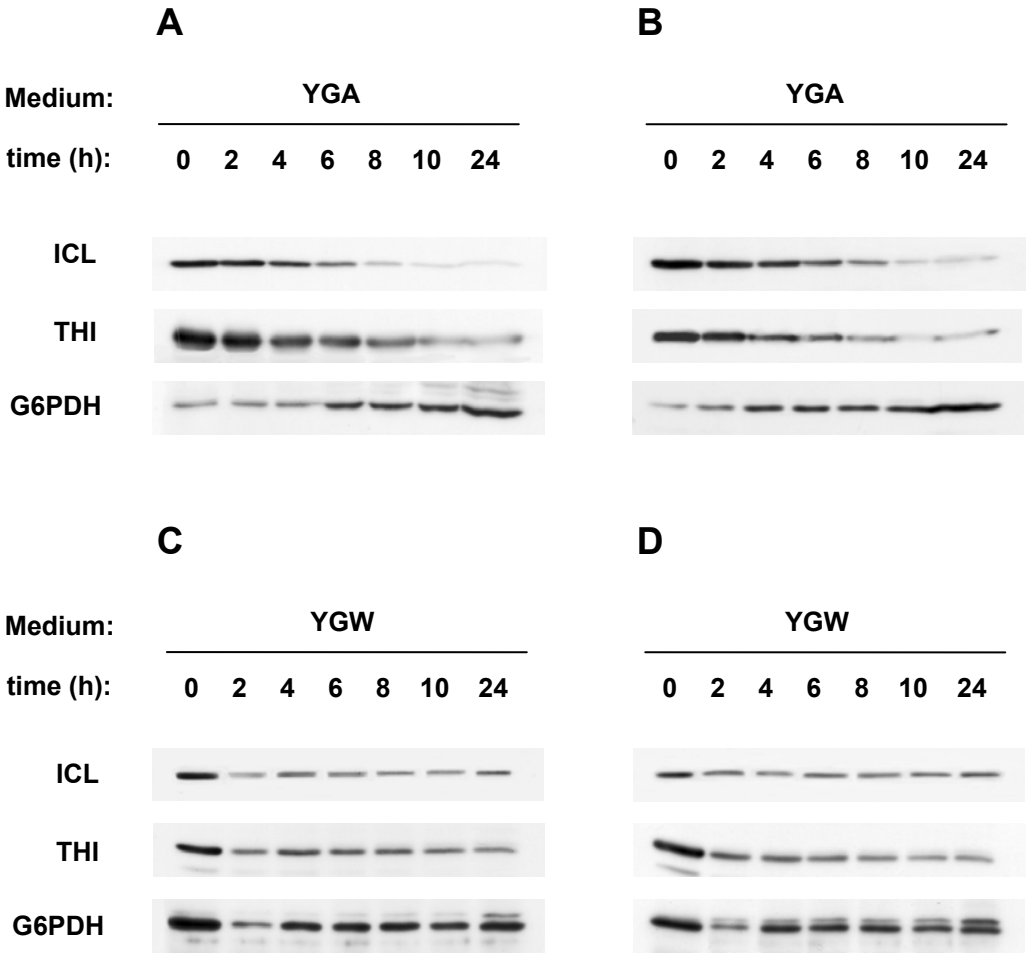

Figure 3.20 Changes in the levels of some marker proteins in the *Y. lipolytica* WT and *atg11* mutant cells subjected to the peroxisome degradation inducing conditions.
(A, B) Western blots performed with cell-free extracts of the ethanol/ethylamine-grown PO1d(pLG3) **(A)** and *atg11* mutant **(B)** cells shifted into a glucose/ammonium sulfate-containing medium. Equal volumes of cell-free extracts were loaded per line.
(C, D) Western blots performed with cell-free extracts of the ethanol/ethylamine-grown PO1d(pLG3) **(C)** and *atg11* mutant **(D)** cells shifted into a glucose medium lacking nitrogen. Equal volumes of cell-free extracts were loaded per line.
Abbreviations used for marker proteins: ICL, isocitrate lyase; THI, thiolase; G6PDH, glucoso-6-phosphate dehydrogenase.
Abbreviations used for media: YGA, yeast extract/glucose/ammonium sulfate; YGW, yeast extract/glucose without nitrogen source.

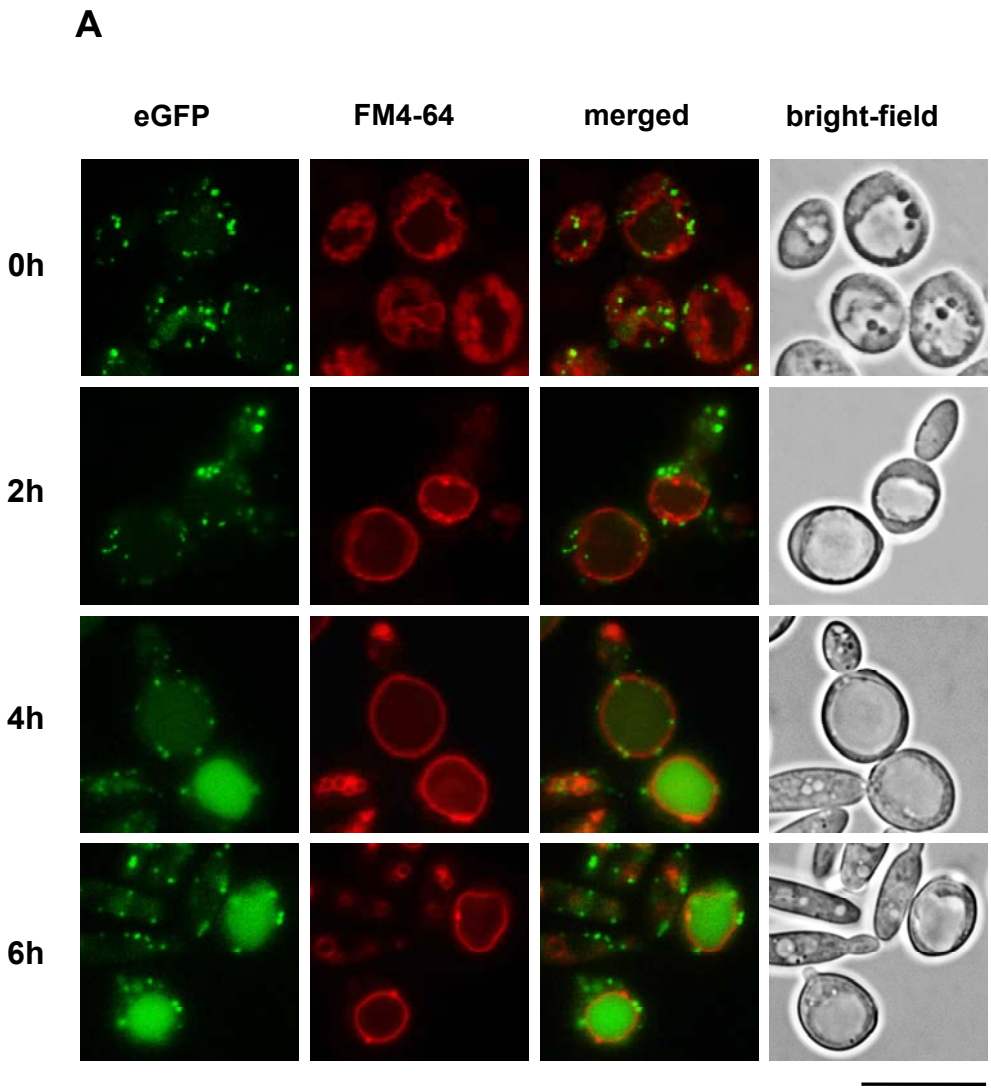

Figure 3.21 Fluorescence microscopic detection of peroxisome degradation in the *atg11* mutant of *Y. lipolytica*. Yeast cells were cultivated in an ethanol/ethylamine-containing medium to induce peroxisome biogenesis as described in *Materials and Methods (2.5.2)* and then transferred into glucose-containing media with **(A)** and without **(B)** nitrogen source. Probes were taken at the indicated time points, processed as described *(2.9)* and analyzed by fluorescent microscope. Peroxisomes were viewed with eGFP (green fluorescence). Vacuolar membranes were stained with FM4-64 (red fluorescence).
(A) Pexophagy is delayed in the *atg11* mutant cells grown in a medium containing glucose and ammonium sulfate.
The scale bar is equal to 20 μm.

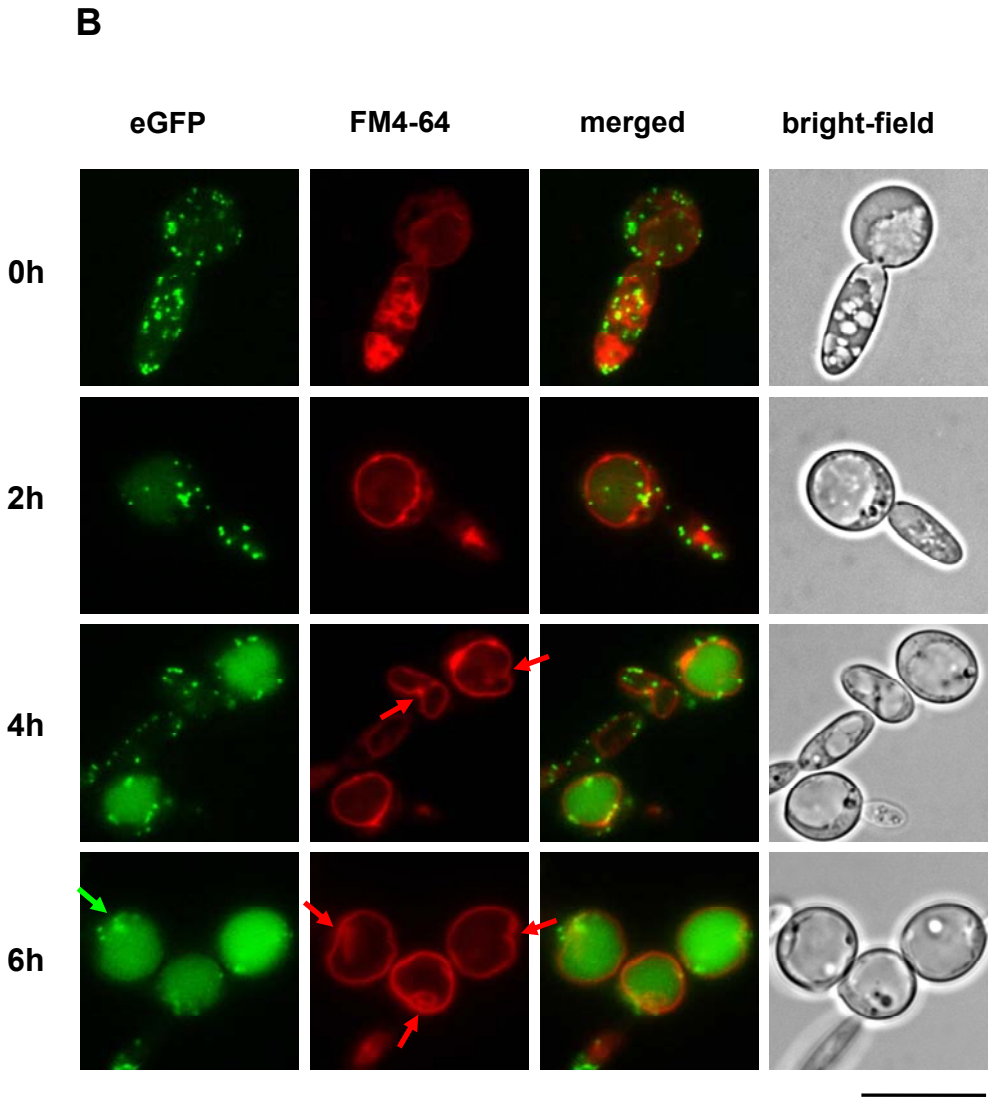

Figure 3.21 (continuation) Fluorescence microscopic detection of peroxisome degradation in the *atg11* mutant of *Y. lipolytica*.
(B) Pexophagy is delayed in the *atg11* mutant cells under the conditions of nitrogen starvation. Red arrows point to invaginations of the vacuolar membranes. A green arrow points to a cluster of non-degraded peroxisomes.
The scale bar is equal to 20 µm.

3.5.2.4 The atg18 mutant of Y. lipolytica

Shift of the ethanol/ethylamine-grown *Y. lipolytica* wild type and *atg18* mutant cells into a glucose/ammonium sulfate-containing medium led to the rapid inactivation of both ICL and β-galactosidase **(Fig. 3.22: A, B)**. Following Western blotting with the same cell-free extracts revealed a decrease in levels of the peroxisomal marker proteins ICL and THI, as well **(Fig. 3.23: A, B)**. At the same time, amounts of the cytosolic G6PDH did not significantly varied indicating selective character of peroxisome degradation under these conditions. However, opposite results were obtained after transfer of the ethanol/ethylamine-grown *atg18* cells into a minimal glucose medium lacking nitrogen. In this case, no obvious decrease in the activities of marker enzymes could be observed in the *atg18* mutant **(Fig. 3.22: C, D)**. Furthermore, no visible reduction in levels of peroxisomal (ICL and THI) and cytoplasmic (G6PDH) proteins could be found in the *atg18* mutant cells cultivated under the glucose and nitrogen starvation conditions **(Fig. 3.23: D)**. In the initial strain, on the contrary, degradation of all these proteins was detectable **(Fig. 3.23: C)**. The above observations were subsequently confirmed by the fluorescence microscopic analysis of the glucose-grown *Y. lipolytica atg18* cells. It was found that pexophagy was not disturbed in the *atg18* mutant subjected to glucose and ammonium sulfate simultaneously. As shown in **Fig. 3.24 (A)**, the organelles were normally targeted to and fused with the vacuoles in *atg18* cells during first 2-4 h of cultivation. 6 h after transfer into glucose and ammonium sulfate, a bulk of peroxisomal population was seen to be already removed by the vacuoles. Conversely, the autophagic degradation of peroxisomes appeared to be damaged in the ethanol/ethylamine-grown *atg18* cells transferred into a glucose medium lacking nitrogen. Under these conditions, distinct clusters of non-degraded organelles were observed at the vacuolar membranes of the *atg18* mutant cells **(Fig. 3.24: B, arrows)**. Furthermore, no peroxisomes could be detected inside the vacuoles in this mutant even after 6 h of incubation under glucose and nitrogen starvation that confirmed the phenotypic defects described above. In conclusion, it is suggested that the Atg18 homolog of *Y. lipolytica* is implicated in the course of peroxisome degradation under conditions of nitrogen depletion. On the other hand, YlAtg18p seems to be dispensable for pexophagy if both carbon and nitrogen sources are available. Another interesting observation is that development of the vacuolar membrane invaginations seemed to be disturbed in the *atg18* cells grown under conditions of nitrogen depletion. Together with unusual membranous formations observed in the cytoplasm of the nitrogen-starved *atg18* cells, it may suggest the involvement of the *YlATG18* gene product in the membrane dynamics during autophagic processes.

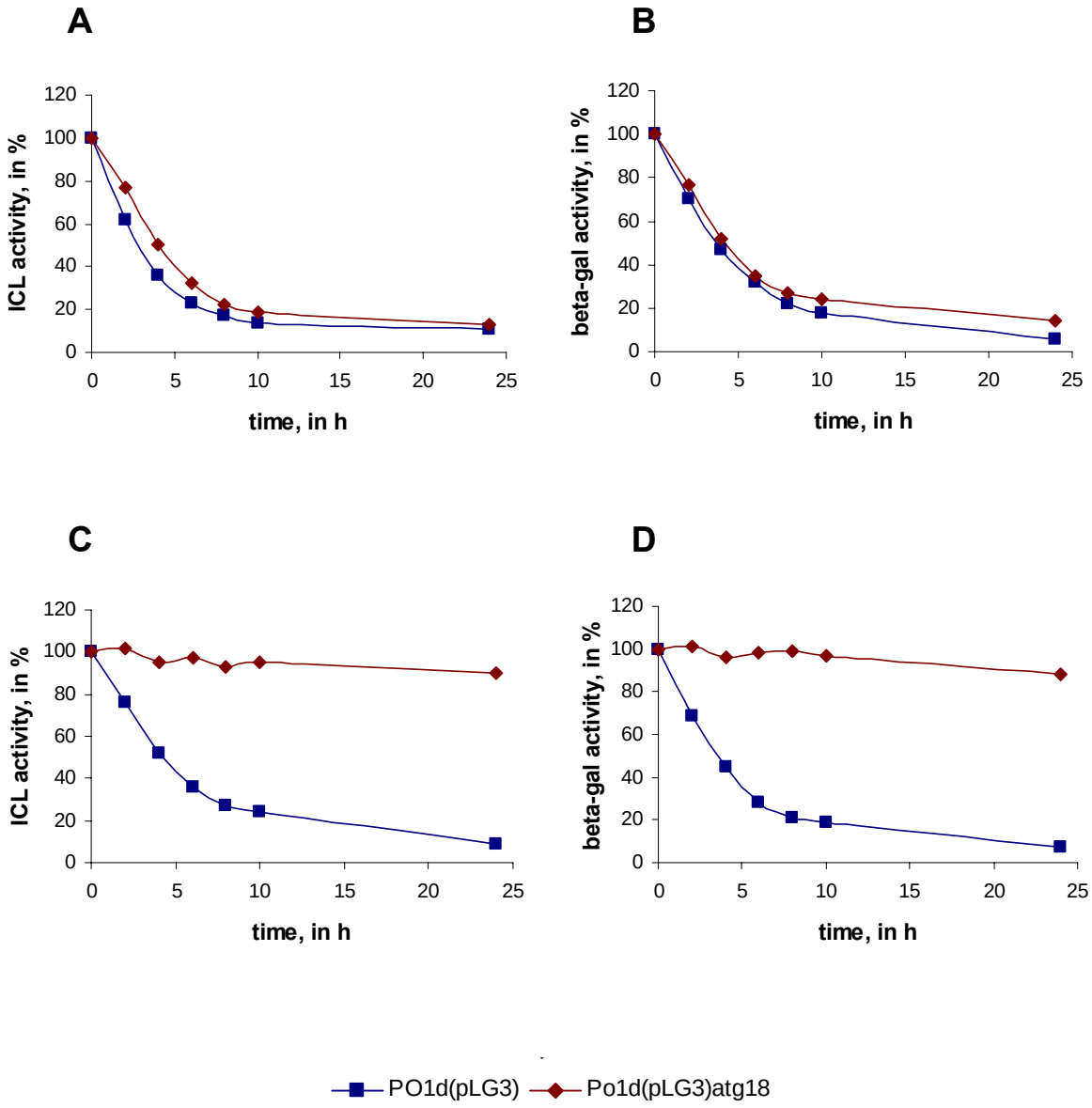

Figure 3.22 Changes in the relative activities of isocitrate lyase and β-galactosidase in the *Y. lipolytica* WT and *atg18* mutant cells under the peroxisome degradation inducing conditions. Ethanol/ethylamine-grown cells of the parental strain PO1d(pLG3) and the *atg18* mutant of *Y. lipolytica* were transferred into glucose media with **(A, B)** and without **(C, D)** nitrogen source as described above *(Materials and Methods, 2.5.2)*. Samples were collected immediately (0 h) and after 2, 4, 6, 8 and 24 h of incubation. Cell-free extracts were then prepared and activities of the peroxisomal ICL **(A, C)** and β-galactosidase **(B, D)** were determined as described *(2.7.7)*. Results of a representative experiment are shown. Specific enzyme activities are expressed as a percentage of the initial value (0 h) which is set to 100 %.

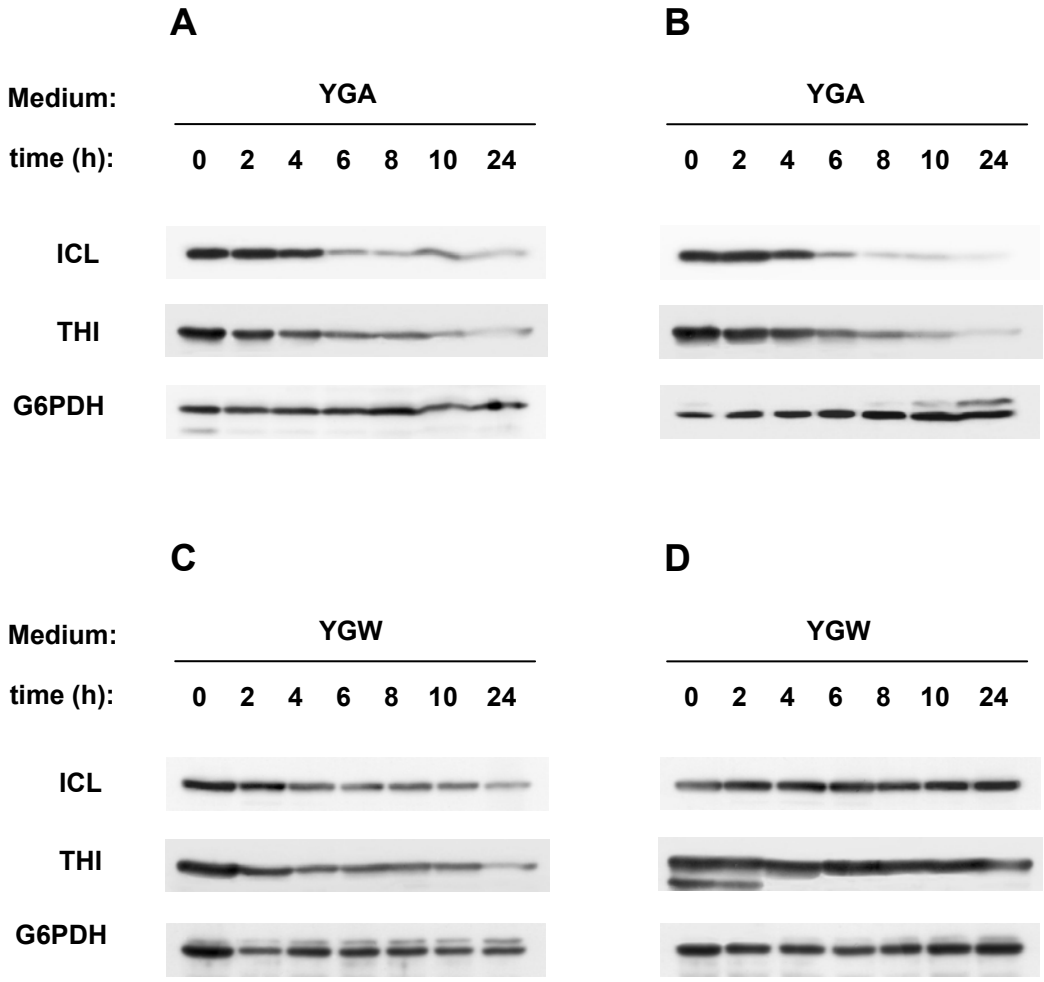

Figure 3.23 Changes in the levels of some marker proteins in the *Y. lipolytica* WT and *atg18* mutant cells subjected to the peroxisome degradation inducing conditions.

(A, B) Western blots performed with cell-free extracts of the ethanol/ethylamine-grown PO1d(pLG3) **(A)** and *atg18* **(B)** cells shifted into a glucose/ammonium sulfate-containing medium. Equal volumes of cell-free extracts were loaded per line.

(C, D) Western blots performed with cell-free extracts of the ethanol/ethylamine-grown PO1d(pLG3) **(C)** and *atg18* mutant **(D)** cells shifted into a glucose medium lacking nitrogen. Equal volumes of cell-free extracts were loaded per line.

Abbreviations used for marker proteins: ICL, isocitrate lyase; THI, thiolase; G6PDH, glucoso-6-phosphate dehydrogenase.

Abbreviations used for media: YGA, yeast extract/glucose/ammonium sulfate; YGW, yeast extract/glucose without nitrogen source.

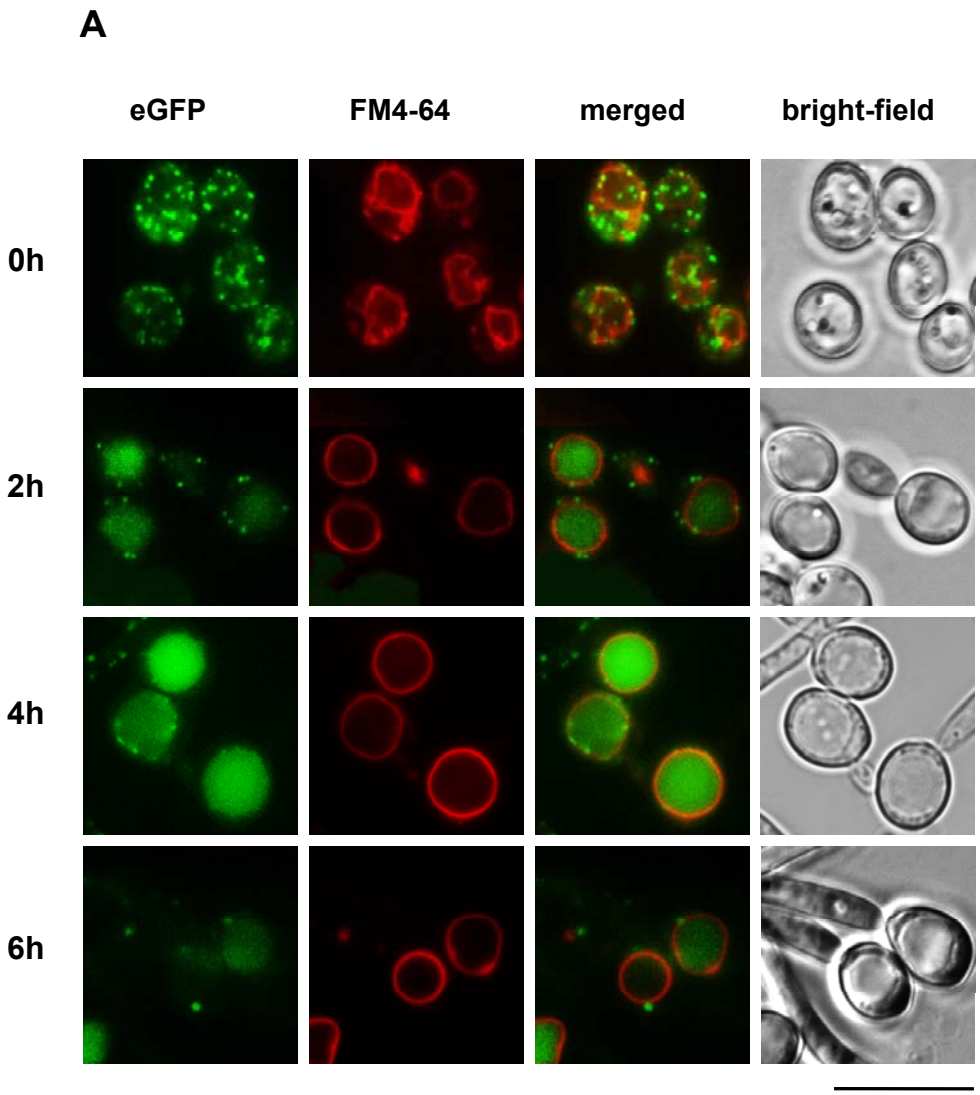

Figure 3.24 Fluorescence microscopic detection of peroxisome degradation in the *atg18* mutant of *Y. lipolytica*. Yeast cells were cultivated in an ethanol/ethylamine-containing medium to induce peroxisome biogenesis as described in *Materials and Methods (2.5.2)* and then transferred into glucose media with **(A)** and without **(B)** nitrogen source. Probes were taken at the indicated time points, processed as described *(2.9)* and analyzed by fluorescent microscope. Peroxisomes were viewed with eGFP (green fluorescence). Vacuolar membranes were stained with FM4-64 (red fluorescence).
(A) A bulk of peroxisomal population is removed by the vacuoles in the *atg18* mutant cells subjected to glucose and ammonium sulfate.
The scale bar is equal to 20 µm.

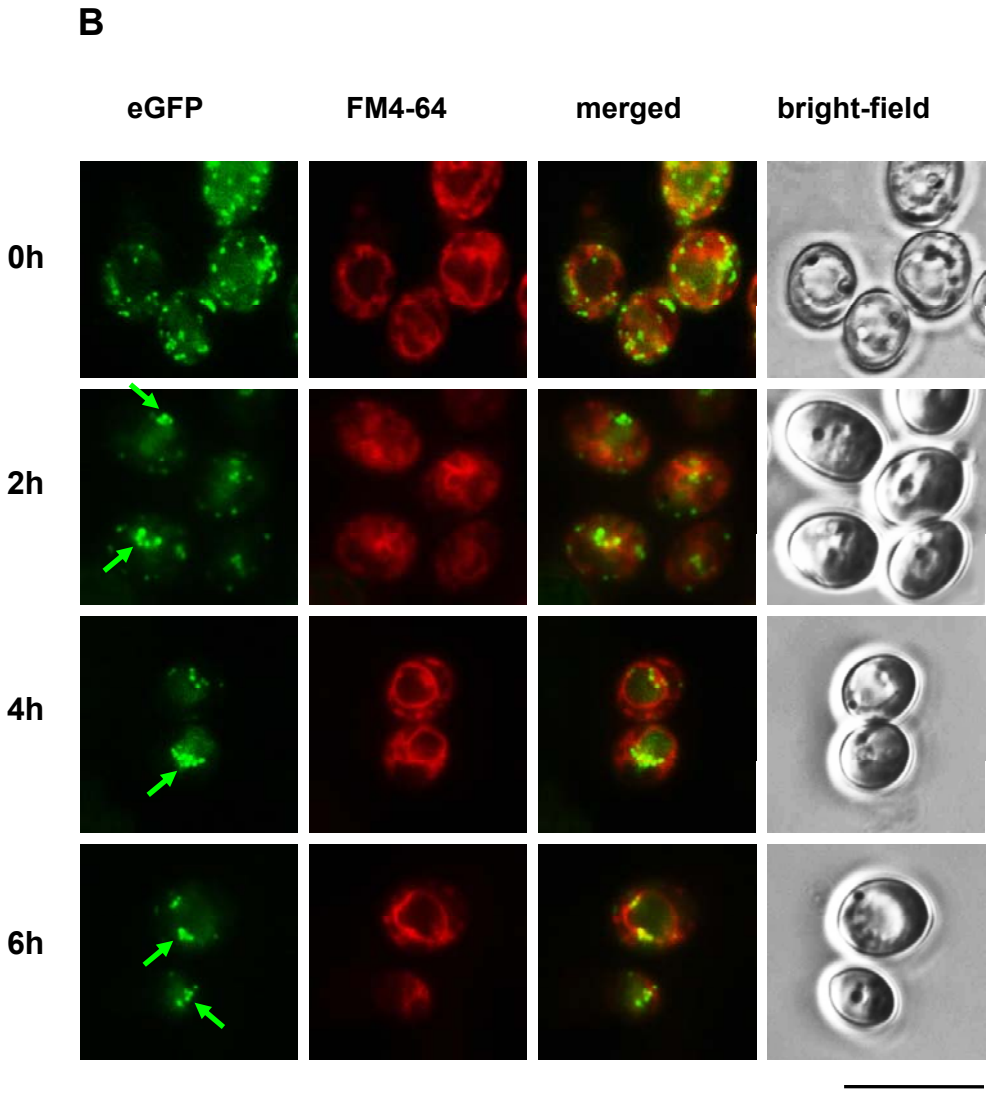

Figure 3.24 (continuation) Fluorescence microscopic detection of peroxisome degradation in the *atg18* mutant of *Y. lipolytica*.
(B) The degradation of peroxisomes is disturbed in the *atg18* mutant cells grown in a glucose medium lacking nitrogen.
Arrows point to clusters of non-degraded peroxisomes.
The scale bar is equal to 20 µm.

3.5.2.5 The gcn2 mutant of Y. lipolytica

Measuring of enzymatic activities of the homologous ICL and heterologous β-galactosidase did not reveal any significant differences between the parental and the *gcn2* mutant strains of *Y. lipolytica* shifted into glucose-containing media with and without source of nitrogen. In general, a rapid inactivation of these enzymes could be observed under both tested conditions **(Fig. 3.25)**. Results obtained biochemically were confirmed by the following Western blotting. In this experiment, a peroxisomal marker protein THI was found to degrade in both wild type and *gcn2* mutant cells upon transfer into glucose/ammonium sulfate-containing medium **(Fig. 3.26: A, B)**. At the same time, the levels of the control cytosolic marker enzyme G6PDH remained generally unchangeable in the parental as well as in the *gcn2* mutant strains of *Y. lipolytica*. Essentially the same observations were made for the ethanol/ethylamine-grown yeast cells subjected to glucose and nitrogen starvation conditions. As shown in **Fig. 3.26 (C, D)**, the degradation patter of THI showed basically the same tendency in the wild type and *gcn2* mutant, except for a probable 2 h-degradation delay. However, the last observation is most likely an artifact. Further immunological detection of the G6PDH didn't reveal any noticeable differences between the wild type and the mutant strains. To verify these results, fluorescence microscopy of the glucose-grown *gcn2* cells was performed. As expected, pexophagy appeared to be not impaired in the ethanol/ethylamine-grown *gcn2* mutant cells transferred into glucose and ammonium sulfate. As is evident from **Fig. 3.27 (A)**, the organelles underwent normal degradation in the vacuoles of mutant cells since a 4 h-shift into glucose/ammonium sulfate-containing medium resulted in a strong vacuolar staining with eGFP. Similarly, no obvious defects in the peroxisome degradation could be revealed in the *gcn2* mutant under conditions of glucose and nitrogen starvation **(Fig. 3.27: B)**. Taken together, these results indicate that the Gcn2 homolog of *Y. lipolytica* is apparently not involved in the degradation of peroxisomes since disruption of the corresponding *YlGCN2* gene didn't appear to be essential for the course of pexophagy in this yeast. However, an absence of well-formed invaginations of the vacuolar membranes under conditions of nitrogen depletion remains a remarkable feature of the *gcn2* mutant phenotype **(Fig. 3.27: B, arrows)**, which, in turn, could be due to a defect in the microautophagic process normally triggered by starvation.

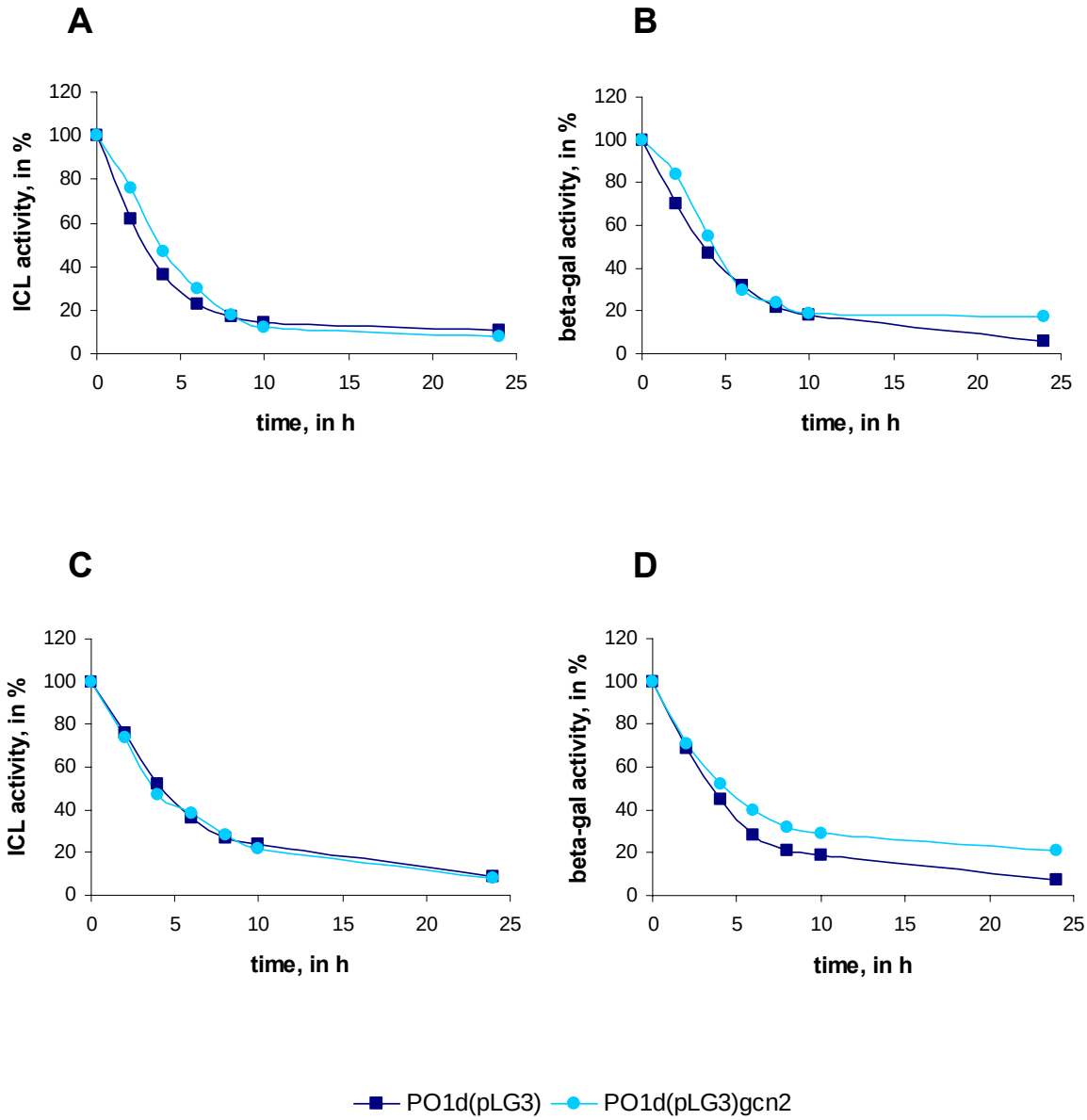

Figure 3.25 Changes in the relative activities of isocitrate lyase and β-galactosidase in the *Y. lipolytica* WT and *gcn2* mutant cells under the peroxisome degradation-inducing conditions. Ethanol/ethylamine-grown cells of the parental strain PO1d(pLG3) and the *gcn2* mutant of *Y. lipolytica* were transferred into glucose media with **(A, B)** and without **(C, D)** nitrogen source as described above *(Materials and Methods, 2.5.2)*. Samples were taken immediately (0 h) and after 2, 4, 6, 8 and 24 h of incubation. Cell-free extracts were prepared and activities of the peroxisomal ICL **(A, C)** and β-galactosidase **(B, D)** were determined as described *(2.7.7)*. Results of a representative experiment are shown. Specific enzyme activities are expressed as a percentage of the initial value (0 h) which is set to 100 %.

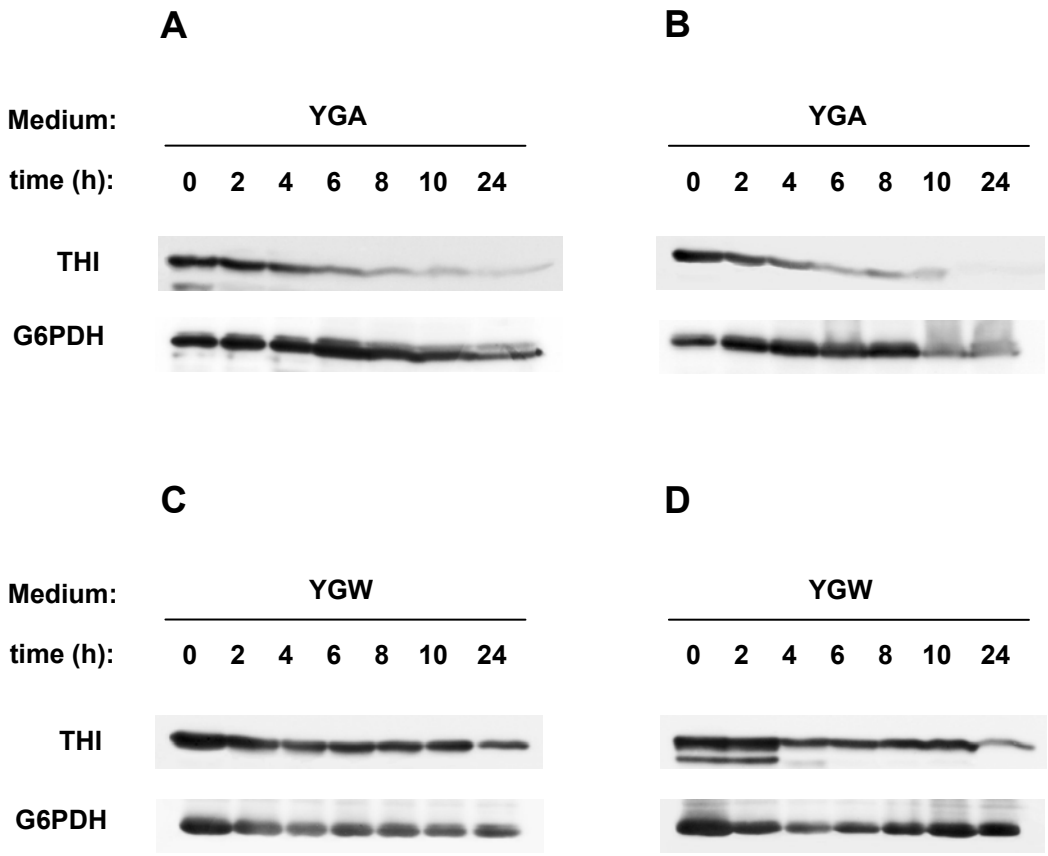

Figure 3.26 Changes in the levels of some marker proteins in the *Y. lipolytica* WT and *gcn2* mutant cells subjected to the peroxisome degradation inducing conditions.
(A, B) Western blots performed with cell-free extracts of the ethanol/ethylamine-grown PO1d(pLG3) **(A)** and *gcn2* **(B)** cells shifted into a glucose/ammonium sulfate-containing medium. Equal volumes of cell-free extracts were loaded per line.
(C, D) Western blots performed with cell-free extracts of the ethanol/ethylamine-grown PO1d(pLG3) **(C)** and *gcn2* **(D)** cells shifted into a glucose medium lacking nitrogen. Equal volumes of cell-free extracts were loaded per line.
Abbreviations used for marker proteins: THI, thiolase; G6PDH, glucoso-6-phosphate dehydrogenase.
Abbreviations used for media: YGA, yeast extract/glucose/ammonium sulfate; YGW, yeast extract/glucose without nitrogen source.

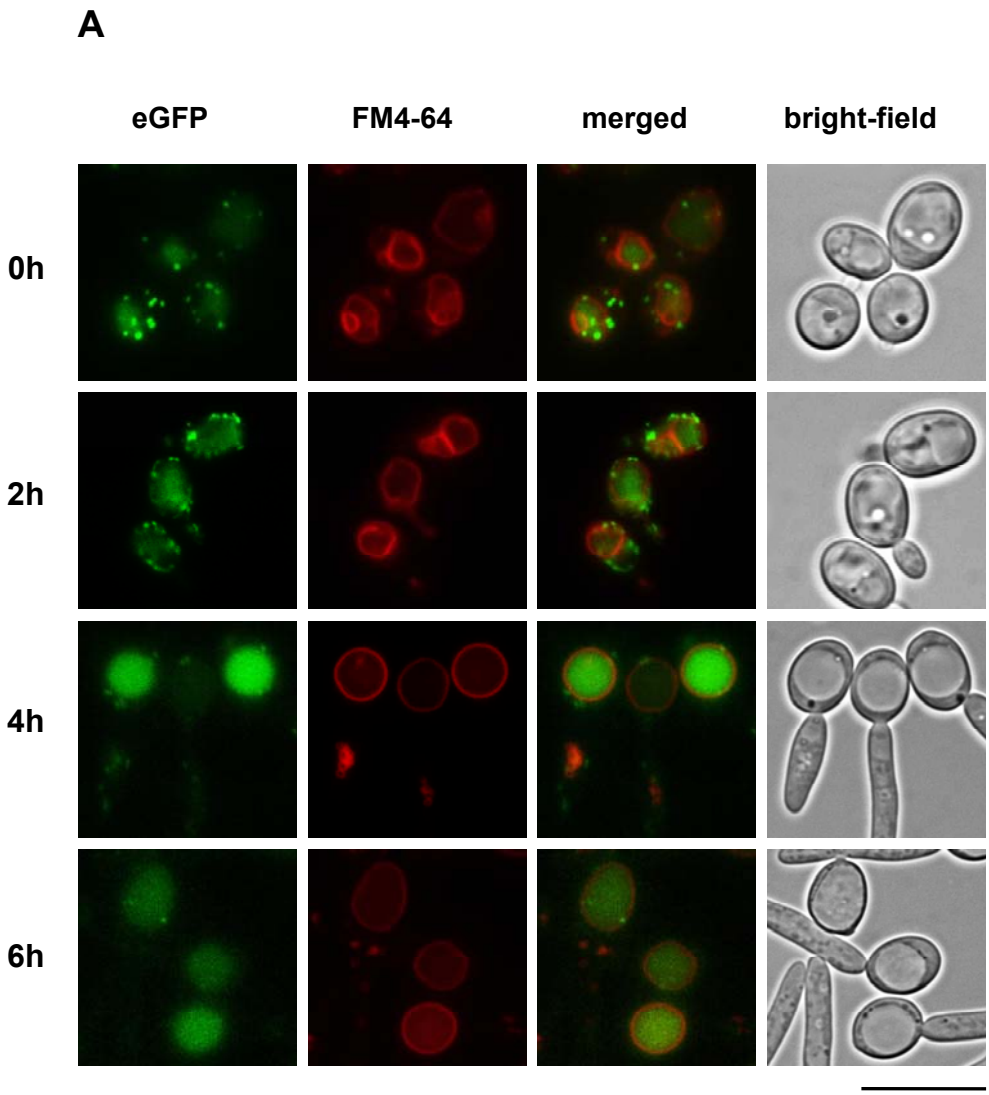

Figure 3.27 Fluorescence microscopic detection of peroxisome degradation in the *gcn2* mutant of *Y. lipolytica*. Yeast cells were cultivated in an ethanol/ethylamine-containing medium to induce peroxisome biogenesis as described in *Materials and Methods (2.5.2)* and then transferred into glucose-containing media with **(A)** and without **(B)** nitrogen. Probes were taken at the indicated time points, processed as described *(2.9)* and analyzed by fluorescent microscope. Peroxisomes were viewed with eGFP (green fluorescence). Vacuolar membranes were stained with FM4-64 (red fluorescence).
(A) Peroxisomes are selectively degraded in the vacuoles upon transfer of the ethanol/ethylamine-grown *gcn2* mutant cells into a glucose/ammonium sulfate-containing medium.
The scale bar is equal to 20 μm.

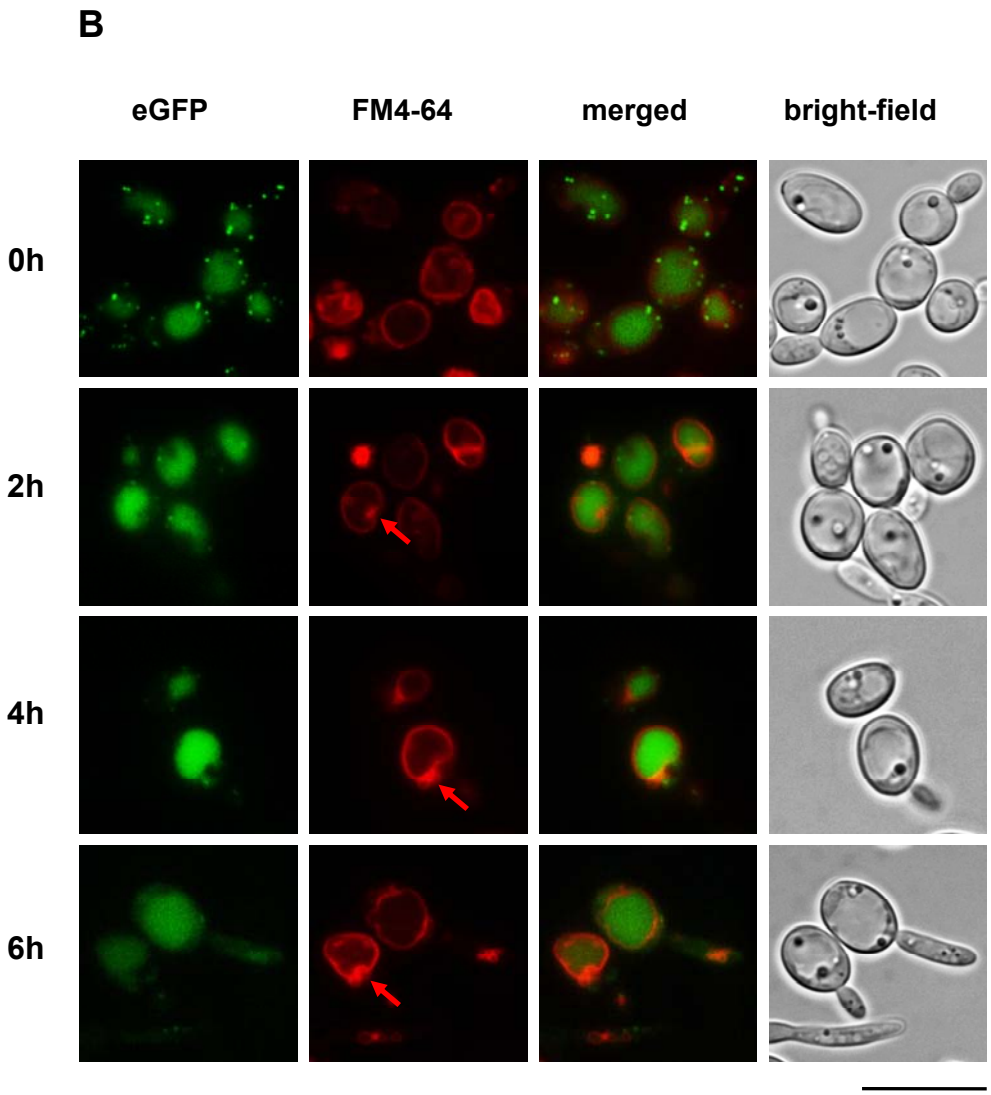

Figure 3.27 (continuation) Fluorescence microscopic detection of peroxisome degradation in the *gcn2* mutant of *Y. lipolytica*.
(B) Peroxisomes are targeted to and degraded in the vacuoles of the *gcn2* mutant cells in a glucose medium lacking nitrogen.
Arrows point to uncompleted invaginations of the vacuolar membranes.
The scale bar is equal to 20 µm.

3.5.2.6 The pep4 mutant of Y. lipolytica

Transfer of the wild type and *pep4* mutant cells from ethanol/ethylamine- into glucose-containing media followed by measurements of the activities of peroxisomal enzymes ICL and β-galactosidase revealed an obvious delay in the decrease of these activities in the *pep4* mutant. As is evident from **Fig. 3.28**, in the initial strain, a half-reduction of the tested enzyme activities was detected already during the first 4 h of cell growth in glucose media with and without nitrogen source. On the contrary, only about 10-20 % decrease of these activities could be observed in the *pep4* cells under the same conditions. The acquired enzyme activity profiles were confirmed by the following Western blot analysis. As shown in **Fig. 3.29 (A, B)**, degradation of the peroxisomal marker proteins ICL and THI was clearly retarded in the *pep4* cells subjected to glucose and ammonium sulfate in comparison with the parental *Y. lipolytica* strain PO1d(pLG3). Likewise, only a slight reduction in levels of the examined peroxisomal proteins could be found in the *pep4* mutant during its growth in glucose-containing nitrogen-depleted medium whereas these proteins underwent normal degradation in the corresponding wild type cells **(Fig. 3.29: C, D)**. Furthermore, degradation of the cytosolic G6PDH appeared to be reduced in the *pep4* cells under conditions of nitrogen starvation, as well, suggesting possible defects in the course of autophagy in this *Y. lipolytica* mutant. Assumed mutant phenotype of the *pep4* strain could be also confirmed by further fluorescence microscopic analysis of the glucose-grown mutant cells. As shown in **Fig. 3.30**, vacuolar degradation of peroxisomes was clearly affected in the *pep4* cells subjected to glucose/ammonium sulfate and glucose/nitrogen starvation media. Under both conditions, degradation event was first normally initiated as the organelles were found to be directed to the vacuoles 2 h after transfer into the peroxisome degradation-inducing media. Also, fusion events between the auto(pexo)phagosomal and vacuolar membranes seemed to be not disturbed in the *pep4* mutant cells. However, the subsequent vacuolar degradation of peroxisomes appeared to be reduced during cultivation of the *pep4* cells in glucose/ammonium sulfate-containing medium **(Fig. 3.30: A)**. Under conditions of nitrogen starvation, this process was obviously delayed since a strong eGFP fluorescence could be observed within the vacuoles of the *pep4* cells even 8 h after the shift into minimal medium with glucose and without any source of nitrogen **(Fig 3.30: B)**. Furthermore, the vacuolar membranes of the *pep4* mutant were found to form numerous invaginations and protrusions not only upon starvation but also under normal growth conditions probably to compensate the lack of degradation capacity of the vacuoles **(arrows)**. Altogether, these results strongly suggest that YlPep4p is required for sufficient peroxisome degradation in glucose-grown yeast cells both in the presence and in the absence of a nitrogen source.

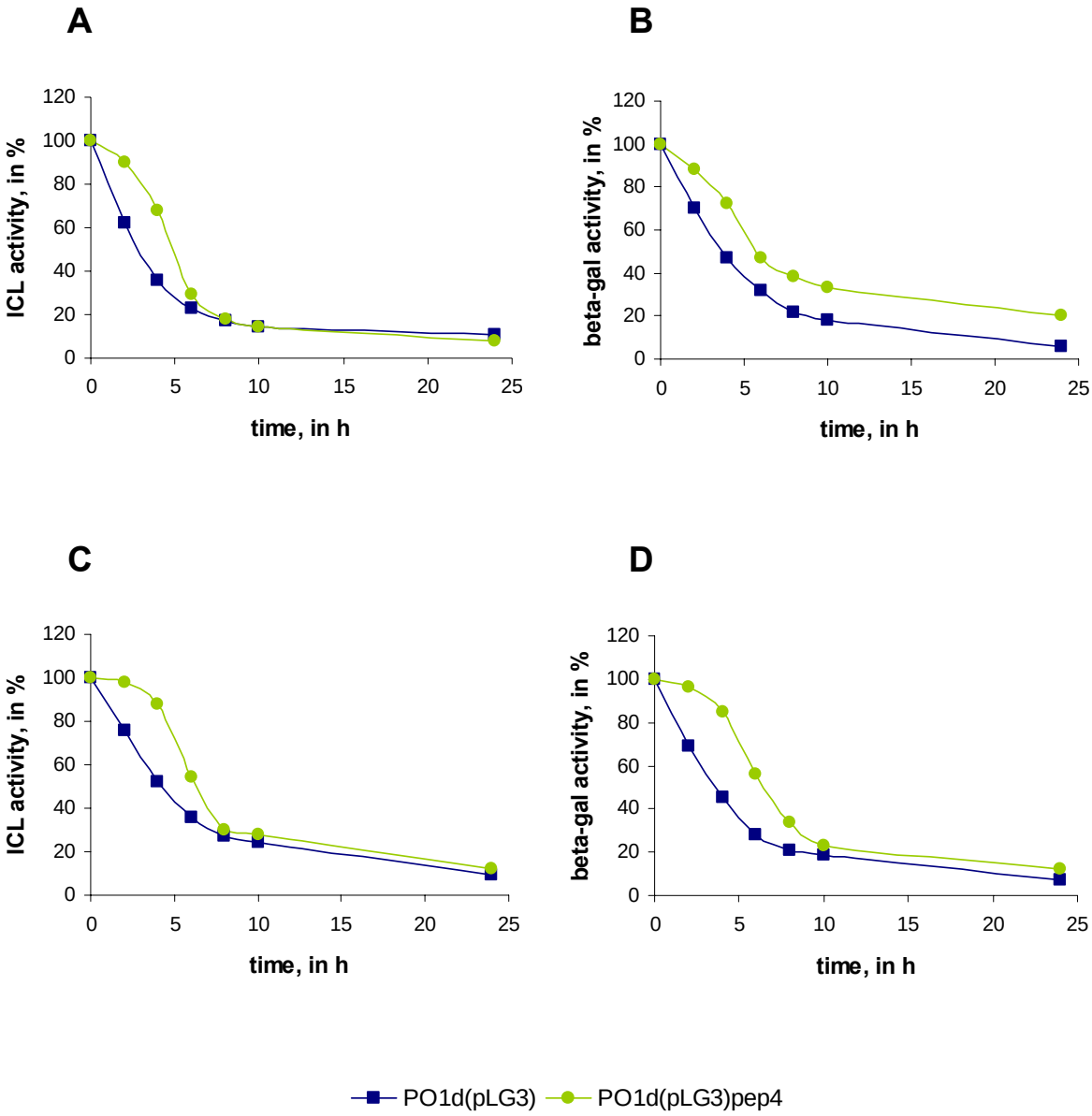

Figure 3.28 Changes in the relative activities of isocitrate lyase and β-galactosidase in the *Y. lipolytica* WT and *pep4* mutant cells under the peroxisome degradation inducing conditions. Ethanol/ethylamine-grown cells of the parental strain PO1d(pLG3) and *pep4* mutant of *Y. lipolytica* were transferred into glucose media with **(A, B)** and without **(C, D)** source of nitrogen as described above *(Materials and Methods, 2.5.2)*. Samples were collected immediately (0 h) and after 2, 4, 6, 8 and 24 h of incubation. Cell-free extracts were then prepared and activities of the peroxisomal ICL **(A, C)** and β-galactosidase **(B, D)** were determined as described *(2.7.7)*. Results of a representative experiment are shown. Specific enzyme activities are expressed as a percentage of the initial value (0 h) which is set to 100 %.

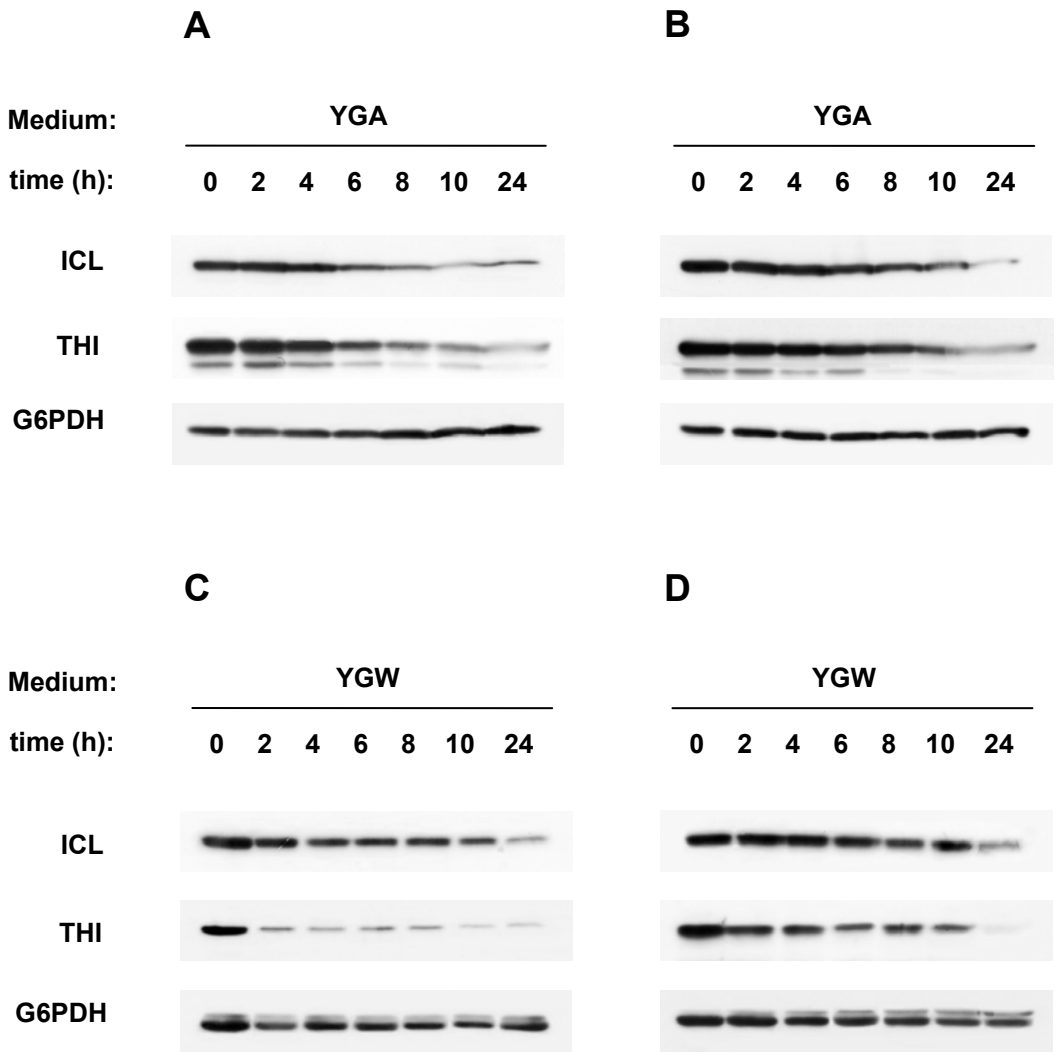

Figure 3.29 Changes in the levels of some marker proteins in the *Y. lipolytica* WT and *pep4* mutant cells subjected to the peroxisome degradation inducing conditions.
(A, B) Western blots performed with cell-free extracts of the ethanol/ethylamine-grown PO1d(pLG3) **(A)** and *pep4* **(B)** cells shifted into a glucose/ammonium sulfate-containing medium. Equal volumes of cell-free extracts were loaded per line.
(C, D) Western blots performed with cell-free extracts of the ethanol/ethylamine-grown PO1d(pLG3) **(C)** and *pep4* mutant **(D)** cells shifted into a glucose medium lacking nitrogen. Equal volumes of cell-free extracts were loaded per line.
Abbreviations used for marker proteins: ICL, isocitrate lyase; THI, thiolase; G6PDH, glucoso-6-phosphate dehydrogenase.
Abbreviations used for media: YGA, yeast extract/glucose/ammonium sulfate; YGW, yeast extract/glucose without nitrogen source.

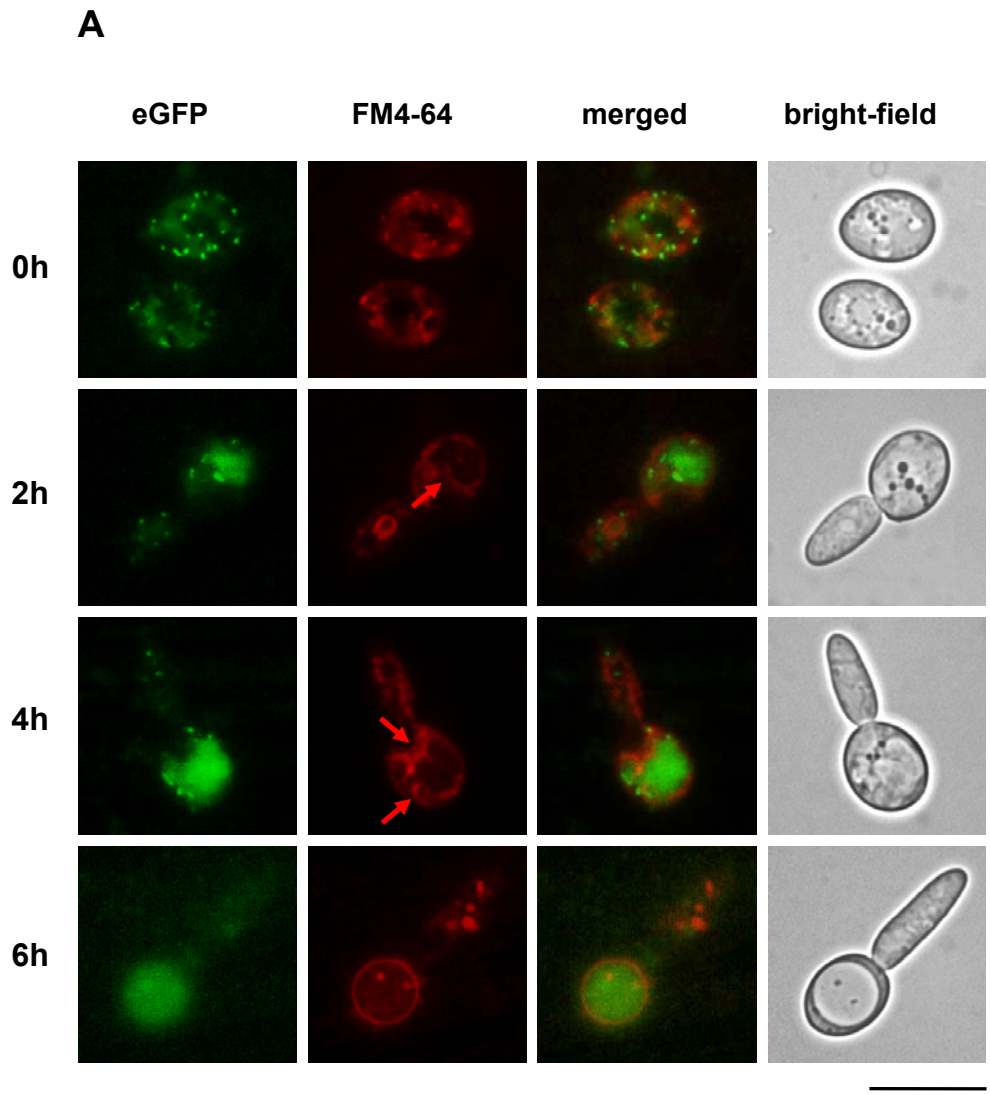

Figure 3.30 Fluorescent microscopic detection of peroxisome degradation in the *pep4* mutant of *Y. lipolytica*. Yeast cells were cultivated in an ethanol/ethylamine-containing medium to induce peroxisome biogenesis as described in *Materials and Methods (2.5.2)* and then transferred into glucose-containing media with **(A)** and without **(B)** nitrogen. Probes were taken at the indicated time points, processed as described *(2.9)* and analyzed by fluorescent microscope. Peroxisomes were viewed with eGFP (green fluorescence). Vacuolar membranes were stained with FM4-64 (red fluorescence).
(A) The rate of pexophagy is reduced in the *pep4* cells subjected to glucose and ammonium sulfate.
Arrows point to invaginations of the vacuolar membranes.
The scale bar is equal to 20 μm.

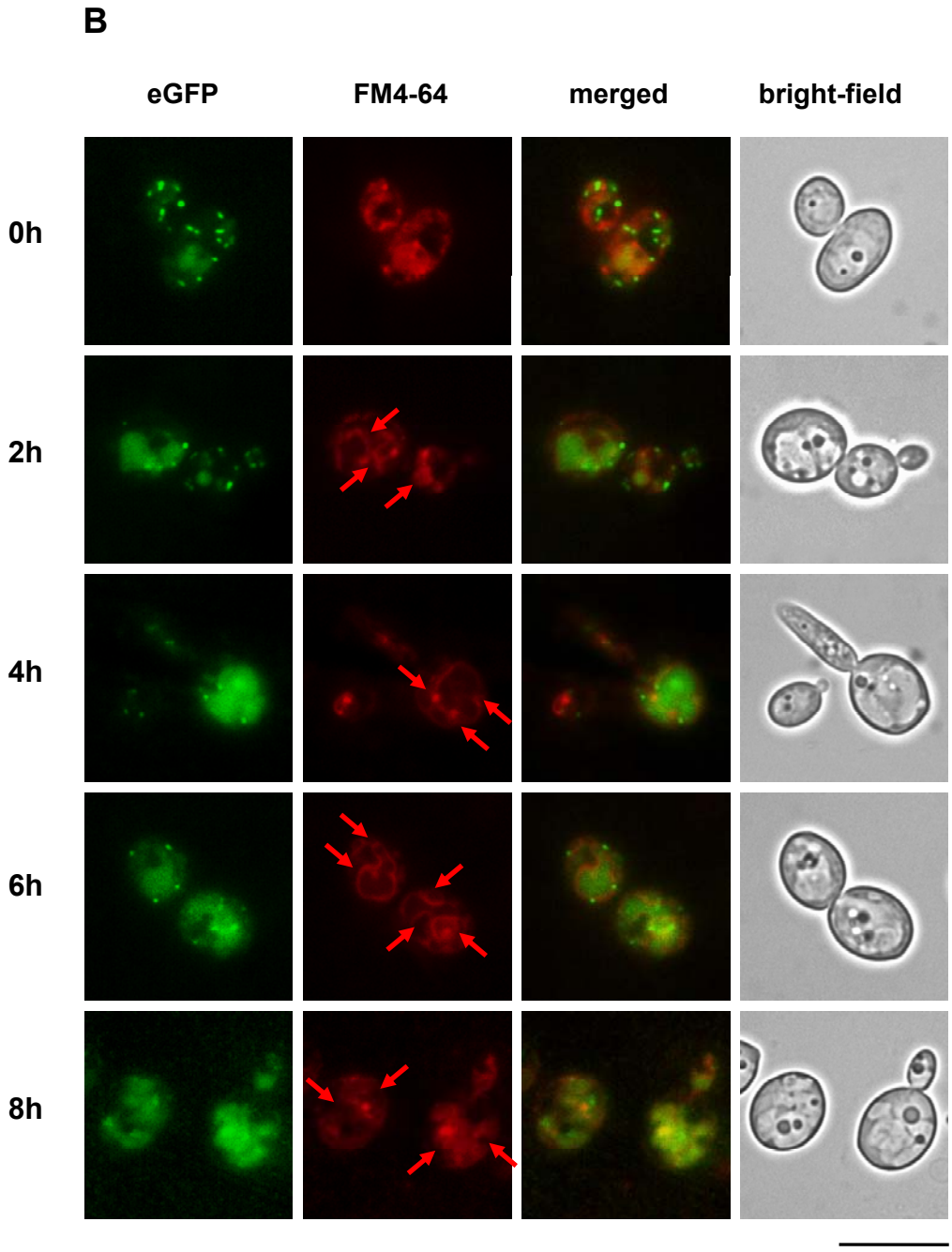

Figure 3.30 (continuation) Fluorescent microscopic detection of peroxisome degradation in the *pep4* mutant of *Y. lipolytica*.
(B) The degradation of peroxisomes is delayed in the *pep4* mutant cells transferred into a glucose-containing medium depleted by nitrogen.
Arrows point to numerous protrusions and invaginations of the vacuolar membranes.
The scale bar is equal to 20 µm.

3.6 Isolation of novel *Y. lipolytica* peroxisome degradation deficient mutants by the use of chimerical protein βGal-eGFP(SKL)

The last part of this thesis project was focused on isolation of novel *Y. lipolytica* mutant strains affected in the autophagic degradation of peroxisomes (so-called *pdd* mutants). For this purpose, a visual screening method was devised utilizing heterologous β-galactosidase as a marker enzyme for peroxisomes (for its detailed description, see *Materials and Methods, 2.8*). In this screening, *Y. lipolytica* strain PO1d(pLG3) expressing the chimerical protein βGal-eGFP(SKL) under the control of a strongly regulated homologous *YlICL1* promoter was used as initial one. MNNG-treated yeast cells were first grown on ethanol/ethylamine agar plates in order to induce peroxisome biogenesis and then transferred onto glucose/ammonium sulfate and glucose/nitrogen starved plates to provoke turnover of these organelles. The cell-carrying filters were subsequently subjected to the β-galactosidase activity assay *(Fig. 7.17 in Appendix)*. Yeast colonies exhibited blue coloring on both ethanol/ethylamine- and glucose-containing plates were kept for the secondary screen. Progenies of individual strains with stable mutant phenotypes were then tested for their ability to degrade peroxisomes. Fluorescence microscopic analysis of peroxisomal turnover in two of selected *Y. lipolytica* mutants (№№ 32 and 55) showing most robust phenotypic alterations was done as describe above *(Materials and Methods, 2.9)*.

As shown in **Fig. 3.31 (A)**, pexophagy was not damaged in the ethanol/ethylamine-grown cells of the strain № 32 transferred into glucose and ammonium sulfate as most of organelles were found to degrade in the vacuoles 6 h after transfer. However, shift of the mutant cells into glucose-containing medium lacking nitrogen source revealed a clear delay in the degradation of peroxisomes **(Fig. 3.31: B)**. Remarkably, delivery of peroxisomes to and their uptake by the vacuoles was not impaired as seen 4 h after exposing of cell to the glucose/nitrogen starvation conditions. The following degradation step, however, turned out to be obstructed since a strong green fluorescence could be still observed in the vacuolar lumina of the mutant cells after 6 h of cultivation. A most obvious reason for this mutant phenotype could be a strong alteration of the vacuolar morphology as revealed by the FM4-64 staining. Displaying firstly a normal morphology, the vacuoles of mutant cells appeared to be many times folded forming numerous wrinkles and cisterna after transfer into the glucose-containing medium lacking nitrogen **(Fig. 3.31: B)**. Taking into account this fact, we couldn't rule out a possibility that the delay in peroxisome degradation in the strain № 32 results rather from abnormal morphology of the vacuoles than from a defect in the course of degradation itself. However, it still remains a good example of an exciting mutant phenotype which can be screened by this system.

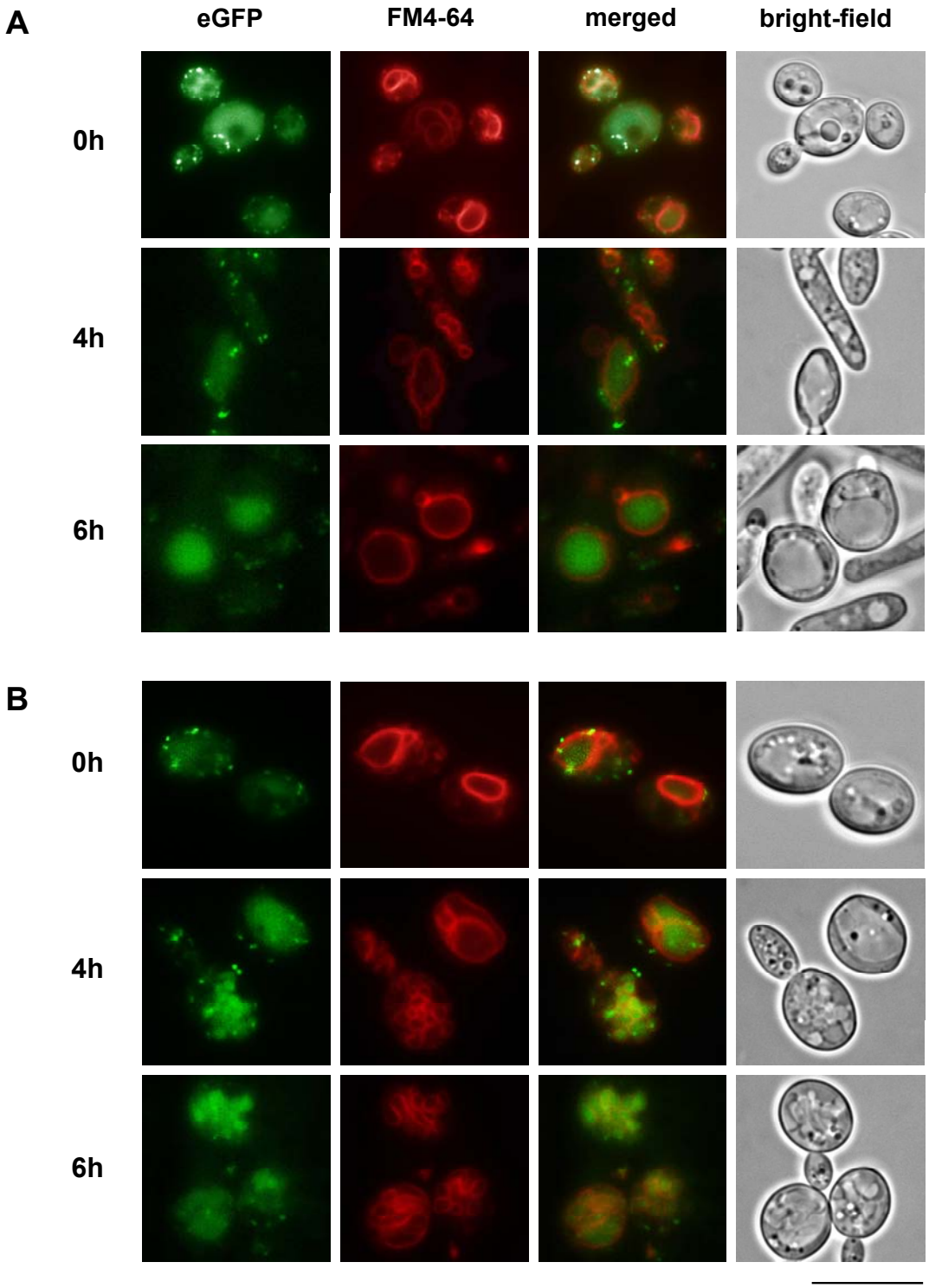

Figure 3.31 Fluorescence microscopic detection of peroxisome degradation in the *Y. lipolytica* mutant № 32. Peroxisomal turnover was induced by the glucose/ammonium sulfate **(A)** and glucose/nitrogen starvation **(B)** conditions exactly as described above (*Materials and Methods, 2.5.2)*. Probes were taken at the indicated time points, processed as in *Materials and Methods (2.9)* and viewed under the fluorescent microscope. Peroxisomes are targeted with eGFP(SKL) (green fluorescence). Vacuolar membranes are stained with FM4-64 (red fluorescence). The scale bar is equal to 20 μm. The vacuolar degradation of peroxisomes is impaired in the mutant cells subjected to glucose and nitrogen depletion. Also, morphology of the vacuoles appeared to be disturbed under conditions of nitrogen limitation.

A mutant phenotype of the strain № 55 appeared to be one of the most interesting for pexophagy studies. Fluorescence microscopy of mutant cells shifted into glucose-containing media with and without nitrogen clearly revealed that degradation of peroxisomes was impaired under both tested conditions. As is evident from **Fig. 3.32**, the organelles were prevented from entering the vacuoles since no green fluorescence could be found in the vacuolar lumina even 6 h after glucose adaptation. Noteworthy, a formation of the autophagic tubes seemed to be impaired in mutant cells of the strain № 55 subjected to glucose and nitrogen depletion simultaneously **(Fig. 3.32: B)**. Interestingly, peroxisomes looked like to form clusters at the sites of the potential vacuolar invaginations **(arrows)** although a full engulfment of such peroxisomal clusters was never observed. Also cellular morphology of cells of the strain № 55 appeared to be affected. As indicated by microscopic studies, mutant cells exhibited a characteristic prolonged form. Moreover, almost no buds could be observed upon cultivation hinting at a possible cell cycle arrest in this mutant strain of *Y. lipolytica* **(Fig. 3.32)**. However, it cannot be definitely suggested whether this mutant possessed any defects in cell cycle progression since its temperature sensitivity was not explored in this study.

Taken together, the data presented in this chapter provide a strong evidence for the proposed screening system to be a suitable one to obtain novel *pdd* mutants of *Y. lipolytica*. The alkane-assimilating yeast *Y. lipolytica* can be therefore efficiently used as an alternative model system for studying molecular machineries implicated in the selective autophagic turnover of peroxisomes.

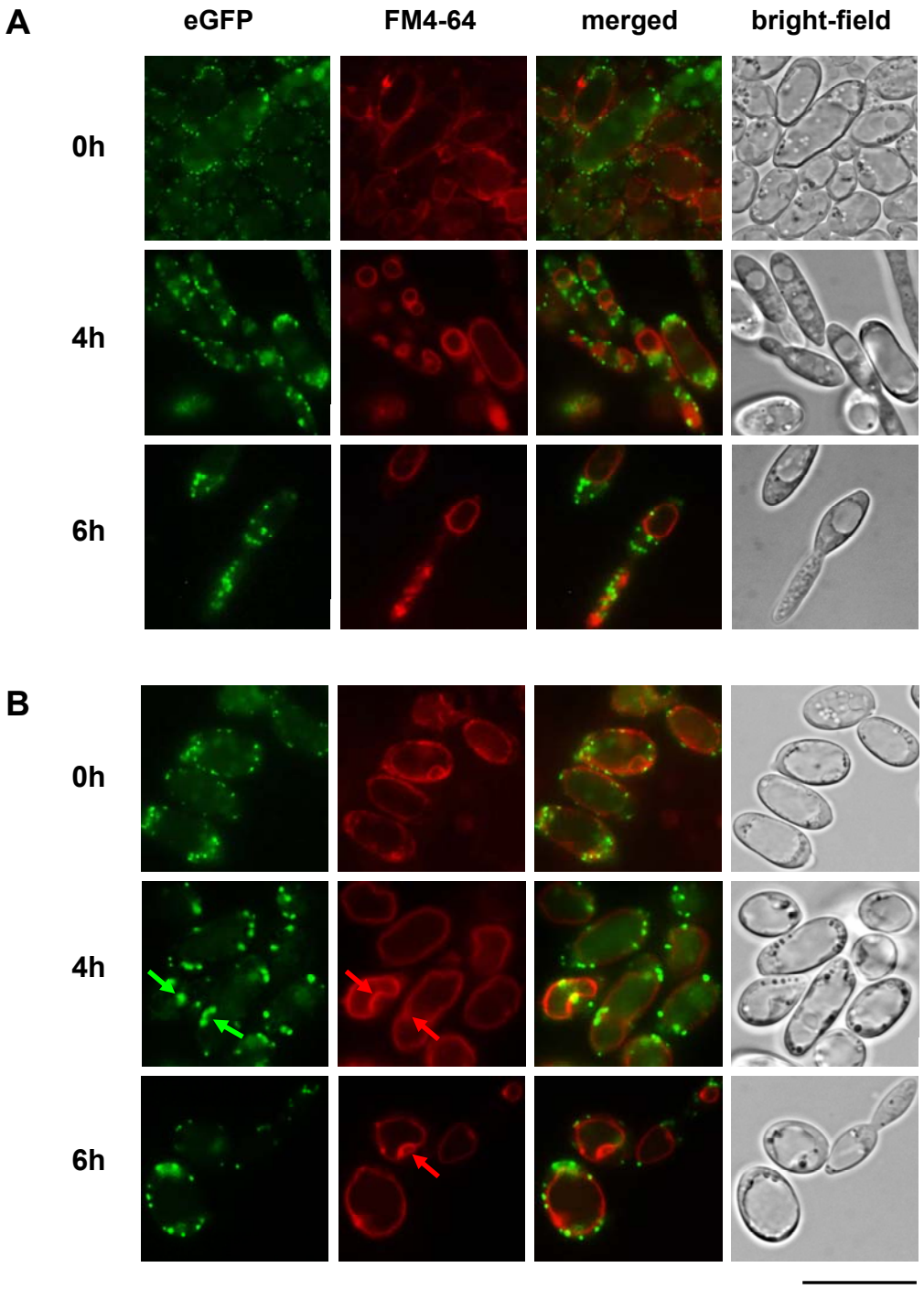

Figure 3.32 Fluorescence microscopic detection of peroxisome degradation in the *Y. lipolytica* mutant № 55. Peroxisomal turnover was induced by the glucose/ammonium sulfate **(A)** and glucose/nitrogen starvation **(B)** conditions exactly as described above (*Materials and Methods, 2.5.2)*. Probes were taken at the indicated time points, processed as in *Materials and Methods (2.9)* and viewed under the fluorescent microscope. Peroxisomes are targeted with eGFP(SKL) (green fluorescence). Vacuolar membranes are stained with FM4-64 (red fluorescence). The scale bar is equal to 20 μm. Peroxisomes are prevented from entering the degradation pathway under both tested conditions. Red arrows point to invaginations of the vacuolar membrane. Green arrows point to the peroxisomal clusters.

4 Discussion

The study presented in this thesis project aims at gaining insights into the molecular mechanisms behind the autophagic degradation of peroxisomes in the alkane-assimilating yeast *Y. lipolytica*. The first part of this research deals with the establishment of *Y. lipolytica* as a new model system to explore turnover of peroxisomes using a chimerical protein βGal-eGFP(SKL) as a peroxisomal marker. The central part of this project is devoted to the identification and characterization of several *Y. lipolytica* genes and proteins involved in the degradation of peroxisome in this microorganism. For this purpose, a bioinformatic screen of the *Y. lipolytica* genome was applied. The last part of this thesis describes development of a new screening procedure for isolation of novel *Y. lipolytica* peroxisome degradation deficient mutants using heterologous β-galactosidase as a reporter enzyme. This study belongs to the pioneer researches on pexophagy in *Y. lipolytica*. Its results should provide the platform for future investigations on autophagy-related processes in this non-conventional yeast species.

4.1 Establishment of the yeast *Y. lipolytica* as a model system to study autophagic peroxisome degradation

4.1.1 Application of chimerical protein βGal-eGFP(SKL) as a peroxisomal marker in the *Y. lipolytica* system

Investigation of a "life cycle" of peroxisomes requires in the first place a suitable easy-handling marker allowing one to examine the fate of these organelles under different growth conditions. In the methylotrophic yeasts *H. polymorpha* and *P. pastoris,* alcohol oxidase, a key enzyme of methanol assimilation, has been proved to be an excellent tool to study peroxisomal turnover (Veenhuis *et al.*, 1983; Waterham *et al.*, 1997). In methanol-limited continuous cultures, the amount of alcohol oxidase reaches more than 30% of the total soluble protein (van der Klei *et al.*, 1991). Conversely, addition of glucose or ethanol strongly represses synthesis of this enzyme (Egli *et al.*, 1980). Furthermore, changes in the activity of alcohol oxidase can be simply visualized by a color reaction using 2, 2′-azinodi-3-ethylbenzthiazolim sulfonate (ABTS) as a substrate. Based on this fact, a screening procedure for selection of mutants affected in peroxisome degradation was elaborated and first *pdd*, *gsa* and *pag* mutants* of the

* According to the unified nomenclature for yeast autophagy-related genes (Klionsky *et al.*, 2003), all known *PDD, PAG* and *GSA* genes are now classified as *ATG* genes.

methylotrophic yeasts *H. polymorpha* and *P. pastoris* were isolated (Titorenko *et al.*, 1995; Tuttle and Dunn, 1995; Sakai *et al.*, 1998).

Research on the alkane-assimilating yeast *Y. lipolytica* has contributed considerably to elucidation of principles of peroxisome biogenesis (Titorenko *et al.*, 2000). However, this organism has been explored to a limited degree for studying molecular mechanisms behind the degradation of these organelles. *Y. lipolytica* doesn't grow on methanol and its peroxisomes do not possess any enzymatic equipment prominent for methyloptrophic yeasts. Furthermore, preliminary studies on *Y. lipolytica* have shown that a chimerical protein Mox1-eGFP(SKL) consisting of the methanol oxidase from *H. polymorpha* C-terminally fused to the SKL-tagged version of eGFP is not functional in this microorganism (Gunkel, 2000). This observation made us to look for an alternative reporter for peroxisomes in *Y. lipolytica*. In our case, we have chosen the bacterial β-galactosidase for the following reasons. First, this very popular reporter enzyme is known to be functionally expressed and, therefore, is commonly applied in expression studies in yeast cells (Mount *et al.*, 1996). Second, β-galactosidase is not only well applicable for biochemical analyses but also offers a good possibility to screen yeast colonies on plates that allows one to carry out a selection of appropriate mutants (see also *Chapter 4.2.3*). Moreover, to make possible *in vivo* fluorescence analysis of peroxisomal turnover, the enhanced version of GFP (eGFP) was C-terminally fused to the β-galactosidase (βGal). In addition, the peroxisomal targeting signal 1 (SKL) appended to the C-terminus of eGFP should provide correct direction of the βGal-eGFP(SKL) fusion into its target organelle, the peroxisome. The whole construct was put under the control of a strong, inducible homologous promoter of the *Y. lipolytica* isocitrate lyase gene (*ICL1*) and cloned into the plasmid pINA354b-icl1 (Gunkel, 2000). The obtained plasmid pLG3 bearing the artificial construct *pICL1-LacZ-eGFP(SKL)* was linearized and introduced into the genome of *Y. lipolytica* strain PO1d yielding the recombinant strain PO1d(pLG3). Results presented in *Chapter 3.1* showed that the chimerical *YlICL1*-controlled protein βGal-eGFP(SKL) expressed by this strain fulfills the functional properties expected for a peroxisomal enzyme. Immunocytochemical microscopy revealed its localization into peroxisomes in the ethanol/ethylamine-grown *Y. lipolytica* cells. Biochemical studies with β-galactosidase and ICL showed that the activity pattern of the heterologous βGal-eGFP(SKL) protein is very similar to that obtained for the homologous peroxisomal enzyme. Finally, Western blot analyses indicated that this protein is expressed and degraded as a peroxisomal one under conditions leading to turnover of these organelles. Thus, the artificial fusion protein βGal-eGFP(SKL) can be exploited as a marker for peroxisomal compartment to examine the course of pexophagy in *Y. lipolytica*, for example, by fluorescence microscopy.

4.1.2 Fluorescence microscopic dissection of pexophagy in *Y. lipolytica*

Degradation of peroxisomes (pexophagy) is a specific membrane trafficking process that directs the destined for degradation organelles into the vacuoles of yeast cells. Monosov *et al.* (1996) first successfully applied the GFP(SKL) fusion to label peroxisomal matrix in living methanol-grown *P. pastoris* cells. In order to facilitate the fluorescence microscopical exploration of the yeast vacuolar membrane dynamics, Vida and Emr (1995) proposed an additional staining of the vacuolar membrane with a red styryl dye FM4-64. This double-fluorescent technique for simultaneous visualizing of peroxisomes and vacuoles in a yeast cell has been successfully utilized later on to study *in vivo* autophagic degradation of peroxisomes in *S. cerevisiae*, *H. polymorpha* and *P. pastoris* (Sakai *et al.*, 1998; Noda *et al.*, 2000; Guan *et al.*, 2001; Monastyrska *et al.*, 2005).

In my thesis, I used the eGFP(SKL)/FM4-64 double fluorescent labeling of peroxisomes/vacuoles to follow the peroxisome-to-vacuole dynamics in the living ethanol/ethylamine-grown *Y. lipolytica* cells transferred into glucose-containing media with and without source of nitrogen. The obtained results indicated that the degradation of peroxisomes takes place under both tested conditions. As is evident from Fig. 3.7 *(Chapter 3.2)*, upon induction of pexophagy, majority of the cellular peroxisomal population was targeted to and degraded in the vacuoles of cells of the examined strain PO1d(pLG3). Interestingly, a rate of the peroxisome degradation in the glucose-grown *Y. lipolytica* cells seems to be dependent on the presence or absence of the source of nitrogen in the growth media. So, pexophagy appears to be almost completed during the first 4 h after transfer of cells into glucose/ammonium sulfate, whereas the same process takes at least 6 h in cells subjected to excess glucose and nitrogen starvation simultaneously (Fig. 3.7). This finding is also in line with the degradation rates of the peroxisomal enzymes isocitrate lyase and thiolase determined by Western blot analysis (see *Chapter 3.1.4*).

How could these kinetic differences in peroxisome degradation be explained? A most plausible reason is that two distinct mechanisms may contribute to pexophagy under nitrogen-rich and nitrogen-starved conditions. It is generally known, that a character of signaling strongly determines the mode by which the cargo-organelle is delivered into the vacuole (Klionsky and Ohsumi, 1999). So, different nutrient starvations (i.e., N-starvation) trigger a bulk degradation of cytosolic proteins and organelles via autophagy (Klionsky and Emr, 2000). On the other hand, changing of carbon, but not nitrogen, source causes a selective turnover of peroxisomes in yeasts (Veenhuis *et al.*, 2000). Our previous observations in *Y. lipolytica* have shown that selective macropexophagy occurs after a shift of the acetate/oleic acid/ethylamine-grown cells into

glucose/ammonium sulfate-containing medium (Gunkel *et al.*, 1999). A more recent study with Aox3-eYFP(SKL)-labeled peroxisomes have confirmed the macroautophagic character of peroxisome degradation in the *Y. lipolytica* cells transferred from oleate/ethylamine- into glucose/ammonium chloride-containing medium (Nazarko *et al.*, 2005). Results achieved in the course of my thesis project clearly strengthen the fact that peroxisomes in *Y. lipolytic*a are degraded via macropexophagy if both glucose and a source of nitrogen are present in the growth medium. Firstly, peroxisomes were found to be individually targeted to and taken up by the vacuole that is strongly believed to be a common feature of the macropexophagic degradation mechanism described for *H. polymorpha* and *P. pastoris* (Veenhuis *et al.*, 1983; Tuttle and Dunn, 1995). Secondly, no vacuolar membrane structures typical for micropexophagy, such as formation of membrane protrusions, engulfment of a cluster of peroxisomes by the vacuolar membrane, etc. (Sakai *et al.*, 1998), could be revealed in the wild type *Y. lipolytica* cells in the presence of glucose and ammonium sulfate. Alternatively, under autophagy-triggering conditions, numerous invaginations of the vacuolar membranes, so-called autophagic tubes (Müller *et al.*, 2000), were observed indicating beginning of the microautophagy. However, it could not be surely assumed whether the sites of autophagic tubes formation correspond to those of peroxisomal uptake. Moreover, also under glucose/nitrogen starvation conditions, the organelles appear to be taken up individually by the vacuoles suggesting rather macroautophagic then microautophagic degradation mode. Analysis of *Y. lipolytica* mutants affected at different steps of peroxisome degradation will definitely shed more light on this intriguing question.

4.1.3 Influence of PMSF addition on the course of pexophagy in *Y. lipolytica*

PMSF (phenylmethylsulphonyl fluoride) is a general inhibitor of serine proteases which is known to block a number of yeast vacuolar proteases, such as proteinase B and carboxypeptidase Y (Lee and Goldberg, 1996). Takeshige *et al.* (1992) showed that addition of 1 mM PMSF resulted in the extensive accumulation of autophagic bodies in the vacuoles of the wild type yeast cells subjected to a minimal medium lacking nitrogen. The same phenotype was also observed in the *H. polymorpha* cells subjected to nitrogen starvation (Bellu *et al.*, 2001). Moreover, PMSF was also shown to inhibit the last step of macropexophagy in *P. pastoris* (Sakai *et al.*, 1998). Taking into account the last fact, it was interesting to test whether PMSF treatment also affects pexophagy in *Y. lipolytica* cells exposed to different peroxisome degradation-inducing conditions. Results obtained in the course of this project revealed that addition of 1 mM PMSF to the peroxisome-containing yeast cells transferred into glucose with and without nitrogen source indeed disturbs degradation of these organelles. As is shown in

Chapter 3.3, PMSF efficiently prevented inactivation of the peroxisomal marker enzymes isocitrate lyase and β-galactosidase. Furthermore, the ICL protein was shown not to degrade in the presence of PMSF, whereas a control treatment with DMSO had no impact on its degradation pattern. Following fluorescent microscopy of the recombinant *Y. lipolytica* cells expressing the artificial fusion protein βGal-eGFP(SKL) revealed a clear impairment in the vacuolar degradation of peroxisomes in the PMSF-treated cells subjected to both glucose/ammonium sulfate and glucose/nitrogen starvation conditions. Thus, in *Y. lipolytica*, the vacuolar serine-dependent proteases are directly involved in the autophagic degradation of peroxisomes.

An interesting point is that, upon PMSF treatment, uptake of peroxisomes by the vacuoles was delayed. The simplest explanation for this phenomenon could be a probable dynamic correlation between the vacuolar engulfment on the one hand and the vacuolar degradation on the other hand. However, also formation of the autophagic tubes appeared to be affected in the PMSF-treated nitrogen-starved yeast cells (Fig. 3.10: C) suggesting a feasible influence of PMSF addition on the microautophagic membrane apparatus. So, the whole picture seems to be more complex than we had imagined. Unfortunately, we still have little knowledge of how PMSF influences the cellular metabolism. It has been reported that addition of PMSF efficiently abolishes the glucose catabolite inactivation of some enzymes of the glyoxylate cycle and gluconeogenesis in *S. cerevisiae* (Grossmann, 1980). Furthermore, PMSF was found to almost completely inhibit a specific phosphoinositide turnover (Sekar and Roufogalis, 1984) as well as activity of the membrane-associated acetylcholine esterase in brain and muscle (Skau and Shipley, 1999). My study on *Y. lipolytica* as well as earlier observations done on the *P. pastoris* system (Sakai *et al.*, 1998) has shown that addition of PMSF also affects the engulfment of peroxisomes during pexophagy. Further experiments are certainly required to identify specific molecular targets of this compound.

4.2 Exploration of molecular mechanisms of peroxisome degradation in *Y. lipolytica*

A most suitable approach to explore a complex molecular pathway is its genetical dissection by isolation of mutants impaired at different stages with the aim of identifying molecular players involved in each step of this process. In this study, two main strategies were used to isolate *Y. lipolytica* mutants deficient in the autophagic degradation of peroxisomes. On the one hand, a bioinformatic genome-wide screen for *Y. lipolytica* counterparts which display homology to already known autophagy-related proteins from other organisms was performed. On the other hand, a random chemical mutagenesis of cells expressing a chimerical βGal-eGFP(SKL) fusion was carried out in order to obtain pexophagy deficient mutants with novel phenotypes. In the last case, a screening system based on the expression of the bacterial β-galactosidase under the control of *ICL1* promoter from *Y. lipolytica* was devised.

4.2.1 Genome-wide bioinformatic analysis of autophagy-related proteins from *Y. lipolytica*

Autophagy and pexophagy are distinct catabolic membrane trafficking routes that occur in response to dramatic changes in the nutrients available to yeast cells, for example during starvation for nitrogen (autophagy) or upon transfer of cells to a preferred carbon source such as glucose (pexophagy) (reviewed in Abeliovich and Klionsky, 2001). Notably, autophagy and pexophagy[*] was found to be topologically similar processes. In both pathways, the cargo components should be initially sequestered in double-membrane vesicles called auto- or pexophagosomes, respectively, which then fuse with the yeast lytic compartment, the vacuole, whereupon these vesicles are gradually degraded by the vacuolar hydrolases. Thus, it would be not surprising if both processes may share overlapping mechanistic components. Indeed, previous genetic studies in yeasts have revealed a number of proteins encoded by so-called *ATG* genes (Klionsky *et al.*, 2003) known to form a common molecular machinery involved in the general (autophagy) as well as in the selective catabolic (pexophagy) and anabolic (the Cvt-pathway) membrane trafficking routes (Hutchins *et al.*, 1999; Kim and Klionsky, 2000; Bellu *et al.*, 2003). However, some protein factors specific for the Cvt or pexophagy also do exist, i.g., at the stages of signaling and cargo sorting (Scott *et al.*, 2001; Kim *et al.*, 2001; Mukaiyama *et al.*, 2002), that underlines significance of such specificity for the cellular metabolism.

[*] In this case, macroautophagy and macropexophagy are meant.

In my study, I sought to apply bioinformatic tools to identify putative Atg proteins from the genome of *Y. lipolytica* which whole sequence has recently become available (Dujon *et al.*, 2004). Following the computational genome-wide screen, I was succeeded in identifying of 33 protein candidates of *Y. lipolytica* displaying considerable homology to Atg proteins described in other yeast species, namely *S. cerevisiae*, *P. pastoris* and *H. polymorpha*. As shown in Table 3.1 *(Chapter 3.4.1)*, the identified *Y. lipolytica* Atg-homologs appeared to be involved at the different stages of both selective and non-selective degradation processes. For instance, all proteins known to be essential for the induction of autophagic response (i.e., members of the Tor signaling pathway as well as Atg1 and PI3K protein complexes) were revealed to possess corresponding *Y. lipolytica* counterparts. Furthermore, almost all components of two yeast ubiquitin-like systems involved in the autophagosome formation (except for Atg10 and Atg16 proteins) were shown to have homologs in *Y. lipolytica*. Also, proteins exhibiting high homology rates to certain components of the yeast pexophagy-specific machinery, such as Atg11, Atg27, Tup1 and Gcn1-4 proteins, could be identified in the *Y. lipolytica* genome. Hence, these results underline a conserved character of the molecular mechanisms implied in different types of autophagic degradation in yeasts.

A very interesting finding is that no *Y. lipolytica* counterparts could be identified for yeast Atg10, Atg16, Atg19, Atg21, Atg23 and Atg28 proteins during this search. As already mentioned above, Atg10 and Atg16 proteins from *S. cerevisiae* were shown to contribute to the yeast Atg5-Atg12 conjugation system required for efficient vesicular formation (reviewed in Ohsumi, 2001). In addition, a *P. pastoris* homolog of ScAtg16p (Paz3p) has been recently found to control the vacuolar engulfment of peroxisomes during micropexophagy in this yeast (Mukaiyama *et al.*, 2002). So, it looks very surprising why exactly these components of the UBL system could not be found in *Y. lipolytica*. The next Atg protein, Atg19, was described to be essential for the Cvt-pathway but not for autophagy in *S. cerevisiae* (Shintani *et al.*, 2002). Since the selective transport of aminopeptidase I and α-mannosidase to the vacuole has been so far observed only in baker's yeast, it can be proposed that this protein is unique for this microorganism. A similar situation may occur in the case of Atg28 protein from *P. pastoris* which has been recently shown to be selectively involved in pexophagy but not in autophagy in this yeast and until now no apparent homologs of Atg28p could be found in the *S. cerevisiae* genome (Stasyk *et al.*, 2006). Furthermore, the *ATG23* gene product was first demonstrated to be required for both the Cvt-pathway and autophagy but not for selective peroxisome degradation in *S. cerevisiae* (Tucker *et al.*, 2003). Another recent study, however, indicated an important role of ScAtg23p in the Cvt pathway but disproved its function in autophagy (Meiling-Wesse *et al.*,

2004). Thus, also in this case, the absence of a well-conserved *Y. lipolytica* homolog could be explained by an exclusive role of its corresponding *S. cerevisiae* counterpart in the Cvt pathway. Finally, ScAtg21p is more likely to be paralogous to his counterpart, ScAtg18p (will be discussed in detail below) and, consequently, its function may be adopted by the related Atg18 protein from *Y. lipolytica*.

What reasons may be accounted for the absence of well-defined *Y. lipolytica* Atg10 and Atg16 homologs? A most probable explanation could be that the corresponding *Y. lipolytica* counterparts do exist but they display much higher evolutionary divergence to be identified by this computational search. In fact, former data on the exploration of *Y. lipolytica* genome demonstrated that this yeast significantly differs from other hemiascomycetous yeasts. Moreover, several features of the organization of its genome place this microorganism closer to higher eukaryotes (Casaregola *et al.*, 2000). Indeed, another BLAST search against Atg10- and Atg16-related proteins from *Mus musculus* and *Homo sapiens* revealed 1 and 3 hypothetical proteins from *Y. lipolytica,* respectively, which display about 20-25% of amino acids identity to corresponding query sequences (this data is not included in this study). Remarkably, no *S. cerevisiae* counterparts could be identified in this search using *Y. lipolytica* Atg10 and Atg16 protein sequences as queries. Taken together, this data suggests that the set of molecular players involved in autophagy-related processes in different organisms has been considerably diverged during evolution and, therefore, its study requires a simultaneous application of both molecular-biological and computational approaches.

4.2.2 Phenotypic analysis of constructed *Y. lipolytica atg* mutants: cell growth and cell viability under nitrogen starvation conditions

A process of vacuolar autophagic degradation has been proven to be crucial for survival of wild type yeast cells subjected to nitrogen deprivation (Klionsky and Emr, 2000). In the yeast *atg* mutants, conversely, impairment of this process was shown to significantly reduce cell growth and viability under nitrogen-limited conditions (Tsukada and Ohsumi, 1993). Thus, diminished cell growth and survival upon starvation can be used as a marker for *atg*-mutant phenotype. In my thesis, I applied this phenotypic difference for a rapid prediction of phenotypes of six constructed *Y. lipolytica* mutant strains, namely *atg1*, *atg6, atg11, atg18, gcn2* and *pep4*. Results presented in *Chapter 3.5.1* clearly showed a reduction of viability rates of *atg1*, *atg6* and *atg18* mutant cells cultivated under conditions of nitrogen starvation (Figs. 3.11, 3.12). On the other hand, no significant differences in cell survival could be revealed for other tested mutants, i.e. *atg11*, *gcn2* and *pep4*, when compared to the parental *Y. lipolytica* strain PO1d(pLG3), although

defects in cell growth were obvious for all these strains. It is well known that nutrient deprivation not only induces autophagy but also arrests cells at early G1 phase. In eukaryotes, the rapamycin-sensitive Tor kinase was demonstrated to be an essential part of a signal transduction pathway which coordinates nutritional and mitogenic signals (Cutler *et al.*, 1999). In yeast, inactivation of Tor by rapamycin treatment or by using a temperature-sensitive allele of *TOR2* was shown to efficiently promote autophagy even under nitrogen-rich conditions (Barbet *et al.*, 1996). However, the G1 arrest itself did not appear to trigger autophagy and, therefore, both events were proposed to be induced in a parallel manner by the inactivation of Tor under starvation conditions (Noda and Ohsumi, 1998). According to obtained data, the autophagic degradation turned up to be impaired in *Y. lipolytica atg1*, *atg6* and *atg18* mutant strains, whereas no apparent defects in the course of autophagy could be suggested for *atg11*, *gcn2* and *pep4* mutants. These results are in line with early observations done for the related *S. cerevisiae* mutants (will be discussed in detail below). So, the discernible phenotypes of the constructed mutant strains seem to agree with the predicted ones that hints at a probable involvement of the corresponding *Y. lipolytica* proteins in autophagy-related processes in this yeast species.

4.2.3 Functional characterization of some Atg proteins from *Y. lipolytica*

4.2.3.1 The Atg1 protein from Y. lipolytica

ATG1 (alias *APG1, AUT3*) gene from *S. cerevisiae* was the first autophagy-related gene identified in yeasts (Matsuura *et al.*, 1997; Straub *et al.*, 1997). ScAtg1p encoded by this gene has been determined as a serine/threonine kinase which forms a complex at the perivacuolar membrane compartment implied in switching between Cvt transport and autophagy (Kim *et al.*, 2002). The kinase activity of Atg1 was shown to depend on upstream nutrient signals initially relayed through the Tor kinase (Kamada *et al.*, 2000). Interestingly, a non-kinase role of ScAtg1p in the initiation of formation of autophagosomes but not Cvt vesicles has been recently revealed suggesting principal differences in the membrane trafficking requirements of these two pathways (Abeliovich *et al.*, 2003). Moreover, yeast Atg1 counterparts were demonstrated to be essential for selective peroxisome degradation in *S. cerevisiae* (Hutchins *et al.*, 1999) and *P. pastoris* (Mukaiyama *et al.*, 2002) as well as for both macropexophagy and microautophagy in *H. polymorpha* (Komduur *et al.*, 2003). Remarkably, Atg1 homologous proteins could be also found in a number of higher eukaryotes including human and mouse suggesting its conservation over large evolutionary distances (Khalfan and Klionsky, 2002).

The Atg1 homolog from *Y. lipolytica* is a protein of 710 amino acids with a predicted N-terminal kinase domain that spans amino acids 7-299. YlAtg1p was found to share a high rate of

homology with correspondent proteins from *H. polymorpha* and *P. pastoris* as well as with ULK1/2 protein kinases from human (Fig. 7.9 in Appendix). Disruption of the *YlATG1* gene resulted in the damaged degradation of some peroxisomal, cytosolic and mitochondrial marker enzymes in *atg1* cells subjected to glucose without nitrogen source (see Fig. 3.14). A possible defect in the bulk autophagic degradation was also confirmed by the phloxin B test with *atg1* mutant incubated on glucose-containing plates without a nitrogen source (Fig. 3.12) Fluorescence microscopic study of the nitrogen-starved *atg1* mutant cells revealed a clear impairment of peroxisome degradation most likely at the stage of the organelles uptake by the vacuoles (Fig. 3.15: B). On the other hand, no obvious defects in the course of pexophagy could be observed in the *atg1* mutant if both glucose and ammonium sulfate were present in growth medium (Fig. 3.15: A).

What function could be presumed for *Y. lipolytica* Atg1 protein? A first definitive conclusion which can be made from these results is that the Atg1 homolog from *Y. lipolytica* is not essential for glucose-induced macropexophagy in this yeast. It seems to be a little bit surprising since a corresponding *S. cerevisiae* counterpart was shown to be involved in selective degradation of peroxisomes (Hutchins *et al.*, 1999). However, it should be taken into account that, in baker's yeast, peroxisomal turnover has been explored only under conditions of glucose and nitrogen starvation, so, we can not compare these studies directly. In any case, a presumed role of YlAtg1p in peroxisome degradation appears to be restricted to the conditions of nitrogen deprivation. A second important observation is that the induction of pexophagy is not impaired in *atg1* mutant cells subjected to glucose and nitrogen deprivation simultaneously. This fact objects against a well-established role of Atg1 as a key regulator of general autophagic events in response to nitrogen starvation and supports a recently described structural function of this protein (Abeliovich *et al.*, 2003). It has been previously shown that ScAtg1p forms a large protein complex which includes Atg11, Atg13, Atg17, Vac8 and most likely additional interaction partners and regulates the conversion between the Cvt pathway and autophagy at the level of vesicle formation (Wang *et al.*, 1998; Scott *et al.*, 2000; Kim *et al.*, 2001). Furthermore, Atg1 and Atg11 subunits of the Atg1 protein kinase complex were found to be localized to a specific perivacuolar compartment called pre-autophagosomal structure shown to be essential for vesicle formation (Kim *et al.*, 2002). Thus, it can be proposed that, in *Y. lipolytica*, Atg1 homolog may be also involved in the autophagosome formation in response to nitrogen starvation. Indeed, in the nitrogen-starved *atg1* cells, peroxisomal clusters were found at the close proximity to the vacuolar membranes which may imply a defect in the sequestration of these organelles. At the same time, microautophagy itself is not obviously impaired since the

formation of autophagic tubes could be observed in the same cells. Taking together, it can be supposed that YlAtg1p is implied in the formation of autophagic membranes during macroautophagy in *Y. lipolytica* cells subjected to glucose without source of nitrogen but not to glucose with ammonium sulfate. Another important assumption which comes from these data is that, in *Y. lipolytica*, membranes involved in the formation of autophagosomes and pexophagosomes may differ qualitatively. Of course, further electron microscopic and immunocytochemical analyses are necessary to verify this hypothesis.

4.2.3.2 The Atg6 protein from Y. lipolytica

The sequestration and delivery of cytoplasmic material to the vacuole require the dynamic rearrangement of intracellular membranes by specialized molecular machinery consisting of different protein-protein and protein-lipid complexes. A good example of such interaction partner is Atg6 protein from *S. cerevisiae* originally described as a component of the PI3K complexes I and II involved in autophagy, Cvt pathway and endocytosis (Kametaka *et al.*, 1998; Kihara *et al.*, 2001). Also a human Atg6 counterpart called beclin 1 was identified and its important role in the inhibition of tumorogenesis was demonstrated (Liang *et al.*, 1999). Remarkably, it has been shown recently that inactivation of the beclin 1 ortholog from *C. elegans* may trigger apoptotic cell death that provides an additional molecular link between autophagy and apoptosis (Takacs-Vellai *et al.*, 2005).

In *Y. lipolytica*, the Atg6 counterpart is a protein of 434 amino acids with a predicted Apg6 domain occupying three quarters of its whole length (amino acids 102-433). YlAtg6p exhibits a high similarity to both ScAtg6 and beclin1, so, all three proteins could be suggested to be orthologous. Biochemical and fluorescence microscopic studies confirmed the idea that YlAtg6p is implicated in the autophagic degradation of peroxisomes. As shown in Fig. 3.18, pexo(auto)phagosomal membranes failed to fuse with the vacuoles in the glucose-grown *atg6* cells both in the presence and in the absence of a nitrogen source. This fact together with the observation that *Y. lipolytica atg6* mutant cells accumulate atypical membranous structures hints at a possible function of YlAtg6p in dynamic membrane flow. Indeed, in baker's yeast, it was shown that Atg6 together with Atg14 peripherally associates with a novel intracellular membrane formation (Kametaka *et al.*, 1998) later determined as pre-autophagosomal structure playing a crucial role in generating autophagosomes (Suzuki *et al.*, 2001). At the same time, Atg6 was revealed to be a part of the Vps34 PIK3-kinase complexes I and II which trigger formation of the Cvt vesicles and autophagosomes in *S. cerevisiae* (Kihara *et al.*, 2001). Finally, Atg6 (originally described as Vps30) functions in a selective protein sorting of the

carboxypeptidase Y to the vacuole (Seaman *et al.*, 1997). Taking together, these data suggest Atg6 to be a protein implicated in a "cross-talk" between different intracellular transport processes. The present study shows for the first time that, in *Y. lipolytica*, Atg6 is additionally required for the degradation of peroxisomes via both macropexophagy and macroautophagy. This is so far the only known *Y. lipolytica* protein displaying such features. Further investigations are required to elucidate its multiple roles in the intracellular membrane trafficking in more detail.

4.2.3.3 The Atg11 protein from Y. lipolytica

Selective incorporation of cargo molecules into certain vesicles appears to be an important aspect of membrane trafficking which facilitates the proper vesicular formation (Shintani *et al.*, 2002; Shintani and Klionsky, 2004b). There are a large number of proteins known to participate in this complex event. Among them, Atg11 protein from *S. cerevisiae* has been shown to be required for the Cvt pathway and pexophagy – two transport processes resulting in selective cargo delivery to the vacuoles (Kim *et al.*, 2001). Conversely, ScAtg11p was found to be dispensable for bulk autophagy, thus, it is a good example of an autophagy-related protein (Atg) with no true autophagic function[*]. Importantly, also in baker's yeast, Atg11 has been recently demonstrated to be involved in self-assembly and interactions with other proteins from the pre-autophagosomal structure and, therefore, it was suggested to play an integral role in connecting cargo molecules with components of the vesicle-forming machinery (Yorimitsu and Klionsky, 2005). Finally, Atg11 homologs from other yeasts were revealed to be specifically involved in the selective peroxisome degradation via macropexophagy in *H. polymorpha* (Monastyrska *et al.*, 2005b) and via micropexophagy in *P. pastoris* (Kim *et al.*, 2001). The last observation strengthens the reason for Atg11 protein to be of a particular interest for this thesis project.

The Atg11 homolog from *Y. lipolytica* appears to be a large protein of 924 amino acids which displays rather moderate similarity to other known yeast homologous proteins. Computational analysis of YlAtg11p predicted two putative membrane-spanning segments (amino acid residues 444-464 and 519-539) suggesting its probable membranous localization. Disruption of the *ATG11* gene in *Y. lipolytica* did not lead to any decrease in cell viability of the *atg11* mutant comparing to the wild type (Fig. 3.12). Furthermore, it was found out that degradation of a cytosolic marker protein G6PDH as well as formation of the autophagic tubes was not affected in the *atg11* cells grown in a glucose-containing medium depleted by nitrogen (Figs. 3.20; 3.21).

[*] See a new unified nomenclature for yeast autophagy-related genes (Klionsky *et al.*, 2003).

Taken together, these observations imply that general autophagy is not impaired in this *Y. lipolytica* mutant which is in line with theoretical predictions described above. However, the picture becomes more complex regarding the degradation of peroxisomes in the *atg11* mutant strain. As shown in Fig. 3.21, pexophagy appeared to be delayed in the *Y. lipolytica atg11* cells subjected to glucose with and without source of nitrogen. Nevertheless, this defect seemed to be not crucial since the organelles were finally found to be degraded in the vacuoles of the glucose-grown mutant cells. Such "leaky" mutant phenotype is typical for proteins involved in huge, dynamic protein complexes in which other molecular players may also contribute to a main function. As a "leaky" degradation defect caused by disruption of *YlATG11* occurs at the stage of peroxisome uptake by the vacuoles, it could be proposed that YlAtg11p is a part of a putative protein complex required either for vesicle formation or for a heterotypic membrane fusion between vesicular and vacuolar membranes. Detailed electron microscopical analysis of the *atg11* mutant of *Y. lipolytica* will shed more light on this question. Another interesting point concerns the nature of the peroxisome-containing vesicles which arose under different physiological conditions. Since Atg11 homologs from *S. cerevisiae*, *P. pastoris* and *H. polymorpha* are known to be specifically involved in the recruitment of selective cargos for the Cvt vesicles and pexo- but not autophagosomes (Kim *et al.*, 2001; Yorimitsu and Klionsky, 2005; Monastyrska *et al.*, 2005b), it is highly attractive to speculate that also in *Y. lipolytica* Atg11 protein may play the same function. From this point of view, it would be interesting to identify a specific marker for the *Y. lipolytica* pexophagosomes if it does exist. Regarding conditions of glucose and nitrogen starvation, we can not exclude a probable contribution of microautophagy to the peroxisome degradation. Unfortunately, it is impossible to answer this question using a fluorescence microscopic analysis only, so, further electron microscopic studies are necessary. The last but not the least is an assumption that, in *Y. lipolytica*, alike in *H. polymorpha*, two diverse simultaneous stimuli may initiate two different degradation mechanisms, namely specific macropexophagy and non-selective microautophagy (Monastyrska *et al.*, 2004). Other *Y. lipolytica* mutants are surely required to dissect these two pathways genetically, biochemically and morphologically.

4.2.3.4 The Atg18 protein from Y. lipolytica

Atg18 protein represents a member of a novel WD-repeat family of phospholipid-binding effectors which display autophagic capacity (so-called WIPI-family, from WD-repeat protein interacting with phosphoinosides). There are two paralogous groups of WIPI proteins in human, namely WIPI-1 (WIPI49/Atg18) and WIPI-2. WIPI-1 counterpart has been recently shown to link the mammalian amino acid deprivation-induced autophagy to cellular transformation during cancer progression (Proikas- Cezanne *et al.*, 2004). In baker's yeast, three homologous proteins from the WIPI-family have been identified till now, i.e. Atg18, Atg21 and Hsv2. Whereas ScAtg18p is essential for all autophagy-related processes including pexophagy (Barth *et al.*, 2001; Guan *et al.*, 2001), ScAtg21p was found to be required only for the Cvt pathway (Stromhaug *et al.*, 2004; Meiling-Wesse *et al.*, 2004). Also corresponding orthologs from the methylotrophic yeasts – Gsa12 protein from *P. pastoris* and Atg21 counterpart from *H. polymorpha* – were shown to be essential for selective degradation of peroxisomes in these microorganisms (Guan *et al.*, 2001; Leão-Helder *et al.*, 2004). Interestingly, no strong phenotypic effects have yet been determined for the third member of the WIPI-family, ScHsv2p (Stromhaug *et al.*, 2004).

Bioinformatic analysis of the genome of *Y. lipolytica* revealed two putative members of the WIPI-protein family - YlAtg18p and YlHsv2p (Table 3.1). A predicted YlAtg18p is 400 amino acids long and possesses a highly conserved core region consisting of several WD-repeats (residues 70-273). WD-repeat was originally defined as a core unit of approximately 40 amino acids, ending with the tryptophan and aspartic acid residues (WD) (van der Voorn and Ploegh, 1992). WD-repeat-containing proteins are generally known to be regulatory proteins forming a beta-propeller platform which enables the assembly of multiprotein complexes (Neer *et al.*, 2004). Based on this property, WD-repeat proteins were found to regulate a number of essential cellular functions, such as cell cycle control, apoptosis, signal transduction, assembly of chromatin and vesicular trafficking. Phenotypic analysis of the *Y. lipolytica atg18* mutant cells demonstrated a reduced rate of cell viability under conditions of nitrogen starvation which hints at a probable deficiency of general autophagy in this mutant. Further biochemical and immunological studies showed that, in line with the first observation, degradation of some peroxisomal and cytosolic marker proteins were impaired in the glucose/nitrogen-starved *atg18* cells. Finally, fluorescence microscopy of the *Y. lipolytica atg18* mutant grown under conditions of glucose and nitrogen depletion revealed an obvious defect at the early stage of peroxisome degradation as numerous clusters of non-degraded organelles were observed in close vicinity to the vacuolar membranes (Fig. 3.24). Conversely, glucose-triggered pexophagy was unaffected in

the *atg18* mutant cells if both carbon and nitrogen sources were available. Thus, YlAtg18p is essential for degradation of peroxisomes under conditions of nitrogen starvation but it seems to be dispensable for this process if ammonium sulphate is present in growth medium.

What role could *YlATG18* gene product play in peroxisome degradation? Previous studies on *S. cerevisiae* demonstrated that *atg18* mutant is blocked in the development of sequestering membranes during both auto- and pexophagic processes (Guan *et al.*, 2001). Furthermore, sequestration of the Cvt cargo aminopeptidase I was reported to be disturbed in *S. cerevisiae atg18* and *atg21* mutants (Guan *et al.*, 2001). Also in methylotrophs, deletion of the *PpATG18* and *HpATG21* genes was shown to cause essential defects in development of the pexophagosomal membranes and their further fusion with the vacuoles (Guan *et al.*, 2001; Leão-Helder *et al.*, 2004). In *Y. lipolytica atg18* mutant cells, peroxisomes were never observed to enter the vacuoles upon induction of autophagy. Thus, it could be proposed that *Y. lipolytica* Atg18 homolog may be involved in the formation of autophagosomal membranes in response to nitrogen starvation. It should be pointed out that also appearance of the autophagic tubes was found to be disturbed in *atg18* mutant implying a possible role of YlAtg18p in microautophagy in *Y. lipolytica* (Fig. 3.24: B). Interestingly, *S. cerevisiae* Atg21 counterpart has been reported to be required for efficient lipidation and localization of another essential autophagy-related protein, Atg8, to the pre-autophagosomal compartment (PAS) (Stromhaug *et al.*, 2004). Recently, a related membranous structure, called micropexophagy-specific membrane apparatus (MIPA), has been revealed to be necessary for complete peroxisome engulfment during micropexophagy in *P. pastoris*, and the Atg8-PE conjugate was found to be localized to this structure (Mukaiyama *et al.*, 2004). It is not clear whether membrane structures equivalent to the PAS or MIPA also exist in *Y. lipolytica*. However, the preservation of these molecular events in different yeast species strongly supports a hypothesis that yeast WIPI-proteins might perform equivalent functions. If it holds true, yeast proteins from the WIPI-family may present a good example of the functional redundancy and divergence between diverse yeast genomes described previously (Dujon *et al.*, 2004).

4.2.3.5 The Gcn2 protein from Y. lipolytica

Under conditions of nutrient limitation, eukaryotic cells not only increase rates of intracellular degradation via general autophagy but also decrease overall protein synthesis. The last process has been described as a stress-induced translational arrest which is tightly regulated by a family of evolutionary conserved serine/threonine kinases (Hinnebusch, 1994). The yeast eIF2 kinase Gcn2 has been previously reported to be required for setting off the general amino acid control pathway by activation of a downstream transcriptional regulator Gcn4 in response to starvation (Dever *et al.*, 1992). Another study linked the eIF2 kinase signaling pathway to the starvation-induced autophagy in baker's yeast and to both starvation- and virus-induced autophagy in mammals (Talloczy *et al.*, 2002). Finally, a Gcn2 homolog from *P. pastoris* (Paz11) was shown to be involved in the stage 2 of micropexophagy, i.e. fusion of peroxisomal clusters with the vacuoles (Mukaiyama *et al.*, 2002).

The predicted Gcn2 counterpart of *Y. lipolytica* is a large protein of 1609 amino acid residues with two putative protein kinase domains. Multiple sequence alignment revealed a high similarity between YlGcn2p and its homologs from *S. cerevisias* and human. In *Y. lipolytica*, disruption of the predicted *GCN2* gene appeared to have no obvious effect on degradation of peroxisomal marker proteins under both tested conditions (Fig. 3.26). Also fluorescence microscopic analysis failed to discover any clear defects in the course of pexophagy in the ethanol/ethylamine-grown *gcn2* cells transferred into glucose/ammonium sulfate and glucose/nitrogen starved media. Thus, Gcn2 is apparently not essential for degradation of peroxisomes in *Y. lipolytica*. Another important characteristic of the *Y. lipolytica gcn2* mutant phenotype is a noticeable defect in formation of the autophagic tubes which are known to be the vacuolar membrane invaginations typical for microautophagy (Müller *et al.*, 2000). Nevertheless, pexophagy still occurs efficiently in the glucose-grown *gcn2* mutant cells starved by nitrogen. So, it is most likely that microautophagy plays a minor role in peroxisome degradation under conditions of nitrogen starvation, and in this case peroxisomes are apparently degraded mostly in the macroautophagic manner. At present, it remains unclear, how YlGcn2p may affect microautophagy. A previous study in *P. pastoris* demonstrated that glucose-induced micropexophagy requires protein synthesis (Tuttle and Dunn, 1995). Since yeast Gcn2 kinase was shown to phosphorylate the downstream translation initiation factor eIF2 upon nutrient starvation which, in turn, leads to the efficient translation of a transcriptional activator Gcn4 (Dever *et al.*, 1992), it may be suggested that also in *Y. lipolytica* efficient microautophagy involves a synthesis of novel protein(s). The validity of this hypothesis needs further experimental conformations.

4.2.3.6 The Pep4 protein from Y. lipolytica

The yeast vacuole is a degradative organelle equivalent to the lysosomes of higher eukaryotes and contains a number of proteases required for its proteolytic function (reviewed by van den Hazel *et al.*, 1995). Among them, proteinase A encoded by *PEP4* gene is one of the major vacuolar aspartic proteases known to be essential for post-translational modification of a number of vacuolar zymogens (Ammerer *et al.*, 1986; Woolford *et al.*, 1986). Firstly synthesized as a precursor, this protease is transported to the vacuole via the early secretory pathway, and then the active mature protein is generated by specific proteolysis implying another vacuolar endopeptidase, proteinase B (Klionsky *et al.*, 1988; Wolff *et al.*, 1996). Yeast mutants lacking proteinases A and B were shown to accumulate the autophagic bodies within the vacuoles if subjected to nitrogen depletion (Takeshige *et al.*, 1992) suggesting that activities of these enzymes greatly contribute to the degradative capacity of the vacuole under starvation conditions. Noteworthy, Pep4 homolog from *P. pastoris* (Paz14) was reported to be required for the vacuolar degradation of peroxisomes via micropexophagy (Tuttle and Dunn, 1995; Mukaiyama *et al.*, 2002). In *H. polymorpha*, Pep4 protein has been recently demonstrated to be engaged in the proteolytic activation of carboxypeptidase Y (Bae *et al.*, 2005), although its possible role in the peroxisome degradation has not been addressed.

The predicted amino acid sequence of Pep4 protein from *Y. lipolytica* is 396 residues long. This protein was found to share about 65% of identity with correspondent counterparts from *S. cerevisiae* and *H. polymorpha* (Table 3.1). The most conserved region of YlPep4p belongs to the catalytic domain of the family of aspartyl proteases and shows a significant similarity degree with yeast yapsin proteases as well as with a human cathepsin D (Fig. 7.13 in Appendix). Biochemical analysis of the *pep4* mutant cells grown under peroxisome degradation-inducing conditions revealed an obvious delay in the degradation of some peroxisomal and cytosolic proteins (Fig. 3.29). These results were verified by the following fluorescence microscopy of the *pep4* cells. The rate of pexophagy appeared to be reduced in the ethanol/ethylamine-grown mutant cells transferred into a minimal medium with glucose and ammonium sulfate (Fig. 3.30: A). However, this process seemed to be not completely abolished since a gradual reduction of intensity of the green fluorescent signal could be observed within the vacuoles of the *pep4* mutant cells with prolonged incubation time. Conversely, a clear delay in the autophagic degradation of peroxisomes was revealed in the *pep4* strain under conditions of glucose and nitrogen depletion (Fig. 3.30: B). Also, degradation of the cytosolic protein G6PDH was provisionally shifted in this mutant (Fig. 3.29: D) hinting at a probable defect in non-specific

bulk autophagy as well. Thus, disruption of the *YlPEP4* gene has an impact on the degradation capacity of the vacuole, although its effect appears to be much more pronounced under starvation conditions. However, the proteolytic activity of the vacuole does not seem to be completely blocked in the *pep4* strain. Also, phoxin B test did not reveal any defects in cell viability of the glucose-grown *pep4* mutant cells starved by nitrogen which is in line with this suggestion. A most plausible explanation of this finding could be a presence of an alternative proteinase A-independent pathway which may activate vacuolar proteases if the proteolytic activity of Pep4 is missing. Indeed, a previous study have shown that Pep4-dependent maturation of yeast vacuolar proteins can be functionally replaced by a plant cystein protease from the family of vacuolar processing enzymes (Hiraiwa *et al.*, 1997). Furthermore, there are some examples of a self-activation of the vacuolar proteolytic enzymes by self-catalysis (Wolff *et al.*, 1996; Hiraiwa *et al.*, 1999). Finally, an existence of other proteinase(s) essential for the degradation capability of the vacuole couldn't be excluded. Taking together, results described above confirm a prediction that proteinase A encoded by the yeast *PEP4* gene partially contributes to the proteolytic activity of the vacuole.

Another interesting observation concerns dynamics of the vacuolar membranes in the *pep4* cells. As shown in Fig. 3.30, an intensive proliferation of the microautophagic tubes was observed in mutant cells grown in the absence of nitrogen source. However, if ammonium sulfate was present in growth medium, some invaginations and protrusion of the vacuolar membranes could be also revealed. It seems likely that development of such structures by the vacuole is required to reimburse a lack of degradation caused by the Pep4 depletion. This observation imply that microautophagy – besides its important degradation function - may play a role as a subsidiary mechanism to contribute to cell respond to the intracellular changes. If it holds true, it would be interesting to investigate which molecular signals trigger microautophagy in this case.

4.2.4 Isolation of novel peroxisome degradation deficient *(pdd)* mutants of *Y. lipolytica*

The suitability of the alkane-utilizing yeast *Y. lipolytica* as a model system to identify genes implicated in different pathways, such as metabolism of hydrophobic substrates, dimorphic transition, secretion pathway, etc. has been demonstrated by many genetic screens (see Barth *et al.* (2003) for review). Being a unicellular organism, *Y. lipolytica* is amenable to a large-scale plate screening. Furthermore, this yeast grows well on alkanes, alcohols and fatty acids and its growth was shown to be accompanied by an enhanced proliferation of peroxisomes (Titorenko *et al.*, 2000a). The last feature has been successfully used to initiate studies on biogenesis of these organelles in *Y. lipolytica* which resulted in a recently developed viewpoint about dynamic,

heterogeneous structure of the peroxisomal population in a yeast cell (Titorenko and Rachubinski, 2001a).

Exploration of pexophagy in *Y. lipolytica* started with an observation that addition of ethylamine to growth medium induces a peroxisomal amine oxidase activity which may be used as a marker to monitor turnover of peroxisomes in *Y. lipolytica* (Gunkel *et al.*, 1999). Furthermore, applying a modified plate activity assay to visualize yeast colonies expressing amine oxidase, Gunkel *et al.* (1999) and later on Nazarko *et al.* (2004) succeeded in isolation of *Y. lipolytica* mutants deficient in the specific inactivation of peroxisomal enzymes. Recently, a first *Y. lipolytica pdd* mutant with mutation in the early secretory pathway gene *TRS85* has been described to be impaired in selective macropexophagy in this yeast species (Nazarko *et al.*, 2005a). This finding supports a previous suggestion that the early secretory route may contribute to autophagy-related pathways. In this thesis project, a different approach based on expression of the chimerical protein βGal-eGFP(SKL) under the control of homologous *YlICL1* promoter was used to isolate *pdd* mutants of *Y. lipolytica*. This method implies a direct monitoring of the heterologous β-galactosidase activity by a filter assay (Gunkel, 2000) which serves as a platform for visual screen of yeast mutants affected in the course of autophagic degradation of peroxisomes. During this study, a number of *Y. lipolytica* mutant strains defected in the specific inactivation of β-galactosidase by glucose was obtained. Mutants displaying most prominent phenotypes were then analyzed by fluorescence microscopy.

A mutant № 55 turned out to exhibit a most interesting phenotype. As described in Chapter 3.6, mutation in this strain led to an early block in peroxisome degradation at a point prior to uptake of the organelles by the vacuoles. In particular, the transport of peroxisomes to the vacuoles appeared to be delayed in the mutant cells grown in medium containing glucose and ammonium sulfate (Fig. 3.32: A). On the other hand, under conditions of nitrogen starvation, individual organelles as well as peroxisomal clusters were found at close proximity to the vacuolar membranes; however, no fusion between the vacuolar and auto(pexo)phagosomal membranes occurred (Fig. 3.32: B). These data imply that a gene affected in the mutant 55 apparently has a role in both selective pexophagy and non-selective autophagy pathways. Noteworthy, a product of the mutated gene seem to be unnecessary for the initial signaling and recognition steps of these degradation processes but is most likely involved in later stages, such as the cargo sequestration and targeting and/or membrane fusion events. Another observation giving us some clues what indeed may happen in the mutant cells under peroxisome degradation-inducing conditions is their abnormal morphology. The mutant cells exhibited a characteristic prolonged cellular form which may results from a possible defect in the cytoskeleton. The association of

peroxisomes with cytoskeletal structures has been demonstrated previously by many studies (see Schrader *et al.* (2003) for review). Recently, microtubules and dynein motors have been shown to be required for biogenesis of these organelles in human (Brocard *et al.*, 2005). Another current study revealed the actin cytoskeleton to be essential for the selective types of autophagy, i.e. pexophagy and the Cvt pathway, in baker's yeast (Reggiori *et al.*, 2005). Finally, a yeast homolog of a mammalian microtubule-associated protein, Atg8p, was proven to be pivotal for autophagy in *S. cerevisiae* (Lang *et al.*, 1998) as well as for micro- and macropexophagy in *P. pastoris* and *H. polymorpha,* respectively (Mukaiyama *et al.*, 2002; Monastyrska *et al.*, 2005a). Since phenotypic features of the mutant № 55 for the most part resemble morphological alterations described for nutrient depleted cells treated with microfilament depolymerazing drugs (Aplin *et al.*, 1992), it is highly attractive to speculate that mutation(s) in the strain 55 may have an effect on organization and/or functioning of the cytoskeleton. This, in turn, may lead to defects in peroxisomal motility and/or in the formation of auto(pexo)phagosomes (Aplin *et al.*, 1992). Alternatively, this mutant phenotype may results from mutation(s) in a putative *Y. lipolytica* gene associated with the control of cell cycle progression although temperature-sensitivity of this strain was not addressed in this study. Finally, the mutant № 55 may possess mutation(s) in several genes making its phenotype really complex. Additional studies are certainly required to distinguish between these possible explanations.

Another *Y. lipolytica* mutant strain № 32 was found to display a strong alteration in the vacuolar morphology when grown under conditions of nitrogen depletion (Fig. 3.31: B). This fact appears to be a most plausible reason for why the degradation of peroxisomes was disturbed in the nitrogen-starved mutant cells, so that this mutant strain could be selected by the β-galactosidase screen. Being most likely not a true *pdd* mutant, the strain № 32 may serve a good illustration of an interesting mutant phenotype which may be found out by this method. The devised β-galactosidase-based screening system also offers a good possibility to isolate mutants impaired in glucose signaling, vacuolar degradation, import of peroxisomal proteins, etc. Development of similar assays will further improve the suitability of *Y. lipolytica* as a model organism to study the turnover of peroxisomes.

4.3 Functional overview of *Y. lipolytica* mutants explored in this study

Most of our current knowledge on the autophagic degradation of peroxisomes in yeasts come from studies performed in three microorganisms, namely in baker's yeast *S. cerevisiae* and in two non-conventional methylotrophic yeast species *P. pastoris* and *H. polymorpha* (Bellu *et al.*, 2003; Kiel and Veenhuis, 2003). Most recently, a non-conventional alkane-assimilating yeast *Y. lipolytica* has been introduced into pexophagy studies (reviewed in Dunn *et al.*, 2005). This thesis project aimed at further elucidation of molecular mechanisms behind the autophagic peroxisome degradation in this yeast. For this purpose, several *Y. lipolytica atg* mutants displaying defects at different stages of pexophagy and/or other autophagy-related processes were isolated and characterized. This chapter provides an overview of phenotypic effects of the *Y. lipolytica* mutant strains explored in this study in comparison with data summarized for other yeast systems. As described in **Table 4.1**, phenotypes of the most studied *Y. lipolytica* mutants agree well with those assigned to corresponding mutants of *S. cerevisiae*, *H. polymorpha* and *P. pastoris*. So, *atg1*, *atg6* and *atg18* strains of *Y. lipolytica* were revealed to exhibit defects in a bulk autophagy triggered by nitrogen starvation which is in line with data obtained previously (see appropriate chapters for detail). Furthermore, the phenotype of *Y. lipolytica atg11* mutant was found to correspond to a predicted one although the *YlATG11* gene disruption appeared to have no drastic effect on peroxisome degradation in *Y. lipolytica* unlike in other yeast species. On the other hand, some results gained in the course of this project provide new insights on the molecular machinery involved in autophagy-like processes. This study showed for the first time that Atg6p, a yeast homolog of a human beclin 1, is required for efficient pexophagy in *Y. lipolytica*. Furthermore, disruption of *YlATG1* and *YlATG18* genes did not affect pexophagy upon shift of *Y. lipolytica* cells into glucose medium supplied by nitrogen, whereas an opposite situation is known to occur in other yeasts. Finally, Gcn2 protein of *Y. lipolytica* was shown to be dispensable for selective autophagy of peroxisomes as well as for a bulk nitrogen-starvation induced autophagy which is not in agreement with data reported earlier. Isolation and characterization of novel *Y. lipolytica* mutants affected in pexophagy will definitely shed more light on molecular machineries implicated in this pathway in different yeast species. Thus, this study, together with previous data indicating common but also unique features of some Atg proteins from different organisms, underlines the importance of using alternative model systems for the formation of a general view on autophagy-related pathways.

Table 4.1 Overview of *Y. lipolytica atg* mutants explored in this study.

Abbreviations: *atg*, autophagy-related (mutant); PAS, pre-autophagosomal structure.

Strain	Shift to glucose with nitrogen source		Shift to glucose w/o nitrogen source		Proposed role in *Y. lipolytica*	Known function(s)
	Degradation of peroxisomal proteins	Morphological defects	Degradation of peroxisomal proteins	Morphological defects		
atg1	Not affected	Not observed	Blocked	Formation of clusters of peroxisomes; organelles were not taken up by the vacuoles	Formation of autophagic membranes during macroautophagy	Autophagosome formation, associated with PAS
atg6	Blocked	Peroxisomes were targeted to the vacuoles but not taken up by them	Blocked	Peroxisomes were targeted to the vacuoles but not taken up by them; altered morphology of intracellular membranes	Involved in intracellular membrane trafficking; required for both glucose- and nitrogen starvation-induced pexophagy	Formation of autophagosomes and Cvt vesicles, associated with PAS
atg11	Not significantly affected	Slower uptake of peroxisomes by the vacuole	Not significantly affected	Slower uptake of peroxisomes by the vacuole	Recruitment of selective cargo for pexophagosomes	Recruitment of selective cargos for the Cvt vesicles and pexophagosomes; dispensable for bulk autophagy
atg18	Not affected	Not affected	Blocked	Formation of clusters of peroxisomes; organelles were not taken up by the vacuoles	Formation of autophagosomal membranes in response to nitrogen starvation	Formation of sequestering membranes during auto- and pexophagy, associated with PAS
gcn2	Not affected	Not affected	Not affected	Not affected	Not required for peroxisome degradation	Activation of starvation-induced autophagy
pep4	Delayed	Slower degradation of peroxisomes inside the vacuoles; no defect in uptake of peroxisomes	Delayed	Slower degradation of peroxisomes inside the vacuoles; no defect in uptake of peroxisomes	Involved in the vacuolar degradation but not crucial for pexophagy	One of the major vacuolar aspartic proteases
#32	Not examined	Not affected	Not examined	Alterations in the vacuolar morphology	Involved in organizing and(or) functioning of the vacuoles	-
#55	Not examined	No uptake of peroxisomes by the vacuole; changes in cell morphology	Not examined	No uptake of peroxisomes by the vacuole; changes in cell morphology	Formation of auto(pexo)phagosomal membranes	-

4.4 Outlook: Modes of autophagic peroxisome degradation in *Y. lipolytica*

In yeasts, two morphologically distinct modes of pexophagy, macro- and micropexophagy, may contribute to the degradation of peroxisomes (Dunn *et al.*, 2005). Macropexophagy implies the sequestration of an individual peroxisome within a pexophagosome by additional membrane layers and its subsequent fusion with the vacuole for degradation. Micropexophagy is a process whereby cytosolic substances and clusters of organelles are engulfed by specific protrusions formed at the vacuolar surface following by their recycling in the vacuolar lumina. Despite obvious differences in their morphology, macro- and micropexophagy share many components with each other and with other known autophagy-related pathways, i.e. macro- and micro-autophagy as well as the Cvt pathway (Hutchins *et al.*, 1999; Veenhuis *et al.*, 2000; Farre and Subramani, 2004). In *Y. lipolytica*, macropexophagy was revealed to be a major route of the selective peroxisome degradation started upon transfer of peroxisome-containing cells into glucose medium supplied by nitrogen (Gunkel *et al.*, 1999; Nazarko *et al.*, 2005). However, no data were presented on the mode of pexophagy which occurs in *Y. lipolytica* if two different stimuli, i.e. glucose and nitrogen depletion, are available simultaneously. In the course of my thesis project, I attempted to address this question as well. Consequently, a following model for the autophagic degradation of peroxisomes in *Y. lipolytica* may be proposed.

When *Y. lipolytica* cells are switched from an ethanol/ethylamine medium to one containing glucose and ammonium sulfate, peroxisomes are degraded by the macroautophagic process. Remarkably, this degradation mode appears to be selective for peroxisomes and, therefore, can be referred to macropexophagy. In contrast, shift of the ethanol/ethylamine-grown *Y. lipolytica* cells into a glucose-containing nitrogen-depleted medium obviously triggers two different degradation modes, namely macro- and microautophagy. Interestingly, all three processes can be genetically separated in *Y. lipolytica*. Thus, *atg1* and *atg18 Y. lipolytica* mutants display defects in starvation-induced macroautophagy and, in the case of *atg18*, also microautophagy, but are not affected in glucose-induced macropexophagy. Conversely, in *atg6* mutant as well as in the strain № 55, all these processes appear to be disturbed since peroxisomes are not degraded by any of the aforementioned modes. On the other hand, *Y. lipolytica atg11* mutant exhibits slight defects in the selective degradation of peroxisomes, whereas bulk autophagy is not impaired in this strain. Finally, microautophagic mode of degradation appears to be affected in *gcn2* mutant of *Y. lipolytica* which, however, does not have any considerable effect on peroxisome degradation by other pathways.

Which molecular signals determine a switch between different degradation modes in response to environmental changes, is still poorly understood. In the methylotrophic yeast *P. pastoris*, for instance, micro- and macropexophagy are shown to be induced by adaptation of methanol-grown cells to glucose- and ethanol-containing media, respectively (Tuttle and Dunn, 1995). However, a recent study in this yeast has revealed that rather the level of intracellular ATP than the kind of provided carbon source (so-called "inducer") influences the manner of peroxisome degradation (Ano *et al.*, 2005). Another line of evidence for a probable correlation between different modes of pexophagy comes from a finding that both degradation processes can partially substitute for each other. For example, it was noted that in a *P. pastoris* mutant completely disturbed in glucose-induced micropexophagy peroxisomes were still slowly degraded during glucose adaptation, presumably by a macropexophagic mode (Yuan *et al.*, 1997). Similarly, in a *H. polymorpha* mutant affected in macropexophagy, degradation of peroxisomes might still occur by a constitutive process resembling microautophagy (Bellu and Kiel, 2003). In the case of *H. polymorpha*, these processes have been already shown to proceed simultaneously in cells subjected to excess glucose and nitrogen depletion at once (Monastyrska *et al.*, 2004). Finally, recent studies on a role of membrane dynamics in autophagy-like processes have indicated that many *ATG* gene products, including the ubiquitin-like Atg8-system, share common functions in the formation of membrane structures, e.g., the pre-autophagosomal structure (PAS) during macroauto(pexo)phagy and the micropexophagic apparatus (MIPA) during micropexophagy (Suzuki *et al.*, 2001; Mukaiyama *et al.*, 2002; Farre and Subramani, 2004). So, it is also conceivable that a choice of a proper degradation pathway takes place not only at the stage of nutrient signaling but occurs also during later steps of vesicle formation and cargo recognition.

The pexophagy model proposed for *Y. lipolytica* is still largely speculative, mainly because of the lack of experimental data, and, therefore, is less clear than in the case of methylotrophic yeasts. The data gained in this study provides first evidence that molecular mechanisms of the autophagic degradation of peroxisomes in *Y. lipolytica* not only share a lot of common with those described for other yeast species but also display clear differences. Being phylogenetically well isolated from other hemiascomycetes, this yeast offers a good alternative to methylotrophs. In conclusion, further studies on *Y. lipolityca* are certainly required to provide a more complete insight into pexophagy which, in turn, will help us to create a unified model of autophagy-related processes in eukaryotes.

5 Summary

The dimorphic alkane-assimilating yeast *Y. lipolytica* is at present one of the most intensively studied non-conventional yeast species. A complete set of molecular genetic techniques has been developed for this organism. Recently, the full sequence of *Y. lipolytica* genome has become available (Dujon *et al.*, 2004). During the past few years, substantial progress has been made towards understanding the basic mechanisms underlying peroxisomal biogenesis in *Y. lipolytica* (Titorenko *et al.*, 2000b). A new view on peroxisomes as dynamic, structurally and functionally distinct compartments, organized into a so-called multistep peroxisome assembly pathway, has been developed using *Y. lipolytica* as a model organism (Titorenko and Rachubinski, 2001). However, until recent times, only little attention has been paid to pexophagy, a converse process leading to degradation of peroxisomes in yeast vacuoles by a specific autophagy-related mode. It was Gunkel *et al.* (1999) who first introduced *Y. lipolytica* into pexophagy studies. It was revealed that peroxisomes are subjected to selective degradation via macropexophagy in *Y. lipolytica* cells transferred from oleate/acetate/ethylamine into glucose media with ammonium sulfate or ammonium chloride (Gunkel *et al.*, 1999; Nazarko *et al.*, 2005). Recently, a first *Y. lipolytica* gene implicated in both selective pexophagy and bulk autophagy has been identified (Nazarko *et al.*, 2005a). However, the field of pexophagic research on this yeast remains quite unexplored. This study focused on the molecular mechanisms behind the autophagic degradation of peroxisomes in *Y. lipolytica*. The following results were obtained:

1. A recombinant *Y. lipolytica* strain PO1d(pLG3) bearing an artificial gene fusion *LacZ-eGFP(SKL)* placed under the control of a strong inducible promoter of the homologous isocitrate lyase gene *(YlICL1)* was constructed. A chimerical protein βGal-eGFP(SKL) encoded by this construct was localized to peroxisomes and possessed expression and degradation profiles characteristic for a peroxisomal enzyme. This data suggests that the βGal-eGFP(SKL) protein is a suitable marker for the peroxisomal compartment in *Y. lipolytica* system.

2. The course of autophagic peroxisome degradation in *Y. lipolytica* was analyzed by fluorescence microscopy using eGFP(SKL)/FM4-64 double fluorescent labeling of peroxisomes/vacuoles. Macropexophagy was confirmed to be the mode of peroxisome degradation in *Y. lipolytica* cells transferred from ethanol/ethylamine- into glucose/ ammonium sulfate-containing media. Under autophagy-triggering conditions however, both macro- and microautophagic degradation pathways were functional.

3. The influence of the serine protease inhibitor PMSF on pexophagy in *Y. lipolytica* was tested. Addition of PMSF affected not only the vacuolar degradation of peroxisomes, but also the uptake of these organelles by the vacuoles. Remarkably, the formation of autophagic tubes was disturbed in the PMSF-treated nitrogen-starved yeast cell as well. Thus, PMSF has a complex effect on the degradation of peroxisomes in *Y. lipolytica*.

4. Bioinformatic analysis of the genome of *Y. lipolytica* revealed 33 putative homologous proteins displaying different rates of homology to their counterparts from other yeast species. Interestingly, in this screen, no homologs of yeast Atg10, Atg16, Atg19, Atg21, Atg23 or Atg28 proteins could be identified in *Y. lipolytica*. Nevertheless, we identified homologs for *Y. lipolytica* Atg1, Atg6, Atg11, Atg18, Gcn2 and Pep4 proteins that were analyzed in more detail.

5. Phenotypic analysis of the *Y. lipolytica atg* mutants grown under nitrogen starvation conditions demonstrated an obvious reduction of cell viability of *atg1, atg6* and *atg18* mutant cells. In contrast, no significant differences in cell survival were observed for *atg11, gcn2* and *pep4* mutants compared to the initial *Y. lipolytica* strain PO1d(pLG3). Thus, bulk nitrogen-starvation-triggered autophagy is impaired in *atg1, atg6* and *atg18*, but is apparently unaffected in *atg11, gcn2* and *pep4* mutants of *Y. lipolytica*.

6. Biochemical and fluorescence microscopy studies of pexophagy in *Y. lipolytica* mutants revealed clear defects in peroxisome degradation in the *atg1, atg6* and *atg18* mutant cells subjected to a glucose-containing medium lacking nitrogen. Noticeably, pexophagy was also impaired in the *atg6* cells upon their shift into glucose/ammonium sulfate, which is the first evidence linking a yeast pexophagy protein to tumour suppression. On the other hand, degradation of peroxisomes was unaffected in the glucose/ammonium sulfate-grown *atg1* and *atg18* mutants of *Y. lipolytica*, hinting at a possible difference between the molecular profiles of peroxisome-containing vesicles produced by yeast cells under different physiological conditions. Furthermore, disruption of the *YlATG11* gene had no significant effect on peroxisome degradation that could be explained through the complex role that YlAtg11p, together with its potential interaction partners, might play in selective autophagy-related processes. Conversely, YlGcn2p was dispensable for the selective degradation of peroxisomes via macropexophagy under both nitrogen-rich and nitrogen-starved conditions. Since formation of autophagic tubes was impaired in the *gcn2* mutant, it is proposed that microautophagy plays rather a minor role in peroxisome degradation in *Y. lipolytica.* Finally, pexophagy was slowed down, but not completely blocked, in the

Y. lipolytica pep4 mutant, suggesting a partial contribution of proteinase A to the proteolytic capacity of the vacuole.

7. A novel approach for a visual screening of *pdd* mutants of *Y. lipolytica* was developed, based on the *YlICL1*-driven expression of heterologous β-galactosidase as part of chimerical protein βGal-eGFP(SKL). Using this method, a mutant, № 55, was discovered which had an effect on peroxisome degradation under both nitrogen-rich and nitrogen-starved conditions. The discovery of this mutant shows the suitability of this approach for the isolation of *Y. lipolytica* mutants impaired in pexophagy that will allow us to learn more about the molecular background of autopahgy-related pathways in yeasts.

On the basis of this data and data from literature, a model of peroxisome degradation in *Y. lipolytica* can be proposed. According to this model, two different mechanisms can contribute to the degradation of peroxisomes in *Y. lipolytica* depending on the growth conditions. Macropexophagy occurs in yeast cells only if both carbon and nitrogen sources are present in the growth medium. In contrast, both macro- and microautophagic degradation take place in cells grown in the medium containing only carbon but no nitrogen source. However, there is no direct evidence so far that microautophagy contributes to peroxisome degradation in *Y. lipolytica*. Studies on mutants indicate that these processes may be distinguished not only mechanically but also genetically. Taken together, this data emphasizes that as a model organism *Y. lipolytica* will provide significant insight into the molecular mechanisms of selective autophagy-related processes in eukaryotes.

6 References

Abeliovich, H., Zhang, C., Dunn, W. A., Jr., Shokat, K. M. and Klionsky, D. J. (2003). Chemical genetic analysis of Apg1 reveals a non-kinase role in the induction of autophagy. *Mol Biol Cell* 14, 477-90.

Abeliovich, H. and Klionsky, D. J. (2001). Autophagy in yeast: mechanistic insights and physiological function. *Microbiol Mol Biol Rev* 65, 463-79, table of contents.

Ammerer, G., Hunter, C. P., Rothman, J. H., Saari, G. C., Valls, L. A. and Stevens, T. H. (1986). *PEP4* gene of *Saccharomyces cerevisiae* encodes proteinase A, a vacuolar enzyme required for processing of vacuolar precursors. *Mol Cell Biol* 6, 2490-9.

Ano, Y., Hattori, T., Kato, N. and Sakai, Y. (2005). Intracellular ATP correlates with mode of pexophagy in *Pichia pastoris*. *Biosci Biotechnol Biochem* 69, 1527-33.

Aplin, A., Jasionowski, T., Tuttle, D. L., Lenk, S. E. and Dunn, W. A., Jr. (1992). Cytoskeletal elements are required for the formation and maturation of autophagic vacuoles. *J Cell Physiol* 152, 458-66.

Aubourg, P. (1994). Adrenoleukodystrophy and other peroxisomal diseases. *Curr Opin Genet Dev* 4, 407-11.

Baba, M., Osumi, M., Scott, S. V., Klionsky, D. J. and Ohsumi, Y. (1997). Two distinct pathways for targeting proteins from the cytoplasm to the vacuole/lysosome. *J Cell Biol* 139, 1687-95.

Baba, M., Takeshige, K., Baba, N. and Ohsumi, Y. (1994). Ultrastructural analysis of the autophagic process in yeast: detection of autophagosomes and their characterization. *J Cell Biol* 124, 903-13.

Bae, J. H., Sohn, J. H., Rhee, S. K. and Choi, E. S. (2005). Cloning and characterization of the *Hansenula polymorpha PEP4* gene encoding proteinase A. *Yeast* 22, 13-9.

Baehrecke, E. H. (2003). Autophagic programmed cell death in *Drosophila*. *Cell Death Differ* 10, 940-5.

Baerends, R. J., Faber, K. N., Kiel, J. A., van der Klei, I. J., Harder, W. and Veenhuis, M. (2000). Sorting and function of peroxisomal membrane proteins. *FEMS Microbiol Rev* 24, 291-301.

Barbet, N. C., Schneider, U., Helliwell, S. B., Stansfield, I., Tuite, M. F. and Hall, M. N. (1996). TOR controls translation initiation and early G1 progression in yeast. *Mol Biol Cell* 7, 25-42.

Barth, G., Beckerich, J.-M., Dominguez, A., Kerscher, S., Ogrydziak, D., Titorenko, V. and Gaillardin, C. (2003). Functional genetics of *Yarrowia lipolytica*. In: Functional Genetics of Industrial Yeasts. J. H. de Winde (ed.) Berlin, Heidelberg, Springer, 227-271.

Barth, G. and Gaillardin, C. (1997). Physiology and genetics of the dimorphic fungus *Yarrowia lipolytica*. *FEMS Microbiol Rev* 19, 219-37.

Barth, G. and Gaillardin, C. (1996). *Yarrowia lipolytica*. In: Non-conventional Yeasts in Biotechnology: a handbook. K. Wolf (ed.) Berlin, Heidelberg, Springer, 313-388.

Barth, G. and Weber, H. (1985). Improvement of sporulation in the yeast *Yarrowia lipolytica*. *Antonie van Leeuwenhoek J Microbiol* 51, 167-177.

Barth, H., Meiling-Wesse, K., Epple, U. D. and Thumm, M. (2001). Autophagy and the cytoplasm to vacuole targeting pathway both require Aut10p. *FEBS Lett* 508, 23-8.

Beckerich, J. M., Boisrame-Baudevin, A. and Gaillardin, C. (1998). *Yarrowia lipolytica*: a model organism for protein secretion studies. *Int Microbiol* 1, 123-30.

Bellu, A. R. and Kiel, J. A. (2003). Selective degradation of peroxisomes in yeasts. *Microsc Res Tech* 61, 161-70.

Bellu, A. R., Salomons, F. A., Kiel, J. A., Veenhuis, M. and Van Der Klei, I. J. (2002). Removal of Pex3p is an important initial stage in selective peroxisome degradation in *Hansenula polymorpha*. *J Biol Chem* 277, 42875-80.

Bellu, A. R., Komori, M., van der Klei, I. J., Kiel, J. A. and Veenhuis, M. (2001). Peroxisome biogenesis and selective degradation converge at Pex14p. *J Biol Chem* 276, 44570-4.

Bellu, A. R., Kram, A. M., Kiel, J. A., Veenhuis, M. and van der Klei, I. J. (2001a). Glucose-induced and nitrogen-starvation-induced peroxisome degradation are distinct processes in *Hansenula polymorpha* that involve both common and unique genes. *FEMS Yeast Res* 1, 23-31.

Berlanga J., Santoyo J. and De Haro C. (1999). Characterization of a mammalian homolog of the GCN2 eukaryotic initiation factor 2alpha kinase. *Eur J Biochem* 265, 754-62.

Bodinus, C. (2004) Charakterisierung der Gene *YlCVT18* und *YlYGR223c* hinsichtlich ihrer Rolle im Abbau von Peroxisomen durch Autophagie und Pexophagie in der Hefe *Yarrowia lipolytica*. Diplomarbeit, Institut für Mikrobiologie, Technische Universität Dresden.

Borst, P. and Elferink, R. O. (2002). Mammalian ABC transporters in health and disease. *Annu Rev Biochem* 71, 537-92.

Brocard, C. B., Boucher, K. K., Jedeszko, C., Kim, P. K. and Walton, P. A. (2005). Requirement for microtubules and dynein motors in the earliest stages of peroxisome biogenesis. *Traffic* 6, 386-95.

Bryant, N. J. and Stevens, T. H. (1998). Vacuole biogenesis in *Saccharomyces cerevisiae*: protein transport pathways to the yeast vacuole. *Microbiol Mol Biol Rev* 62, 230-47.

Bursch, W., Ellinger, A., Gerner, C., Frohwein, U. and Schulte-Hermann, R. (2000). Programmed cell death (PCD). Apoptosis, autophagic PCD, or others? *Ann N Y Acad Sci* 926, 1-12.

Casaregola, S., Neuveglise, C., Bon, E. and Gaillardin, C. (2002). Ylli, a non-LTR retrotransposon L1 family in the dimorphic yeast *Yarrowia lipolytica*. *Mol Biol Evol* 19, 664-77.

Casaregola, S., Neuveglise, C., Lepingle, A., Bon, E., Feynerol, C., Artiguenave, F., Wincker, P. and Gaillardin, C. (2000). Genomic exploration of the hemiascomycetous yeasts: 17. *Yarrowia lipolytica*. *FEBS Lett* 487, 95-100.

Casaregola, S., Feynerol, C., Diez, M., Fournier, P. and Gaillardin, C. (1997). Genomic organization of the yeast *Yarrowia lipolytica*. *Chromosoma* 106, 380-90.

Chiang, H. L., Schekman, R. and Hamamoto, S. (1996). Selective uptake of cytosolic, peroxisomal, and plasma membrane proteins into the yeast lysosome for degradation. *J Biol Chem* 271, 9934-41.

Cirigliano, M. C. and Carman, G. M. (1984). Isolation of a bioemulsifier from *Candida lipolytic*a. *Appl Environ Microbiol* 48, 747-50.

Cutler, N. S., Heitman, J. and Cardenas, M. E. (1999). TOR kinase homologs function in a signal transduction pathway that is conserved from yeast to mammals. *Mol Cell Endocrinol* 155, 135-42.

De Camilli, P., Emr, S. D., McPherson, P. S. and Novick, P. (1996). Phosphoinositides as regulators in membrane traffic. *Science* 271, 1533-9.

De Duve, C. and Baudhuin, P. (1966). Peroxisomes (microbodies and related particles). *Physiol Rev* 46, 323-57.

De Waal, E. J., Vreeling-Sindelarova, H., Schellens, J. P. and James, J. (1986). Starvation-induced microautophagic vacuoles in rat myocardial cells. *Cell Biol Int Rep* 10, 527-33.

Dever, T. E., Feng, L., Wek, R. C., Cigan, A. M., Donahue, T. F. and Hinnebusch, A. G. (1992). Phosphorylation of initiation factor 2 alpha by protein kinase GCN2 mediates gene-specific translational control of GCN4 in yeast. *Cell* 68, 585-96.

Dixon, G. and Kornberg, H. (1959). Assay methods for key enzymes of the glyoxylate cycle. *Biochem J* 72, 3.

Dodt, G. and Gould, S. J. (1996). Multiple *PEX* genes are required for proper subcellular distribution and stability of Pex5p, the PTS1 receptor: evidence that PTS1 protein import is mediated by a cycling receptor. *J Cell Biol* 135, 1763-74.

Dominguez, A., Costas, M., Longo, M. A. and Sanroman, A. (2003). A novel application of solid state culture: production of lipases by *Yarrowia lipolytica*. *Biotechnol Lett* 25, 1225-9.

Dower, W., Miller, J. and Ragsdale C. (1988.9 High efficiency transformation of *E. coli* by high voltage electroporation. *Nucleic Acids Res* 16, 6127-6145.

Dujon, B., Sherman, D., Fischer, G., Durrens, P., Casaregola, S., Lafontaine, I *et al.* (2004). Genome evolution in yeasts. *Nature* 430, 35-44.

Dunn, W. A., Jr., Cregg, J. M., Kiel, J. A.K.W., van der Klei, I. J., Oku, M., Sakai, Y., Sibirny, A., Stysyk, O. and Veenhuis, M. *et al.* (2005). Pexophagy: the selective autophagy of peroxisomes. *Autophagy* 1:2, 75-83.

Dunn, W. A., Jr. (1990). Studies on the mechanisms of autophagy: formation of the autophagic vacuole. *J Cell Biol* 110, 1923-33.

Eckert, J. H. and Erdmann, R. (2003). Peroxisome biogenesis. *Rev Physiol Biochem Pharmacol* 147, 75-121.

Egli, T., van Dijken, J. P., Veenhuis, M., Harder, W. and Fiechter, A (1980). Methanol metabolism in yeasts: Regulation of the synthesis of catabolic enzymes. *Arch. Microbiol* 124, 115-121.

Elmore, S. P., Qian, T., Grissom, S. F. and Lemasters, J. J. (2001). The mitochondrial permeability transition initiates autophagy in rat hepatocytes. *Faseb J* 15, 2286-7.

Erdmann, R. and Schliebs, W. (2005). Opinion: Peroxisomal matrix protein import: the transient pore model. *Nat Rev Mol Cell Biol* 6(9), 738-42.

Farre, J. C. and Subramani, S. (2004). Peroxisome turnover by micropexophagy: an autophagy-related process. *Trends Cell Biol* 14, 515-23.

Faust P., Kornfeld S. and Chirgwin J. (1985). Cloning and sequence analysis of cDNA for human cathepsin D. *Proc Natl Acad Sci USA* 82, 4910-4.

Fickers, P., Benetti, P. H., Wache, Y., Marty, A., Mauersberger, S., Smit, M. S. and Nicaud, J. M. (2005). Hydrophobic substrate utilisation by the yeast *Yarrowia lipolytica*, and its potential applications. *FEMS Yeast Res* 5, 527-43.

Fickers, P., Fudalej, F., Nicaud, J. M., Destain, J. and Thonart, P. (2005a). Selection of new over-producing derivatives for the improvement of extracellular lipase production by the non-conventional yeast *Yarrowia lipolytica*. *J Biotechnol* 115, 379-86.

Fickers, P., Le Dall, M. T., Gaillardin, C., Thonart, P. and Nicaud, J. M. (2003). New disruption cassettes for rapid gene disruption and marker rescue in the yeast *Yarrowia lipolytica*. *J Microbiol Methods* 55, 727-37.

Flores, C. L., Rodriguez, C., Petit, T. and Gancedo, C. (2000). Carbohydrate and energy-yielding metabolism in non-conventional yeasts. *FEMS Microbiol Rev* 24, 507-29.

Fournier, P., Abbas, A., Chasles, M., Kudla, B., Ogrydziak, D. M., Yaver, D., Xuan, J. W., Peito, A., Ribet, A. M., Feynerol, C. and et al. (1993). Colocalization of centromeric and replicative functions on autonomously replicating sequences isolated from the yeast *Yarrowia lipolytica*. *Proc Natl Acad Sci U S A* 90, 4912-6.

Fujiki, Y. (1997). Molecular defects in genetic diseases of peroxisomes. *Biochim Biophys Acta* 1361, 235-50.

Funakoshi, T., Matsuura, A., Noda, T. and Ohsumi, Y. (1997). Analyses of *APG13* gene involved in autophagy in yeast, *Saccharomyces cerevisiae*. *Gene* 192, 207-13.

George, M. D., Baba, M., Scott, S. V., Mizushima, N., Garrison, B. S., Ohsumi, Y. and Klionsky, D. J. (2000). Apg5p functions in the sequestration step in the cytoplasm-to-vacuole targeting and macroautophagy pathways. *Mol Biol Cell* 11, 969-82.

Gould, S. J. and Collins, C. S. (2002). Opinion: peroxisomal-protein import: is it really that complex? *Nat Rev Mol Cell Biol* 3, 382-9.

Gould, S. J. and Valle, D. (2000). Peroxisome biogenesis disorders: genetics and cell biology. *Trends Genet* 16, 340-5.

Grossmann, M. K. (1980). The use of phenylmethylsulfonyl fluoride in the study of catabolite inactivation and repression in intact cells of *Saccharomyces cervisiae*. *Arch Microbiol* 124, 293-5.

Guan, J., Stromhaug, P. E., George, M. D., Habibzadegah-Tari, P., Bevan, A., Dunn, W. A., Jr. and Klionsky, D. J. (2001). Cvt18/Gsa12 is required for cytoplasm-to-vacuole transport, pexophagy, and autophagy in *Saccharomyces cerevisiae* and *Pichia pastoris*. *Mol Biol Cell* 12, 3821-38.

Gunkel, K., van Dijk, R., Veenhuis, M. and van der Klei, I. (2004). Routing of *Hansenula polymorpha* alcohol oxidase: An alternative peroxisomal protein-sorting machinery. *Mol Biol Cell* 15, 1347-1355.

Gunkel, K. (2000) Etablierung von Screeningsystemen von Peroxisomedabbaudefekten Mutanten in der Hefe *Yarrowia lipolytica*. Diplomarbeit, Institut für Mikrobiologie, Technische Universität Dresden.

Gunkel, K., van der Klei, I. J., Barth, G. and Veenhuis, M. (1999). Selective peroxisome degradation in *Yarrowia lipolytica* after a shift of cells from acetate/oleate/ethylamine into glucose/ammonium sulfate-containing media. *FEBS Lett* 451, 1-4.

Hammond, E. M., Brunet, C. L., Johnson, G. D., Parkhill, J., Milner, A. E., Brady, G., Gregory, C. D. and Grand, R. J. (1998). Homology between a human apoptosis specific protein and the product of *APG5*, a gene involved in autophagy in yeast. *FEBS Lett* 425, 391-5.

Hamsa, P. V., Kachroo, P. and Chattoo, B. B. (1998). Production and secretion of biologically active human epidermal growth factor in *Yarrowia lipolytica*. *Curr Genet* 33, 231-7.

Hazra, P. P., Suriapranata, I., Snyder, W. B. and Subramani, S. (2002). Peroxisome remnants in pex3delta cells and the requirement of Pex3p for interactions between the peroxisomal docking and translocation subcomplexes. *Traffic* 3, 560-74.

Heiland, I. and Erdmann, R. (2005). Biogenesis of peroxisomes. Topogenesis of the peroxisomal membrane and matrix proteins. *Febs J* 272, 2362-72.

Herman, P. K. and Emr, S. D. (1990). Characterization of *VPS34*, a gene required for vacuolar protein sorting and vacuole segregation in Saccharomyces cerevisiae. *Mol Cell Biol* 10, 6742-54.

Hill, D. J., Hann, A. C. and Lloyd, D. (1985). Degradative inactivation of the peroxisomal enzyme, alcohol oxidase, during adaptation of methanol-grown Candida boidinii to ethanol. *Biochem J* 232, 743-50.

Hinnebusch, A. G. (1994). The eIF-2 alpha kinases: regulators of protein synthesis in starvation and stress. *Semin Cell Biol* 5, 417-26.

Hiraiwa, N., Nishimura, M. and Hara-Nishimura, I. (1999). Vacuolar processing enzyme is self-catalytically activated by sequential removal of the C-terminal and N-terminal propeptides. *FEBS Lett* 447, 213-6.

Hiraiwa, N., Nishimura, M. and Hara-Nishimura, I. (1997). Expression and activation of the vacuolar processing enzyme in *Saccharomyces cerevisiae*. *Plant J* 12, 819-29.

Hoffmann, C. (2004) Untersuchungen zur Funktion der Gene *YlVPS15* und *YlAPG6* bei der Autophagie und Pexophagie in der Hefe *Yarrowia lipolytica*. Diplomarbeit, Institut für Mikrobiologie, Technische Universität Dresden.

Holzschu, D. L., Chandler, F. W., Ajello, L. and Ahearn, D. G. (1979). Evaluation of industrial yeasts for pathogenicity. *Sabouraudia* 17, 71-8.

Hoepfner, D., Schildknegt, D., Braakman, I., Philippsen, P. and Tabak, H. F. (2005) Contribution of the endoplasmatic reticulum to peroxisome formation. *Cell* 122(1), 85-95.

Hutchins, M. U. and Klionsky, D. J. (2001). Vacuolar localization of oligomeric alpha-mannosidase requires the cytoplasm to vacuole targeting and autophagy pathway components in *Saccharomyces cerevisiae*. *J Biol Chem* 276, 20491-8.

Hutchins, M. U., Veenhuis, M. and Klionsky, D. J. (1999). Peroxisome degradation in *Saccharomyces cerevisiae* is dependent on machinery of macroautophagy and the Cvt pathway. *J Cell Sci* 112**,** 4079-87.

Ichimura, Y., Kirisako, T., Takao, T., Satomi, Y., Shimonishi, Y., Ishihara, N., Mizushima, N., Tanida, I., Kominami, E., Ohsumi, M., Noda, T. and Ohsumi, Y. (2000). A ubiquitin-like system mediates protein lipidation. *Nature* 408, 488-92.

Iida, T., Sumita, T., Ohta, A. and Takagi, M. (2000). The cytochrome P450ALK multigene family of n-alkane-assimilating yeast, *Yarrowia lipolytica*: cloning and characterization of genes coding for new CYP52 family members. *Yeast* 16, 1077-87.

Il'chenko, A. P., Mauersberger, S., Matiashova, R. N. and Lozinov, A. B. (1980). Cytochrome P-450 induction during yeast organism growth on various substrates. *Mikrobiologiia* 49, 452-8.

Ishihara, N., Hamasaki, M., Yokota, S., Suzuki, K., Kamada, Y., Kihara, A., Yoshimori, T., Noda, T. and Ohsumi, Y. (2001). Autophagosome requires specific early Sec proteins for its formation and NSF/SNARE for vacuolar fusion. *Mol Biol Cell* 12, 3690-702.

Jacobi, A. (2005) Herstellung und Charakterisierung von Pdd-Mutanten in der Hefe *Yarrowia lipolytica*. Diplomarbeit, Institut für Mikrobiologie, Technische Universität Dresden.

Juretzek, T., Le Dall, M., Mauersberger, S., Gaillardin, C., Barth, G. and Nicaud, J. (2001). Vectors for gene expression and amplification in the yeast *Yarrowia lipolytica*. *Yeast* 18, 97-113.

Juretzek, T. (1999). Entwicklung von Wirts-Vektor-Systemen zur heterologen Expression von Proteinen in der nichtkonventionellen Hefe *Yarrowia lipolytica* und ihre Anwendung für die Cytochrom P450-katalysierte Stoffumwandlung. Dissertation, Institut für Mikrobiologie, Technische Universität Dresden.

Kabani, M., Boisrame, A., Beckerich, J. M. and Gaillardin, C. (2000). A highly representative two-hybrid genomic library for the yeast *Yarrowia lipolytica*. *Gene* 241, 309-15.

Kamada, Y., Funakoshi, T., Shintani, T., Nagano, K., Ohsumi, M. and Ohsumi, Y. (2000). Tor-mediated induction of autophagy via an Apg1 protein kinase complex. *J Cell Biol* 150, 1507-13.

Kametaka, S., Okano, T., Ohsumi, M. and Ohsumi, Y. (1998). Apg14p and Apg6/Vps30p form a protein complex essential for autophagy in the yeast, *Saccharomyces cerevisiae*. *J Biol Chem* 273, 22284-91.

Khalfan, W. A. and Klionsky, D. J. (2002). Molecular machinery required for autophagy and the cytoplasm to vacuole targeting (Cvt) pathway in *S. cerevisiae*. *Curr Opin Cell Biol* 14, 468-75.

Kiel, J. A and Veenhuis, M. (2003). Selective degradation of peroxisomes in the methylotrophic yeast *Hansenula polymorpha*. In: Autophagy. Ed. by D. Klionsky, Landes Bioscience, Georgetown, Texas

Kiel, J. A., Komduur, J. A., van der Klei, I. J. and Veenhuis, M. (2003a). Macropexophagy in *Hansenula polymorpha*: facts and views. *FEBS Lett* 549, 1-6.

Kiel, J. A., Rechinger, K. B., van der Klei, I. J., Salomons, F. A., Titorenko, V. I. and Veenhuis, M. (1999). The *Hansenula polymorpha PDD1* gene product, essential for the selective degradation of peroxisomes, is a homologue of *Saccharomyces cerevisiae* Vps34p. *Yeast* 15, 741-54.

Kihara, A., Noda, T., Ishihara, N. and Ohsumi, Y. (2001). Two distinct Vps34 phosphatidylinositol 3-kinase complexes function in autophagy and carboxypeptidase Y sorting in *Saccharomyces cerevisiae*. *J Cell Biol* 152, 519-30.

Kim, J., Huang, W. P., Stromhaug, P. E. and Klionsky, D. J. (2002). Convergence of multiple autophagy and cytoplasm to vacuole targeting components to a perivacuolar membrane compartment prior to de novo vesicle formation. *J Biol Chem* 277, 763-73.

Kim, J., Kamada, Y., Stromhaug, P. E., Guan, J., Hefner-Gravink, A., Baba, M., Scott, S. V., Ohsumi, Y., Dunn, W. A., Jr. and Klionsky, D. J. (2001). Cvt9/Gsa9 functions in sequestering selective cytosolic cargo destined for the vacuole. *J Cell Biol* 153, 381-96.

Kim, J. and Klionsky, D. J. (2000). Autophagy, cytoplasm-to-vacuole targeting pathway, and pexophagy in yeast and mammalian cells. *Annu Rev Biochem* 69, 303-42.

Kim, J., Dalton, V. M., Eggerton, K. P., Scott, S. V. and Klionsky, D. J. (1999). Apg7p/Cvt2p is required for the cytoplasm-to-vacuole targeting, macroautophagy, and peroxisome degradation pathways. *Mol Biol Cell* 10, 1337-51.

Kim, J., Scott, S., Oda, M. and Klionsky, D. (1997). Transport of a large oligomeric protein by the cytoplasm to vacuole protein targeting pathway. *J Cell Biol* 137, 609-618.

Kirisako, T., Baba, M., Ishihara, N., Miyazawa, K., Ohsumi, M., Yoshimori, T., Noda, T. and Ohsumi, Y. (1999). Formation process of autophagosome is traced with Apg8/Aut7p in yeast. *J Cell Biol* 147, 435-46.

Klionsky, D. (2005). The molecular machinery of autophagy: the unanswered questions. *J Cell Sci* 118, 7-18.

Klionsky, D. J., Cregg, J. M. *et al.* (2003). A unified nomenclature for yeast autophagy-related genes. *Dev Cell* 5, 539-45.

Klionsky, D. J. and Emr, S. D. (2000). Autophagy as a regulated pathway of cellular degradation. *Science* 290, 1717-21.

Klionsky, D. J. and Ohsumi, Y. (1999). Vacuolar import of proteins and organelles from the cytoplasm. *Annu Rev Cell Dev Biol* 15, 1-32.

Klionsky, D. J. (1998). Nonclassical protein sorting to the yeast vacuole. *J Biol Chem* 273, 10807-10.

Klionsky, D. J., Cueva, R. and Yaver, D. S. (1992). Aminopeptidase I of *Saccharomyces cerevisiae* is localized to the vacuole independent of the secretory pathway. *J Cell Biol* 119, 287-99.

Klionsky, D. J., Banta, L. M. and Emr, S. D. (1988). Intracellular sorting and processing of a yeast vacuolar hydrolase: proteinase A propeptide contains vacuolar targeting information. *Mol Cell Biol* 8, 2105-16.

Kohlwein, S. D. (2000). The beauty of the yeast: live cell microscopy at the limits of optical resolution. *Microsc Res Tech* 51, 511-29.

Komduur, J. A., Veenhuis, M. and Kiel, J. A. (2003). The *Hansenula polymorpha PDD7* gene is essential for macropexophagy and microautophagy. *FEMS Yeast Res* 3, 27-34.

Kovalchuk, A., Senam, S., Mauersberger, S. and Barth, G. (2005). Tyl6, a novel Ty3/gypsy-like retrotransposon in the genome of the dimorphic fungus *Yarrowia lipolytic*a. *Yeast* 22, 979-91.

Kulachkovsky, A. R., Moroz, O. M. and Sibirny, A. A. (1997). Impairment of peroxisome degradation in *Pichia methanolica* mutants defective in acetyl-CoA synthetase or isocitrate lyase. *Yeast* 13, 1043-52.

Kunau, W. H. (2001). Peroxisomes: the extended shuttle to the peroxisome matrix. *Curr Biol* 11, R659-62.

Kunau, W. H., Agne, B. and Girzalsky, W. (2001a). The diversity of organelle protein import mechanisms. *Trends Cell Biol* 11, 358-61.

Kunau, W. H. (1998). Peroxisome biogenesis: from yeast to man. *Curr Opin Microbiol* 1, 232-7.

Kuroyanagi H., Jan J., Seki N., Yamanouchi S., Suzuki Y., Takano T., Muramatsu M. and Shirasawa T. (1998). Human ULK1, a novel serine/threonine kinase related to UNC-51 kinase of *Caenorhabditis elegans*. *Genomics* 51: 76-85.

Laemmli, U. K. (1970). Cleavage of structural proteins during the assembly of the head of bacteriophage T4. *Nature* 227: 680-5.

Lang, T., Schaeffeler, E., Bernreuther, D., Bredschneider, M., Wolf, D. H. and Thumm, M. (1998). Aut2p and Aut7p, two novel microtubule-associated proteins are essential for delivery of autophagic vesicles to the vacuole. *Embo J* 17, 3597-607.

Larsen, K. E. and Sulzer, D. (2002). Autophagy in neurons: a review. *Histol Histopathol* 17, 897-908.

Lazarow, P. B. and Fujiki, Y. (1985). Biogenesis of peroxisomes. *Annu Rev Cell Biol* 1, 489-530.

Le Dall, M. T., Nicaud, J. M. and Gaillardin, C. (1994). Multiple-copy integration in the yeast *Yarrowia lipolytica*. *Curr Genet* 26, 38-44.

Leao-Helder, A. N., Krikken, A. M., Gellissen, G., van der Klei, I. J., Veenhuis, M. and Kiel, J. A. (2004). Atg21p is essential for macropexophagy and microautophagy in the yeast *Hansenula polymorpha*. *FEBS Lett* 577, 491-5.

Leao-Helder, A. N., Krikken, A. M., van der Klei, I. J., Kiel, J. A. and Veenhuis, M. (2003). Transcriptional down-regulation of peroxisome numbers affects selective peroxisome degradation in *Hansenula polymorpha*. *J Biol Chem* 278, 40749-56.

Leao, A. N. and Kiel, J. A. (2003). Peroxisome homeostasis in *Hansenula polymorpha*. *FEMS Yeast Res* 4, 131-9.

Lee, D. H. and Goldberg, A. L. (1996). Selective inhibitors of the proteasome-dependent and vacuolar pathways of protein degradation in *Saccharomyces cerevisiae.* *J Biol Chem* 271, 27280-4.

Levine, B. and Klionsky, D. J. (2004). Development by self-digestion: molecular mechanisms and biological functions of autophagy. *Dev Cell* 6, 463-77.

Liang, X. H., Jackson, S., Seaman, M., Brown, K., Kempkes, B., Hibshoosh, H. and Levine, B. (1999). Induction of autophagy and inhibition of tumorigenesis by beclin 1. *Nature* 402, 672-6.

Lopez-Boado, Y. S., Herrero, P., Fernandez, T., Fernandez, R. and Moreno, F. (1988). Glucose-stimulated phosphorylation of yeast isocitrate lyase in vivo. *J Gen Microbiol* 134, 2499-505.

Lowry, O. H., Rosenbrough, N. J., Farr, A. L. and Randall, R. J. (1951). Protein measurement with the Folin phenol reagent. *J Biol Chem* 193: 265-75.

Madzak, C., Gaillardin, C. and Beckerich, J. M. (2004). Heterologous protein expression and secretion in the non-conventional yeast *Yarrowia lipolytica*: a review. *J Biotechnol* 109, 63-81.

Majeski, A. E. and Dice, J. F. (2004). Mechanisms of chaperone-mediated autophagy. *Int J Biochem Cell Biol* 36, 2435-44.

Marino, G. and Lopez-Otin, C. (2004). Autophagy: molecular mechanisms, physiological functions and relevance in human pathology. *Cell Mol Life Sci* 61, 1439-54.

Marzella, L., Ahlberg, J. and Glaumann, H. (1981). Autophagy, heterophagy, microautophagy and crinophagy as the means for intracellular degradation. *Virchows Arch B Cell Pathol Incl Mol Pathol* 36, 219-34.

Matsuura, A., Tsukada, M., Wada, Y. and Ohsumi, Y. (1997). Apg1p, a novel protein kinase required for the autophagic process in *Saccharomyces cerevisiae*. *Gene* 192, 245-50.

Mauersberger, S., Wang, H. J., Gaillardin, C., Barth, G. and Nicaud, J. M. (2001). Insertional mutagenesis in the n-alkane-assimilating yeast *Yarrowia lipolytica*: generation of tagged mutations in genes involved in hydrophobic substrate utilization. *J Bacteriol* 183, 5102-9.

Meiling-Wesse, K., Barth, H., Voss, C., Eskelinen, E. L., Epple, U. D. and Thumm, M. (2004). Atg21 is required for effective recruitment of Atg8 to the preautophagosomal structure during the Cvt pathway. *J Biol Chem* 279, 37741-50.

Melendez, A., Talloczy, Z., Seaman, M., Eskelinen, E. L., Hall, D. H. and Levine, B. (2003). Autophagy genes are essential for dauer development and life-span extension in *C. elegans*. *Science* 301, 1387-91.

Michels, P. A., Moyersoen, J., Krazy, H., Galland, N., Herman, M. and Hannaert, V. (2005). Peroxisomes, glyoxysomes and glycosomes (review). *Mol Membr Biol* 22, 133-45.

Mizushima, N., Ohsumi, Y. and Yoshimori, T. (2002). Autophagosome formation in mammalian cells. *Cell Struct Funct* 27, 421-9.

Mizushima, N., Yamamoto, A., Hatano, M., Kobayashi, Y., Kabeya, Y., Suzuki, K., Tokuhisa, T., Ohsumi, Y. and Yoshimori, T. (2001). Dissection of autophagosome formation using Apg5-deficient mouse embryonic stem cells. *J Cell Biol* 152, 657-68.

Mizushima, N., Noda, T., Yoshimori, T., Tanaka, Y., Ishii, T., George, M. D., Klionsky, D. J., Ohsumi, M. and Ohsumi, Y. (1998). A protein conjugation system essential for autophagy. *Nature* 395, 395-8.

Mlickova, K., Roux, E., Athenstaedt, K., d'Andrea, S., Daum, G., Chardot, T. and Nicaud, J. M. (2004). Lipid accumulation, lipid body formation, and acyl coenzyme A oxidases of the yeast *Yarrowia lipolytica*. *Appl Environ Microbiol* 70, 3918-24.

Monastyrska, I., van der Heide, M., Krikken, A. M., Kiel, J. A., van der Klei, I. J. and Veenhuis, M. (2005). Atg8 is essential for macropexophagy in *Hansenula polymorpha*. *Traffic* 6, 66-74.

Monastyrska, I., Kiel, J. A.K.W., Krikken, A. M., Komduur, J. A., Veenhuis, M. and van der Klei, I. J. (2005a). The *Hansenula polymorpha ATG25* gene encodes a novel coiled-coil protein that is required for macropexophagy. *Autophagy* 1:2, 92-100.

Monastryska, I., Sjollema, K., van der Klei, I. J., Kiel, J. A. and Veenhuis, M. (2004). Microautophagy and macropexophagy may occur simultaneously in *Hansenula polymorpha*. *FEBS Lett* 568, 135-8.

Monosov, E. Z., Wenzel, T. J., Luers, G. H., Heyman, J. A. and Subramani, S. (1996). Labeling of peroxisomes with green fluorescent protein in living *P. pastoris* cells. *J Histochem Cytochem* 44, 581-9.

Mortimore, G. E., Poso, A. R. and Lardeux, B. R. (1989). Mechanism and regulation of protein degradation in liver. *Diabetes Metab Rev* 5, 49-70.

Mount, R. C., Jordan, B. E. and Hadfield, C. (1996). Reporter gene systems for assaying gene expression in yeast. *Methods Mol Biol* 53, 239-48.

Mukaiyama, H., Baba, M., Osumi, M., Aoyagi, S., Kato, N., Ohsumi, Y. and Sakai, Y. (2004). Modification of a ubiquitin-like protein Paz2 conducted micropexophagy through formation of a novel membrane structure. *Mol Biol Cell* 15, 58-70.

Mukaiyama, H., Oku, M., Baba, M., Samizo, T., Hammond, A. T., Glick, B. S., Kato, N. and Sakai, Y. (2002). *Paz2* and 13 other *PAZ* gene products regulate vacuolar engulfment of peroxisomes during micropexophagy. *Genes Cells* 7, 75-90.

Muller, O., Sattler, T., Flotenmeyer, M., Schwarz, H., Plattner, H. and Mayer, A. (2000). Autophagic tubes: Vacuolar invaginations involved in lateral membrane sorting and inverse vesicle budding. *J Cell Biol* 151, 519-528.

Muller, W. H., Bovenberg, R. A., Groothuis, M. H., Kattevilder, F., Smaal, E. B., Van der Voort, L. H. and Verkleij, A. J. (1992). Involvement of microbodies in penicillin biosynthesis. *Biochim Biophys Acta* 1116, 210-3.

Naumova, E., Naumov, G., Fournier, P., Nguyen, H. V. and Gaillardin, C. (1993). Chromosomal polymorphism of the yeast *Yarrowia lipolytica* and related species: electrophoretic karyotyping and hybridization with cloned genes. *Curr Genet* 23, 450-4.

Nazarko, T. Y., Nicaud, J. M. and Sibirny, A. A. (2005). Observation of the *Yarrowia lipolytica* peroxisome-vacuole dynamics by fluorescence microscopy with a single filter set. *Cell Biol Int* 29, 65-70.

Nazarko, T. Y., Huang, J., Nicaud, J.-M., Klionsky, D. J. and Sibirny, A. A. (2005a) Trs85 is required for macroautophagy, pexophagy and cytoplasm to vacuole targeting in *Yarrowia lipolytica* and *Saccharomyces cerevisiae*. *Autophagy* 1:1, 37-34.

Nazarko, T. Y., Mala, M. J. and Sibirny, A. A. (2002) Development of the plate assay screening procedure for isolation of the mutants deficient in inactivation of peroxisomal enzymes in the yeast *Yarrowia lipolytica*. *Biopolymers and Cell* (Ukr.) 18, 135-38.

Neer, E. J., Schmidt, C. J., Nambudripad, R. and Smith, T. F. (1994). The ancient regulatory-protein family of WD-repeat proteins. *Nature* 371, 297-300.

Neuveglise, C., Chalvet, F., Wincker, P., Gaillardin, C. and Casaregola, S. (2005). Mutator-like element in the yeast *Yarrowia lipolytica* displays multiple alternative splicings. *Eukaryot Cell* 4, 615-24.

Nicaud, J. M., Madzak, C., van den Broek, P., Gysler, C., Duboc, P., Niederberger, P. and Gaillardin, C. (2002). Protein expression and secretion in the yeast *Yarrowia lipolytica*. *FEMS Yeast Res* 2, 371-9.

Nicaud, J. M., Fabre, E. and Gaillardin, C. (1989). Expression of invertase activity in *Yarrowia lipolytica* and its use as a selective marker. *Curr Genet* 16, 253-60.

Noda, T., Suzuki, K. and Ohsumi, Y. (2002). Yeast autophagosomes: de novo formation of a membrane structure. *Trends Cell Biol* 12, 231-5.

Noda, T., Kim, J., Huang, W. P., Baba, M., Tokunaga, C., Ohsumi, Y. and Klionsky, D. J. (2000). Apg9p/Cvt7p is an integral membrane protein required for transport vesicle formation in the Cvt and autophagy pathways. *J Cell Biol* 148, 465-80.

Noda, T. and Ohsumi, Y. (1998). Tor, a phosphatidylinositol kinase homologue, controls autophagy in yeast. *J Biol Chem* 273, 3963-6.

Nuttley W., Brade, A., Gaillardin, C., Eitzen, G., Glover, J., Aitchison, J and Rachubinski, R. (1993). Rapid identification and characterization of peroxisomal assembly mutants in *Yarrowia lipolytica*. *Yeast* 9, 507-17.

Ogier-Denis, E. and Codogno, P. (2003). Autophagy: a barrier or an adaptive response to cancer. *Biochim Biophys Acta* 1603, 113-28.

Ohsumi, Y. (2001). Molecular dissection of autophagy: two ubiquitin-like systems. *Nat Rev Mol Cell Biol* **2,** 211-6.

Ohsumi, Y. (1999). Molecular mechanism of autophagy in yeast, *Saccharomyces cerevisiae*. *Philos Trans R Soc Lond B Biol Sci* 354, 1577-80; discussion 1580-1.

Oku, M., Warnecke, D., Noda, T., Muller, F., Heinz, E., Mukaiyama, H., Kato, N. and Sakai, Y. (2003). Peroxisome degradation requires catalytically active sterol glucosyltransferase with a GRAM domain. *Embo J* 22, 3231-41.

Park, C. S., Chang, C. C., Kim, J. Y., Ogrydziak, D. M. and Ryu, D. D. (1997). Expression, secretion, and processing of rice alpha-amylase in the yeast *Yarrowia lipolytica*. *J Biol Chem* 272, 6876-81.

Parsons, M., Furuya, T., Pal, S. and Kessler, P. (2001). Biogenesis and function of peroxisomes and glycosomes. *Mol Biochem Parasitol* 115, 19-28.

Perez-Campo, F. M. and Dominguez, A. (2001). Factors affecting the morphogenetic switch in *Yarrowia lipolytica*. *Curr Microbiol* **43,** 429-33.

Petriv, O., Tang, L., Titorenko, V. and Rachubinski, R. (2004). A new definition for the consensus sequence of the peroxisome targeting signal type 2. *J Mol Biol* 341, 119-134.

Proikas-Cezanne, T., Waddell, S., Gaugel, A., Frickey, T., Lupas, A. and Nordheim, A. (2004). WIPI-1alpha (WIPI49), a member of the novel 7-bladed WIPI protein family, is aberrantly expressed in human cancer and is linked to starvation-induced autophagy. *Oncogene* 23, 9314-25.

Purdue, P. E. and Lazarow, P. B. (2001). Peroxisome biogenesis. *Annu Rev Cell Dev Biol* 17, 701-52.

Rachubinski, R. A. and Subramani, S. (1995). How proteins penetrate peroxisomes. *Cell* 83, 525-8.

Raught, B., Gingras, A. C. and Sonenberg, N. (2001). The target of rapamycin (TOR) proteins. *Proc Natl Acad Sci U S A* 98, 7037-44.

Reggiori, F. and Klionsky, D. J. (2002). Autophagy in the eukaryotic cell. *Eukaryot Cell* 1, 11-21.

Reggiori, F., Monastyrska, I., Shintani, T. and Klionsky, D. J. (2005). The actin cytoskeleton is required for selective types of autophagy, but not nonspecific autophagy, in the yeast *Saccharomyces cerevisiae*. *Mol Biol Cell* 16, 5843-56.

Roussou I., Thireous G. and Hauge, B. (1988). Transcriptional-translational regulatory circuit in *Saccharomyce cerevisia* which involves the GCN4 transcriptional activator and the GCN2 protein kinase. *Mol Cell Biol* 8, *2132-9.*

Sakai, Y., Koller, A., Rangell, L. K., Keller, G. A. and Subramani, S. (1998). Peroxisome degradation by microautophagy in Pichia pastoris: identification of specific steps and morphological intermediates. *J Cell Biol* 141, 625-36.

Sato, T. K., Rehling, P., Peterson, M. R. and Emr, S. D. (2000). Class C Vps protein complex regulates vacuolar SNARE pairing and is required for vesicle docking/fusion. *Mol Cell* 6, 661-71.

Schmelzle, T. and Hall, M. N. (2000). TOR, a central controller of cell growth. *Cell* 103, 253-62.

Schmid-Berger, N., Schmid, B. and Barth, G. (1994). Ylt1, a highly repetitive retrotransposon in the genome of the dimorphic fungus *Yarrowia lipolytica*. *J Bacteriol* 176, 2477-82.

Schrader, M., Thiemann, M. and Fahimi, H. D. (2003). Peroxisomal motility and interaction with microtubules. *Microsc Res Tech* 61, 171-8.

Schu, P. V., Takegawa, K., Fry, M. J., Stack, J. H., Waterfield, M. D. and Emr, S. D. (1993). Phosphatidylinositol 3-kinase encoded by yeast *VPS34* gene essential for protein sorting. *Science* 260, 88-91.

Scott, S. V., Guan, J., Hutchins, M. U., Kim, J. and Klionsky, D. J. (2001). Cvt19 is a receptor for the cytoplasm-to-vacuole targeting pathway. *Mol Cell* 7, 1131-41.

Scott, S. V., Nice, D. C., 3rd, Nau, J. J., Weisman, L. S., Kamada, Y., Keizer-Gunnink, I., Funakoshi, T., Veenhuis, M., Ohsumi, Y. and Klionsky, D. J. (2000). Apg13p and Vac8p are part of a complex of phosphoproteins that are required for cytoplasm to vacuole targeting. *J Biol Chem* 275, 25840-9.

Scott, S. V. and Klionsky, D. J. (1998). Delivery of proteins and organelles to the vacuole from the cytoplasm. *Curr Opin Cell Biol* 10, 523-9.

Scott, S. V., Hefner-Gravink, A., Morano, K. A., Noda, T., Ohsumi, Y. and Klionsky, D. J. (1996). Cytoplasm-to-vacuole targeting and autophagy employ the same machinery to deliver proteins to the yeast vacuole. *Proc Natl Acad Sci U S A* 93, 12304-8.

Seaman, M. N., Marcusson, E. G., Cereghino, J. L. and Emr, S. D. (1997). Endosome to Golgi retrieval of the vacuolar protein sorting receptor, Vps10p, requires the function of the VPS29, VPS30, and VPS35 gene products. *J Cell Biol* 137, 79-92.

Sekar, M. C. and Roufogalis, B. D. (1984). Differential effects of phenylmethanesulfonyl fluoride (PMSF) on carbachol and potassium stimulated phosphoinositide turnover and contraction in longitudinal smooth muscle of guinea pig ileum. *Cell Calcium* 5, 191-203.

Shimozawa, N., Nagase, T., Takemoto, Y., Funato, M., Kondo, N. and Suzuki, Y. (2005). Molecular and neurologic findings of peroxisome biogenesis disorders. *J Child Neurol* 20, 326-9.

Shintani, T. and Klionsky, D. J. (2004). Autophagy in health and disease: a double-edged sword. *Science* 306, 990-5.

Shintani, T. and Klionsky, D. J. (2004a). Cargo proteins facilitate the formation of transport vesicles in the cytoplasm to vacuole targeting pathway. *J Biol Chem* 279, 29889-94.

Shintani, T., Huang, W. P., Stromhaug, P. E. and Klionsky, D. J. (2002). Mechanism of cargo selection in the cytoplasm to vacuole targeting pathway. *Dev Cell* 3, 825-37.

Shintani, T., Mizushima, N., Ogawa, Y., Matsuura, A., Noda, T. and Ohsumi, Y. (1999). Apg10p, a novel protein-conjugating enzyme essential for autophagy in yeast. *Embo J* 18, 5234-41.

Skau, K. A. and Shipley, M. T. (1999). Phenylmethylsulfonyl fluoride inhibitory effects on acetylcholinesterase of brain and muscle. *Neuropharmacology* 38, 691-8.

Stack, J. H., Herman, P. K., Schu, P. V. and Emr, S. D. (1993). A membrane-associated complex containing the Vps15 protein kinase and the Vps34 PI 3-kinase is essential for protein sorting to the yeast lysosome-like vacuole. *Embo J* 12, 2195-204.

Stasyk, O. V., Stasyk, O. G., Mathewson, R. D., Farre, J.-C., Nazarko, V. Y., Krasovska, O. S., Subramani, S., Cregg, J. M and Sibirny, A. A. (2006). Atg28, a novel coulde-coil protein involved in autophagic degradation of peroxisomes in the methylotrophic yeast *Pichia pastoris*. *Autophagy* 2:1, 30-8.

Stasyk, O. V., van der Klei, I. J., Bellu, A. R., Shen, S., Kiel, J. A., Cregg, J. M. and Veenhuis, M. (1999). A *Pichia pastoris VPS15* homologue is required in selective peroxisome autophagy. *Curr Genet* 36, 262-9.

Straub, M., Bredschneider, M. and Thumm, M. (1997). *AUT3*, a serine/threonine kinase gene, is essential for autophagocytosis in *Saccharomyces cerevisiae*. *J Bacteriol* 179, 3875-83.

Strausberg R., Feingold E., Grouse E., Derge J. et al. (2002). Generation and initial analysis of more than 15,000 full-length human and mouse cDNA sequences. *Proc. Natl. Acad. Sci.*99, 16899-

Stromhaug, P. E., Reggiori, F., Guan, J., Wang, C. W. and Klionsky, D. J. (2004). Atg21 is a phosphoinositide binding protein required for efficient lipidation and localization of Atg8 during uptake of aminopeptidase I by selective autophagy. *Mol Biol Cell* 15, 3553-66.

Stromhaug, P. E. and Klionsky, D. J. (2001). Approaching the molecular mechanism of autophagy. *Traffic* 2, 524-31.

Stromhaug, P. E., Bevan, A. and Dunn, W. A., Jr. (2001a). GSA11 encodes a unique 208-kDa protein required for pexophagy and autophagy in *Pichia pastoris*. *J Biol Chem* 276, 42422-35.

Subramani, S. (2001). Self-destruction in the line of duty. *Dev Cell* 1, 6-8.

Subramani, S., Koller, A. and Snyder, W. B. (2000). Import of peroxisomal matrix and membrane proteins. *Annu Rev Biochem* 69, 399-418.

Subramani, S. (1998). Components involved in peroxisome import, biogenesis, proliferation, turnover, and movement. *Physiol Rev* 78, 171-88.

Subramani, S. (1996). Protein translocation into peroxisomes. *J Biol Chem* 271, 32483-6.

Sumita, T., Iida, T., Hirata, A., Horiuchi, H., Takagi, M. and Ohta, A. (2002). Peroxisome deficiency represses the expression of n-alkane-inducible *YlALK1* encoding cytochrome P450ALK1 in *Yarrowia lipolytica*. *FEMS Microbiol Lett* 214, 31-8.

Suzuki, K., Kirisako, T., Kamada, Y., Mizushima, N., Noda, T. and Ohsumi, Y. (2001). The pre-autophagosomal structure organized by concerted functions of *APG* genes is essential for autophagosome formation. *Embo J* 20, 5971-81.

Tabak, H. F., Murk, J. L., Braakman, I. and Geuze, H. J. (2003). Peroxisomes start their life in the endoplasmic reticulum. *Traffic* 4, 512-8.

Takacs-Vellai, K., Vellai, T., Puoti, A., Passannante, M., Wicky, C., Streit, A., Kovacs, A. L. and Muller, F. (2005). Inactivation of the autophagy gene bec-1 triggers apoptotic cell death in *C. elegans*. *Curr Biol* 15, 1513-7.

Takeshige, K., Baba, M., Tsuboi, S., Noda, T. and Ohsumi, Y. (1992). Autophagy in yeast demonstrated with proteinase-deficient mutants and conditions for its induction. *J Cell Biol* 119, 301-11.

Talloczy, Z., Jiang, W., Virgin, H. W. t., Leib, D. A., Scheuner, D., Kaufman, R. J., Eskelinen, E. L. and Levine, B. (2002). Regulation of starvation- and virus-induced autophagy by the eIF2alpha kinase signaling pathway. *Proc Natl Acad Sci U S A* 99, 190-5.

Thumm, M., Egner, R., Koch, B., Schlumpberger, M., Straub, M., Veenhuis, M. and Wolf, D. H. (1994). Isolation of autophagocytosis mutants of Saccharomyces cerevisiae. *FEBS Lett* 349, 275-80.

Tettelin H., Agostoni C., Carbone M., Albermann K. et al. (1997). The nucleotide sequence of *Saccharomyces cerevisiae* chromosome VII. *Nature* 387, 81-4.

Titorenko, V. I. and Rachubinski, R. A. (2001). Dynamics of peroxisome assembly and function. *Trends Cell Biol* 11, 22-29.

Titorenko, V. I. and Rachubinski, R. A. (2001a). The life cycle of the peroxisome. *Nat Rev Mol Cell Biol* 2, 357-68.

Titorenko, V. I., Chan, H. and Rachubinski, R. A. (2000). Fusion of small peroxisomal vesicles in vitro reconstructs an early step in the *in vivo* multistep peroxisome assembly pathway of *Yarrowia lipolytica*. *J Cell Biol* 148, 29-44.

Titorenko, V. I. and Rachubinski, R. A. (2000a). Peroxisomal membrane fusion requires two AAA family ATPases, Pex1p and Pex6p. *J Cell Biol* 150, 881-6.

Titorenko, V. I., Smith, J. J., Szilard, R. K. and Rachubinski, R. A. (2000b). Peroxisome biogenesis in the yeast *Yarrowia lipolytica*. *Cell Biochem Biophys* 32 Spring, 21-6.

Titorenko, V. I. and Rachubinski, R. A. (1998). The endoplasmic reticulum plays an essential role in peroxisome biogenesis. *Trends Biochem Sci* 23, 231-3.

Titorenko, V. I., Keizer, I., Harder, W. and Veenhuis, M. (1995). Isolation and characterization of mutants impaired in the selective degradation of peroxisomes in the yeast *Hansenula polymorpha*. *J Bacteriol* 177, 357-63.

Tomoda, T., Bhatt, R. S., Kuroyanagi, H., Shirasawa, T. and Hatten, M. E. (1999). A mouse serine/threonine kinase homologous to *C. elegans UNC51* functions in parallel fiber formation of cerebella granule neurons. *Neuron* 24, 833-46.

Treton, B., Le Dall, M. and Heslot, H. (1985). Virus-like particles from the yeast *Yarrowia lipolytica*. *Current Genetics* 9, 279-284.

Tsukada, M. and Ohsumi, Y. (1993). Isolation and characterization of autophagy-defective mutants of *Saccharomyces cerevisiae*. *FEBS Lett* 333, 169-74.

Tucker, K. A., Reggiori, F., Dunn, W. A., Jr. and Klionsky, D. J. (2003). Atg23 is essential for the cytoplasm to vacuole targeting pathway and efficient autophagy but not pexophagy. *J Biol Chem* **278,** 48445-52.

Tuttle, D. L. and Dunn, W. A., Jr. (1995). Divergent modes of autophagy in the methylotrophic yeast *Pichia pastoris*. *J Cell Sci* 108, 25-35.

Tuttle, D. L., Lewin, A. S. and Dunn, W. A., Jr. (1993). Selective autophagy of peroxisomes in methylotrophic yeasts. *Eur J Cell Biol* 60, 283-90.

van den Bosch, H., Schutgens, R. B., Wanders, R. J. and Tager, J. M. (1992). Biochemistry of peroxisomes. *Annu Rev Biochem* 61, 157-97.

van den Hazel, H., B., Kielland-Brandt, M. C. and Winther, J. R. (1995) Biosynthesis and function of yeast vacuolar proteases. *Yeast* 12, 1-6.

van der Klei, I. J., Harder, W. and Veenhuis, M. (1991). Biosynthesis and assembly of alcohol oxidase, a peroxisomal matrix protein in methylotrophic yeasts: a review. *Yeast* 7, 195-209.

van der Klei, I. J., Harder, W. and Veenhuis, M. (1991a). Selective inactivation of alcohol oxidase in two peroxisome-deficient mutants of the yeast *Hansenula polymorpha*. *Yeast* 7, 813-21.

van der Klei, I. J. and Veenhuis, M. (1996). Peroxisome biogenesis in the yeast *Hansenula polymorpha*: a structural and functional analysis. *Ann N Y Acad Sci* 804, 47-59.

van der Voorn, L. and Ploegh, H. L. (1992). The WD-40 repeat. *FEBS Lett* 307**,** 131-4.

van der Walt, J. P. and von Arx, J. A. (1980). The yeast genus *Yarrowia* gen. nov. *Antonie Van Leeuwenhoek* 46, 517-21.

Veenhuis, M., Salomons, F. A. and Van Der Klei, I. J. (2000). Peroxisome biogenesis and degradation in yeast: a structure/function analysis. *Microsc Res Tech* 51, 584-600.

Veenhuis, M., Komori, M., Salomons, F., Hilbrands, R. E., Hut, H., Baerends, R. J., Kiel, J. A. and van der Klei, I. J. (1996). Peroxisomal remnants in peroxisome-deficient mutants of the yeast *Hansenula polymorpha*. *FEBS Lett* 383, 114-8.

Veenhuis, M., Douma, A., Harder, W. and Osumi, M. (1983). Degradation and turnover of peroxisomes in the yeast *Hansenula polymorpha* induced by selective inactivation of peroxisomal enzymes. *Arch Microbiol* 134, 193-203.

Veenhuis, M. and Harder, W. (1988). Microbodies in yeasts: structure, function and biogenesis. *Microbiol Sci* 5, 347-51.

Vernis, L., Poljak, L., Chasles, M., Uchida, K., Casaregola, S., Kas, E., Matsuoka, M., Gaillardin, C. and Fournier, P. (2001). Only centromeres can supply the partition system required for *ARS* function in the yeast *Yarrowia lipolytica*. *J Mol Biol* 305, 203-17.

Vida, T. A. and Emr, S. D. (1995). A new vital stain for visualizing vacuolar membrane dynamics and endocytosis in yeast. *J Cell Biol* 128, 779-92.

Wache, Y., Aguedo, M., Nicaud, J. M. and Belin, J. M. (2003). Catabolism of hydroxyacids and biotechnological production of lactones by *Yarrowia lipolytica*. *Appl Microbiol Biotechnol* 61, 393-404.

Wache, Y., Aguedo, M., Choquet, A., Gatfield, I. L., Nicaud, J. M. and Belin, J. M. (2001). Role of beta-oxidation enzymes in gamma-decalactone production by the yeast *Yarrowia lipolytica*. *Appl Environ Microbiol* 67, 5700-4.

Wanders, R. J. and Waterham, H. R. (2005). Peroxisomal disorders I: biochemistry and genetics of peroxisome biogenesis disorders. *Clin Genet* 67, 107-33.

Wang, Y. X., Catlett, N. L. and Weisman, L. S. (1998). Vac8p, a vacuolar protein with armadillo repeats, functions in both vacuole inheritance and protein targeting from the cytoplasm to vacuole. *J Cell Biol* 140, 1063-74.

Waterham, H. R., Russell, K. A., Vries, Y. and Cregg, J. M. (1997). Peroxisomal targeting, import, and assembly of alcohol oxidase in *Pichia pastoris*. *J Cell Biol* 139, 1419-31.

Weber, H. and Kurischko, C. (1989). Sexual behaviour in the alkane-utilizing yeast Yarrowia lipolytica. *Yeast* 5 Spec No, S279-85.

Werten M. and de Wolf F. (2005). Reduced proteolysis of secreted gelatin and Yps-1 mediated alpha-factor leader processing in a *Pichia pastoris kex2* disruptant. *Appl Environ Microbiol* 71, 2310-7.

Wolff, A. M., Din, N. and Petersen, J. G. (1996). Vacuolar and extracellular maturation of *Saccharomyces cerevisiae* proteinase A. *Yeast* 12, 823-32.

Woolford, C. A., Daniels, L. B., Park, F. J., Jones, E. W., Van Arsdell, J. N. and Innis, M. A. (1986). The *PEP4* gene encodes an aspartyl protease implicated in the posttranslational regulation of *Saccharomyces cerevisiae* vacuolar hydrolases. *Mol Cell Biol* 6, 2500-10.

Wurmser, A. E., Sato, T. K. and Emr, S. D. (2000). New component of the vacuolar class C-Vps complex couples nucleotide exchange on the Ypt7 GTPase to SNARE-dependent docking and fusion. *J Cell Biol* 151, 551-62.

Yamagami, S., Iida, T., Nagata, Y., Ohta, A. and Takagi, M. (2001). Isolation and characterization of acetoacetyl-CoA thiolase gene essential for n-decane assimilation in yeast *Yarrowia lipolytica*. *Biochem Biophys Res Commun* 282, 832-8.

Yan J., Kuroyanagi T., Tomemore T., Okazaki N., Asato K., Matsuda Y., Suzuki Y., Ohshima Y., Mitani S., Masuho Y., Shirasawa T. and Muramatsu M. (1999). Mouse ULK2, a novel member of the UNK-51-like protein kinases. *Oncogene* 18, 5850-9.

Yorimitsu, T. and Klionsky, D. J. (2005). Atg11 links cargo to the vesicle-forming machinery in the cytoplasm to vacuole targeting pathway. *Mol Biol Cell* 16, 1593-605.

Yuan, W., Stromhaug, P. E. and Dunn, W. A., Jr. (1999). Glucose-induced autophagy of peroxisomes in *Pichia pastoris* requires a unique E1-like protein. *Mol Biol Cell* 10, 1353-66.

Yuan, W., Tuttle, D. L., Shi, Y. J., Ralph, G. S. and Dunn, W. A., Jr. (1997). Glucose-induced microautophagy in *Pichia pastoris* requires the alpha-subunit of phosphofructokinase. *J Cell Sci* 110, 1935-45.

Yue, Z., Jin, S., Yang, C., Levine, A. J. and Heintz, N. (2003). Beclin 1, an autophagy gene essential for early embryonic development, is a haploinsufficient tumor suppressor. *Proc Natl Acad Sci USA* 100, 15077-82.

7 Appendix

7.1 Plasmid maps

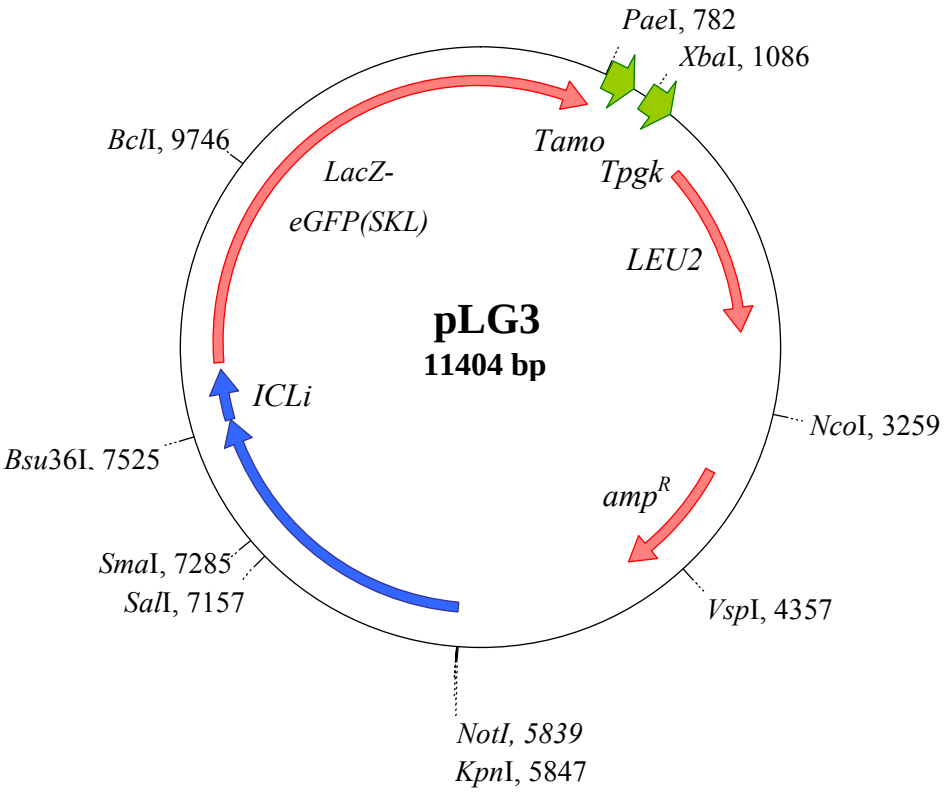

Figure 7.1 The plasmid pLG3 used for expression of the βGal-eGFP(SKL) fusion protein under the control of *YlICL1* promoter.

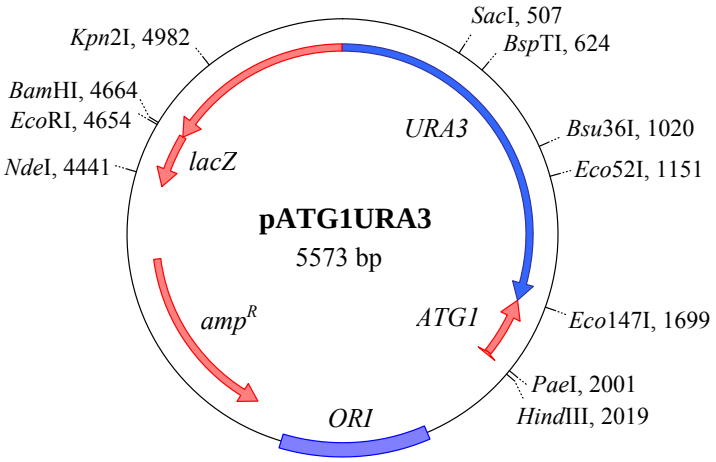

Figure 7.2 The plasmid pATG1URA3 carrying the *ATG1::URA3* cassette for disruption of the *ATG1* gene of *Y. lipolytica*.

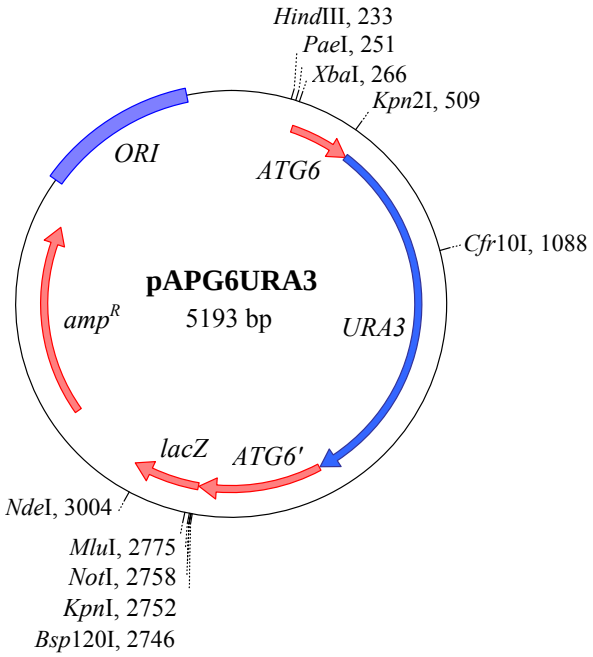

Figure 7.3 The plasmid pATG6URA3 carrying the *ATG6::URA3* cassette for disruption of the *ATG6* gene of *Y. lipolytica*.

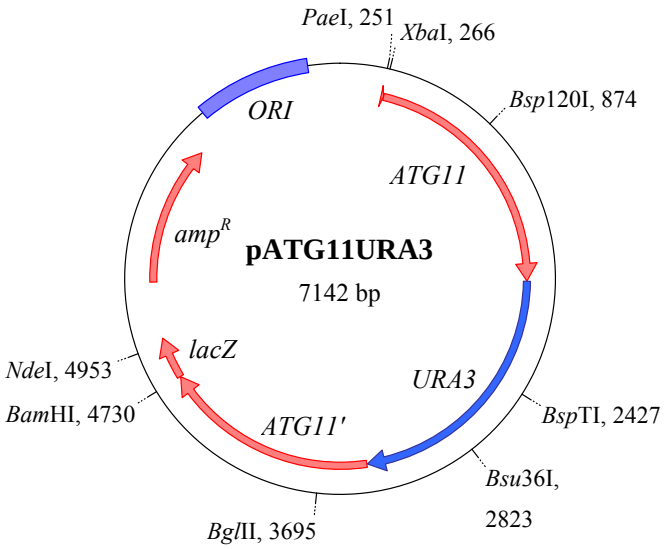

Figure 7.4 The plasmid pATG11URA3 carrying the *ATG11::URA3* cassette for disruption of the *Y. lipolytica ATG11* gene.

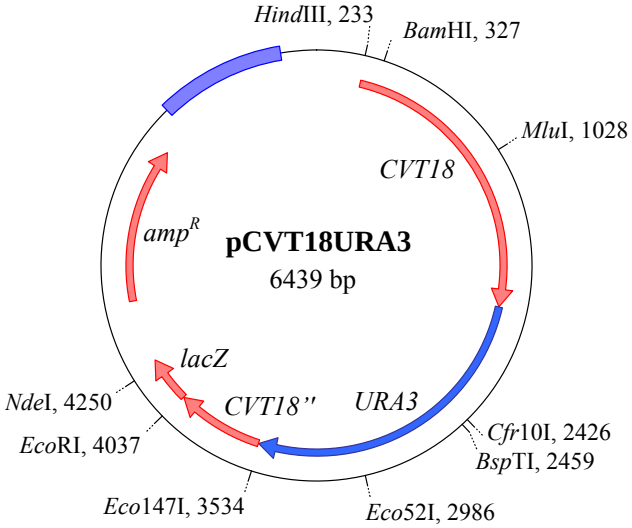

Figure 7.5 The plasmid pCVT18URA3 carrying the CVT18::URA3 cassette for disruption of the *ATG18 (alias CVT18)* gene of *Y. lipolytica*.

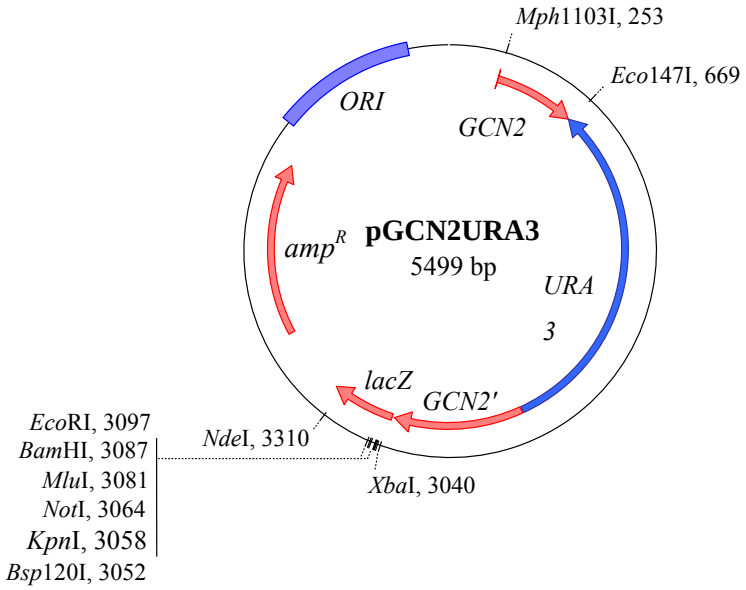

Figure 7.6 The plasmid pGCN2URA3 carrying the *GCN2::URA3* cassette for disruption of the *Y. lipolytica GCN2* gene.

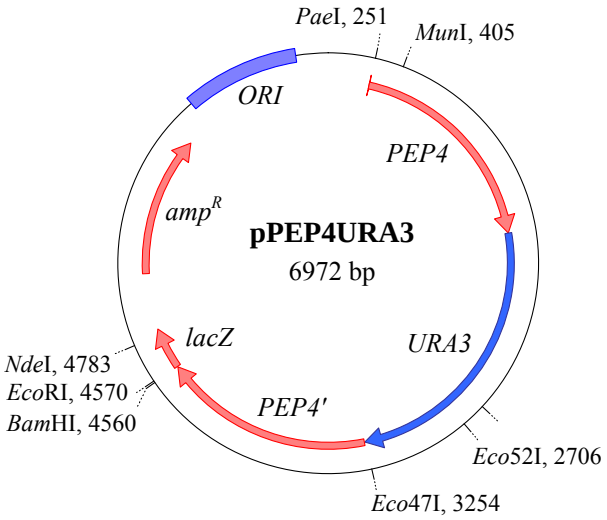

Figure 7.7 The plasmid pPEP4URA3 carrying the *PEP4::URA3* cassette for disruption of the *Y. lipolytica PEP4* gene.

7.2 Protein alignments and phylogenetic trees

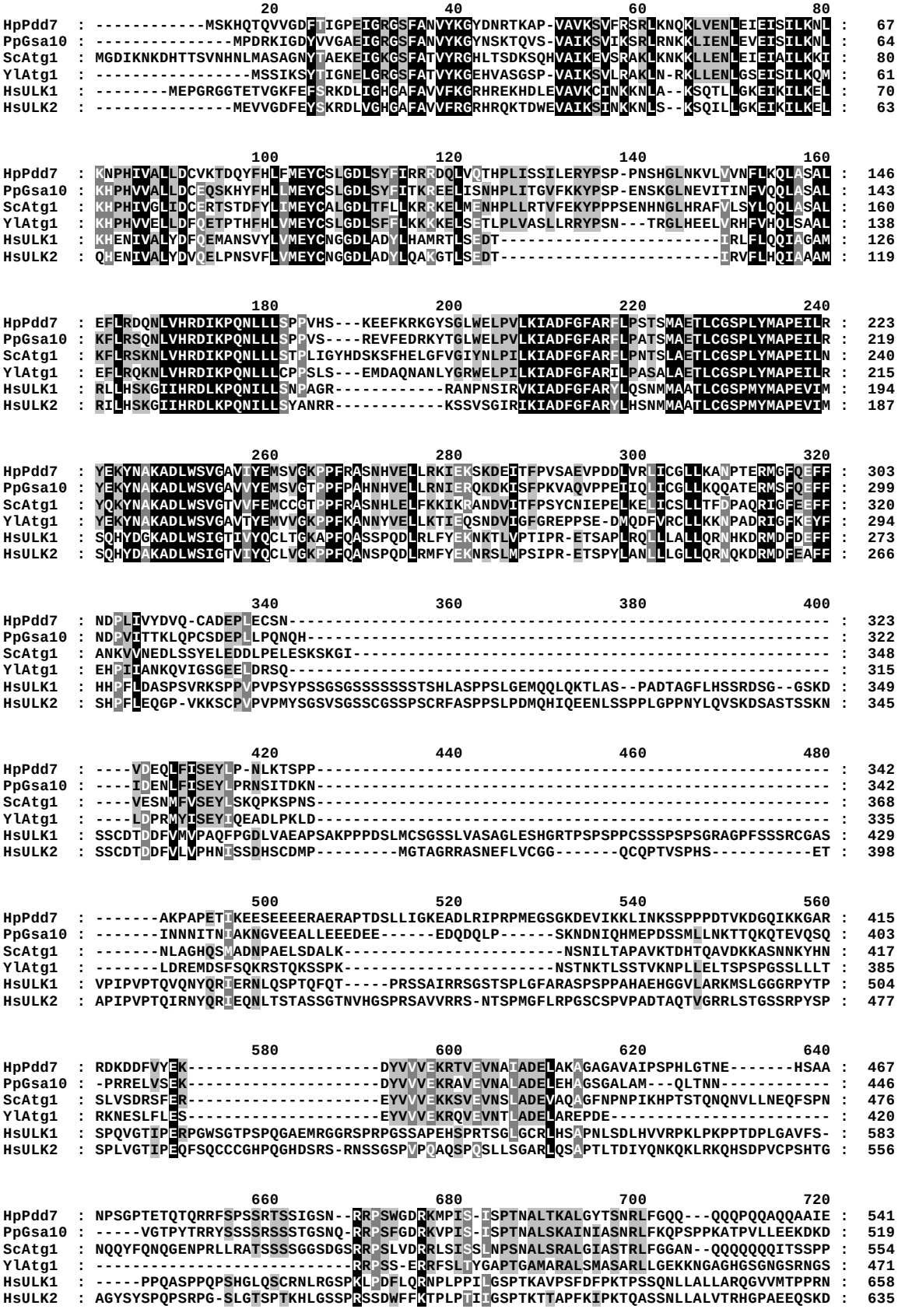

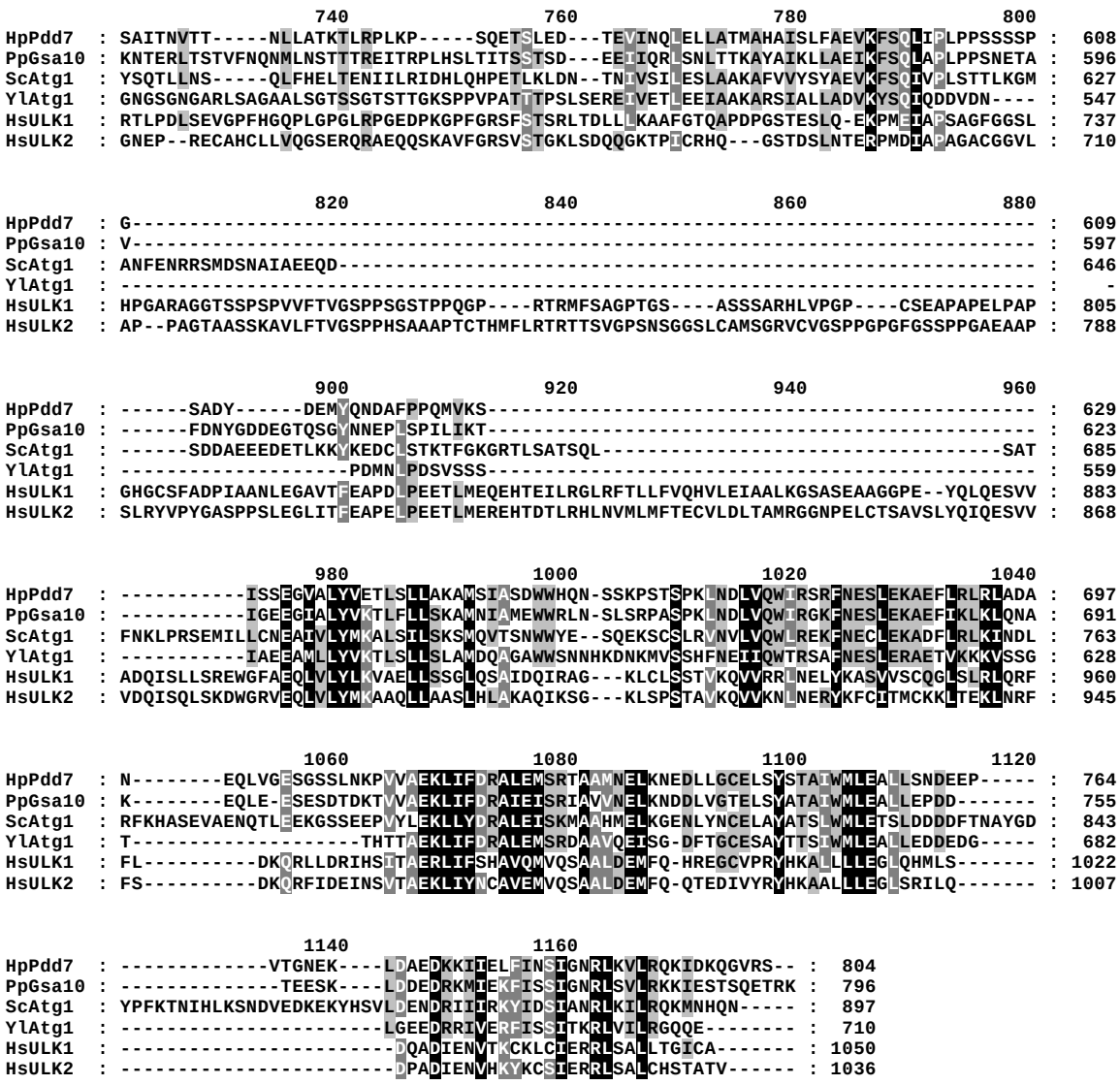

Figure 7.8 Multiple alignments of Atg1 homologs from yeasts and human. The Atg1 protein sequence from *Y. lipolytica* is aligned with amino acid sequences of the indicated proteins: *H. polymorpha* Pdd7, *P. pastoris* Gsa10, *S. cerevisiae* Atg1 and *H. sapiens* ULK1/2.

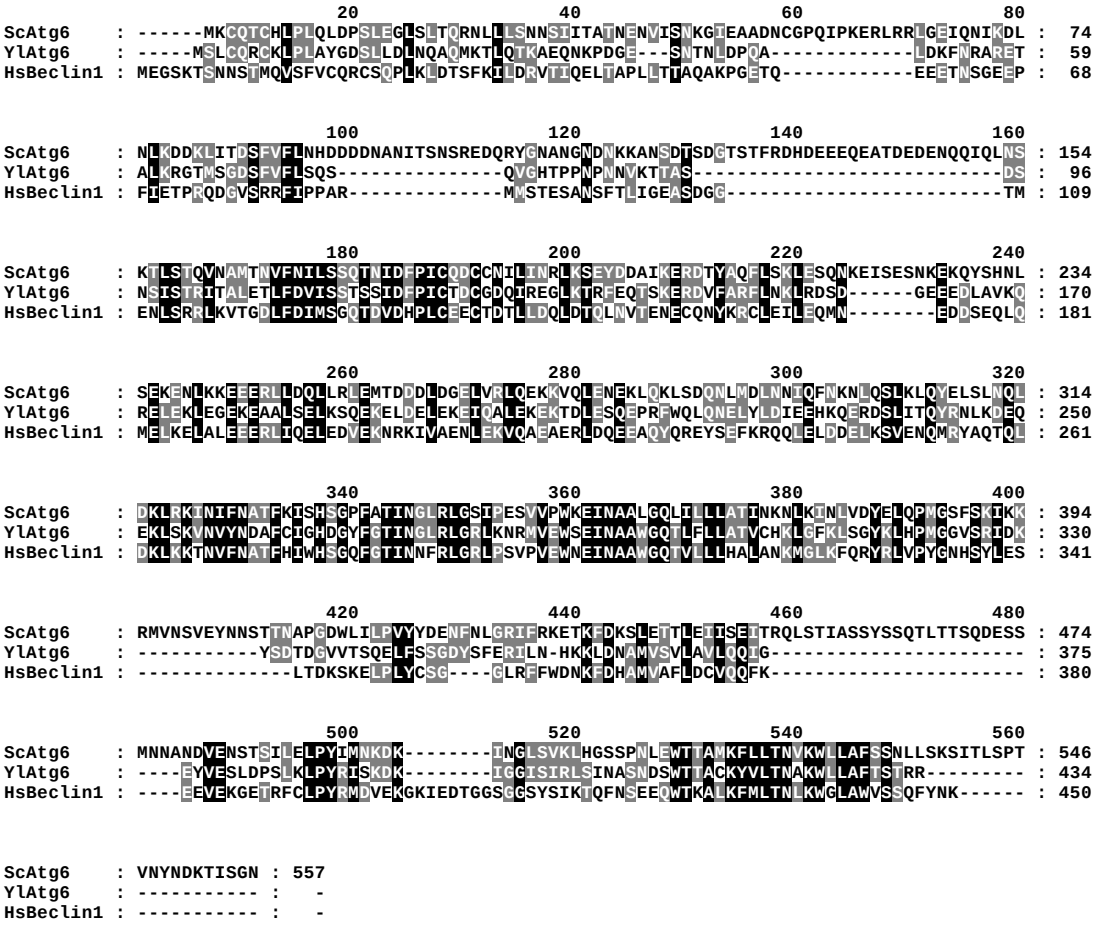

Figure 7.9 Multiple alignments of Atg6 homologs from yeasts and human. The Atg6 protein sequence from *Y. lipolytica* is aligned with amino acid sequences of the indicated proteins: *S. cerevisiae* Atg6 and *H. sapiens* beclin 1.

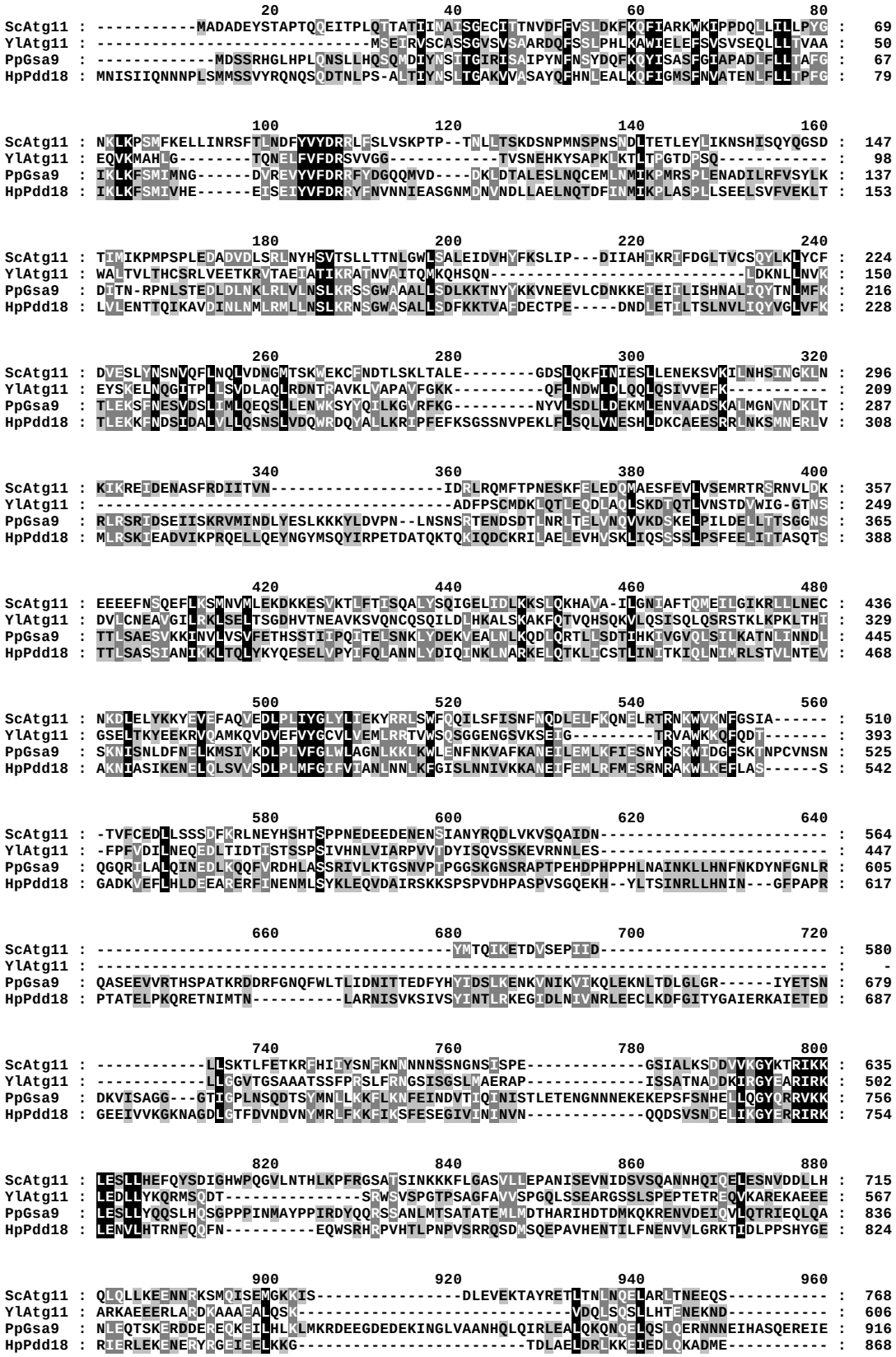

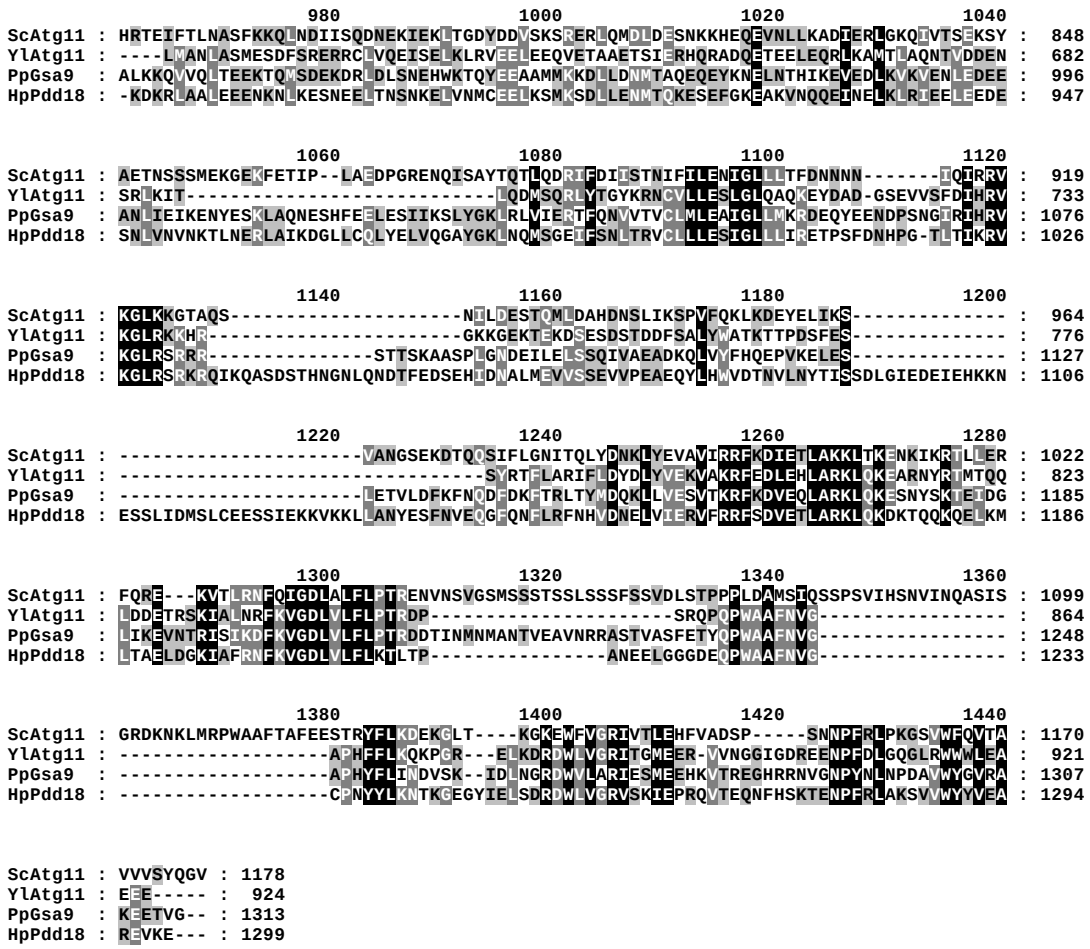

Figure 7.10 Multiple alignments of Atg11 homologs from yeasts. The Atg11 protein of *Y. lipolytica* is aligned with respective amino acid sequences of the following yeast proteins: *S. cerevisiae* Atg11, *P. pastoris* Gsa9 and *H. polymorpha* Pdd18.

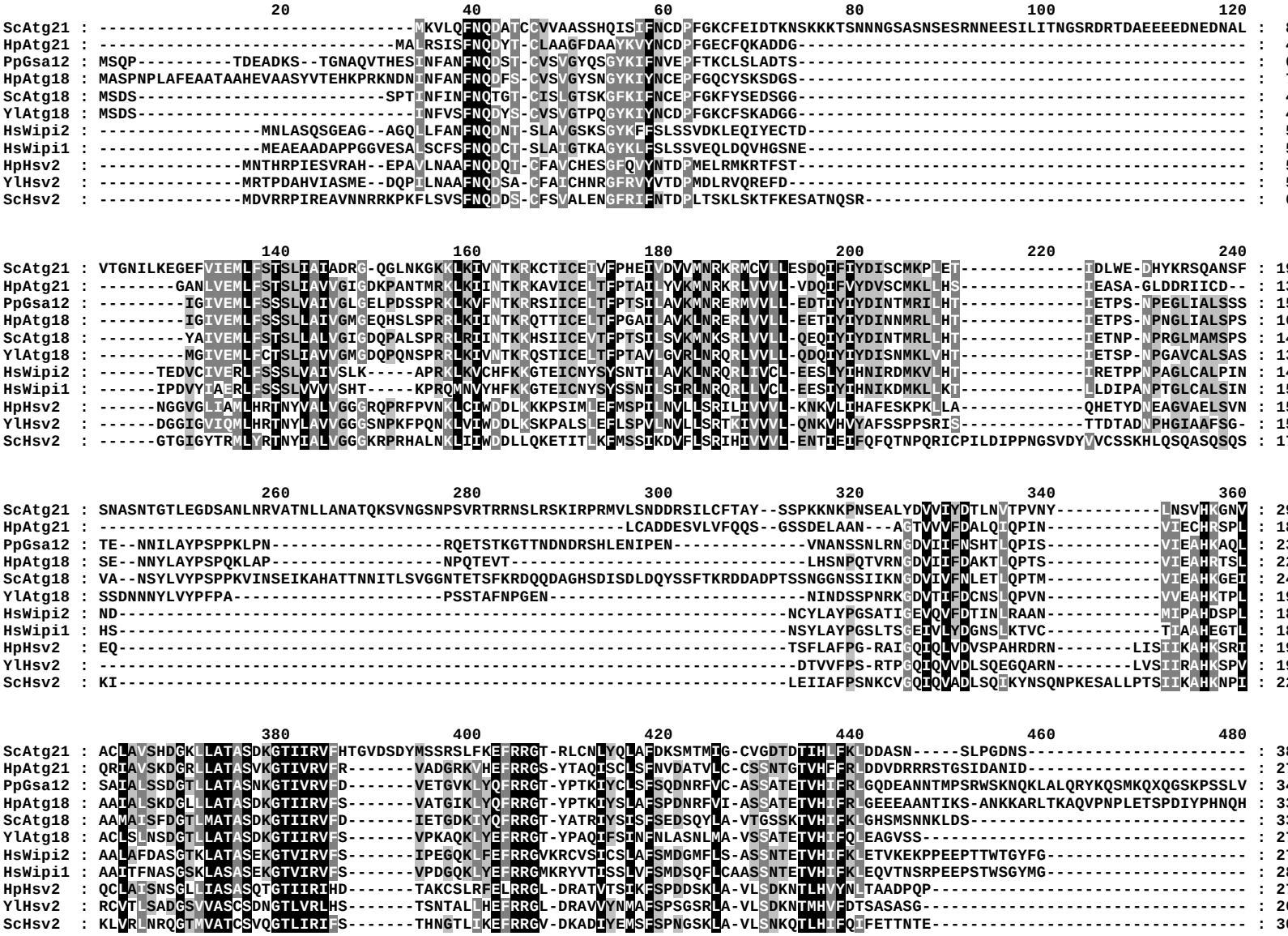
ScAtg21
HpAtg21
PpGsa12
HpAtg18
ScAtg18
YlAtg18
HsWipi2
HsWipi1
HpHsv2
YlHsv2
ScHsv2

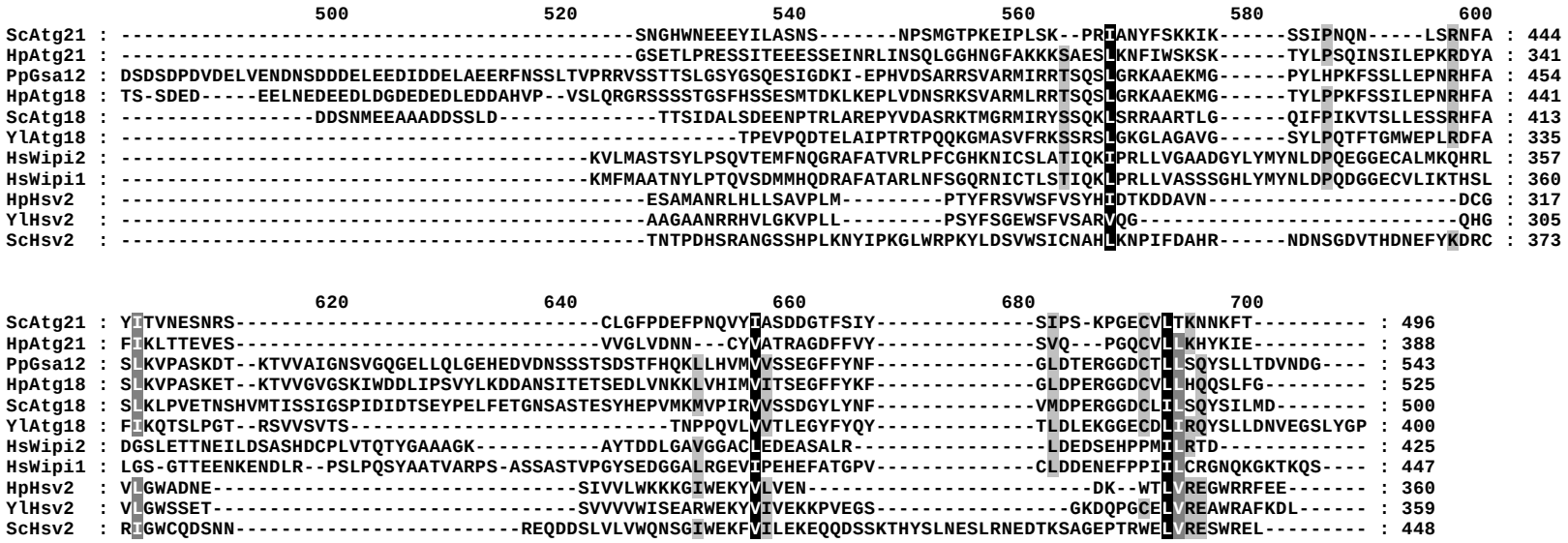

Figure 7.11 Multiple alignments of Atg18-related proteins from selected organisms. YlAtg18 protein sequence is aligned with respective amino acid sequences of the following proteins: *S. cerevisiae* Atg18, Atg21 and Hsv2; *H. polymorpha* Atg18, Atg21 and Hsv2; *P. pastoris* Gsa12; *Y. lipolytica* Hsv2p and *H. sapiens* Wipi1/2.

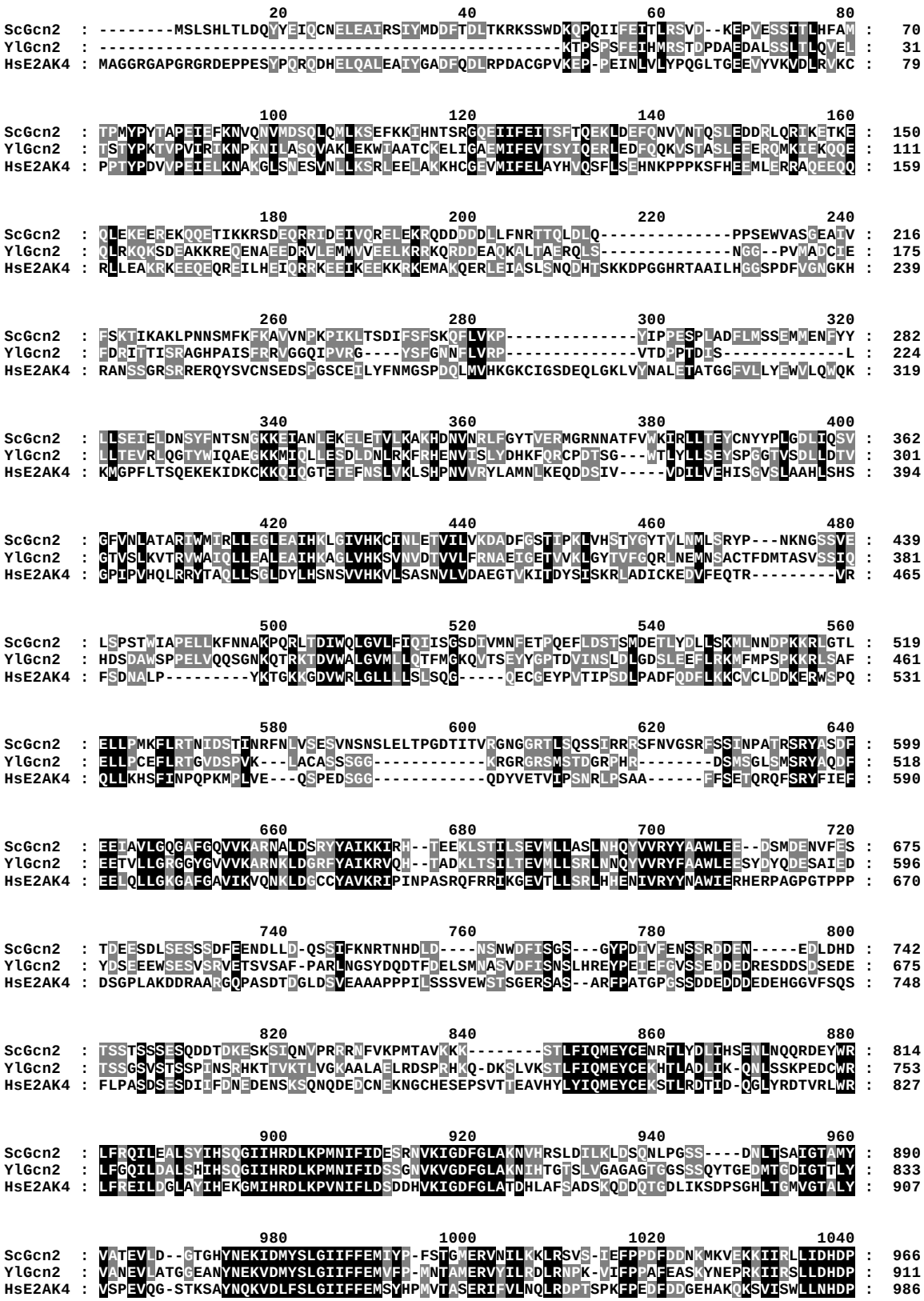
ScGcn2
YlGcn2
HsE2AK4

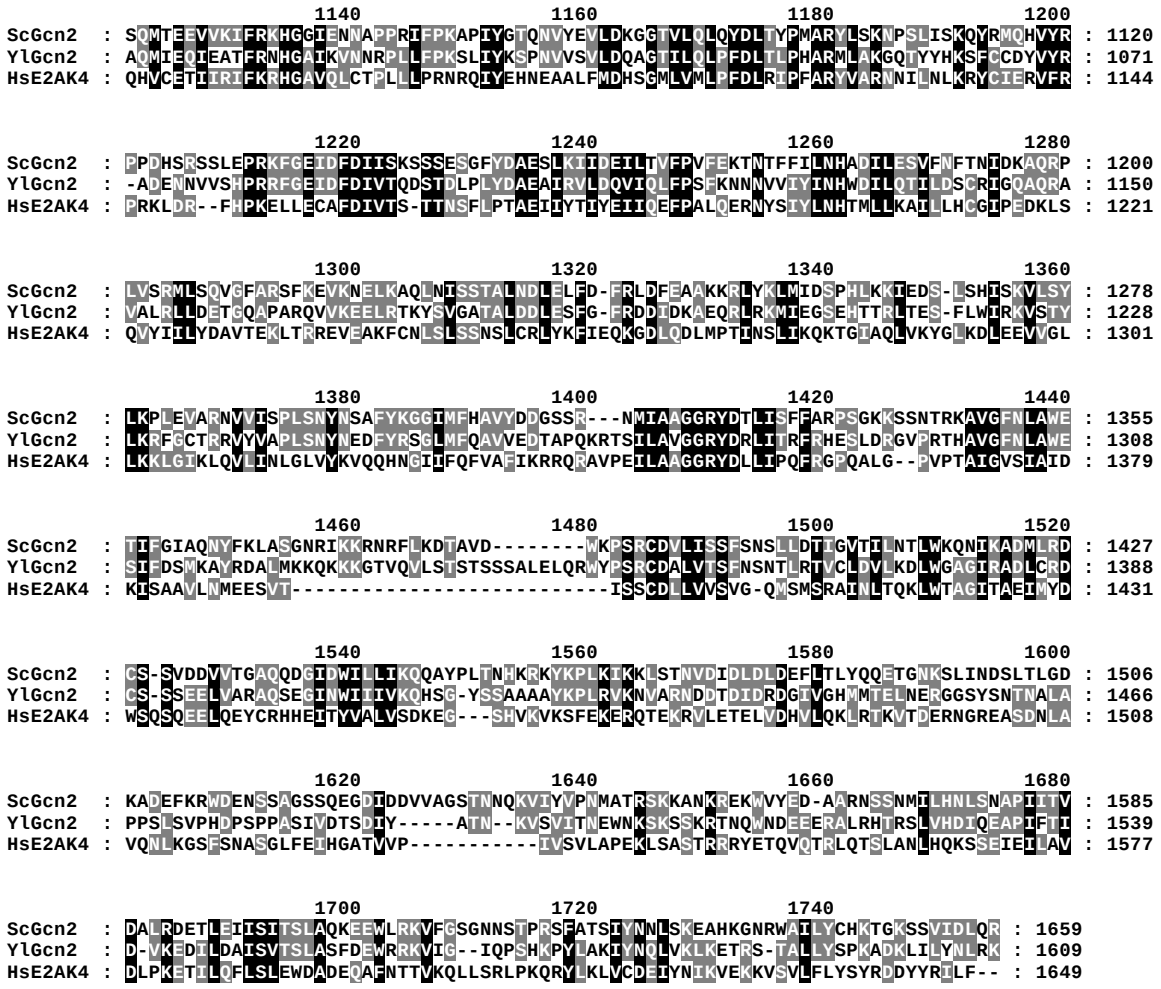

Figure 7.12 Multiple alignments of Gcn2 homologs from selected organisms. The protein sequence of YlGcn2p is aligned with amino acid sequences of the following organisms: *S. cerevisiae* Gcn2 and *H. sapiens* E2AK4 (eIF2).

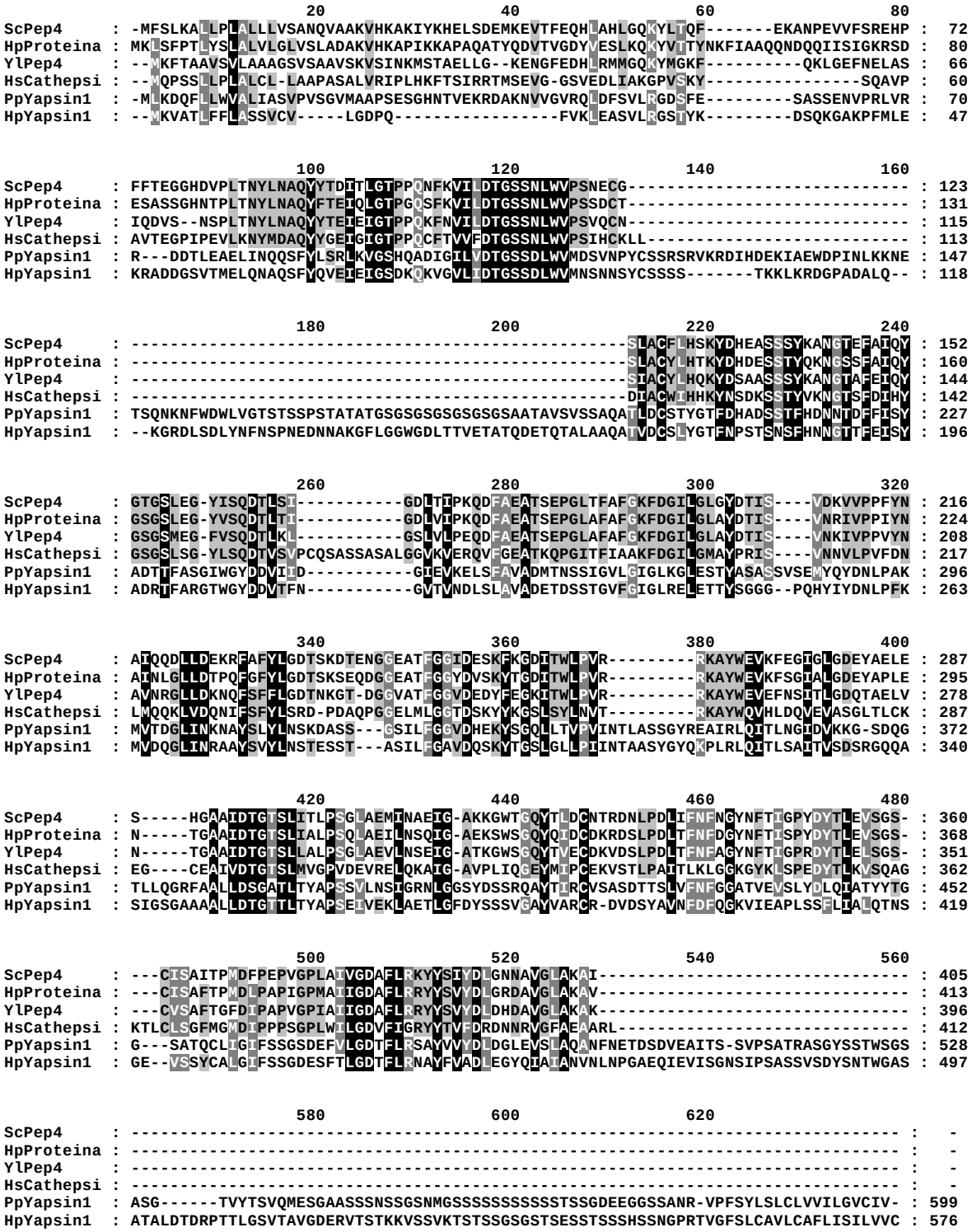

Figure 7.13 Multiple alignments of Pep4 and related proteases from selected organisms. The protein sequence of YlPep4p is aligned with respective amino acid sequences of the following organisms: *S. cerevisiae* Pep4p, *H. polymorpha* proteinase A and yapsin1, *P. pastoris* yapsin1 and *H. sapiens* cathepsin D.

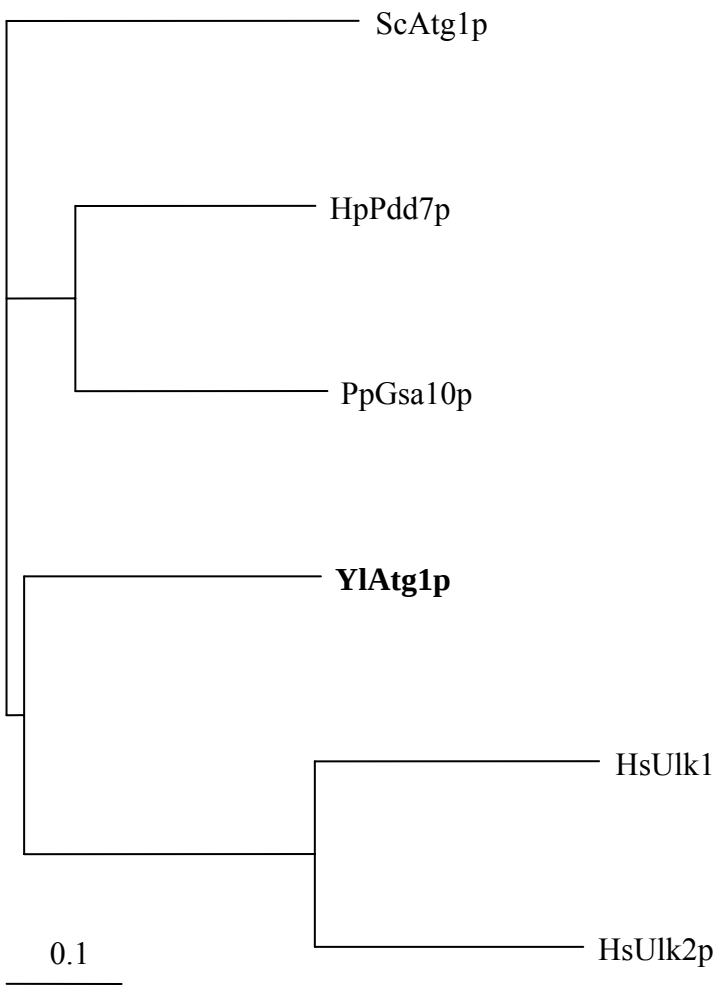

Figure 7.14 Phylogenetic tree of selected Atg1 homologous proteins. Fungal (ScAtg1, HpPdd7, PpGsa10) and human (HsUlk1/2) proteins are clustered together forming two groups, respectively. YlAtg1p is placed between these groups but seems to be closer to the correspondent human homologs.

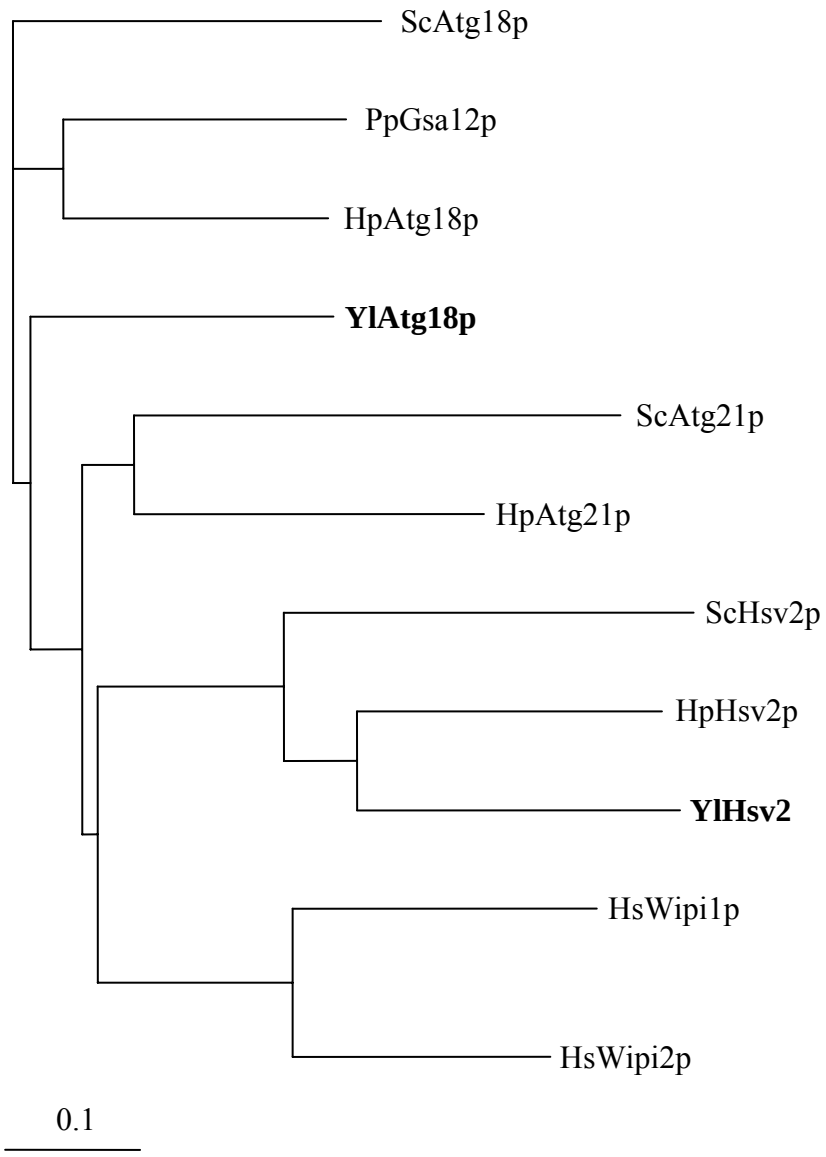

Figure 7.15 Phylogenetic tree of selected yeast and human proteins from the WIPI family. YlHsv2p is grouped together with Hsv2 proteins from *H. polymorpha* and *S. cerevisiae*. YlAtg18p is placed outside of yeast groups including Atg18- and Atg21-related proteins. Human homologs (HsWipi1/2) are clustered together at the separate branch.

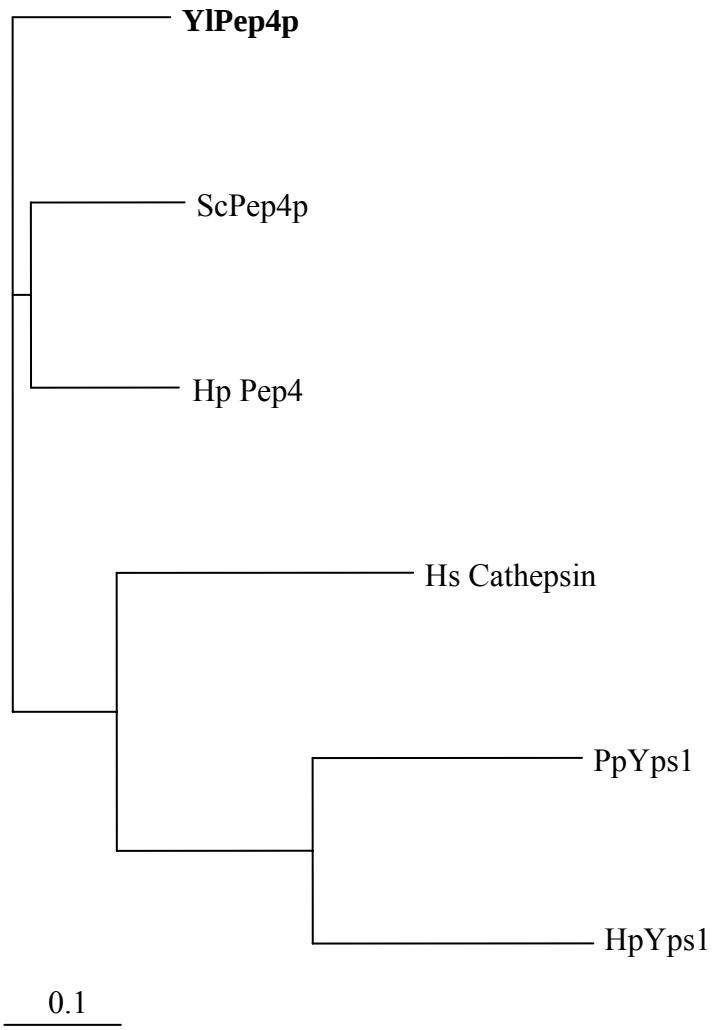

Figure 7.16 Phylogenetic tree of some Pep4-related proteases from yeasts and human. Yeast Pep4 proteins (ScPep4, HpPep4 and YlPep4) are placed outside of the branch including fungal yapsins (PpYps1 and HpYps1) and a human cathepsin proteases.

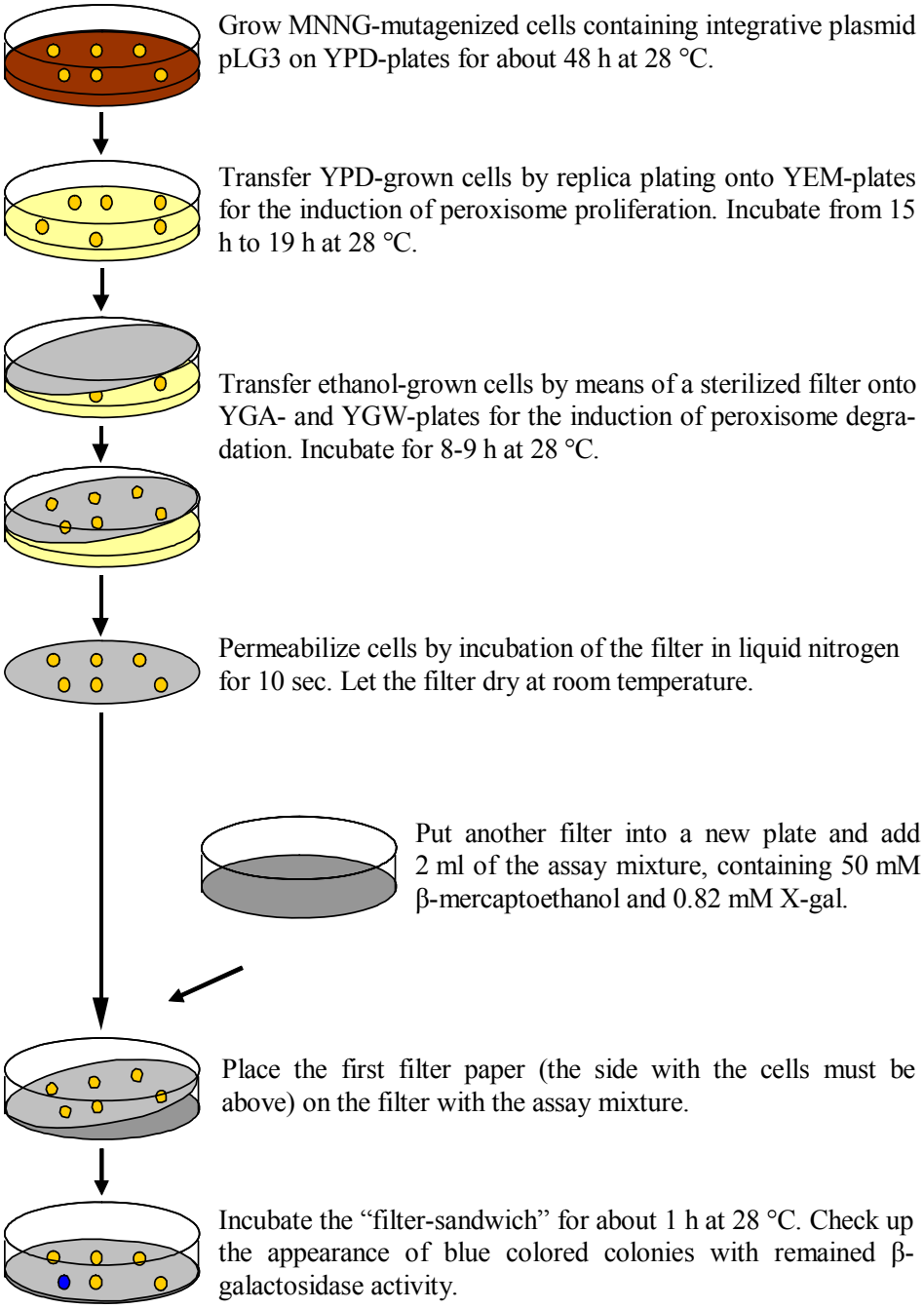

Figure 7.17 β-galactosidase plate activity assay used for isolation of peroxisome degradation deficient *(pdd)* mutants of *Y. lipolytica* (modified after Gunkel, 2000). The assay is based on the *YlICL1*-driven expression of heterologous β-galactosidase as part of peroxisomal-targeted chimerical protein βGal-eGFP(SKL).

Danksagung

An dieser Stelle möchte ich mich insbesondere bei Herrn Prof. Dr. Gerold Barth für die Überlassung des interessanten Themas, sein stetiges Interesse am Fortgang dieser Arbeit, wertvollen Anregungen sowie sein Verständnis und persönlichen Unterstützung bedanken.

Herrn Prof. Dr. Michael Kasper vom Institut für Anatomie des Universitätsklinikums Dresden möchte ich für die Möglichkeit danken, an seinem Institut die fluoreszenzmikroskopischen Untersuchungen durchführen zu können.

Andriy Kovalchuk danke ich vor allem für seine Unterstützung während der Arbeit, für die Durchsicht des Manuskriptes und die wertvollen wissenschaftlichen Diskussionen mit ihm.

Weiterhin bedanke ich mich auch meinen Studenten Carola Hoffmann, Christian Bodinus und Angela Jacobi für ihr ständiges Interesse, zahlreichen Fragen und Anregungen, die sehr zum Gelingen dieser Arbeit beigetragen haben.

Mein herzlicher Dank gilt auch allen jetzigen und ehemaligen Mitarbeitern des Institutes für Mikrobiologie, die für eine gute Arbeitsatmosphäre besorgt haben und mir immer zur Seite standen.

Nicht zuletzt möchte ich mich bei meiner lieben Familie bedanken. Ihr seid weit weg, aber in meinem Herzen bleibt ihr immer bei mir.

Versicherung

Hiermit versichere ich, dass ich die vorliegende Arbeit ohne unzulässige Hilfe Dritter und ohne Benutzung anderer als der angegebenen Hilfsmittel angefertigt habe; die aus fremden Quellen direkt oder indirekt übernommenen Gedanken sind als solche kenntlich gemacht. Die Arbeit wurde bisher weder im Inland noch im Ausland in gleicher oder ähnlicher Form einer anderen Prüfungsbehörde vorgelegt.

Die vorliegende Arbeit wurde am Institut für Mikrobiologie der Technischen Universität Dresden unter Betreuung von Herrn Prof. Dr. G. Barth angefertigt.

Die Promotionsordnung wird anerkannt.

Dresden, den 16. Mai 2006

Iryna Parshyna